

**Molecular Dissection of Ras Protein
Signalling in *Schizosaccharomyces
pombe***

A thesis submitted for the
degree of Doctor of Philosophy

by

Emma Jane Kelsall BSc (Hons)

Department of Biochemistry

University of Leicester

September 2013

Molecular Dissection of Ras Protein Signalling in *Schizosaccharomyces pombe*

Emma Jane Kelsall

Department of Biochemistry, University of Leicester

Thesis submitted for the degree of Doctor of Philosophy, September 2013

ABSTRACT

Fission yeast mating pheromone triggers the RAS-MAPK signalling pathway essential for meiotic differentiation. It also induces a dramatic morphological change of the cells leading to mating, a cell fusion event between cells of opposite mating types. The system is ideal to dissect the mechanisms by which the RAS-MAPK signal activation is regulated and highlight basic regulatory concepts of RAS protein signalling. In this work we evaluated the role of Ras1 in coordinating both MAPK activation due to pheromone signalling and activation of the Cdc42 pathway responsible for actin reorganisation. We established a condition to induce highly synchronous mating of fission yeast cells and we also established an assay system to monitor the MAPK phosphorylation status with an anti-phospho ERK monoclonal antibody. In addition, the changes in cellular morphology during the time course of meiotic differentiation were monitored. These tools allowed us to carry out quantitative measurements of the MAPK phosphorylation status in cells harbouring various mutations in the signalling components.

We confirmed that a constitutively active mutation of the MEK induces constitutive phosphorylation of the MAPK. Strikingly however, with a canonical oncogenic Ras mutation (*ras1.val17*), although the MAPK activation occurs acutely, it is rapidly down-regulated therefore identifying the role of an unidentified modulator of the pathway at the level of the MEKK or MEK. We have also identified that unlike Ras1 and its GEF, Ste6, the G-protein, Gpa1 and the adaptor protein Ste4 are essential for MAPK phosphorylation although Ras1 appears to be the main activator of MAPK phosphorylation exclusively through the MAPK cascade. We therefore conclude that Ras1 is activating both the MAPK branch - which leads to expression of meiotic genes - and the Cdc42 pathway for polarised growth in response to pheromone. Successful MAPK activation is required for a morphological response even in the presence of oncogenic Ras1 indicating that MAPK activation is likely to be essential for site selection for polarised growth and that preventing MAPK activation can successfully prevent the oncogenic Ras1 phenotype. Importantly, the oncogenic phenotype of *ras1.val17* can be rescued by the overexpression of the Ras1GAP, Gap1, therefore highlighting the importance of Ras proteins as potential therapeutic targets.

ACKNOWLEDGEMENTS

I would firstly like to thank Kayoko for all her encouragement, support and guidance over the past four years, you have made this time a bright and vibrant period of my life and I couldn't have done it without you!

My acknowledgments to our collaborators in Berlin; Professor Edda Klipp, Abel Vertesy and Dr Gabriele Schreiber for help with experimental design and project direction. My PhD committee members; Professor Andrew Fry, Dr Miguel Martins and Dr Raffael Schaffrath for stimulating discussion and useful comments and Dr Kees Straatman for all his technical support with the microscopy work.

Thank you to past and present members of the Tanaka lab; Shivanthi who made me feel welcome when I first arrived and all the technical support she provided, Deep, who never fails to make me smile, we've had some dramas together but somehow always come out laughing! And the newest member of the lab, Zsolt, for being a wonderful conference buddy and who is always there when I need advice.

Thank you to Sam, Jesvin, Ellie, Sarah, Maggie, Nico and Mark for their friendship and for making the Biochemistry department such a great place to work.

Finally, I would like to thank all my family and friends for their continuing love and support, especially to my parents, my brother Adam and my grandparents for being so understanding and always being there for me.

ABBREVIATIONS

(in alphabetical order)

ATP	- Adenosine-5'-triphosphate
bp	- Base pairs
cAMP	- Cyclic adenosine 3, 5-monophosphate
<i>clonNAT^R</i>	- Nourseothricin-dihydrogen sulphate resistance
DMSO	- Di-methyl sulphoxide
DNA	- Deoxyribonucleic acid
dNTP	- Deoxynucleoside triphosphate
<i>E.coli</i>	- <i>Escherichia Coli</i>
EDTA	- Ethylenediaminetetraacetic acid
EGFR	- Epidermal growth factor receptor
ERK	- Extracellular regulated kinase
GAP	- GTPase activating protein
GDP	- Guanosine-5'-diphosphate
GEF	- Guanine nucleotide exchange factor
GFP	- Green fluorescent protein
G-protein	- Guanosine nucleotide binding protein
GPCR	- G-protein coupled receptor
GTP	- Guanosine-5'triphosphate
<i>hyg^R</i>	- Hygromycin resistance
<i>kan^R</i>	- Kanamycin resistance
Kb	- Kilobases
LB	- Luria-Bertani medium
MAPK	- Mitogen Activated Protein Kinase
MAPKK	- Mitogen Activated Protein Kinase Kinase
MAPKKK	- Mitogen Activated Protein Kinase Kinase Kinase
MFSP	- Mating factor signalling pathway
MKPs	- MAPK phosphatases
MM-N	- Minimal media minus nitrogen
MM+N	- Minimal media plus nitrogen
mRNA	- Messenger ribonucleic acid
OBB	- Odyssey blocking buffer
ORF	- Open reading frame
PBS	- Phosphate buffer saline
PCR	- Polymerase chain reaction
PMSF	- Phenylmethylsulphonyl fluoride
PNACL	- Protein nucleic acid chemistry lab
PVDF	- Polyvinylidene difluoride
RNA	- Ribonucleic acid
RGS	- Regulator of G-protein signalling
RTKs	- Receptor Tyrosine Kinases
SDS	- Sodium dodecyl sulphate
<i>S.cerevisiae</i>	- <i>Saccharomyces cerevisiae</i>
<i>S.pombe</i>	- <i>Schizosaccharomyces pombe</i>
SPA	- Sporulation media agar

TBS	- Tris buffer saline
TBST	- Tris buffer saline plus Tween
TCA	- Trichloroacetic acid
TE	- 10 mM Tris-HCL, 1 mM EDTA: pH8.0
TF	- Transcription factor
WCE	- Whole cell protein extract
WT	- Wild type
YE+ade	- Yeast extract plus adenine

LIST OF CONTENTS

ABSTRACT	i
ACKNOWLEDGEMENTS	ii
ABBREVIATIONS	iii
LIST OF CONTENTS	v
LIST OF FIGURES	x
CHAPTER 1 INTRODUCTION	1
1.1 Ras proteins	1
1.1.1 Discovery of Ras proteins	1
1.1.2 Upstream of Ras.....	2
1.1.3 Ras effectors	6
1.1.4 Oncogenic Ras	7
1.1.5 RASopathies	11
1.2 Mammalian Ras-MAPK Pathways	11
1.2.1 The Ras-Raf-MEK-ERK pathway	12
1.2.2 Activation of Raf	12
1.2.3 Downstream of ERK1/2.....	13
1.2.4 Regulation	15
1.3 Fission Yeast Meiosis: a Ras-MAPK model system.....	16
1.3.1 Fission yeast as a model organism.....	16
1.3.2 Fission yeast cell cycle	17
1.3.3 Fission Yeast Meiosis	18
1.3.4 Signalling pathways involved in the initiation of meiosis.....	20
1.3.5 Pheromone Signalling.....	25
1.3.6 Ras1	29
1.3.7 Activation of the MAPK cascade	34
1.3.8 Cdc42 GTPase and the control of polarised growth.....	48
1.3.9 Genetic control of meiosis - The Pat1-Mei2 switch	66
1.4 Aims and Objectives	72
CHAPTER 2 MATERIALS AND METHODS	74
2.1 Materials.....	74

2.1.1	Yeast Strains	74
2.1.2	Oligonucleotides	74
2.1.3	Media	75
2.1.4	Antibodies	84
2.1.5	Molecular weight markers	84
2.2	Methods.....	86
2.2.1	Agarose gel electrophoresis	86
2.2.2	Preparation of yeast genomic DNA	86
2.2.3	Plasmid preparation	87
2.2.4	<i>E.coli</i> Transformation	89
2.2.5	<i>E.coli</i> Plasmid Isolation	89
2.2.6	Polymerase Chain reaction	90
2.2.7	DNA Purification	91
2.2.8	DNA sequencing	91
2.2.9	Gene disruption.....	92
2.2.10	Checking for correct chromosomal insertion.....	99
2.2.11	Yeast Transformations	99
2.2.12	Induction of meiotic differentiation	100
2.2.13	Collection of Cells - The Cdc2 STOP buffer method vs. the Trichloroacetic acid (TCA) method.....	103
2.2.14	Calculating mating efficiency	104
2.2.15	Preparation of total protein extracts.....	106
2.2.16	Western Blotting	107
2.2.17	Established protocol for measuring phospho-Spk1 by western blotting	108
2.2.18	Live Cell Imaging	109
 CHAPTER 3 ASSESSMENT OF MAPK ACTIVATION IN RESPONSE TO PHEROMONE 110		
3.1	Introduction	110
3.2	Establishing a mating assay system	116
3.2.1	Large scale liquid culture.....	116
3.2.2	Agar Plate Assay	119
3.3	Denaturation of Cell Extracts.....	124
3.4	Validation of the use of a phospho-ERK antibody to detect phospho-Spk1..	128
3.4.1	Detection of Spk1 MAPK.....	128

3.4.2	Detection of phosphorylated Spk1 MAPK	129
3.5	MAPK dynamics in WT and Ras1-MAPK mutants	134
3.5.1	WT cells; changes in MAPK activation and cellular localisation during meiosis	134
3.5.2	Meiotic phenotype of a constitutively active MEK mutant	142
3.5.3	MAPK dynamics in an oncogenic Ras mutant	151
3.6	Discussion	159
3.6.1	WT MAPK dynamics	159
3.6.2	The <i>byr1.DD</i> phenotype	160
3.6.3	The <i>ras1.val17</i> phenotype.....	162
CHAPTER 4 RAS ACTIVATES TWO INDEPENDENT PATHWAYS DURING MEIOTIC DIFFERENTIATION		166
4.1	Introduction	166
4.2	Constitutively active MEK can bypass the requirement of Ras1 for MAPK phosphorylation but not the morphological defect	169
4.3	MAPK activation does not define the morphological phenotype	172
4.4	MAPK activation is essential for a morphological response	181
4.4.1	Byr2 is exclusive to the activation of the MAPK cascade.....	181
4.4.2	Scd1 is exclusive to activation of the morphology branch	185
4.4.3	Activation of the morphology branch still requires MAPK activation in the presence of oncogenic Ras1.....	187
4.5	Does the morphology pathway feeding into MAPK activation?	191
4.6	Discussion	196
4.6.1	The potential Spk1 MAPK target of the morphology branch.....	200
4.6.2	Does the Cdc42 pathway contribute to MAPK activation?	202
4.6.3	Targeting Cdc42 in Ras-induced transformation.....	204
CHAPTER 5 SIGNAL TRANSDUCTION UPSTREAM OF RAS1: COORDINATION OF MAPK AND MORPHOLOGY ACTIVATION.....		206
5.1	Introduction	206
5.2	Gpa1 plays a key role in activation of both the pheromone and morphology pathways	208
5.2.1	Role of Gpa1	208
5.2.2	Gpa1.QL	216
5.3	The role of Ste4 in mating signal transduction	224
5.4	Role of Ste6 for Ras1 activation	227

5.5	Discussion	236
5.5.1	The role of Ste4 in Byr2 activation.....	239
5.5.2	Ste6 and the activation of Ras1 during mating.....	244
5.5.3	Coordinated activation of the MAPK cascade and the morphology pathway	248
CHAPTER 6 THE ROLE OF NEGATIVE REGULATORS IN SHAPING MAPK ACTIVATION 250		
6.1	Introduction	250
6.2	Role of Gap1	254
6.3	Role of Sxa2.....	260
6.4	Role of Rgs1.....	265
6.5	Discussion - Downregulation of the MFSP	271
CHAPTER 7 BIOCHEMICAL MANIPULATION OF PHEOMONE SIGNAL TRANSDUCTION		
7.1	Introduction	277
7.2	Creation of an ATP-analogue sensitive MAPK.....	280
7.2.1	Creation of ATP-analogue sensitive Spk1	286
7.2.2	Rescue of <i>byr1.DD</i>	296
7.2.3	Potential use of <i>spk1.as</i> to identify direct Spk1 substrates.....	297
7.3	Lifeact – Visualisation of F-actin in live cells	298
7.3.1	<i>Actin Localisation in Wildtype Cells</i>	299
7.3.2	<i>Actin localisation in Ras-MAPK mutants</i>	302
7.4	Discussion of the <i>byr1.DD</i> phenotype	308
7.5	Direct manipulation of Ras1	312
7.5.1	Gap1 overexpression in <i>ras1.val17</i>	312
7.5.2	Overexpression of GAP deficient and N- and C-terminal truncation Gap1 mutants	317
7.6	Discussion - GAPs as potential therapeutics.....	322
CHAPTER 8 DISCUSSION AND FUTURE DIRECTIONS		
8.1	Original aims and objectives.....	325
8.1.1	An undefined down regulatory mechanism at the level of MEKK or MEK	328
8.1.2	Ras1 plays an essential role in coordination <i>S.pombe</i> mating events.....	331
8.1.3	Gpa1 and Ste4 are essential for activation of the MAPK cascade.....	332

8.1.4	Ste6 is the Ras1 GEF controlling the activation of both the MAPK branch and the morphology branch	335
8.1.5	The Importance of Negative Regulators	336
8.1.6	GAPs as therapeutic targets	336
8.1.7	Targeting the Cdc42 pathway as a therapeutic approach	337
8.1.8	The <i>ras1.val17</i> elongated phenotype	338
8.2	Conclusions	340
APPENDICES		342
BIBLIOGRAPHY		347

LIST OF FIGURES

Figure 1.1 Post-translational processing of Ras proteins (Reproduced from (Downward, 2003)).....	4
Figure 1.2 Ras GDP-GTP Cycle.....	5
Figure 1.3. Ras effector pathways (Reproduced from (Schubbert <i>et al.</i> , 2007)).....	10
Figure 1.4 Fission yeast mitosis and meiosis.....	19
Figure 1.5 The initiation of meiosis (reproduced from (Yamamoto, 2010)).....	24
Figure 1.6. The Mating Factor Signalling Pathway.....	27
Figure 1.7 Mitotic and meiotic oncogenic Ras1 phenotypes in <i>S.pombe</i>	31
Figure 1.8 Byr2 protein domains.....	39
Figure 1.9 Hypothesis: Activation of Byr2 (Reproduced from (Tu <i>et al.</i> , 1997)).....	41
Figure 1.10 Mitotic and meiotic phenotypes of <i>byr1.DD</i> in <i>S.pombe</i>	44
Figure 1.11 Ras1-Cdc42 cell morphology pathway in <i>S.pombe</i>	54
Figure 1.12 Mitotic polarised cell growth in <i>S.cerevisiae</i> and <i>S. pombe</i> . Reproduced from (Perez & Rincon, 2010)).....	57
Figure 1.13 Polarised growth during meiosis in <i>S.cerevisiae</i> and <i>S.pombe</i> . Reproduced from ((Merlini <i>et al.</i> , 2013)).....	60
Figure 1.14 Cell fusion process in <i>S.cerevisiae</i> and <i>S.pombe</i> (Reproduced from (Merlini <i>et al.</i> , 2013)).....	65
Figure 1.15 Genetic basis of meiosis in <i>Schizosaccharomyces pombe</i>	69
Figure 2.1: Gene deletion at the endogenous locus.....	94
Figure 2.2 GFP-Tagging of a gene at the endogenous locus.....	96
Figure 2.3 Site-directed mutagenesis.....	98
Figure 2.4 Liquid mating assay.....	102
Figure 2.5 Plate mating assay.....	105
Figure 3.1 The mating factor signalling pathway.....	112
Figure 3.2 Pat1.114 (Pat1.ts) synchronous meiosis.....	115
Figure 3.3 Liquid mating assay.....	118
Figure 3.4 Plate mating assay.....	121
Figure 3.5 Quantification of WT mating efficiency using the Plate assay.....	123
Figure 3.6 Experimental design for quantitative mating assay and protein extraction.....	126
Figure 3.7: Validation of the use of a commercially available anti-GFP and anti-phospho-MAPK specific antibody.....	133
Figure 3.8 Wildtype MAPK dynamics during sexual differentiation.....	137
Figure 3.9 Imaging of Spk1-GFP over a 24 hour time-course in WT cells.....	140
Figure 3.10 A direct comparison of Spk1 MAPK dynamics in WT and <i>byr1.DD</i> strains during a mating time-course.....	146
Figure 3.11 Imaging of Spk1-GFP over a 24 hour time-course in <i>byr1.DD</i> cells.....	149
Figure 3.12 Ras1 plays roles in both the MFSP and the Cdc42 morphology pathway.....	152
Figure 3.13 A direct comparison of the MAPK signalling dynamics in WT and <i>ras1.val17</i> during a mating time-course.....	156
Figure 3.14 Imaging of Spk1-GFP over a 24 hour time-course in <i>ras1.val17</i> cells.....	158

Figure 4.1 Hypothesis: Ras1 activates two independent pathways upon pheromone signalling.....	168
Figure 4.2 <i>byr1.DD</i> can bypass the requirement of Ras1 for MAPK activation but not the morphological defect.	171
Figure 4.3 Direct comparison of MAPK phosphorylation in <i>byr1.DD</i> and <i>ras1.val17 byr1.DD</i> by quantitative western blot.....	175
Figure 4.4 The terminal mating phenotype of <i>ras1.val17 byr1.DD</i> is a phenocopy of <i>ras1.val17</i>	178
Figure 4.5 Byr1.DD signals independently of Byr2	183
Figure 4.6. The <i>byr1.DD</i> "paired" phenotype is independent of Byr2	184
Figure 4.7 <i>Scd1</i> is an essential part of the morphology branch	186
Figure 4.8 No morphological change in the absence of MAPK signalling	189
Figure 4.9 Morphological change associated with the <i>ras1.val17</i> occurs at <i>later time points</i> in the <i>byr1.DD</i> mutant	190
Figure 4.10 Does the morphology pathway influence MAPK activation?.....	194
Figure 4.11 <i>scd1Δ</i> morphology	195
Figure 4.12 Conclusion: Ras1 activates two independent pathways and activated MAPK feeds into the morphology branch	199
Figure 5.1 Aim of Chapter 5.....	207
Figure 5.2 <i>Gpa1</i> is an essential component for MAPK phosphorylation.	212
Figure 5.3 Rescue of the <i>gpa1Δ</i> phenotype is dependent on reactivation of both the morphology pathway and MAPK pathway	213
Figure 5.4 Activation of both of the two pathways is required and sufficient to mimic the pheromone signal	215
Figure 5.5 <i>Gpa1.QL</i> causes MAPK phosphorylation upon nitrogen starvation.....	220
Figure 5.6 <i>Gpa1.QL</i> causes the elongated phenotype in response to nitrogen starvation	221
Figure 5.7 Hypothesis: <i>Ste4</i> links <i>Byr2</i> and <i>Ras1</i>	223
Figure 5.8 The role of <i>Ste4</i> as an exclusive MAPK pathway activator.....	226
Figure 5.9 The control of <i>Ras1</i> activation during mating.....	230
Figure 5.10 <i>Ras1</i> and <i>Ste6</i> are not essential for MAPK activation.	231
Figure 5.11 Comparison of morphology between various MFSP.....	232
Figure 5.12 <i>Ste6</i> is required for both MAPK activation and a morphological response	234
Figure 5.13 Proposed model for coordination of MAPK activation and morphology pathway activation	238
Figure 5.14 Proposed model for <i>Byr2</i> activation.....	243
Figure 5.15 The proposed model for activation of <i>Ras1</i>	247
Figure 6.1 Identified negative regulators of the MFSP	252
Figure 6.2 Mutants that phenocopy <i>ras1.val17</i>	253
Figure 6.3 A direct comparison of the MAPK dynamics during aWT and <i>gpa1Δ</i> mating time-course.....	256
Figure 6.4 Imaging of <i>Spk1-GFP</i> over a 24 hour time-course in <i>gpa1Δ</i> cells compared to <i>ras1.val17</i> cells.	259

Figure 6.5 A direct comparison of the MAPK dynamics during a WT and <i>sxa2Δ</i> mating time-course.....	262
Figure 6.6 Imaging of Spk1-GFP over a 24 hour time-course in <i>sxa2Δ</i> cells compared to <i>ras1.val17</i> cells.	264
Figure 6.7 A direct comparison of the signalling dynamics in WT and <i>rgs1Δ</i> during a mating time-course.	268
Figure 6.8 Imaging of Spk1-GFP over a 24 hour time-course in <i>rgs1Δ</i> cells compared to <i>ras1.val17</i> cells.	270
Figure 7.1 Summary of the mating phenotypes and MAPK phosphorylation profiles of WT, <i>ras1.val17</i> and <i>byr1.DD</i>	279
Figure 7.2 The concept of ATP-analogue sensitive kinases.	282
Figure 7.3 Tolerant and intolerant kinases.....	283
Figure 7.4 Generating an ATP-analogue sensitive kinase.....	285
Figure 7.5 Strategy to identify a second site mutation (<i>sogg</i>) for Spk1.	288
Figure 7.6 Spk1-V67I-Q119A Generation	291
Figure 7.7 Spk1-Sho-IA generation.....	292
Figure 7.8 Sequence alignments confirming the GKR mutation and the second site mutations.....	293
Figure 7.9 Rescuing Spk1- <i>as</i> activity and testing 1-NM-PP1 selectivity.....	295
Figure 7.10 Lifeact imaging during conjugation in WT cells.....	301
Figure 7.11 Lifeact-GFP localisation in Ras1-MAPK mutants.....	307
Figure 7.12 Gap1 overexpression in <i>ras1.val17</i>	316
Figure 7.13 Identifying a residue to mutant to create a GTPase deficient Gap1	320
Figure 7.14 Gap1 constructs.	321
Figure 8.1 Summary of the main findings of this work.....	327

CHAPTER 1 INTRODUCTION

1.1 Ras proteins

The Ras proteins are a large super-family of widely conserved small guanine nucleotide-binding proteins. They regulate several crucial signalling pathways that control cellular growth and differentiation and also play a role in cell survival and cytoskeletal arrangement. Importantly, mutations in *Ras* genes are frequently associated with human cancers. Specifically, over a third of all cancers and 90% of adenocarcinomas present in the pancreas have mutated *Ras* (Downward, 2003). *Ras* is also found to be mutated in a high percentage of colorectal, thyroid, liver and lung cancers (Downward, 2003). Germline mutations in *Ras* genes can cause developmental disorders such as Noonan, Costello and cardio-facio-cutaneous (CFC) syndromes (Schubbert *et al.*, 2007). These disorders are collectively known as RASopathies (See 1.1.5). Despite extensive research to uncover the molecular nature of Ras proteins, the range of Ras-mediated signal transduction cascades and the means by which these complex pathways are integrated in cells still requires further studies.

1.1.1 The discovery of Ras proteins

Ras proteins were some of the very first proteins discovered to regulate cell growth and were found to be responsible for the oncogenic nature of the Kirsten and Harvey rat sarcoma viruses (Parada *et al.*, 1982; Der *et al.*, 1982; Santos *et al.*, 1982; Reddy *et al.*, 1982). There are three *Ras* genes in the human genome, *N-Ras*, *H-Ras* and *K-Ras*, with around 85% amino acid sequence identity between the three. *K-Ras* is alternatively spliced at the C-terminus resulting in the K-RasA and K-RasB proteins. All Ras proteins are nearly identical at N-terminus (residues 1-165) but differ substantially at C-terminus, this area is known as the hypervariable region which determines signal

selectivity - reviewed by (Bar-Sagi, 2001). Ras proteins need to posttranslationally modified for function and this usually involves a change in subcellular localisation. All Ras proteins are processed posttranslationally at the conserved CAAX domain at N-terminal, as shown in **Figure 1.1**. The cysteine of the CAAX motif is posttranslationally modified by the addition of a farnesyl group by farnesyltransferase which results in Ras being attached to intracellular membranes (Hancock *et al.*, 1989; Hancock *et al.*, 1990). After several further processing steps, Ras proteins are transported and attached to the plasma membrane by the addition of two palmitoyl fatty acids chains to a different cysteine residue by palmitoyltransferase. Preventing Ras farnesylation has been explored as a therapeutic intervention in human disease but with limited success which is thought to be because when farnesylation is inhibited Ras can be geranylgeranylated instead to anchor it to membranes and attempts to block both farnesylation and geranylgeranylation appears toxic to all cells (Lobell *et al.*, 2001). This is not surprising considering the central role Ras proteins play in fundamental cellular processes.

1.1.2 Upstream of Ras

The activity of Ras is controlled by a simple binary switch mechanism as illustrated in **Figure 1.2**. Ras is activated and will signal to downstream effectors when bound to guanosine-5'triphosphate (GTP) and is considered to be in an inactive when bound to guanosine-5'diphosphate (GDP). Ras contains intrinsic GTPase activity for the hydrolysis of GTP to GDP, this activity is exceptionally slow but is enhanced by several thousand fold by the binding of GTPase Activating Proteins (GAPs) (Gibbs *et al.*, 1984). Ras GAPs are a large family of proteins and examples of Ras GAPs are p120GAP, Neurofibromin (NF1), the GAP1 family, calcium promoted Ras inactivator (CAPRI), Ras GTPase activating-like protein (RASAL) and the SynGAP family (Grewal *et al.*, 2011). Activation of Ras requires Guanine Nucleotide Exchange Factors

(GEFs) for example SOS1 and SOS2, which induce a conformational change to open the nucleotide binding site allowing exchange of GDP for GTP. The concentration of GTP in the cytoplasm is reported to be ten times higher than GDP thereby once GDP is released it can be replaced by the more abundant GTP. It is the balance between the activities of GEFs and GAPs that determines the activation state of Ras.

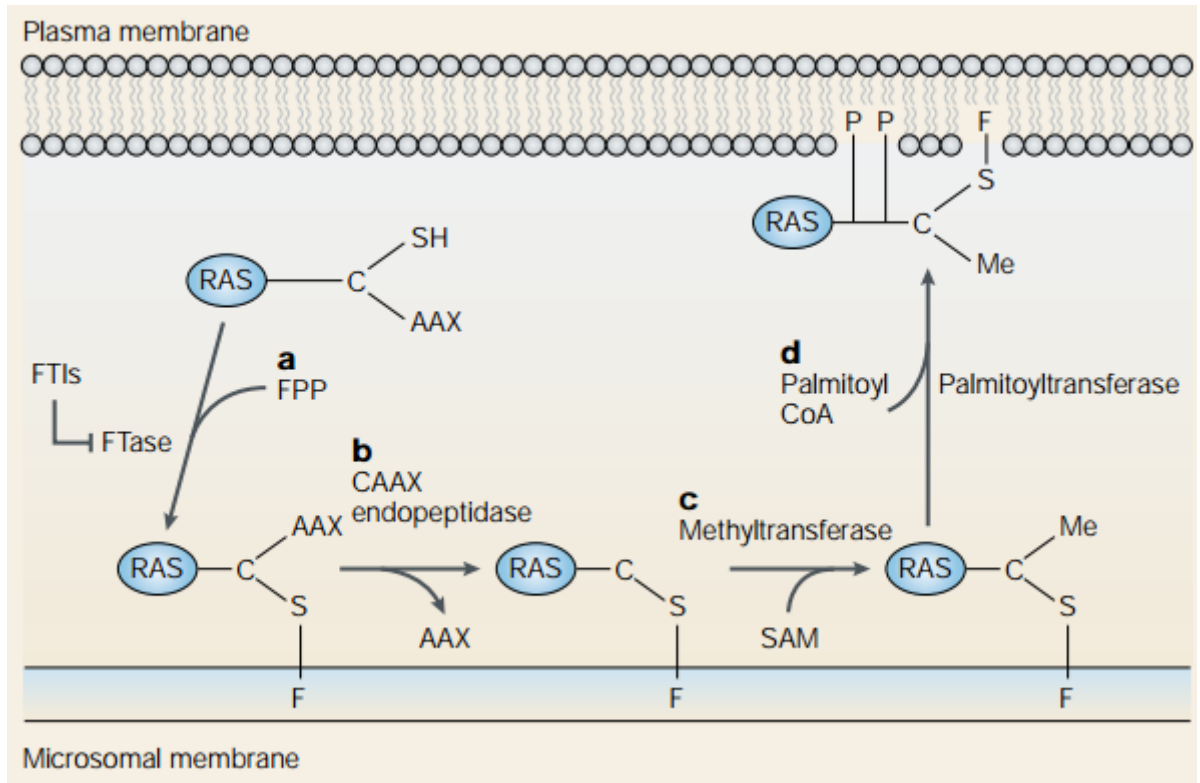


Figure 1.1 Post-translational processing of Ras proteins (Reproduced from Downward, 2003).

Newly synthesised Ras is present in the cytoplasm and requires a number of posttranslational modifications in order to be biologically active. These include farnesylation by farnesyltransferase which results in Ras association with intracellular membranes (a). A CAAX endopeptidase removes the last three amino acids from Ras (b) allowing the terminal cysteine to be methylated (c). Ras can be transported to the plasma membrane where it is further modified by the addition of two palmitoyl long-chain fatty acids which stabilised the interaction with the plasma membrane (d).

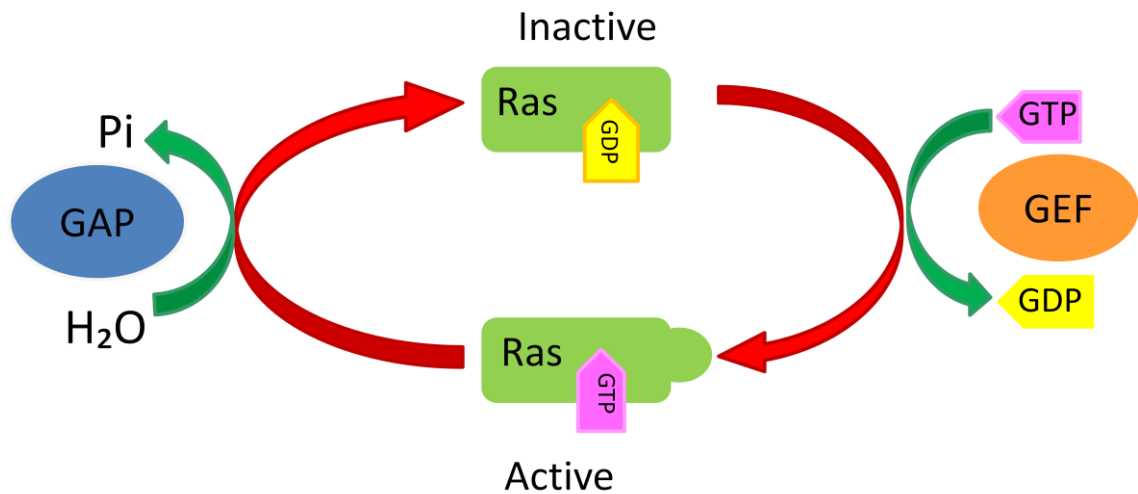


Figure 1.2 Ras GDP-GTP Cycle

The activity of Ras proteins is controlled in a binary switch manner. Ras is activate and signals to downstream effectors when bound to GTP and biologically inactive when bound to GDP. The exchange of GDP for GTP requires Guanine Nucleotide exchange factors (GEFs). Ras proteins have weak intrinsic GTPase activity which will hydrolyse GTP to GDP but at an exceptionally low rate, this hydrolysis rate can be increased several thousand fold by the presence of GTPase Activating Proteins (GAPs).

Ras is activated downstream of a number of extracellular stimuli including activation of the Receptor Tyrosine Kinases (RTKs) which are cell surface receptors as illustrated in **Figure 1.3**. Examples include the epidermal growth factor receptor (EGFR) and the nerve growth factor receptor (NGFR). These receptors are activated by the binding of extracellular ligands which induce a conformational change in the intracellular domain promoting dimerisation and autophosphorylation of the receptor. This allows interactions with adaptor proteins such as SHC and GRB2 and the mammalian RasGEF SOS which can activate plasma membrane bound Ras. Ras can also be activated by G-Protein Coupled Receptors (GPCRs) and a number of different GEFs thereby building complexity into Ras protein activation and signalling - reviewed by (McKay & Morrison, 2007).

1.1.3 Ras effectors

There are four main Ras effector pathways illustrated in **Figure 1.3** and reviewed in (Shields *et al.*, 2000). The best characterised effector pathway is the Raf-MEK-ERK pathway which is a three-tiered mitogen activated protein kinase (MAPK) cascade (See 1.2) . Activated Ras binds to all three Raf isoforms - A-Raf, B-Raf and C-Raf (also known as Raf1), which can form homo- and hetero-dimers. The binding of activated Ras to the Ras binding domain (RBD) of Raf proteins causes membrane translocation and activation of Raf by various means. Activation of Raf is described in 1.2.2. Once activated, RAF proteins activate mitogen activated protein kinase kinases (MEK1 and 2) via dual phosphorylation. MEKs are dual specificity protein kinases which phosphorylate threonine and tyrosine residues on the downstream mitogen activated protein kinases, ERK1 and 2. Some of the major targets are the transcription factors c-Jun and Elk1 which work to promote cell cycle progression.

The second Ras effector pathway is the phosphatidylinositol 3-kinase (PI3K) pathway which leads to the activation of PDK1 and AKT/PKB. This pathway has a strong anti-apoptotic function thereby activation of Ras activates a key cell survival pathway. PI3K also activates the Rho-GTPase, RAC, which is involved in regulation of the actin cytoskeleton.

The third pathway involves the activation of exchange factors for RAL which, once activated, activates phospholipase D (PLD) and the Rho family small GTPase Cdc42. A more detailed description of Cdc42 signalling is given in 1.3.8. This pathway also inhibits the forkhead transcription factors which promote cell cycle arrest and apoptosis thereby through RAL, Ras is sending a pro-survival signal.

The fourth effector is phospholipase C ϵ (PLC ϵ) which acts to hydrolyse phosphatidylinositol-4,5-bisphosphate (PtdIns(4,5)P₂) to diacylglycerol and inositol-1,4,5-trisphosphate (Ins(1,4,5)P₃), this pathway potentially links Ras to the activation of Protein Kinase C (PKC) and calcium mobilisation.

1.1.4 Oncogenic Ras

It is easy to see why hyperactivation of Ras can strongly contribute to malignant phenotypes through these diverse effector pathways. Over the past three decades there has been a huge effort to design effective therapeutic drugs against oncogenic Ras but with limited success.

Around a third of all cancers are found to have mutated *Ras* (Downward, 2003).

Frequently found activating point mutations are in codons 12, 13 and 61 (Bos, 1989) and these mutations result in a Ras protein to which GAPs are ineffective thereby rendering them in a permanent GTP bound activated state. The biochemical reasons as to why mutations at these specific residues confers GAP resistance was brought to light

when the crystal structure of H-Ras bound to the catalytic domain of p120GAP was solved (Scheffzek *et al.*, 1997). It was found that an interaction between glutamine 61 and a highly conserved arginine residue in p120GAP is essential for the stimulation of GTP hydrolysis and point mutations at position 12 and 13 interfere with this interaction (Scheffzek *et al.*, 1997; Scheffzek *et al.*, 1996).

It is proposed that the molecular basis of *Ras* oncogenicity is constitutive effector pathway stimulation but this may not be the case in terms of constitutive ERK pathway activation. Until around a decade ago the effect of hyperactivated Ras was investigated using overexpression of mutated Ras from plasmids, although in reality, amplification of the *Ras* gene is not commonly found in malignancies (Fernandez-Medarde & Santos, 2011). More recently, investigations into the role of endogenously expressed oncogenic Ras have highlighted key points about MAPK output in the presence of oncogenic Ras. In the paper by (Tuveson *et al.*, 2004), by employing a mouse model, they developed a targeting strategy to conditionally express endogenous levels of oncogenic *K-Ras*.

When the mutation is introduced in mouse embryonic fibroblasts (MEFs) there is an increase in the levels of activated Ras as expected. However, upon serum stimulation, the activation of MEK and the kinase activity of ERK appear unchanged compared to the control. Notably, the activation of ERK is still attenuated in these MEFs as shown by a decrease in the amount of phospho-ERK and kinase activity of ERK over time therefore highlighting that in the presence of endogenously expressed oncogenic *Ras* there is still attenuation of the ERK effector pathway. In these MEFs, expression of endogenous levels of oncogenic *K-Ras* caused enhanced proliferation and partial transformation, therefore *K-Ras* oncogenicity is unlikely to be the result of constitutive ERK effector pathway stimulation but some other means and further investigations into the effects of endogenously expressed oncogenic *Ras* will make valuable contributions

to our current understanding of the malignant nature of *Ras* mutations and highlight potential areas of therapeutic intervention. In the past, targeting this pathway has been somewhat problematic in terms of specifically targeting tumour cells as Ras and its effector pathways are important for normal cell survival thereby making the therapeutic window exceptionally small.

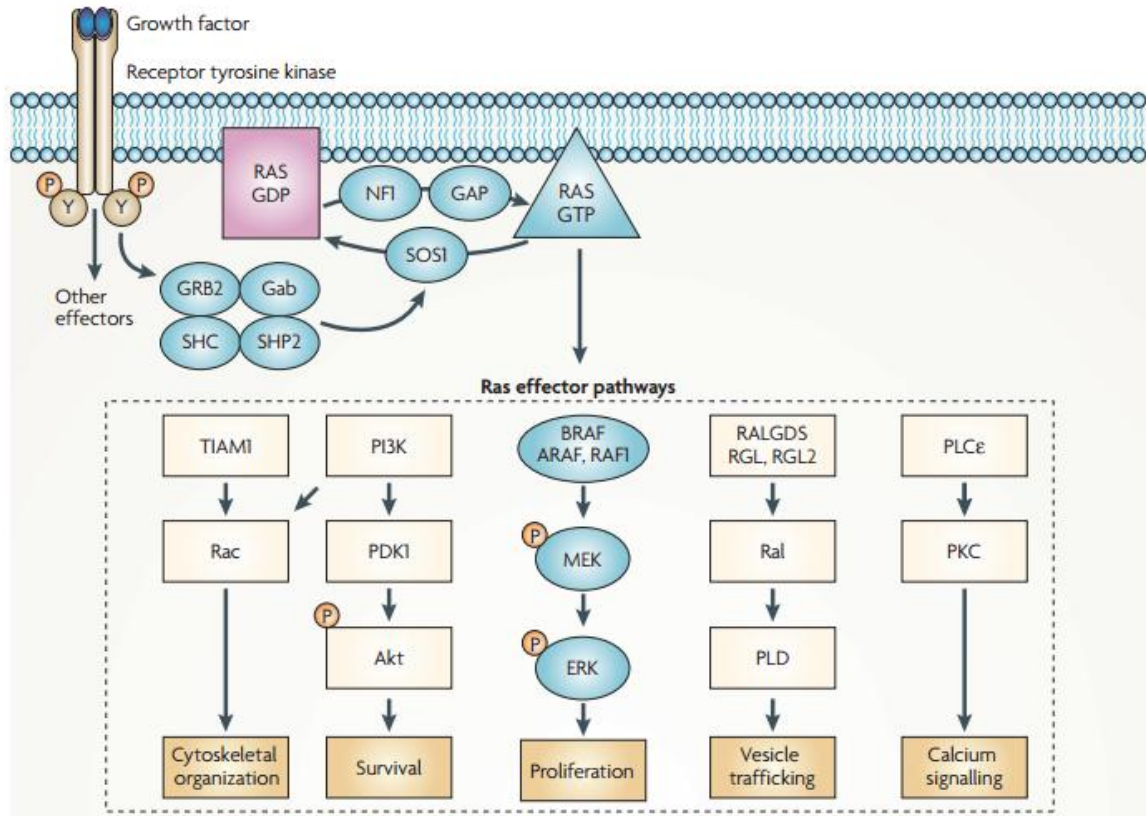


Figure 1.3. Ras effector pathways (Reproduced from Schubert *et al.*, 2007)

Ras is activated in response to growth factor receptor stimulation on the cell membrane involving the adaptor protein GRB2 and the RasGEF SOS1. NF1 and GAP are the two main RasGAPs. In mammalian cells Ras has four main downstream effectors: Raf, PI3K, Ral protein and PLC. These effectors are connected with proliferation, cell survival and anti-apoptotic signals as well as calcium signalling, vesicle trafficking and cytoskeletal organisation..

1.1.5 RASopathies

A group of developmental disorders known as RASopathies results from germline mutations in a number of genes involved in Ras-MAPK signalling, these include; Cardio-facio-cutaneous syndrome (CFC), Costello syndrome, Noonan syndrome and Neurofibromatosis Type 1 (See (Rauen, 2013) for a review). These syndromes are caused by mutations in a number of genes including *H-Ras*, *K-Ras*, *NF1*, *PTPN11* and *B-Raf* (Schubbert *et al.*, 2007). Each RASopathy has a unique phenotype but there are many overlapping characteristics including craniofacial dysmorphology, cardiac malformations, neurocognitive impairment and increased cancer risk (Rauen, 2013). RASopathies represent one of the largest groups of malformation syndromes. Interestingly, these mutations only rarely cause tumours in these patients. A number of activating mutations in these syndromes have been shown to be only weakly activating therefore it is likely that strongly activating mutations, like those associated with malignancies, are not tolerated if present in the germline.

1.2 Mammalian Ras-MAPK Pathways

Mitogen activated protein kinase (MAPK) cascades are evolutionary conserved signalling pathways through from yeast to humans. Each cascade contains three core kinases known as MAPK kinase kinase (MAPKKK), MAPK kinase (MAPKK) and MAPK. The characterised Raf-MEK-ERK pathway is the prototypical MAPK pathway in mammalian cells and is activated upstream by Ras proteins. There are a number of other MAPK pathways in mammalian cells namely the p38, c-Jun N-terminal kinase (JNK) and ERK5 cascades (Plotnikov *et al.*, 2011).

1.2.1 The Ras-Raf-MEK-ERK pathway

The Ras-Raf-MEK-ERK pathway can be activated by a number of different stimuli including cytokines, growth factors, neurotransmitters, hormones and cellular stresses via a number of different types of cell surface receptors including the receptor tyrosine kinases (RTKs) (as described in 1.1), cytokine receptors and G-protein coupled receptors (GPCRs). The MAPKs activated by this pathway are Extracellular Regulated Kinases (ERKs) and they were so named because of the diverse range of extracellular stimuli which can cause their activation. At each level of the MAPK cascade there are a number of isoforms of each protein, for example, there are three Raf isoforms (A-Raf, B-Raf and C-Raf also known as Raf1) and two MEK isoforms (MEK1/2), all of which have been shown to be regulated in slightly different ways in different cells types. MEK1/2 require dual phosphorylation by the upstream Raf kinase for activation. There are also a number of ERK isoforms, ERK1 and ERK2 are the main isoforms of this particular MAPK cascade and they are 44 and 42kDa respectively and share around 85% homology (Roskoski, 2012). They are usually referred to collectively as ERK1/2. ERK1/2 require dual phosphorylation of the threonine and tyrosine residues of the conserved T-x-Y motif in the activation loop of the kinase for activation. Interestingly replacement of these two residues with phosphomimetic residues does not cause functional activation of ERK1/2 highlighting that activation requires more than just phosphorylation of these two residues. This could be the reason why there have been no oncogenic mutations found in ERK1/2 as point mutations do not appear to be enough to cause aberrant activation (Widmann *et al.*, 1999).

1.2.2 Activation of Raf

Activation of Raf requires a number of different post translational steps. Ras-GTP has been shown to recruit Raf proteins to the plasma membrane (Seger & Krebs, 1995)

where they become phosphorylated and adopt an active conformation. All three Raf isoforms contain the conserved Ras binding domain (RBD) in the N-terminal regulatory region (Roy *et al.*, 1997; Wang *et al.*, 2005)(Wan *et al.*, 2004) which is sufficient for translocation of C-Raf to the plasma membrane (Marais *et al.*, 1995). All three Raf isoforms appear to be slightly differently regulated in terms of activation; A-Raf and C-Raf require more residues to be phosphorylated compared to B-Raf which has a higher basal kinase activity (Roskoski, 2010; Mercer & Pritchard, 2003). 14-3-3 proteins bind to CRAF in unstimulated cells and sequester it in the cytoplasm, this localisation changes upon growth factor stimulation and Ras displaces the 14-3-3 protein (Freed *et al.*, 1994). Along with phosphorylation, C-Raf also required dephosphorylation by PP2A for activation (Kubicek *et al.*, 2002). There are a number of identified activating kinases for RAF proteins including SRC-family kinases as well as other Ser/Thr kinases including p21 activated kinase 3 (PAK3) (Roskoski, 2010; King *et al.*, 1998). Dimerisation of Raf proteins is also essential for activation either as homo- or heterodimers (Rajakulendran *et al.*, 2009; Weber *et al.*, 2001).

Raf phosphorylates MEK1 on S218 and S222 (Zheng & Guan, 1994) and ERK1/2 are the only identified MEK1/2 substrates (Robbins *et al.*, 1993). MEKs are dual specificity kinases in that they can phosphorylate both threonine and tyrosine residues of ERK1/2 of the T-x-Y motif. Once ERKs are activated they phosphorylate a diverse number of substrates in a number of subcellular compartments.

1.2.3 Downstream of ERK1/2

ERK1/2 are proline directed Ser/Thr kinases that phosphorylate target proteins which contain the MAPK target consensus sequence Pro-Leu-Ser/Thr-Pro (Widmann *et al.*, 1999). There are over 160 identified direct substrates for ERK1/2 which include nuclear and cytosolic kinases, transcription factors, phosphatases, cytoskeletal proteins

and adhesion/migration proteins (Ramos, 2008). Upon phosphorylation ERKs translocate to the nucleus and this translocation is not dependent on MAPK activity (Seger & Krebs, 1995). Over half of the identified ERK targets are in the nucleus (Plotnikov *et al.*, 2011) and nuclear targets of ERK include proteins that control the transcription and repression of genes as well as chromatin remodelling factors. One of the first identified ERK substrates was the transcription factor Elk1 which is responsible for the activation of a number of early response genes (Plotnikov *et al.*, 2011) including *c-fos* which forms part of the AP-1 complex responsible for the positive regulation of cell cycle genes. Other ERK targets include MAPK-activated protein kinases (MAPKAPKs) for example, RSKs (90kDa Ribosomal protein S6 kinases), MNKs (MAPK interacting kinases) and MSKs (Mitogen and stress activated protein kinases) as well as the previously mentioned nuclear and cytosolic kinases, transcription factors, phosphatases, cytoskeletal proteins and adhesion/migration proteins (Ramos, 2008).

There is evidence that MEK can also translocate to the nucleus upon activation as MEK is usually exclusively cytoplasmic but manipulation of an identified leucine rich nuclear export signal (NES) causes MEK to be both nuclear and cytoplasmic (Jaaro *et al.*, 1997; Tolwinski *et al.*, 1999). It is also shown that MEK may play a role in the nuclear export of ERK1/2 via its NES through CRM1-dependent export (Adachi *et al.*, 2000).

Research using model organisms such as *Saccharomyces cerevisiae* and *Drosophila melanogaster* has made huge contributions to our current understanding of the molecular biology of MAPK pathways. The first scaffold protein was discovered in *S.cerevisiae* which is Ste5. This scaffold provides spatiotemporal regulation to the mating factor signalling pathway by coordinating and segregating specific signalling proteins in order to promote a specific cellular response. They provide a mechanism by which the same proteins can be used to transduce intracellular signals from different

extracellular stimuli. A number of scaffold proteins for MAPK cascades have been discovered in humans, these include the Kinase Suppressor of Ras (KSR), MP-1 and RKIP for the Ras-ERK pathway (Nguyen *et al.*, 2002; Schaeffer *et al.*, 1998; Yeung *et al.*, 1999) and JIP-1 and MEKK1 have been proposed as scaffold for the JNK MAPK pathway (Nguyen *et al.*, 2002).

1.2.4 Regulation

Tight regulation of the Ras-Raf-MEK-ERK pathway is critical for normal cell homeostasis. This is highlighted by the fact that ERK is found to be abnormally activated in around half of all human cancers even when direct components of the pathway are not mutated implementing the importance of regulation of the pathway (Plotnikov *et al.*, 2011). There are a number of identified negative regulators of the pathway that function at various levels. Examples include; RAF kinase inhibitor protein (RKIP1) which is a tumour suppressor and loss of RKIP has been found in breast cancer, colorectal cancer and melanoma (Murphy *et al.*, 2010), the MAPK phosphatases (MKPs) - many of which are themselves early response genes and whose activity can be activated by ERK phosphorylation - and SPROUTY and SPRED (reviewed by (Murphy *et al.*, 2010)). Negative feedback loops are also built into the pathway to terminate the signal. For example, the Epidermal Growth Factor Receptor (EGFR), SOS, Raf1 and MEK1 have all been shown to be ERK targets which are negatively regulated by ERK phosphorylation (Widmann *et al.*, 1999).

MAPK pathways are conserved in eukaryotes and the previous use of model organisms to elucidate their molecular natures has been invaluable. There is a vast amount of research focused on trying to understand the coordination of Ras-MAPK signalling and how this pathway can be best targeted for therapeutic intervention. The oncogenic potential of Ras was firstly discovered over 30-years ago (Downward, 2006) yet,

despite huge efforts, attempts to target hyperactivated Ras remain disappointing. In this work, we use the fission yeast, *Schizosaccharomyces pombe*, as a model organism and the process of fission yeast mating as a Ras-MAPK model system to investigate the basic principles of Ras protein function and signalling coordination/regulation.

1.3 Fission Yeast Meiosis: a Ras-MAPK model system

1.3.1 Fission yeast as a model organism

Schizosaccharomyces pombe, also known as fission yeast, is a rod shaped unicellular eukaryotic yeast which is used as a model organism for studying biological concepts as it shares many homologous genes with higher eukaryotes. Fission yeast is the most commonly used and well characterised yeast after the budding yeast, *Saccharomyces cerevisiae*, for biological research and its genome was fully sequenced in 2002 (Wood *et al.*, 2002). It was the sixth eukaryotic organism to have its genome fully sequenced after *Saccharomyces cerevisiae*, *Caenorhabditis elegans*, *Drosophila melanogaster*, *Arabidopsis thaliana* and *Homo sapiens* and it is thought to have diverged from *Saccharomyces cerevisiae* between 330-420 million years ago (Wood *et al.*, 2002). Fission yeast contains around 4,800 protein coding genes on three chromosomes and usually exists in a haploid state. Information on characterised genes can be found in the *Schizosaccharomyces pombe* gene database, PomBase (<http://www.pombase.org/>).

Fission yeast was first isolated in 1893 by Paul Linder from East African millet beer whilst trying to identify what gave the beer an acidic flavour. However it was not used as a model organism until the 1950's when it was first used for genetic research by Urs Leupold and by Murdoch Mitchison for cell cycle research (http://en.wikipedia.org/wiki/S_pombe). Fission yeast cells can be one of two mating types, h^+ (plus) or h^- (minus) depending on the genetic information at the mating type

locus, *mat1*. Homothallic strains (also known as h^{90} strains) contain approximately equal numbers of both h^+ and h^- cells and these cells switch mating type approximately every third to fourth cell division (Gutz & Doe, 1973; Meade & Gutz, 1976; Egel, 1973). Homothallic strains are called h^{90} strains because the original h^{90} strain used by Leupold had a sporulation efficiency of around 90%. Heterothallic strains which consist exclusively of either h^+ or h^- cells are also used in research. These cells cannot exhibit mating type switching due to deletion of the alternative mating-type cassette at the mating-type locus or impaired recombination at the *mat1* locus.

1.3.2 Fission yeast cell cycle

S.pombe grow and divide mitotically in rich media by binary fission, their cell cycle contains the same four fundamental stages as the mammalian cell cycle; G1, S, G2 and M. The fission yeast cell cycle is predominated by a long G2 phase followed by a relatively short M-phase, G1 and S-phase (**Figure 1.4**). Control of the fission yeast cell cycle is well characterised and has contributed greatly to our understanding of the control of the mammalian cell cycle. One of the key regulators of the cell cycle - the cyclin-dependent kinases- were firstly discovered in yeasts by Paul Nurse and Lee Hartwell and along with the discovery of cyclins by Tim Hunt using sea urchin eggs, these findings were awarded the Nobel Prize in Physiology or Medicine in 2001.

The *S.pombe* mitotic cells cycle is sensitive to the nutritional environment especially the availability of nitrogen and glucose and cells specifically undergo meiotic differentiation when they are starved of nitrogen. This sexual differentiation is a survival mechanism which results in the formation of four haploid spores (**Figure 1.4**) and is described in detail below. *S.pombe* are also capable of another specialised form of invasive cell growth, known as hyphal growth, under certain nutritional conditions which is an adaptive form of growth by which cells attempt to find nutrients during

starvation. During this specialised type of differentiation, cells form elaborate hyphal branches which invade deep into solid media (Amoah-Buahin *et al.*, 2005).

1.3.3 Fission Yeast Meiosis

Meiosis is the conserved process by which eukaryotes produce haploid gametes. It is an essential process consisting of one round of DNA replication followed by two rounds of nuclear division. The extracellular stimuli for cells to enter meiotic differentiation differs greatly between species. For fission yeast, the stimulus is the depletion of nitrogen sources which causes cells of both mating type (h^+ and h^-) to arrest in G1 and secrete mating pheromones. The process of meiotic differentiation is illustrated in **Figure 1.4**. Upon sensing the pheromone, the cell elongates toward a cell of the opposite mating type and the cells fuse with each other to form a zygote. This fusion event is known as conjugation. This is followed by karyogamy - the fusion of the haploid nuclei. The zygote then starts meiotic prophase when premeiotic DNA replication occurs and the fused diploid nucleus moves back and forth between the cell ends. This nuclear movement is called horsetail nuclear movement because of the shape of the nucleus is elongated like a horsetail as it is dragged through the cytoplasm. This process promotes alignment of the two homologous chromosomes leading to efficient meiotic recombination (Ding *et al.*, 2004). After the movement ceases, the nucleus becomes rounded at the centre of the cell and proceeds with the first and second meiotic divisions to create four haploid spores contained within a zygotc ascus (Asakawa *et al.*, 2007). Spores can remain dormant for prolonged periods of time and will only germinate once transferred to rich media. Therefore, in *S.pombe*, meiosis is a form of survival mechanism which allows the organism to survive for long periods of time in starvation conditions.

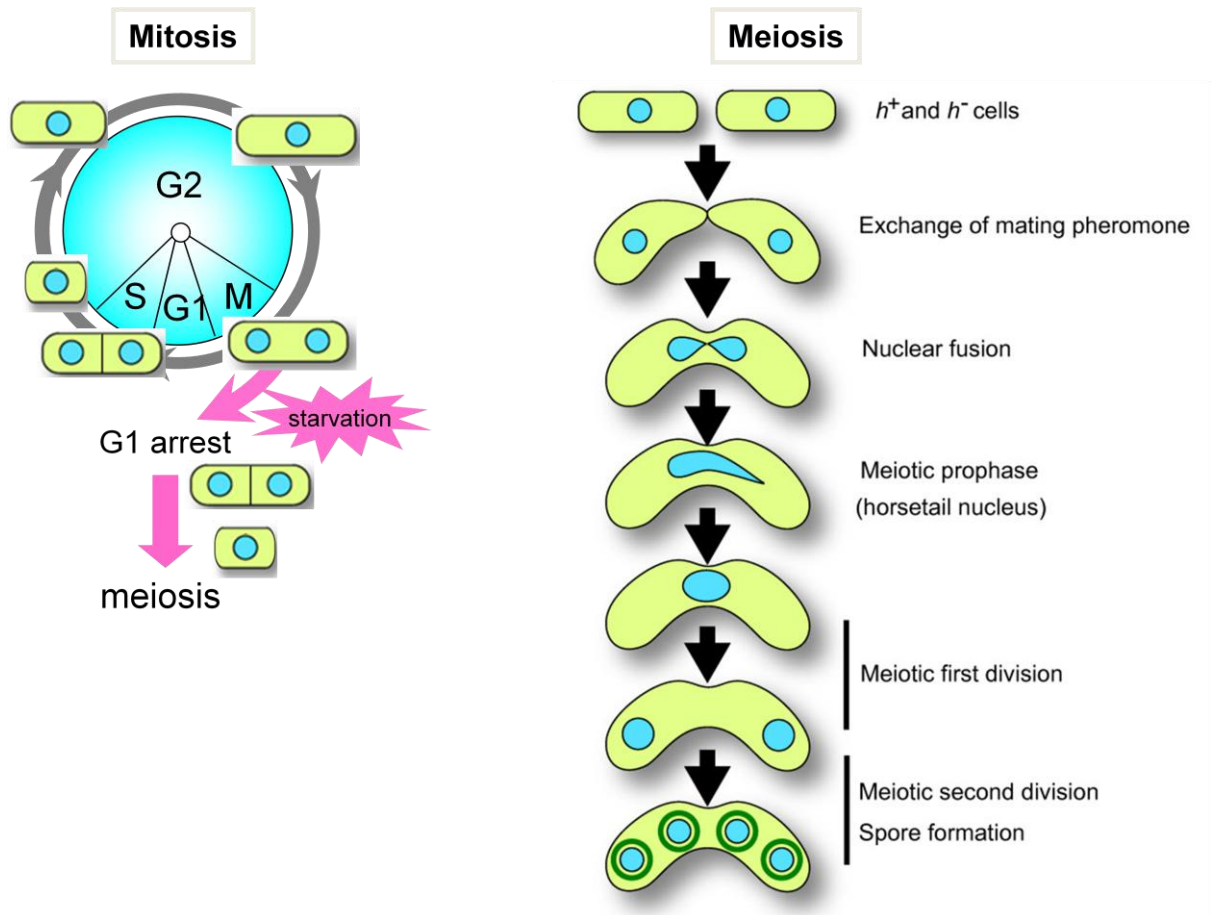


Figure 1.4 Fission yeast mitosis and meiosis

The *S.pombe* mitotic cell cycle is composed of the four fundamental stages seen in higher eukaryotes; G1, S, G2 and M. The cell cycle is dominated by a long G2 phase and a relatively short M, G1 and S phase. Upon nitrogen starvation, cells arrest in G1, this is where the meiotic cell cycle starts from. G1 arrested cells exchange mating pheromones, elongate towards a mating partner and conjugate. The nuclei then fuse (karyogamy), this is followed by pre-meiotic S-phase after which the cells undergo meiotic prophase and two meiotic divisions to create four haploid spores. (Meiosis diagram is adapted from (Asakawa *et al.*, 2007).

1.3.4 Signalling pathways involved in the initiation of meiosis

The switch from a mitotic cell cycle into sexual differentiation is largely controlled by a change in gene expression. The main transcription factor responsible for this change is Ste11 which is a high mobility group (HMG) protein that binds to specific 5'-upstream regions of genes, termed TR-boxes, to influence transcription. Many key meiosis genes contain TR-boxes in their upstream regions including *mat1* (Sugimoto *et al.*, 1991), *ste6* (Hughes *et al.*, 1994) and *ste11* itself (Kunitomo *et al.*, 2000). *ste11* expression is under the control of four signalling pathways illustrated in **Figure 1.5**. A recent review by (Otsubo & Yamamoto, 2012) on the induction of Ste11 summarises these pathways but a brief description is given below.

The cAMP-PKA pathway - The glucose sensing pathway

The first pathway is the cyclic adenosine monophosphate (cAMP) pathway which is sensitive to extracellular glucose levels. When glucose is present in the extracellular environment it binds to the G-protein coupled receptor (GPCR), Git3, which activates the G-protein, Gpa2 (Isshiki *et al.*, 1992; Welton & Hoffman, 2000; Hoffman, 2005), which activates the adenylate cyclase, Cyr1 which generates cAMP from ATP (Kawamukai *et al.*, 1991). cAMP is a well characterised second messenger in many higher eukaryotes. cAMP binds to the regulatory subunit of protein kinase A (PKA), Cgs1 (DeVoti *et al.*, 1991), which releases the catalytic subunit of PKA, Pka1 (Maeda *et al.*, 1994). Pka1 antagonises *ste11* transcription by inhibiting the transcription factor, Rst2 (Kunitomo *et al.*, 2000). During nutritional starvation, there is a decrease in the concentration of intracellular cAMP and therefore there is a decrease in the activity of Pka1 (Maeda *et al.*, 1990) and the repression of *ste11* transcription is lifted (Hoffman & Winston, 1991).

The TORC1 pathway

The second pathway is the TORC1 pathway. Target of Rapamycin (TOR) protein signalling is conserved from yeast to mammals and plays an important role in coordinating the cellular environment with cell growth. In *S.pombe* there are two TOR kinases, Tor1 and Tor2, and two TOR complexes, TORC1 and TORC2. Tor2 is part of the TORC1 complex and Tor1 part of the TORC1 complex (Otsubo & Yamamoto, 2008; Alvarez & Moreno, 2006). Specifically inhibiting Tor2 signalling results in the induction of genes involved in sexual differentiation, and the cells undergo mating and meiosis, even under good nutritional conditions (Alvarez & Moreno, 2006; Valbuena & Moreno, 2010). The complex is activated by the presence of nutrients in the extracellular environment, in this case is it nitrogen and activated TORC1 is repressing *ste11* transcription. This repression is lifted in the absence of nitrogen (Otsubo & Yamamoto, 2012).

The mating factor signalling pathway

The third pathway is the mating factor signalling pathway (MFSP) which involves the Ras1-MAPK cascade. Fission yeast respond to pheromones secreted from cells of the opposite mating type which bind to pheromone receptors on the cell surface and activate the MFSP (Yamamoto, 1996). The expression of mating pheromone and mating pheromone receptors is controlled by Ste11 and therefore pheromone signalling is initiated as a direct consequence of nutritional depletion. Signalling through the MFSP enhances the expression of *ste11* through a positive feedback loop which acts to strengthen the pheromone signal. The MFSP is the main focus of this work and is described in detail in 1.3.5.

The stress response pathway

The fourth pathway is the stress response pathway which is also activated upon nutrient starvation. This pathway involves the stress MAPK Sty1/Spc1 which is the fission yeast homologue of mammalian p38 (Otsubo & Yamamoto, 2012). This stress pathway can be activated by a number of stimuli including oxidative stress, heat shock and osmotic stress as well as nutritional stress. The pathway consists of the MAPKKs, Wis4/Wak1 and Win1, the MAPKK Wis1 and the MAPK Sty1/Spc1 which activates a transcription factor complex of Pcr1 and Atf1 that positively effects the expression of *ste11*. This pathway also plays an important role in G1 arrest in response to nutritional stress (Shiozaki & Russell, 1996; Kanoh *et al.*, 1996). Sty1 phosphorylates and consequently activates Lsk1 which is the catalytic subunit of the CTDK-I complex. This is a CDK-like kinase complex that phosphorylates the C-terminal repeat domain of the largest subunit of RNA polymerase II (Pol II CTD). Specific phosphorylation of Serine 2 of Pol II CTD by CTDK-I influences *ste11* expression (Sukegawa *et al.*, 2011), (Coudreuse *et al.*, 2010). It is important to note that Ste11 is only expressed via the stress response pathway in relation to nutritional starvation and not other stress stimuli but it is unclear how the pathway coordinates this meiosis specific response.

The decision for a cell to enter into meiotic differentiation is a critical one that will ensure survival therefore the process is tightly regulated. For example, Ste11 is not only regulated at transcriptional level, but is also regulated through post-translational modifications, namely, phosphorylation by Pat1 kinase on residues Threonine 173 and Serine 218 (Li & McLeod, 1996) (See 1.3.9.1 for the role of Pat1 in the mitotic-meiotic switch) which creates binding sites for the 14-3-3 protein, Rad24, this binding prevents nuclear localisation of Ste11 (Kitamura *et al.*, 2001; Qin *et al.*, 2003). Ste11 also promotes its own transcription in an auto-stimulatory fashion therefore it is essential to keep Ste11 activity inhibited during mitosis (Kunitomo *et al.*, 2000). Lastly, the

activation of Ste11 is restricted to the G1 phase of the cell cycle when Cdk activity is at its lowest, during the remainder of the cell cycle Ste11 is phosphorylated by Cdk on threonine 82 which prevents it binding to DNA thereby preventing Ste11-induced transcription (Kjaerulff *et al.*, 2005). All four pathways need to be activated for full Ste11 expression and activation that result in the entry into meiosis. There are a number of positive feedback loops built into the system, for example, Ste11 positively regulates its own transcription (Kunitomo *et al.*, 2000), to ensure that once the cell has made the decision to enter meiosis the process is fully initiated.

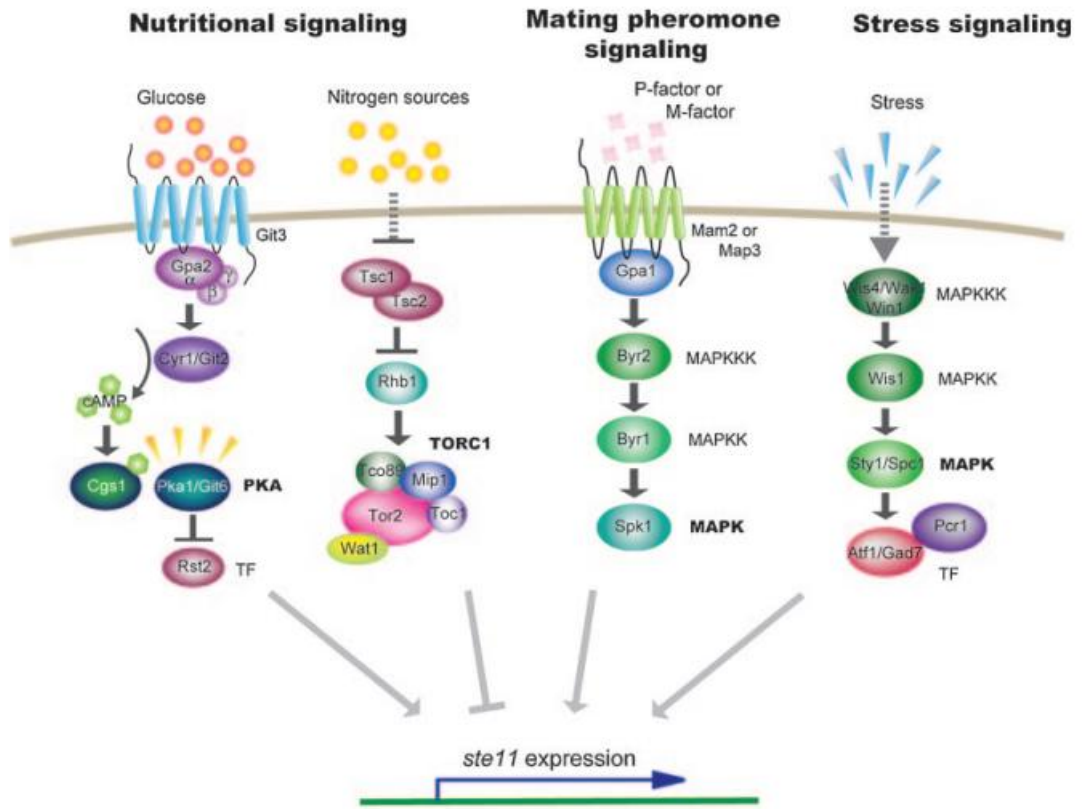


Figure 1.5 The initiation of meiosis (reproduced from Yamamoto, 2010).

Entry into a meiotic cell cycle programme is governed by the transcription factor *Ste11*. The expression of *Ste11* is controlled by four pathways, two of which respond to the availability of nutrients in the extracellular environment, along with the mating factor MAPK pathway and the *Sty1* MAPK stress response pathway.

1.3.5 Pheromone Signalling

Mating types:

The mating type of a cell is defined by the mating type cassette present at the *mat1* locus, this can either be *mat-P* for h^+ (plus) cells or *mat-M* for h^- (minus) cells. This mating type cassette is made up of two transcriptional units, *mat-Pc* and *mat-Pi* or *mat-Mc* and *mat-Mi* (Kelly *et al.*, 1988). Ste11 activates transcription of the *mat-Pc* and *mat-Mc* mating type genes which activates the transcription of the genes for the mating pheromones and the pheromone receptors (Sugimoto *et al.*, 1991; Willer *et al.*, 1995). The Mat-Pi and Mat-Mi proteins play an important role in the inactivation of Pat1 kinase via induction of the *mei3* gene, this is described in 1.3.9.

Mating pheromones and their receptors:

Figure 1.6 is a schematic diagram of proteins known to be involved in the MFSP and outlines the basic view of how this signalling pathway may be transduced.

The mating pheromones, M-factor and P-factor, are expressed and secreted into the extracellular environment upon nutritional starvation. P-factor is produced by cells of the h^+ mating type and binds to the P-factor receptor present on the membranes of cells of the h^- mating type. M-factor is produced by h^- cells and binds to the M-factor receptor on h^+ cells. P-factor is the protein produced from the *map2* gene and consists of 23 amino acids (Imai & Yamamoto, 1994). It is synthesised as a precursor which requires processing before secretion, the P-factor precursor is similar to that of α -factor in *S.cerevisiae*. M-factor contains 9 amino acids and is transcribed from three genes, *mfm1*, *mfm2* and *mfm3* (Davey, 1992). Even though these genes differ slightly in sequence, they all contain the same mature sequence as part of their precursor and all are expressed by WT cells in a redundant manner therefore they are likely to have

arisen by gene duplication. Unlike P-factor, M-factor is also post-translationally modified and is similar to the a-factor of *S.cerevisiae* (Davey, 1992).

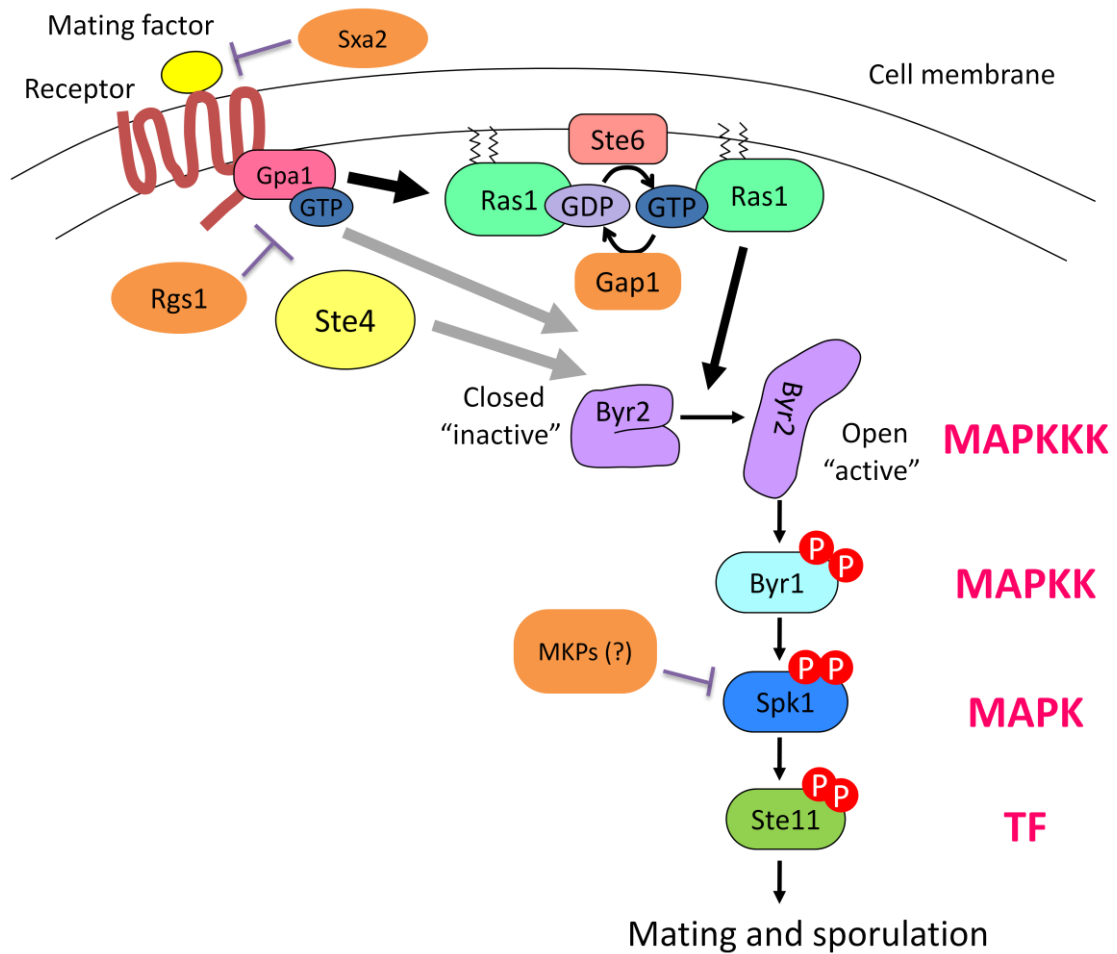


Figure 1.6. The Mating Factor Signalling Pathway

An outline of the structure of the pheromone response pathway in *S. pombe*. Activation of a GPCR leads to dissociation of the G-protein, Gpa1 which along with Ras1 activates the three-tiered MAPK cascade; Byr2-Byr1-Spk1. Spk1 directly phosphorylates the transcription factor Ste11. Full activation of Ste11 is required to activate the meiotic gene programme for successful meiosis. MKPs are MAPK Phosphatases.

The P-factor receptor is encoded by the *mam2* gene and is only expressed in M-cells in contrast to P-cells which only express the M-factor receptor encoded by the *map3* gene (Kitamura & Shimoda, 1991; Tanaka *et al.*, 1993). Both receptors are G-protein coupled receptors (GPCRs) and are homologous to the GPCR families found in higher eukaryotes which bind various molecules including hormones and neurotransmitters. Both receptors are coupled to the G-protein, Gpa1 which activated the mating factor signalling pathway involving a Ras-MAPK cascade which is homologous to the mammalian growth factor signalling pathway. The P-factor receptor has strong homology with the α -factor receptor and the M-factor receptor with the a-factor receptor in *S.cerevisiae* (Nielsen & Davey, 1995). The pheromones and their receptors are key components to signal the presence of a cell of the opposite mating type in close proximity and therefore if the cells are close enough they activate polarised growth (known as shmooing) towards a mating partner. This polarised growth is described further in 1.3.8.

The G-protein:

Activation of the mating factor receptor, via pheromone binding, activates the G-protein, Gpa1, which is a G α subunit of a predicted heterotrimeric G-protein (Obara *et al.*, 1991). The G $\beta\gamma$ subunits are yet to be identified but a potential candidate is Gnr1 which has been shown to interact with Gpa1 using yeast two hybrid (Goddard *et al.*, 2006). Sequence analysis showed some similarity to typical G β subunits in other organisms including mammals. Through deletion and overexpression studies, this work concluded that Gnr1 works as a negative regulator of the pheromone response as observed using an *sxa2-lacZ* reporter strain. However Gnr1 does not appear to be an essential component of the MFSP as deletion of *gnr1* has no effect on the mating efficiency (Goddard *et al.*, 2006). Activation of Gpa1 causes activation of the

downstream MAPK cascade (Obara *et al.*, 1991) via activation of the Ras protein homologue, Ras1 and also a partially Ras1-independent manner (Xu *et al.*, 1994).

1.3.6 Ras1

S. pombe contains one Ras gene homologue, *ras1*, which was first isolated back in 1985 by Fukui *et al* by cross hybridisation using *S.cerevisiae* *RAS1* and *RAS2* DNA as probes (Fukui & Kaziro, 1985). The Ras1 protein is not essential for mitotic growth but disruption of the *ras1* gene results in cells with rounded morphology instead of the usual rod shape and the cells are defective in conjugation and sporulation (Xu *et al.*, 1994; Fukui *et al.*, 1986; Nadin-Davis *et al.*, 1986b; Nadin-Davis *et al.*, 1986a). Unlike *S.cerevisiae* Ras1 and Ras2, *S.pombe* Ras1 is not involved in the regulation of adenylate cyclase and the control of intracellular cAMP levels (Fukui *et al.*, 1986). The human Ras gene can partially complement *S.pombe* Ras1 because overexpression of the human Ras on a plasmid was able to restore mating in a *S.pombe ras1Δ* mutant to around 10% but not to the same extent as the expression of *S.pombe* Ras1 from the same plasmid which rescued mating to around 90% (Nadin-Davis *et al.*, 1986a). This shows there is a degree of homology between the human and *S.pombe* Ras proteins and that the *S.pombe* proteins involved in Ras1 protein regulation (e.g. GEFs and GAPs) are partially effective against the human homologue.

An extensive amount of research is aimed at understanding how Ras proteins are functioning within cells because Ras is found mutated in a large proportion of all human cancers (Downward, 2003) and a number of "RASopathies" (1.1.5). A number of key point mutations in *Ras* have been found to have cell transforming potential (Parada *et al.*, 1982; Reddy *et al.*, 1982; Tabin *et al.*, 1982; Taparowsky *et al.*, 1982; Capon *et al.*, 1983) and the mechanism by which these mutants become transforming is via their inability to hydrolyse GTP in the presence of RasGAPs thereby leaving them

in a permanently activated state (McGrath *et al.*, 1984; Sweet *et al.*, 1984; Scolnick *et al.*, 1979). Investigations into the effect of one of these point mutations, Gly12Val, when introduced into *S.pombe* as Gly17Val, which is the homologous mutation, saw that this activated Ras1 had no obvious effect on the shape of mitotically growing cells but upon nutrient starvation the cells exhibited elongated conjugation tubes and were unable to conjugate (Nadin-Davis *et al.*, 1986a). This phenotype is illustrated in **Figure 1.7**.

The observations that deletion of *ras1* not only causes sterility but also a morphological defect during mitosis, which is not seen with deletion of other genes involved in the MFSP (e.g. *byr2*, *byr1*, *spk1*, *gpa1*) showed that Ras1 is involved in signalling to both a pathway involved in controlling cell morphology (Chang *et al.*, 1994) - details are in 1.3.8 - and Ras1 is a key component of the MFSP working via the MAPKKK, Byr2 (Wang *et al.*, 1991).

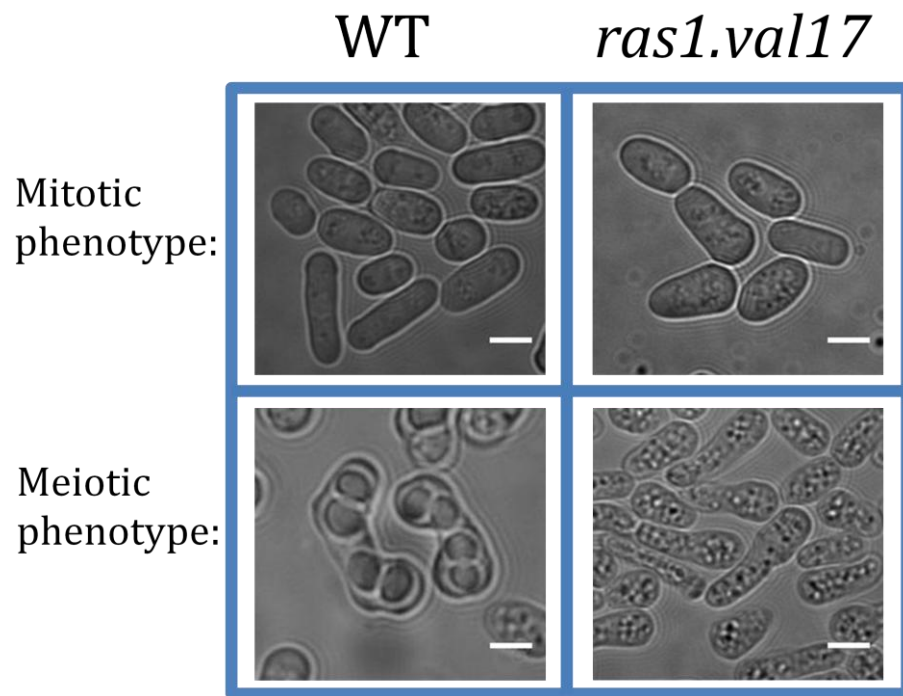


Figure 1.7 Mitotic and meiotic oncogenic Ras1 phenotypes in *S.pombe*

One of the most common cancer causing mutations found in mammalian Ras is the G12V substitution which is known to compromise the intrinsic GTPase activity of Ras and is therefore constitutively active once it is GTP bound as it can no longer hydrolyse GTP back to GDP. When the glycine 17 valine mutation is introduced into *S.pombe* (which is homologous to the mammalian G12V mutation) there is no obvious mitotic phenotype the cells look like wildtype cells. Upon meiotic induction instead of the cells undergoing meiosis and forming zygotes, the cells make elongated conjugation tubes and as a result cells fail to find a mating partner therefore fail to conjugate and proceed through meiosis. This was firstly observed back in the mid 1980s (Fukui et al 1986, Nadin-Davis et al 1986). Scale bar is 5 μm .

1.3.6.1 Ras1 GEFs

The activity of Ras1, like all Ras proteins, is regulated by a binary switch mechanism (**Figure 1.2**) and is controlled by the activities of GEFs and GAPs. There are two known guanine nucleotide exchange factors for Ras1 in *S.pombe*, these are Ste6 and Efc25 (Hughes *et al.*, 1994; Tratner *et al.*, 1997). Ste6 was the first *S.pombe* RasGEF discovered is thought to control the activity of Ras1 exclusively during meiosis as *ste6Δ* results in sterility and *ste6* is a Ste11 target gene therefore its expression is dependent on nutrient depletion and is enhanced upon pheromone signalling (Hughes *et al.*, 1994). *ste6Δ* cells have the normal rod like morphology during mitosis, therefore Ras1 activity is controlled differently during mitosis. This observation lead to the search for another Ras1GEF, resulting in the identification of Efc25 (Tratner *et al.*, 1997).

Characterisation of Efc25 showed that this protein is expressed constitutively during the *S.pombe* cell cycle and deletion of Efc25 results in the same rounded morphology as *ras1Δ* but the cells are capable of conjugation and sporulation (Tratner *et al.*, 1997), therefore Efc25 is thought to control Ras1 activity exclusively during mitosis. Ste6 overexpression cannot rescue to the rounded phenotype of *efc25Δ* cells and *efc25* overexpression cannot rescue the conjugation and sporulation defects of *ste6Δ* cells therefore their functions in activating Ras1 are thought to be completely independent of each other (Papadaki *et al.*, 2002).

1.3.6.2 Ras1 GAP

S.pombe contains one unique Ras1 GAP called Gap1 (also known as Sar1) (Imai *et al.*, 1991; Wang *et al.*, 1991). Gap1 is homologous to the mammalian RasGAP and NF1 and the *S.cerevisiae* proteins Ira1 and Ira2 (Imai *et al.*, 1991; Hughes, 1995). GAPs function by binding to Ras proteins and enhancing their intrinsic GTPase activity thereby promoting the hydrolysis of GTP to GDP and the inactivation of Ras. Gap1 has

been identified as a Ste11 target gene (Mata & Bahler, 2006). Deletion of *gap1* results in sterility therefore highlighting an important role for the regulation of Ras1 during mating. It is possible that Gap1 is the only RasGAP present in *S.pombe* as extensive genetic screens have failed to identify any protein that can complement *gap1Δ* (Wang *et al.*, 1991). Interestingly, *gap1Δ* cells have no mitotic growth defects which brings into question how Ras1 is regulated during mitosis and highlights that the regulation of Ras1 is presently poorly understood.

1.3.6.3 *Ras1 effectors*

Byr2 is a known effector of Ras1 (Wang *et al.*, 1991) and Ras1 has been shown to directly interact with Byr2 (the MAPKKK - see below) via yeast two hybrid (Masuda *et al.*, 1995). Overexpression of *byr2* or *byr1* on multicopy plasmids in *ras1Δ* diploids can partially suppress the meiotic defect which lead to the hypothesis that Ras1-Byr2 and Byr1 are in a linear pathway activated by pheromones (Wang *et al.*, 1991). The observations that *byr2Δ* does not cause the same rounded phenotype in mitotic cells as *ras1Δ* predicted that Ras1 was also involved in the control of cell morphogenesis and a screen for mutants showing the same rounded mitotic phenotype as *ras1Δ* isolated four "ras-like" genes, *ral1-4* (Fukui & Yamamoto, 1988). Investigations into the functions of these identified genes lead to the conclusion that Ras1 forms a complex with two of these *ral* genes - *ral1* and *ral3* - which were renamed *scd1* and *scd2* respectively along with the rho-GTPase, Cdc42 which is involved in a number of processes including cell polarisation and actin organisation (Chang *et al.*, 1994). Functions and regulations of Cdc42 are detailed in 1.3.8.

How is Ras1 regulated to control two independent pathways?

The two pathways which Ras1 is involved in - the Byr2-MAPK pathway and the Scd1-Cdc42 morphology pathway were shown to be independent of each other and not interchangeable as *byr2Δ* cannot be rescued via *scd1* overexpression (Chang *et al.*, 1994; Chen *et al.*, 1999; Li *et al.*, 2000) and *scd1Δ* cannot be rescued by *byr2* overexpression (Papadaki *et al.*, 2002). Work carried out by Eric Chang's lab has proposed ideas about the compartmentalisation of Ras1 signalling and that Ras1 achieves its different roles by localisation to different cellular compartments. They propose that Ras1 localised to the endomembrane primarily activates the Ras1-Cdc42 morphology pathway and Ras1 localised to the plasma membrane activated the Ras1-Byr2 mating factor pathway (Onken *et al.*, 2006; Chang & Philips, 2006) although their result was not reproducible and the hypothesis is still open to debate (Michael Bond and Graham Ladds, University of Warwick, personal communication). The expression of Ste6 is also likely to play a crucial role in Ras1 signalling during meiosis as *ste6* is a Ste11 target gene. The fact that expression of the activated allele of Ras1, *ras1.val17*, shows no obvious cell cycle or morphological defects during the vegetative growth actually tells us that there is likely to be a large amount of Ras1-GTP in mitotic cells (as it plays an essential role in the maintenance of the cell's elongated morphology) and this does not appear to be detrimental to cells, therefore down-regulation of Ras1 via GAPs may be of less importance during mitosis but essential for meiosis. For example, downregulation downstream of Ras1 perhaps at the level of Cdc42 via Cdc42-GAP may be efficient during the mitotic cell cycle to cancel the effect of Ras1 activation towards the morphology pathway.

1.3.7 Activation of the MAPK cascade

The pheromone MAPK cascade consists of the MAPKKK, Byr2, the MAPKK, Byr1 and the MAPK, Spk1 (Wang *et al.*, 1991; Gotoh *et al.*, 1993; Xu *et al.*, 1992; Nadin-

Davis & Nasim, 1988; Neiman *et al.*, 1993) (**Figure 1.6**). Along with Ras1, another protein linked to the activation of the MAPK cascade is Ste4 (Barr *et al.*, 1996).

1.3.7.1 *Ste4*

Ste4 was isolated and characterised as a Ste11 target gene due to the presence of the TR box in the 5'-upstream region and the observation that the mRNA for *ste4* was present only upon nitrogen starvation. There are two mRNA bands present upon nitrogen starvation thought to correspond to a spliced and unspliced species (Okazaki *et al.*, 1991). Deletion of *ste4* caused cells to be defective in mating and meiosis. It was noted that the amino acid sequence of Ste4 contained a "leucine zipper motif" which is found in the Jun family of transcription factors although Ste4 does not contain a characteristic DNA binding domain (Barr *et al.*, 1996). Ste4 shows some homology with the *S.cerevisiae* protein Ste50 which is known to interact and positively regulate Ste11 (the MAPKKK of the *S.cerevisiae* mating response pathway) (Barr *et al.*, 1996; Truckses *et al.*, 2006; Wu *et al.*, 2006). It has been shown that the SAM (sterile alphas motif) of Ste4 and the MAPKKK Byr2 interact and this interaction is essential for meiosis as disruptions to either of the SAMs causes the cells to become sterile (Barr *et al.*, 1996; Tu *et al.*, 1997; Ramachander *et al.*, 2002). Ste4 is thought to act as a trimer (Ramachander *et al.*, 2002) and it not only interacts with itself, but also interacts with Byr2 as confirmed using yeast two hybrid system which also showed that Ste4 failed to interact with Ras1, Gpa1, Byr1 or Spk1 in their system (Barr *et al.*, 1996) therefore making it difficult to place Ste4 in the schematic representation of the pathway in relation to other MFSP components in **Figure 1.6**. A proposed function for Ste4 is the dimerisation/oligomerisation of Byr2 which may be required for Byr2 activation (Tu *et al.*, 1997). A proposed model for Byr2 activation is illustrated in **Figure 1.9**.

1.3.7.2 Activation of Byr2

Activation of the most upstream kinase, Raf, of the mammalian Ras - mediated MAPK cascade consists of a number of regulatory steps involving the correct localisation, dimerisation and phosphorylation (Roskoski, 2010) as described in 1.2.2. The activation of Byr2 in *S.pombe* is not yet fully defined but a number of key findings highlight potential mechanisms of activation. Activation of Byr2 is proposed to be dependent on both Gpa1 and Ras1 which act partially independently as shown by Xu *et al.*, 1994, where Ras1 and Gpa1 can induce *mam2* expression in the absence of each other when expressed from multicopy plasmids. There is also an additive decrease in *mam2* expression in the absence of both Ras1 and Gpa1. The regulatory domain of Byr2 has Ste4 and Ras1 binding sites as well as a catalytic domain binding site which only partially overlap (Tu *et al.*, 1997) (**Figure 1.8**). Using the yeast two-hybrid system, it was shown that Ste4-Byr2-Ras1 form an interaction complex with Byr2 bridging the interaction between Ste4 and Ras1 which do not interact in the absence of Byr2 (Barr *et al.*, 1996). Ste4 is therefore predicted to link the G α protein, Gpa1 and Byr2 but a direct interaction between Gpa1 and Ste4 has yet to be proven. As mentioned previously, the Ste4 homologue in *S.cerevisiae* is Ste50. The Ste50 homologue in the yeast *Kluyveromyces lactis* has been shown to bind the G α subunit and MAPKKK during its mating pheromone response (Sanchez-Paredes *et al.*, 2011) strengthening the idea that Ste4 may act as a scaffold to link Gpa1 activation and Byr2 activation.

Protein kinases are subject to a number of regulatory mechanisms. The idea that some kinases contain an auto-inhibition domain has been around for a long time. When inactive, a kinase is in a locked conformation where the auto inhibition domain is blocking the active site and this needs to be displaced in order for kinase activation (Soderling, 1990). Byr2 has been shown to contain a regulatory domain and a catalytic

domain (**Figure 1.8**) and Ras1 and Ste4 specifically bind the regulatory domain. Tu *et al.*, 1997 performed a number of key experiments to investigate the molecular mechanism of Byr2 activation. Interestingly, they found that the activated form of Shk1 (a Cdc42-associated kinase, also known as Pak1, see 1.3.8.1) was capable of promoting the "open" conformation of Byr2 while Ras1 and Ste4, either individually or cooperatively, were unable to promote this conformation (Tu *et al.*, 1997). Membrane localisation of Byr2 to the site of pheromone stimulation is observed and is known to be dependent on Ras1-GTP but a role for Ste4 in membrane localisation has not been ruled out (Bauman *et al.*, 1998). Ste4 is essential for meiosis and is capable of interacting with itself and Byr2 therefore Ste4 may play a role in dimerisation of Byr2 (Barr *et al.*, 1996) and the proposed model from Tu *et al.*, 1997 is in **Figure 1.9**. Although they accept that the model is very preliminary and speculative, they propose that; Ras1-GTP recruits Byr2 to the membrane where Shk1 acts to release the autoinhibition - possibly through phosphorylation. Ste4 directly binds to Byr2 which may promote dimerisation allowing Byr2 to autophosphorylate itself for full activation.

There is very little evidence to support the proposed mechanism in which Shk1/Pak1 contributes to Byr2 activation and the idea is largely based on comparisons to homologous pathways such as the pheromone pathway in *S.cerevisiae*. Indeed work by Chang *et al* 1994, showed that *scd1* (encoding the Cdc42-GEF) and *scd2* (encoding a scaffold for Scd1 and Cdc42), both of which are required for Cdc42 activation and therefore Shk1/Pak1 activation, are not required for MAPK activation as judged by *mam2* expression level. Therefore, if Shk1/Pak1 is involved in the Byr2 activation, Cdc42 activation of Shk1/Pak1 needs to be occurring independently of Scd1 and Scd2 perhaps via the only other known Cdc42 GEF, Gef1, and perhaps this activation is enough to influence Byr2 activation. The functions of the two Cdc42 GEFs, Scd1 and

Gef1, are not interchangeable as Gef1 activity is not required for mating shmoo formation, where Scd1 plays an essential role (Chang *et al.*, 1994). Further details of regulation and function of the Cdc42 pathway are given in 1.3.8

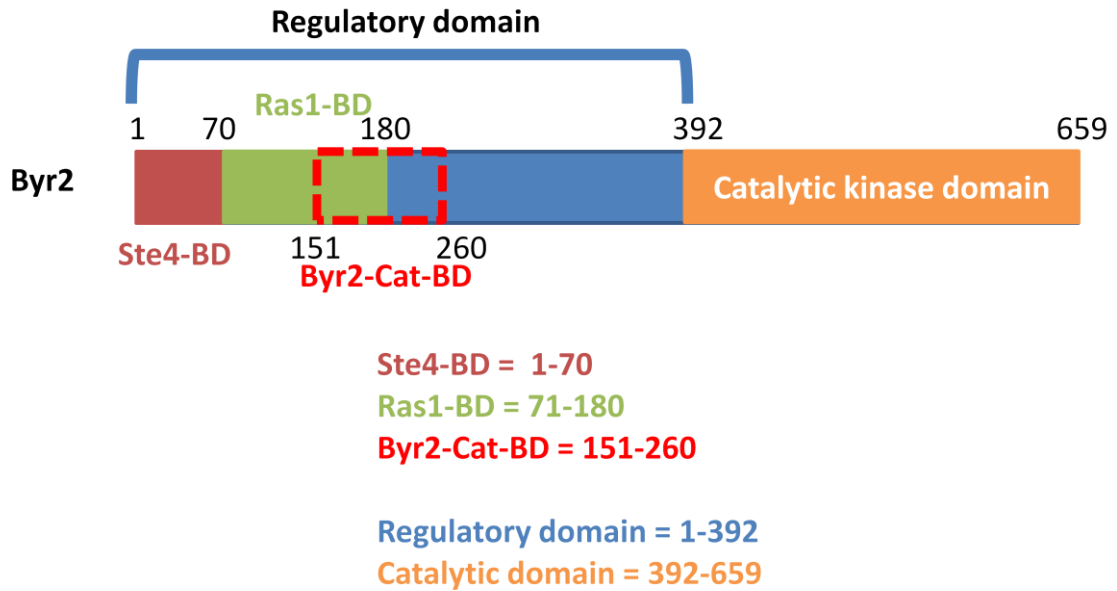


Figure 1.8 Byr2 protein domains

Diagrammatic representation of Byr2 protein domains as described by (Tu *et al.*, 1997). The Ste4 and Ras1 binding domains (BD) are separate but there is a partial overlap between the binding domains of Ras1 and Byr2-catalytic domain which binds to the regulatory region when Byr2 is in an inactive conformation.

The localisation of Byr2 to the plasma membrane upon pheromone stimulation is very important for concerted signalling. It has been shown that the 14-3-3 homologues, Rad24 and Rad25, both bind to Byr2 at the N- and C-terminus and negatively regulate its activity, which was assessed by a decrease in *mam2* expression and sporulation efficiency when Rad24/25 were overexpressed (Ozoe *et al.*, 2002). Byr2 localises to the plasma membrane in a Ras1-GTP dependent manner (Bauman *et al.*, 1998) and this localisation was seen to be faster in cells where either *rad24* or *rad25* had been deleted (Ozoe *et al.*, 2002). The sporulation defect of *ras1Δ* diploids was rescued somewhat by the deletion of either *rad24* or *rad25*, therefore, in their absence, Byr2 can be activated enough in the absence of *ras1* to cause sporulation further confirming a negative role for Rad24/25 in relation to Byr2 function.

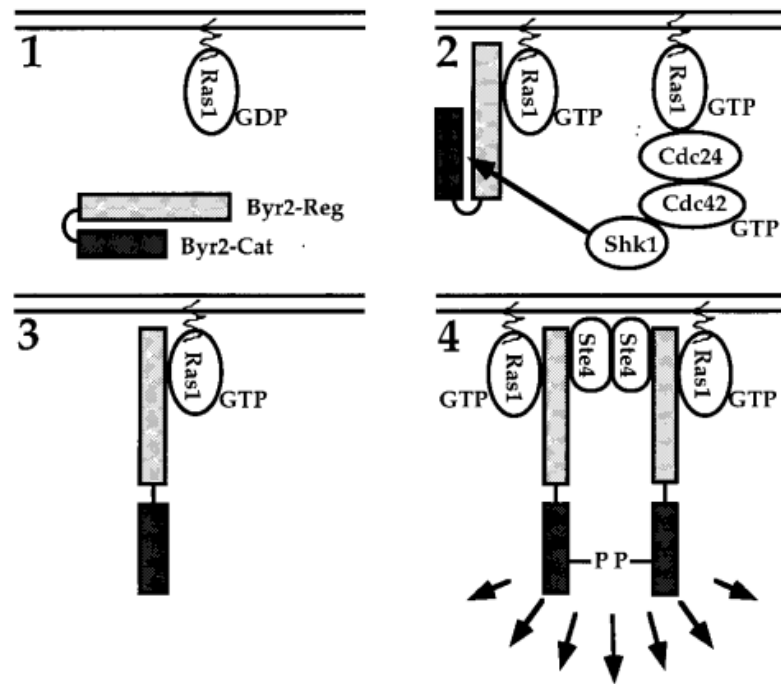


Figure 1.9 Hypothesis: Activation of Byr2 (Reproduced from Tu *et al.*, 1997)

In mitotic cells Ras1 is in its inactive form (Ras1-GDP) and Byr2 is in its closed inactive conformation (1). Activated Ras1 (Ras1-GTP) promotes Byr2 membrane localisation where it is in close proximity to Shk1 (2) which is activated through the Ras1-Cdc42 pathway. Shk1 somehow promotes the open conformation of Byr2 (3). Ste4 acts to dimerise Byr2 allowing autophosphorylation of the catalytic domains (4) leading to full activation of Byr2.

1.3.7.3 *Byr1 and Spk1*

Byr1 and Spk1 are activated by dual phosphorylation via the upstream kinase. Once activated, Spk1 MAPK, activates the major meiosis transcription factor, Ste11 (Kjaerulff *et al.*, 2005), which activates a number of genes responsible for progression through meiosis. The downstream events of Ste11 are described in 1.3.9.

The Byr1 protein has been found to be expressed constitutively in *S.pombe* and its mRNA levels do not appear to change during the mitotic cell cycle (Nadin-Davis & Nasim, 1990) but it is dispensable for the vegetative growth (Nadin-Davis & Nasim, 1988).

A constitutively active Byr1 protein has been previously described in the literature (Ozoe *et al.*, 2002). This mutant is a phospho-mimetic (*byr1.DD*). The molecular concept for this mutant comes from the findings that MEKs require dual phosphorylation by the upstream MEK Kinase for activation (Zheng & Guan, 1994), Byr1 is phosphorylated on Serine 214 and Threonine 218 by Byr2 (Ozoe *et al.*, 2002), if these two residues are mutated to a negative amino acid, in this case aspartic acids, this mimics the negative charge of the covalently added phosphorylation modifications thereby mimicking the phosphorylated state and creating a protein which is constitutively activated and resistant to the action of phosphatases.

Expression of *byr1.DD* from a strong *nmt1* promoter causes cells to undergo haploid meiosis even in rich media (Yamamoto *et al.*, 2004) and without the need of formation of a diploid which is usually required to start the meiotic division process. This haploid meiosis is dependent on *spk1* and *mei2* but not *mei3* thereby predicting that hyperactivation of Spk1 MAPK (in this case via Byr1.DD) is enough to drive the meiotic cell cycle bypassing the need to conjugation with another haploid cell and the

function of Mei3 which forms an essential part of the Pat1/Mei2 switch which is described in 1.3.9.

When expressed from its chromosomal locus, *byr1.DD* (constitutively active MEK) gives a different phenotype to that described for *ras1.val17* (constitutively active Ras1); instead of cells making single elongated conjugation tubes, *byr1.DD* cells can pair but not fuse and are therefore deficient in conjugation. This is shown in **Figure 1.10** and this phenotype is further described in Chapter 3 and Chapter 7.

It is not clear how Gpa1 and Ras1 lead to activation of the MAPK cascade. In the mammalian ERK1/2 growth factor pathway, Ras-GTP is involved in the localisation of Raf (MAPKKK) to the membrane (Marais *et al.*, 1995) where it is then activated by p21 activated kinases (PAKs) (King *et al.*, 1998). Ras is also required for the dimerisation of Raf (Weber *et al.*, 2001; Poulikakos *et al.*, 2010). A similar mechanism may be operating in *S.pombe* but this is yet to be defined although it has been reported that Shk1, which is a kinase activated by Cdc42 (a rho-GTPase), can interact with Byr2 (Tu *et al.*, 1997) as mentioned in 1.3.7.2.

Activation of the MFSP causes a positive feedback effect by which the expression of a number of Ste11 target genes is firstly activated by nutrient starvation and is further activated by pheromone signalling. These genes include the genes for the mating factor signalling, *gpa1*, *ste6*, *ste4*, *spk1* and *ste11* (Mata & Bahler, 2006). This positive feedback reinforces the commitment to meiosis and aids in signalling to a potential mating partner via the increased expression of pheromone. There are also genes whose expression is exclusively dependent on pheromone signalling, these include *sxa2* (Imai & Yamamoto, 1994), *fus1* (Petersen *et al.*, 1995), *rgs1* (Pereira & Jones, 2001) and *mat-pi* (Nielsen *et al.*, 1992).

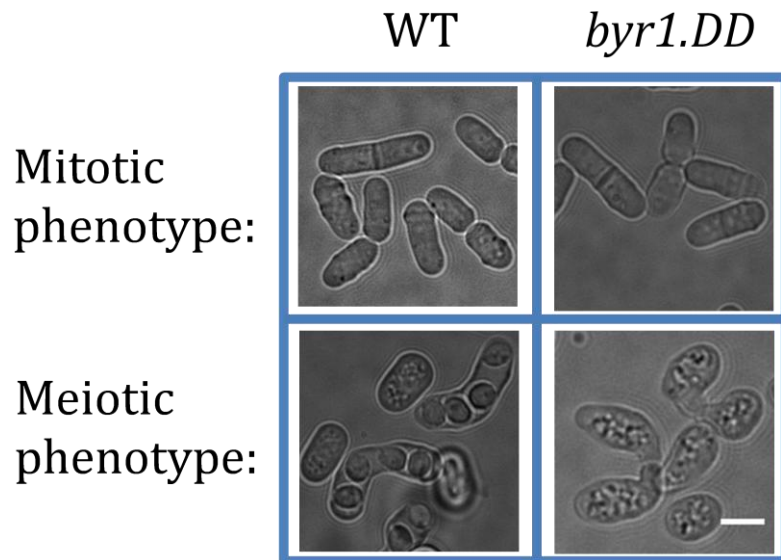


Figure 1.10 Mitotic and meiotic phenotypes of *byr1.DD* in *S.pombe*

A phospho-mimetic mutant of *byr1*, where the two serine residues usually phosphorylated by the upstream kinase *Byr2* have been replaced with aspartic acids, shows a WT mitotic phenotype. Upon the induction of meiosis *byr1.DD* show a prezygotic phenotype where cells appear to be paired but not fused. Scale bar is 5 μm .

1.3.7.4 Down-regulation of the MFSP

Receptor mediated intracellular signalling pathways are known to be desensitised to the effects of ligand binding because continuous stimulation of the receptor generally does not lead to continuous signalling output of that pathway. Desensitisation is an essential process which allows *S.pombe* to enter back into the mitotic cells cycle if mating was not successful (Imai & Yamamoto, 1994; Davey & Nielsen, 1994). There are a number of mechanisms used to terminate the pheromone signal in *S.pombe* which are outlined below and negative regulators are represented in **Figure 1.6** as orange proteins.

Mating factor proteases:

Degradation of the extracellular ligand is a common mechanism for signal termination, in *S.cerevisiae*, α -factor is degraded by the extracellular protease Sst1 and this is an important step for the cells to recover from pheromone stimulation (Chan & Otte, 1982). The *S.pombe* MFSP is subject to regulation by the P-factor protease, Sxa2 (Imai & Yamamoto, 1992; Ladds *et al.*, 1996; Ladds & Davey, 2000) which is a serine carboxypeptidase that works by removing a C-terminal leucine from P-factor. The expression of *sxa2* is solely dependent on pheromone signalling and Sxa2 protein is only secreted by M-type cells. There is another predicted pheromone protease which was isolated at the same time as Sxa2 which is Sxa1. Both M- and P- cells express *sxa1* mRNA during mitotic growth but expression is enhanced two to three fold upon nitrogen starvation (Imai & Yamamoto, 1992). Sxa1 is predicted to be an aspartyl protease based on sequence homology and is likely to degrade M-factor (Imai & Yamamoto, 1992). Both *sxa1* and *sxa2* are essential for meiotic differentiation as single gene deletions of either of them causes sterility (Imai & Yamamoto, 1992).

Rgs1:

There is a family of proteins which act as negative regulators of the G α subunits of heterotrimeric G-proteins, these are known as the "Regulator of G-protein Signalling" (RGS) proteins and there are over 30 identified RGS proteins already identified in mammals (De Vries *et al.*, 2000). *S.pombe* Rgs1 is an RGS protein which functions by activating the intrinsic GTPase activity of the G-protein Gpa1 (Pereira & Jones, 2001; Watson *et al.*, 1999). *rgs1* is a Ste11 target gene and its expression is dependent on pheromone signalling. Deletion of *rgs1* results in sterility and hypersensitivity to mating pheromone (Watson *et al.*, 1999). Rgs1 was identified as a negative regulator of the MFSP as an *rgs1* Δ shows signs of enhanced MAPK activation in the form of quicker G1 arrest and increased expression of *mat1-pm* (Watson *et al.*, 1999). The Rgs1 homologue in *S.cerevisiae* is Sst2 which acts on the G-protein, Gpa1 (Dohlman *et al.*, 1996) therefore Rgs1 is expected to have a similar function although a direct interaction between Rgs1 and Gpa1 has not yet been shown.

Gap1:

Gap1 is the GTPase activating protein for Ras1 and its function is described in 1.3.6.2. Gap1 is essential for meiosis as *gap1* Δ causes sterility (Imai *et al.*, 1991; Wang *et al.*, 1991).

MAPK phosphatases:

Recently there is reported evidence that the MAPK phosphatase, Pmp1, may play a role in the dephosphorylation of Spk1 MAPK (Didmon *et al.*, 2002). Pmp1 is a dual specificity phosphatase for Pmk1 MAPK (Sugiura *et al.*, 1998), which is a MAPK involved in ion homeostasis and cell wall integrity (Toda *et al.*, 1996). Pmp1 is homologous to *S.cerevisiae* Msg5 which is responsible for the dephosphorylation of the pheromone responsive MAPK Fus3 (Doi *et al.*, 1994). Didmon *et al* also showed that

the protein tyrosine phosphatase (PTP) Pyp1 which, along with Pyp2, has been previously shown to dephosphorylate the stress MAPK Sty1 (Shiozaki & Russell, 1995; Millar *et al.*, 1995), may also be involved in Spk1 dephosphorylation. The conclusions about Pmp1 and Pyp1 are based on a defined *LacZ* reporter gene assay using the *sxa2* promoter in which overexpression of both Pmp1 and Pyp1 independently of each other led to a decrease in the amount of β -galactosidase activity in the presence of P-factor and therefore a decrease in the output of the MFSP (Didmon *et al.*, 2002). In our lab, single gene deletions of *pmp1* and *pyp1* in h^{90} WT strains did not appear to affect mating but it is likely that phosphatases play redundant roles within the cell and therefore single deletions are unlikely to show a phenotype.

Receptor internalisation:

Receptor internalisation as an adaptive response has been well studied in *S.cerevisiae* where the pheromone receptor, Ste2, has been shown to be phosphorylated (Chen & Konopka, 1996), ubiquitinated and internalised (Rohrer *et al.*, 1993; Terrell *et al.*, 1998). Details of pheromone receptor internalisation in *S.pombe* are less well characterised but the paper by Hirota *et al* published in 2001 outlines that Map3 (M-factor receptor) is internalised and degraded during a meiotic time course and showed that the last 54-amino acids of the C-terminus are essential for internalisation. When overexpressing the *map3* mutant lacking the last 54-amino acids (*map3.dn9*), pheromone responsive transcription was activated but h^+ *map3.dn9* cells failed to produce any sort of conjugation tube when mixed with a h^- *ras1 Δ* cells which were used as cells that produce M-factor to stimulate h^+ cells but will not respond to P-factor themselves, which suggests that receptor internalisation and the activation of shmooing are closely related (Hirota *et al.*, 2001).

1.3.8 Cdc42 GTPase and the control of polarised growth

Cdc42 in mammalian cells

Cdc42 is a GTPase which belongs to the Rho subfamily of Ras-like GTPases which, like Ras, is activated when bound to GTP and inactive when bound to GDP, the exchange between GDP to GTP is influenced by GEFs and GTP hydrolysis is enhanced by GAPs (Bourne *et al.*, 1990). Cdc42 can be activated by a number of different extracellular stimuli acting through RTKs, GPCRs and cytokine receptors. Activation of Cdc42 effector pathways can effect proliferation, actin remodelling, vesicle trafficking and cell polarity. Cdc42 was originally discovered in *S.cerevisiae* and is highly conserved from yeast through to humans (Stengel & Zheng, 2011). Inappropriate Cdc42 activation has been shown to be oncogenic although activating mutations in the *cdc42* gene have not been found in human cancers but Cdc42 has been found to be overexpressed in non-small cell lung cancer, colorectal adenocarcinoma, melanoma, breast cancer and testicular cancer (Stengel & Zheng, 2011) and has been shown to be important for oncogenic Ras transformation acting through the PI3K-Akt pathway (Stengel & Zheng, 2012). There is potential cross-talk between the Ras-MAPK cascade and Cdc42 through the Cdc42 effector PAK which can phosphorylate Raf and MEK (King *et al.*, 1998; Beeser *et al.*, 2005; Li *et al.*, 2001). More recently, Ras has been shown to localise with Cdc42 on endomembranes which is evidence for potentially pathway cross-talk (Cheng *et al.*, 2011). One of the major roles for Cdc42 is the control of cell polarity (Johnson, 1999).

1.3.8.1 The Cdc42 pathway in S.pombe

S.pombe polarised growth

Polarised cell growth is an essential cellular process that allows cells to successfully grow and divide and also orientate growth in the direction of an extracellular stimulus.

In response to the presence of extracellular pheromone, *S.pombe* orientate polarised cell growth towards a cell of the opposite mating type. This polarised growth is called shmooing and when two shmoos meet the cell walls between the two cells are remodelled to allow plasma membrane fusion and successful conjugation resulting in a diploid cell.

The mechanisms of polarised growth during mating have been extensively studied in *S.cerevisiae* but a lot less is known about the process in *S.pombe*. There are a number of key similarities and differences between shmooing in *S.cerevisiae* and *S.pombe* which are outlined in a current review of polarised growth and cell fusion by Merlini *et al.*, 2013.

S.pombe Rho-GTPases:

The main regulators of cell polarisation are the Rho GTPases and their conserved p21 activated kinase (PAK) effectors. There are six Rho GTPases in *S.pombe*, Rho1-5 and Cdc42 (Perez & Rincon, 2010; Iwaki *et al.*, 2003) but only *rho1* and *cdc42* are essential genes (Nakano *et al.*, 2001; Miller & Johnson, 1994). Cdc42 is very highly conserved between eukaryotes from yeast to humans and *S.pombe* Cdc42 is 83% identical to human Cdc42 (Miller & Johnson, 1994).

S.pombe p21-activated kinases (PAKs):

There are two PAKs in *S.pombe*, *pak1* (also known as *shk1* or *orb2*) and *pak2* (also known as *shk2*) and both are known to be effectors of Cdc42 (Sells *et al.*, 1998; Otilie *et al.*, 1995; Yang *et al.*, 1998; Marcus *et al.*, 1995). Pak1/Shk1 is the Ste20 homologue in *S.cerevisiae* which is capable of signalling to the pheromone responsive MAPK cascade. In *S.pombe*, Pak1 is a regulator of actin cytoskeletal organisation and is an essential protein required for polarised growth, maintenance of cell shape, proper cell

cycle control, normal actin and microtubule cytoskeletal organisation, and sexual differentiation (Miller & Johnson, 1994; Otilie *et al.*, 1995; Marcus *et al.*, 1995; Qyang *et al.*, 2002). The Pak1 protein consists of an N-terminal regulatory domain and a C-terminal kinase domain and, like many kinases, including Byr2, adopts an auto-inhibited conformation which must be altered for activation (Tu & Wigler, 1999)(see 1.3.7.2) . The second known fission yeast PAK, *pak2*, is dispensable for normal growth, morphology, and mating but has been shown to interact with the Mkh1-Pek1-Spm1 pathway, which regulates cytokinesis and cell division in fission yeast (Yang *et al.*, 1998).

S.pombe cdc42 and *pak1* are essential for cell viability (Miller & Johnson, 1994; Marcus *et al.*, 1995) and the conserved Cdc42-Pak1 pathway plays important role in a number of cellular processes including polarised growth during mitosis and meiosis, endocytosis, mitotic spindle formation, chromosome segregation and cytokinesis (Li *et al.*, 2000; Miller & Johnson, 1994; Li & Chang, 2003; Murray & Johnson, 2001).

The Cdc42 morphology pathway in *S.pombe*

A schematic of the proteins known to be involved in the *S.pombe* Cdc42 morphology pathway is presented in **Figure 1.11**. Ras1 is thought to influence the activity of Cdc42 through the formation of a complex containing Scd1, Scd2, Cdc42 and Pak1. There is surprisingly little evidence physically linking Ras1 with this protein complex but it has been shown that Ras1 and Scd1 interact using yeast two hybrid in the presence of overexpressed Scd2 (Chang *et al.*, 1994). Of the two identified RasGEFs, Efc25 is predicted to control Ras1 activation for the morphology pathway (Chang *et al.*, 1994). The only identified RasGAP in *S.pombe* is Gap1 therefore we predict that Gap1 may be working to regulate Ras1 in its morphology pathway context as well as during

pheromone signalling. There are two GEFs for Cdc42, Scd1 which is the main GEF involved in cell shape and mating (Chang *et al.*, 1994) and Gef1 which is also involved in cell polarity and cytokinesis (Coll *et al.*, 2003; Hirota *et al.*, 2003). *scd1Δ* cells are rounded and show the same mitotic phenotype as *ras1Δ* (Fukui & Yamamoto, 1988) whereas *gef1Δ* showed no abnormal cell morphology (Iwaki *et al.*, 2003). Single deletions of these GEFs is not lethal but a *scd1Δ gef1Δ* mutant is not viable therefore these are likely to be the only GEFs for Cdc42 and their functions must somewhat overlap (Coll *et al.*, 2003; Hirota *et al.*, 2003). Unlike *scd1Δ*, *gef1Δ* cells can mate normally (Coll *et al.*, 2003) suggesting that Gef1 function is not required for the polarised growth associated with mating. The *S.cerevisiae* homologue of Scd1 is Cdc24 which is the only GEF for Cdc42 but unlike *scd1*, *cdc24* is an essential gene (Chang *et al.*, 1994). In *S.pombe*, Rga4 is a GAP for Cdc42 (Tatebe *et al.*, 2008) and more recently another protein, Rga6, was shown to be another Cdc42 GAP (Perez lab, Pombe 2013 - International Fission Yeast conference, London 2013).

Originally, Scd1 and Scd2, were isolated in a genetic screen for mutants showing a *ras1*- phenotype to identify proteins involved in the Ras1-morphology pathway (Fukui & Yamamoto, 1988). Scd2 is a scaffold protein which mediates morphology pathway activation by binding to Scd1, Cdc42-GTP and Pak1 (Chang *et al.*, 1994; Endo *et al.*, 2003; Wheatley & Rittinger, 2005; Chang *et al.*, 1999). The observation that Scd2 only binds to activated Cdc42 (Cdc42-GTP) suggests that Scd2 could be an effector of Cdc42 and, via Scd1, could provide a positive feedback platform for further Cdc42 activation (Endo *et al.*, 2003). Pak1 phosphorylates Scd2 *in vitro* (Chang *et al.*, 1999) but the function of this phosphorylation is yet to be explored. This phosphorylation could also act in a negative feedback loop to dissociate the complex thereby limiting Cdc42/Pak1 activation as predicted by (Das *et al.*, 2012). The *scd2* homologue in

S.cerevisiae is Bem1, both contain two SH3 domains which are important for protein-protein interactions with Cdc42 (Wheatley & Rittinger, 2005; Chang *et al.*, 1999).

It was shown by Chang *et al* in 1994 by yeast two hybrid system that Scd1 interacts with human H-Ras only when H-Ras carries an activated mutation G12V, indicating that Scd1 may preferably interact with GTP-bound Ras1. Immunofluorescence studies have shown that activated Cdc42 (visualised with CRIB-GFP) is localised to the growing poles of mitotic cells and the shmoo tips of meiotic cells. Fluorescently tagged Scd1-3GFP and Scd2-mCherry also show this localisation and colocalise with each other. Scd2-mCherry was shown to colocalise with CRIB-GFP therefore the complex containing Scd1-Scd2-Cdc42 is present at the sites of polarised growth in mitotic and meiotic cells (Bendezu & Martin, 2013). Scd1 and Scd2 are mutually dependent for localisation at the growing tips as shown by the loss of cell tip localisation of either protein by deletion of the other and Cdc42 localisation to cell tips is also strongly dependent on Scd1 and Scd2 but not Gef1 (Kelly & Nurse, 2011) showing a more minor role for Gef1 in Cdc42 activation at the cell tips. Live cell fluorescent imaging has shown that, during mitosis, activated Cdc42 is highly dynamic and oscillates between the two cell tips and this is thought to contribute to the control of cell diameter, the switch from monopolar to bipolar growth and the monitoring of cell size (Das *et al.*, 2012). Pak1 also localises to the cell tips in mitotic cells in a Scd1 and Scd2 dependent manner (Kelly & Nurse, 2011). Ras1 is also thought to be part of this morphology complex as Ras1 colocalises with Scd2 (personal communications with Sophie Martin's lab, not published) although this would be contradictory to the previous descriptions by (Chang & Philips, 2006) that Ras1 controls morphology exclusively from the endomembrane. It would be reasonable to predict that the site of activation of Ras1 on

the plasma membrane in response to pheromone would also be closely coordinated with the activation of shmooing via the Ras1-Cdc42 pathway.

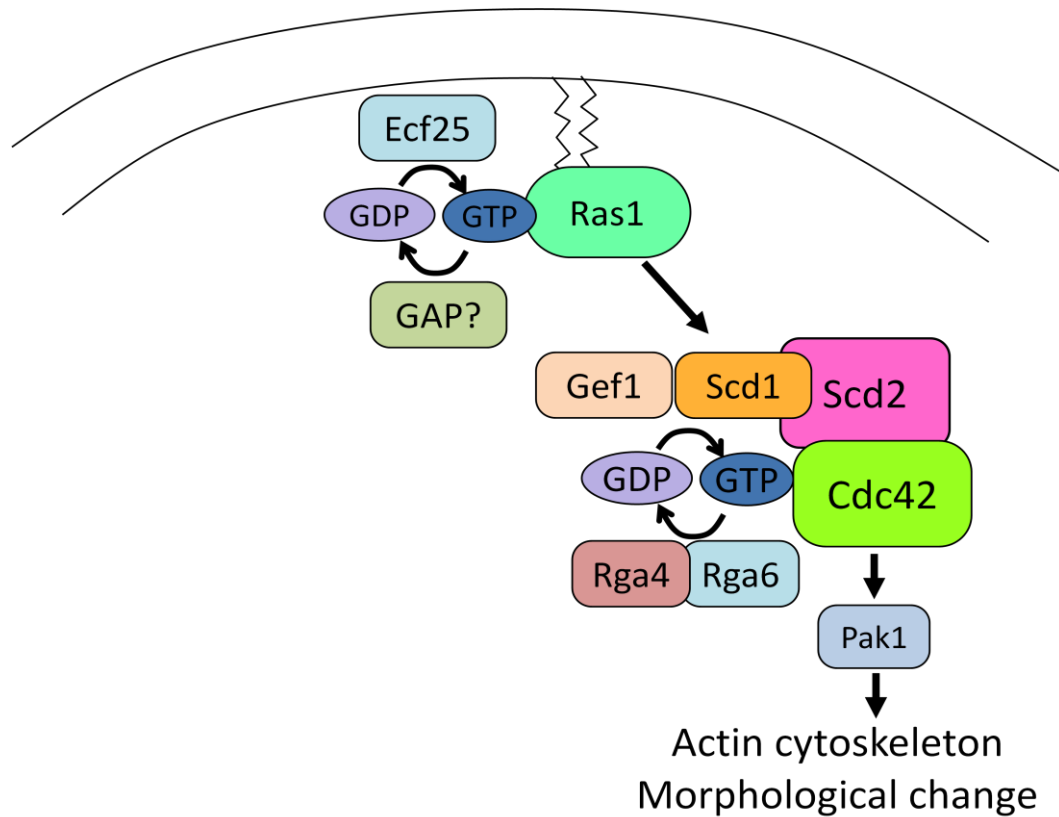


Figure 1.11 Ras1-Cdc42 cell morphology pathway in *S.pombe*

This signalling pathway is involved in actin-cytoskeleton rearrangements and plays a key role in the control of polarised growth in mitotic cells. The activity of Ras1 during mitosis is reported to be controlled by the Efc25 GEF. Ras1 influences the activity of Cdc42 through the activation of Scd1 although there is another GEF for Cdc42 which is Gef1. Scd2 acts as a scaffold. Activated Cdc42 activates the p21-activates kinase, Pak1/Shk1. Rga4 and Rga6 are the GTPase activating protein for Cdc42.

1.3.8.2 *Cdc42 and mitotic growth*

The processes of mitotic cell division between *S.cerevisiae* and *S.pombe* are very different; *S.cerevisiae* have a rounded morphology and divide by the budding of a daughter cell from a mother cell whereas *S.pombe* are rod shaped and divide by binary fission resulting in two identical cells. However, both forms of cell division require the small Rho-GTPase Cdc42 and require polarised growth stimulated and controlled by internal factors. The mitotic processes for both yeasts are summarised below and are illustrated in **Figure 1.12**.

In *S.cerevisiae*, Cdc42 is localised to the bud formation site along with the Cdc42 GEF, Cdc24 (Chang & Peter, 2003). Until it is required at the appropriate stage of the cell cycle, Cdc24 is sequestered in the nucleus by Far1 which is degraded upon G1-cyclin-Cdc28 phosphorylation thereby releasing Cdc24 from the nucleus (Shimada *et al.*, 2000; Nern & Arkowitz, 2000). Localisation of Cdc24 to the site of polarised growth is controlled by two proteins, Rsr1 and Bem1 (Park & Bi, 2007). Bem1 is a scaffold protein which can bind Cdc24, Cdc42 and the PAK, Cla4. Activation of Cdc42 at the bud site promotes polarised cell growth via activation of a number of effectors including the three PAKs, Ste20, Cla4 and Skm1 and the formin, Bni1 which nucleates actin cables (Perez & Rincon, 2010).

In *S.pombe*, cells firstly grow by monopolar extension of the "old end" during the G1-phase but switch to bipolar elongation during G2 in a process called "new end take off" or NETO (Hayles & Nurse, 2001; Martin & Chang, 2005). As well as the actin cytoskeleton, the microtubule cytoskeleton is important for polarised cell growth (Martin, 2009). A large number of proteins are required at the site of growth as seen in **Figure 1.12B**. The Tea1 protein is essential for determining the specific site of growth and is transported there via microtubules (Mata & Nurse, 1997). Mod5, Tea3 and Tea4

all have roles to tether Tea1 to the cell tip (Snaith & Sawin, 2003; Snaith *et al.*, 2005; Martin *et al.*, 2005) and Tea4 links Tea1 with the formin, For3, which is an important actin nucleator (Feierbach & Chang, 2001) which requires both Tea1 and Bud6 for correct localisation (Martin *et al.*, 2007; Glynn *et al.*, 2001). For3 activation by Cdc42 also requires Pob1 (Rincon *et al.*, 2009). Once activated, For3 nucleates actin cables for vesicle transport required for polarised growth and cell wall remodelling (Martin *et al.*, 2007). Cdc42 activation also requires the for-mentioned proteins, Ras1, Scd1 and Scd2 which form a complex at the cell tips along with Pak1 (Chang *et al.*, 1994; Endo *et al.*, 2003). Rga4 is a GTPase activating protein for Cdc42 and is localised exclusively to the sides of the cell and excluded from the growing ends, this localisation is dependent on Pom1 kinase therefore Pom1 plays a crucial role in dictating the areas of Cdc42 activation (Tatebe *et al.*, 2008; Das *et al.*, 2007). Recently, Rga6, another GTPase activating protein, is also proposed to play a role in regulation of Cdc42 (Perez lab, Pombe 2013 - International Fission Yeast conference, London 2013). Both the PAKs, Pak1 and Pak2, interact with Cdc42 (Ottillie *et al.*, 1995; Yang *et al.*, 1998; Marcus *et al.*, 1995) and Pak1 has been shown to phosphorylate Tea1 *in vitro* (Kim *et al.*, 2003). Pak2 interacts with the Mkh1-Pek1-Spm1 pathway, which regulates cytokinesis and cell division in fission yeast (Yang *et al.*, 1998).

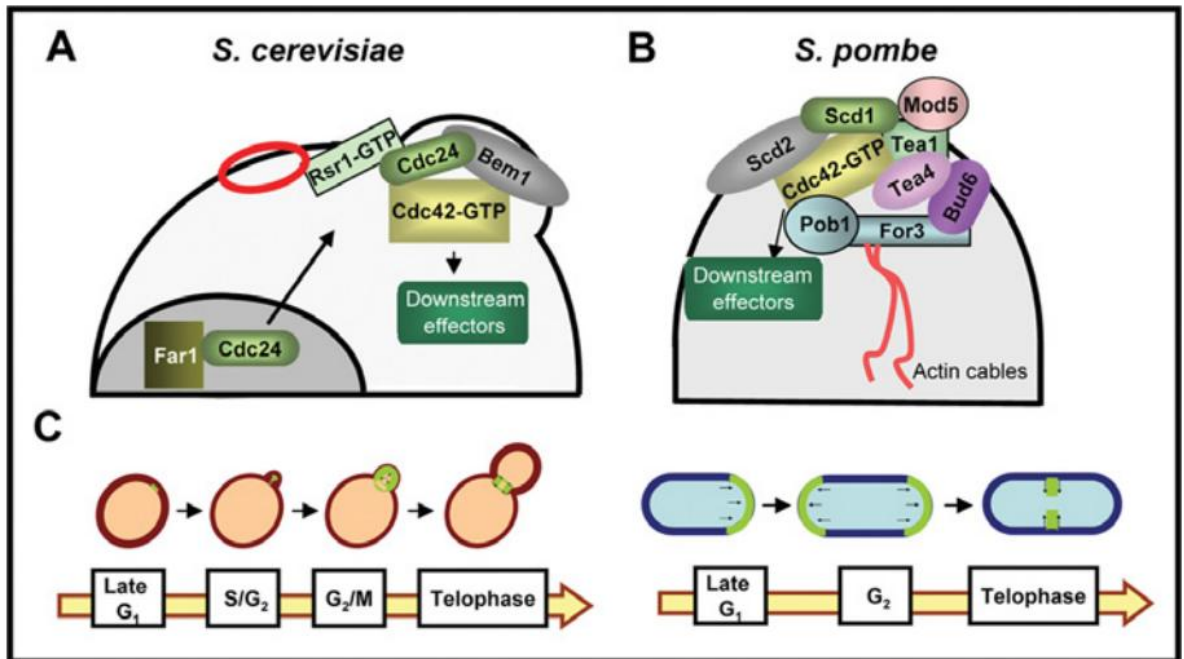


Figure 1.12 Mitotic polarised cell growth in *S.cerevisiae* and *S. pombe*. Reproduced from Perez & Rincon, 2010)

(A) In *S.cerevisiae*, Cdc24 localises to the area of bud growth once it is released from Far1 in the nucleus. Here, it cooperates with Rsr1 and Bem1 to activate Cdc42. (B) In *S.pombe*, a number of proteins are localised and maintained at the growing cell tip these include Tea1, Tea4, Mod5, Bud6 and the formin, For3. (C) Active Cdc42 distribution (in green) in both yeasts throughout their cell cycles.

1.3.8.3 Coordinated activation of the pheromone MAPK pathway and polarised growth in *S.cerevisiae*

Polarised growth during yeast meiotic differentiation is very different to mitosis in the sense that cells orientate growth towards an extracellular stimulus in a monopolar fashion in order to make contact with a cell of the opposite mating type. Upon contact, cells fuse to form a diploid zygote. *S.cerevisiae* spontaneously mate on rich media in the presence of cells of the opposite mating type (a- and α - cells) and grow mitotically as diploids which will only undergo sporulation when starved of nutrients. In contrast, *S.pombe* undergo mating and sporulation in quick succession only when deprived of nutrients and both processes are very closely linked.

The coordinated activation of the pheromone MAPK pathway and polarised growth has been well studied in *S.cerevisiae* and is presented in **Figure 1.13** as well as being described below:

In contrast to *S.pombe*, the G $\beta\gamma$ subunits of the GPCR related heterotrimeric G-protein, Ste4 and Ste18, play the major role in pheromone signal transduction (Elion, 2000). G $\beta\gamma$ binds to a number of key proteins including; the PAK, Ste20, the Ste5 scaffold, the Cdc42 GEF, Cdc24 and the scaffold protein, Far1 (Leeuw *et al.*, 1998; Whiteway *et al.*, 1995; Nern & Arkowitz, 1998; Butty *et al.*, 1998) and therefore plays an important role in localising components of the MAPK pathway and the morphology pathway in close proximity.

The Ste5 scaffold is of major importance as it is essential for Fus3 MAPK activation (Good *et al.*, 2009) and works by binding to the three kinases of the MAPK module (Ste11, Ste7 and Fus3) as well as Ste20 which is required for Ste11 activation (Elion, 2001). Ste5 also binds to Cdc24 to localise and keep in at the cell cortex where is can

activated Cdc42 (Wang *et al.*, 2005). Therefore Ste5 also functions to coordinate MAPK activation and Cdc42 activation.

Cdc42 is positively regulated by the GEF, Cdc24 and the scaffold protein, Bem1 (Perez & Rincon, 2010). Activated Cdc42 recruits and activates the p21-associated kinase (PAK), Ste20 at the plasma membrane and Ste20 has a positive effect on pheromone signal transduction possibly by the direct phosphorylation of the MAPKKK, Ste11 (Simon *et al.*, 1995; Moskow *et al.*, 2000). Disruptions to Cdc42 or Cdc24 affects MAPK signalling (Simon *et al.*, 1995; Zhao *et al.*, 1995) Bem1 also binds to the MAPK cascade scaffold Ste5 and Ste20 (Leeuw *et al.*, 1995) thereby coordinating MAPK activation and polarised growth to a localised area. Far1 is a scaffold which localises activated Cdc42 to the site of polarised growth via Cdc24. During mitosis, Far1 sequesters Cdc24 in the nucleus and is released upon Far1 phosphorylation and degradation (Shimada *et al.*, 2000; Nern & Arkowitz, 2000) but during meiosis the Far1-Cdc24 complex relocates to the cell cortex and recruits Cdc42 and Bem1 away from the bud site to activate a shmoo site (Valtz *et al.*, 1995; Wiget *et al.*, 2004). Pheromone activated MAPK, Fus3 is also localised to the shmoo via G α (Metodiev *et al.*, 2002) and is important for polarised growth as it phosphorylates an important formin protein required for actin assembly, Bni1 (Matheos *et al.*, 2004) and Fus3 phosphorylates G β to stabilise the Far1- G β complex and keep it at the cell cortex (Metodiev *et al.*, 2002).

Overall, extensive research has been carried out in *S.cerevisiae* to understand polarised growth and highlights that several mechanisms work to coordinate the site of pheromone stimulation and the shmooing response (**Figure 1.13**).

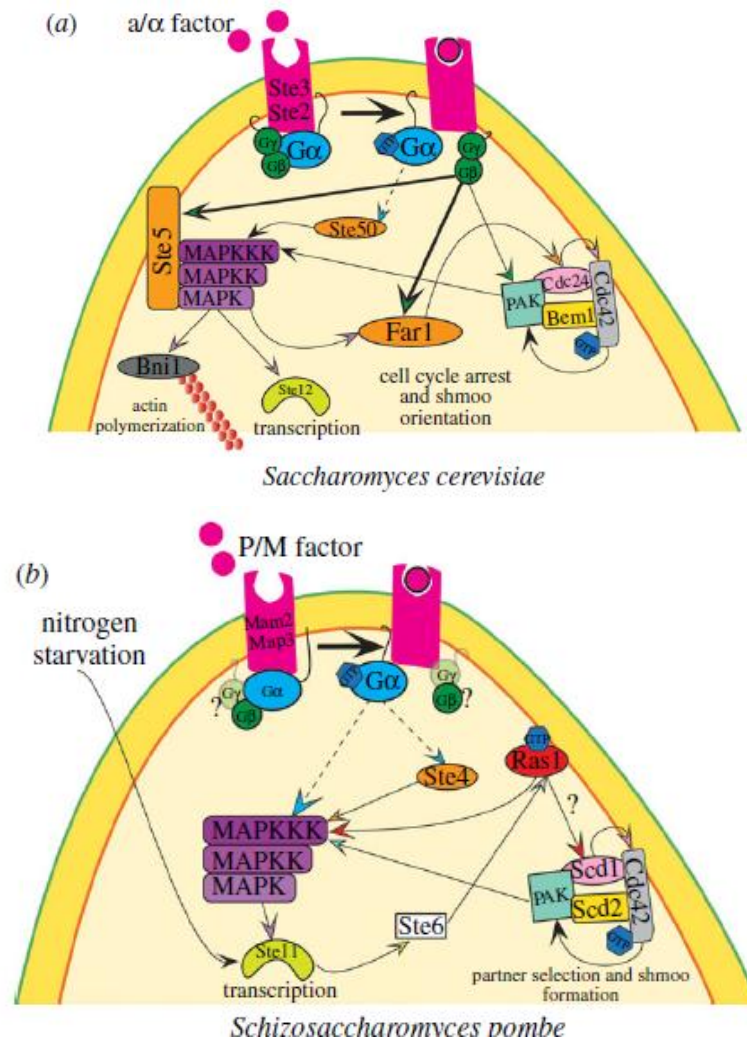


Figure 1.13 Polarised growth during meiosis in *S.cerevisiae* and *S.pombe*.
 Reproduced from (Merlini *et al.*, 2013)

(a) *S.cerevisiae*: Mating factor binds to the mating factor receptor on the cell surface which activates the heterotrimeric G-protein. G $\beta\gamma$ binds to a number of proteins including Ste20 and Ste5. Ste5 is a scaffold binding Ste11, Ste7 and Fus3 as well as Cdc24 and Bem1. (b) *S.pombe*: in a similar manner to *S.cerevisiae*, mating factor binds the mating factor receptor on the cell surface activating a G-protein. G α transduces the signal in an unknown manner, possibly via Ste4, resulting in activation of a MAPK cascade. Ras1 plays an important role in MAPK cascade activation and is linked to activation of the Cdc42 morphology pathway required for polarised growth during mating.

1.3.8.4 Coordination of the MFSP and Meiotic polarised growth in S.pombe

This process is a lot less defined in *S.pombe* and it is difficult to translate over what we know about the process in *S.cerevisiae* to *S.pombe* particularly because *S.pombe* lacks homologues to Ste5 and Far1 which are the essential scaffolds for coordinating the MAPK activation and the polarised growth pathway. Another key difference between the two yeasts is that the pheromone signal is transduced through the G α heterotrimeric G-protein subunit in *S.pombe* and through the G $\beta\gamma$ subunits in *S.cerevisiae*. Potential G $\beta\gamma$ subunits have not been identified in *S.pombe* but a prime candidate for the G β is Gnr1 (Goddard *et al.*, 2006) (See 1.3.5 "The G-protein"). The MFSP in *S.pombe* involves the Ras protein, Ras1. Although *S.cerevisiae* contains two Ras protein homologues, Ras1 and Ras2, they are essential genes involved in the activation of adenylate cyclase and therefore the regulation of cAMP during vegetative growth (Kataoka *et al.*, 1984; Toda *et al.*, 1985).

Figure 1.13b illustrates what is already known in terms coordinated signalling. As outlined in previous sections, Ras1 is an important component of both the Byr2-MAPK pathway and the Scd1-Cdc42 morphology pathway. Deletion of *scd1* or *scd2* results in sterility presumably because they are essential components required for shmooing but neither are required for MAPK output (Chang *et al.*, 1994). There is a potential role for Pak1 to be involved in the activation of Byr2 as work by Tu *et al* showed that Pak1 is capable of promoting the "open" conformation of Byr2 and the two proteins interact in yeast two hybrid (Tu *et al.*, 1997). Ste20, the Pak1 homologue in *S.cerevisiae* complements a strain where *pak1* has been compromised in *S.pombe* therefore it appears likely that their functions are highly related (Marcus *et al.*, 1995). Purified Pak1 has also been shown to induce activation of mammalian MAPK in cell-free extracts of *xenopus laevis* (Polverino *et al.*, 1995).

More recent studies into the factors required for shmooing showed that three key proteins involved in mitotic polarised growth (Tea1, Tea2 and Tip1) are not localised to the shmoo site (Niccoli & Nurse, 2002). Actin polymerisation is required for shmooing as the use of the drug Latrunculin A (LatA), which depolymerises actin, abolished shmoo formation (Niccoli & Nurse, 2002) and in the same paper, they show that depolymerisation of microtubules had no effect on shmooing.

The work of Bendezu and Martin published in 2013, illustrates that upon pheromone signalling, the Cdc42 complex, containing Scd1 and Scd2, dynamically "samples" the cell periphery for a short amount of time before selection of a site for shmoo growth. This "sampling" appears to be important for correct orientation of polarised growth as cells which exhibited altered MAPK activation (in this case *rgs1Δ* and *map3.dn9*) failed to show the "sampling" behaviour resulting in a default shmoo from one of the cell tips (Bendezu & Martin, 2013). This default behaviour to shmoo from a mitotic growth site is also seen in *S.cerevisiae* when there is lack of orientation information (Nern & Arkowitz, 1998; Butty *et al.*, 1998; Valtz *et al.*, 1995; Nern & Arkowitz, 1999).

1.3.8.5 Yeast cell fusion

As with meiotic polarised growth, a lot more is known about the conjugation process in *S.cerevisiae* compared to *S.pombe* and what is known so far highlights that the processes differ significantly between the two yeasts. For both yeast, cell wall remodelling is required in order for the plasma membranes to fuse and allow the formation of a diploid zygote. This process has to be tightly controlled to prevent cell lysis. A schematic of cell fusion is shown in **Figure 1.14**.

In *S.cerevisiae*, high levels of pheromone and activated Fus3 are required for cell fusion (Brizzio *et al.*, 1996; Fujimura, 1994). Localisation of fusion factors is dependent on actin polymerisation and both Fus1 and Fus2 (two factors implicated in cell wall remodelling) localisation is dependent on Cdc42 (Barale *et al.*, 2006; Paterson *et al.*, 2008). Proteins shown to play a role in plasma membrane fusion include, Prm1, Kex2 and Fig1 but their functions remain unclear (Heiman & Walter, 2000; Heiman *et al.*, 2007; Olmo & Grote, 2010; Aguilar *et al.*, 2007).

In *S.pombe*, the meiotic specific formin, Fus1, is essential for cell fusion and *fus1* Δ causes cells to form a characteristic "prezygotic" phenotype in which two cells pair but the cell wall remains intact (Petersen *et al.*, 1995; Petersen *et al.*, 1998b). The expression of *fus1* is dependent on pheromone signalling (Mata & Bahler, 2006). Actin is required at the shmoo tip for cell fusion and actin localisation to the tip is dependent on *fus1* (Petersen *et al.*, 1998b; Petersen *et al.*, 1998a). The tropomyosin, Cdc8, and myosin V, Myo51, also play a role in cell fusion and both proteins have been seen to localise to the fusion site (Kurahashi *et al.*, 2002; Doyle *et al.*, 2009). Localisation of the Dni1 protein to the fusion site is dependent on Fus1 and Dni1 is required for fusion (Angel Clemente-Ramos *et al.*, 2009). Relatively little known about plasma membrane fusion

in *S.pombe* but there is a potential role for the conserved Prm1 protein which also plays a role in *S.cerevisiae* (Merlini *et al.*, 2013).

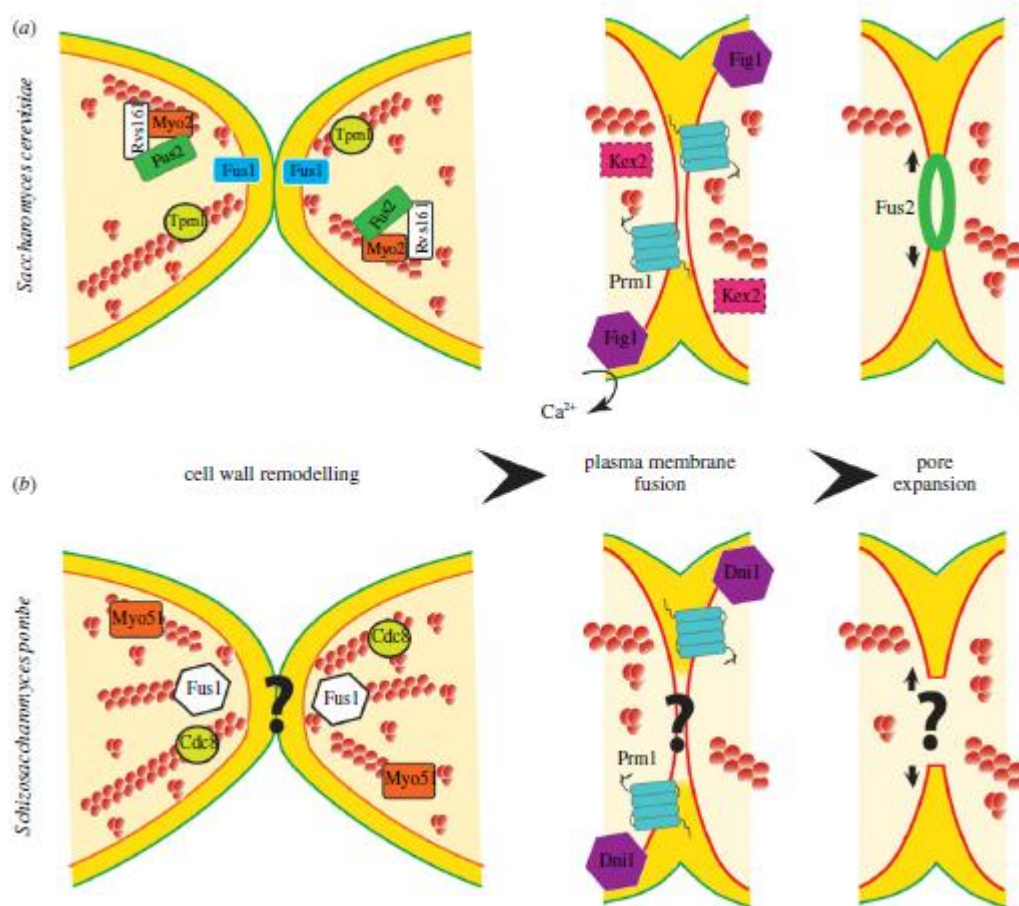


Figure 1.14 Cell fusion process in *S.cerevisiae* and *S.pombe* (Reproduced from Merlini *et al.*, 2013)

The three main steps of cell fusion are cell wall remodelling, plasma membrane fusion and pore expansion (a) In *S.cerevisiae*, Fus1 and Fus2 are implicated in cell wall remodelling. Fus1 is a transmembrane protein whose localization is dependent on active Cdc42. The conserved transmembrane protein Prm1 and transmembrane proteins Kex2 and Fig1 cooperate for plasma membrane fusion. (b) In *S.pombe*, Fus1 is a formin essential for fusion, with tropomyosin Cdc8 and myosin V Myo51 also implicated. The only protein so far implicated in plasma membrane fusion in this organism is Dni1 (Merlini *et al.*, 2013).

1.3.9 Genetic control of meiosis - The Pat1-Mei2 switch

One of the major outcomes of activation of the MFSP is the fusion of two haploid cells to make a diploid zygote which can consequently initiate a meiotic differentiation consisting of one round of DNA replication and two rounds of nuclear division. If transferred to rich media straight after conjugation, the diploid cells will also grow mitotically as diploids which can undergo sporulation upon nitrogen starvation. The control of the mitotic-meiotic cell cycle switch is well defined in *S.pombe* and involves the contrasting actions of the Pat1 and Mei2 proteins.

1.3.9.1 The role of Pat1

Meiosis is inhibited in mitotic cells through the actions of the Pat1 kinase (McLeod & Beach, 1988). Pat1 was first discovered in the mid-1980's and it was observed that a temperature sensitive *pat1* mutant (*pat1.114*) undergoes meiosis in rich media at the restrictive temperature without conjugation between two cells (Beach *et al.*, 1985; Iino & Yamamoto, 1985; Nurse, 1985). This is known as haploid meiosis as the cells do not form a diploid first therefore each spore only contains half the genetic material and is therefore not viable. Pat1 is therefore a key inhibitor of meiosis in mitotic cells and needs to be inactivated for the switch to meiosis. It was also observed that disruptions to *ste11* suppressed *pat1.114* at the restrictive temperature therefore the ectopic meiosis activated in *pat1.114* is working through Ste11.

How does Pat1 inhibit meiosis in mitotic cells?

Another key regulator of meiosis, Mei2, was identified by (Bresch *et al.*, 1968). Disruption to *mei2* is also a suppressor of *pat1.114* ectopic meiosis and is a Ste11 target gene (Sugimoto *et al.*, 1991). Mei2 is therefore an essential meiotic component downstream of Ste11. Mei2 is the major target of Pat1 kinase (Watanabe *et al.*, 1988;

Watanabe & Yamamoto, 1994) and is phosphorylated on two residues (Ser438 and Thr527) (Watanabe *et al.*, 1997). Mutation of these two residues to alanines causes ectopic meiosis therefore Pat1 phosphorylation of Mei2 is the key inhibitory mechanism for Mei2 inhibition during mitosis. This phosphorylation causes a change in the stability of Mei2 and therefore its susceptibility to proteosomal degradation (Kitamura *et al.*, 2001). Phosphorylated Mei2 also binds the 14-3-3 protein, Rad24, which sequesters Mei2 and prevents it binding to its targets (Sato *et al.*, 2002). In order for cells to enter meiosis, Pat1 must be switched off for Mei2 to function. This is accomplished through the expression of another protein, Mei3, which is expressed exclusively in heterozygous diploids after successful conjugation due to the cooperative function of the Mat1-Pi and Mat1-Mi proteins. Mei3 is an inhibitor of Pat1 (Li & McLeod, 1996; Li & McLeod, 1996; McLeod *et al.*, 1987; Van Heeckeren *et al.*, 1998) and it works by acting as a pseudo substrate for Pat1 thereby relieving its inhibition of Mei2 (Watanabe *et al.*, 1997). This is illustrated in **Figure 1.15**.

Inactivation of Pat1 kinase via the temperature sensitive *pat1.114* mutant is routinely used to induce synchronous meiosis (Bahler *et al.*, 1991) but there are a number of limitations to using this mutant as normal meiotic events are not reproduced, for example, 40% of diploid cells and 80% of haploid cells show precocious sister chromatid segregation at meiosis I (Yamamoto & Hiraoka, 2003). Also, although telomeres cluster correctly at the spindle pole body (SPB), centromeres remain partially associated with the spindle pole SPB which affects the timing and effectiveness of meiotic recombination (Chikashige *et al.*, 2004) therefore *pat1.114* driven meiosis does not truly represent WT meiotic events. Haploid meiosis can also be achieved by the overexpression of a constitutively active form of the MEK Byr1 as shown by (Yamamoto *et al.*, 2004) and this is dependent on Spk1 MAPK. In contrast to *pat1.114*

driven meiosis, there was correct dissociation of centromeres from the SPB and correct sister chromatid segregation in Meiosis I therefore there appears to be a Pat1-independent mechanism which requires Spk1 MAPK for correct chromosomal behaviour during meiosis which is absent when using *pat1.114*.

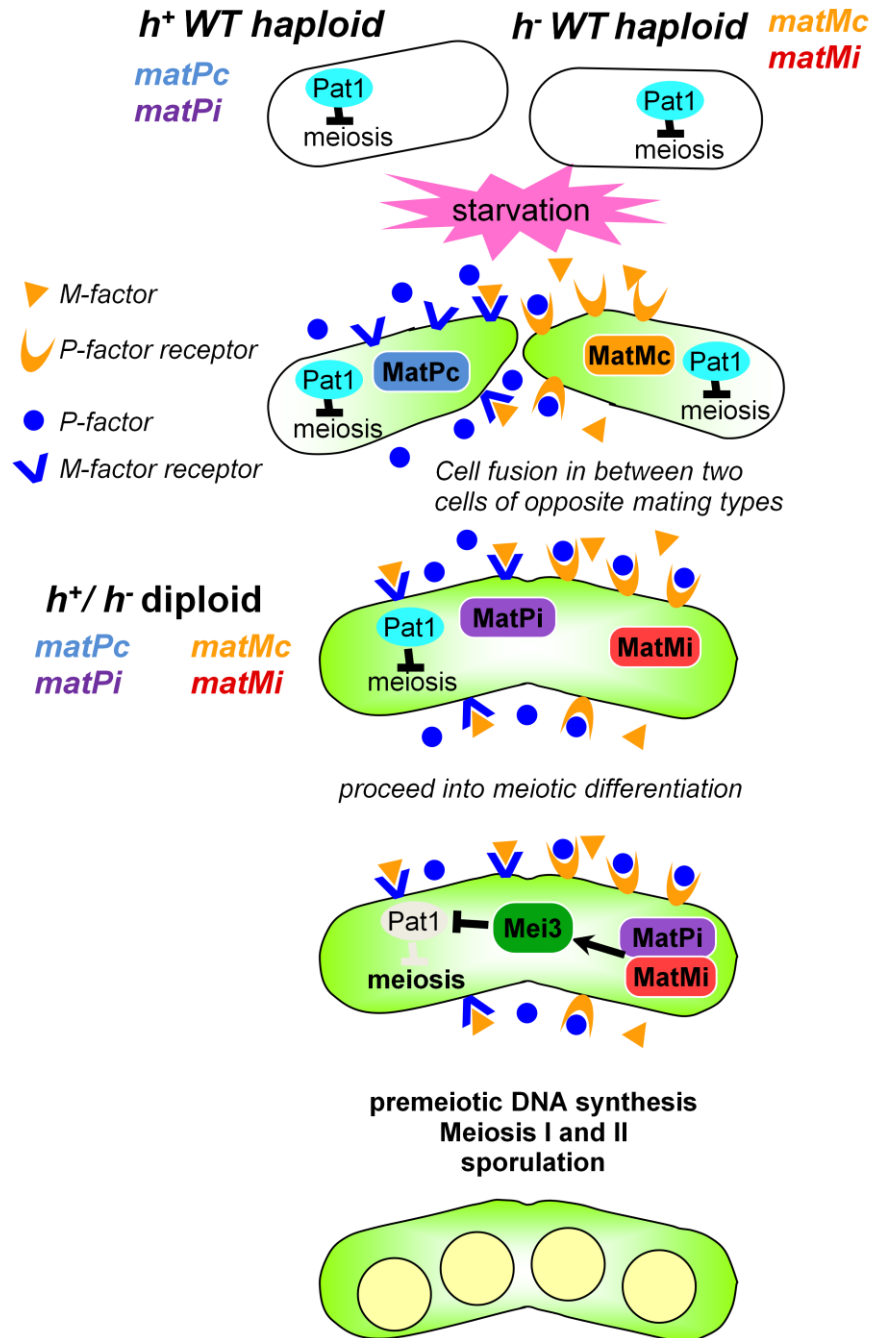


Figure 1.15 Genetic basis of meiosis in *Schizosaccharomyces pombe*

h^+ haploid cells contain the *mat-Pc* and *mat-Pi* genes at their *mat1* mating type locus while h^- cells contain *mat-Mc* and *mat-Mi*, however, these are not expressed until the cells sense nutrient starvation. Pat1 kinase inhibits meiosis in mitotic cells by phosphorylating Mei2. Upon successful conjugation, Mat-Pi and Mat-Mi cooperatively activate the expression of Mei3 which acts as a pseudo-substrate for Pat1 thereby relieving Pat1 inhibition of Mei2.

1.3.9.2 *How does Mei2 activate meiosis?*

Mei2 has been proven to be essential for three key stages of the meiotic cell cycle, firstly it promotes withdrawal from the mitotic cell cycle as the *mei2*-unphosphorylatable mutant (which mimics the activated form) caused cells to go into quiescence and *pat1-114 mei2Δ* cells carry on growing mitotically at the restrictive temperature (Harigaya & Yamamoto, 2007). The mechanism of how Mei2 does this is still unknown. Mei2 is also essential for pre-meiotic S-phase because *mei2Δ* diploids fail to initiate meiotic S-phase. How Mei2 is working here is again unknown but it is likely to involve the meiotic S-phase Cdc2-Cig2 cyclin complex (Harigaya & Yamamoto, 2007). Lastly Mei2 is required for the initiation of meiosis I as diploids containing a temperature sensitive *mei2* (*mei2-33*) could not initiate meiosis I at the restrictive temperature (Watanabe & Yamamoto, 1994).

An important mechanism of action of Mei2 has been recently elucidated and is described in the review by (Yamamoto, 2010). Mei2 is an RNA binding protein (Watanabe *et al.*, 1997) which binds to meiRNA, a non-coding RNA product of the *sme2* locus on chromosome II, during meiosis. Together they form the "Mei2 dot" which is present at the *sme2* locus during meiosis (Watanabe *et al.*, 1997; Yamashita & Yamamoto, 1998; Shimada *et al.*, 2003). It was noted that during mitosis, meiotic mRNA is unable to accumulate even when expressed from a constitutive promoter therefore a system was in place to eliminate meiotic mRNA in mitosis. This has been extensively investigated and is now known as the DSR-Mmi1 system. A number of meiotic mRNAs contain a DSR (determinant of selective removal) region which binds a protein called Mmi1 which recruits a nuclear exosome to degrade the transcript (Yamamoto, 2010). Mmi1 is also present in the "Mei2 dot" therefore it is proposed that the Mei2-meiRNA complex sequesters Mmi1 thereby shutting down the DSR-Mmi1

mRNA degradation system allowing the accumulation of meiotic mRNA (Harigaya & Yamamoto, 2007; Harigaya *et al.*, 2006).

1.3.9.3 Meiotic gene expression

The major changes in gene expression that take place during meiotic differentiation have been studied on a genome wide scale (Mata & Bahler, 2006; Mata *et al.*, 2002; Mata *et al.*, 2007; Xue-Franzen *et al.*, 2006). Around half of the total number of genes in *S.pombe* showed a change in gene expression upon meiosis (Mata *et al.*, 2002) and these have been grouped into the following broad fields; environmental and pheromone response genes, pre-meiotic and S-phase genes and meiotic division and spore formation genes (Mata *et al.*, 2002). Transcriptional regulation appears to occur in waves with each wave controlled by specific transcription factors (Mata *et al.*, 2007). In 2006, Mata *et al* published a paper specifically describing Ste11 dependent genes of which they found 78 (Mata & Bahler, 2006), these included the pheromone response genes *gpa1*, *gap1*, *spk1*, *pyp2*, *pmp1*, *rgs1*, *ste7* and *ste4* along with genes involved in nuclear movement, cell fusion, nuclear fusion and cell cycle regulators. These works show that successful meiosis requires huge changes in gene expression and that transcriptional control of the meiotic gene expression programme is a highly complex and coordinated process.

1.4 Aims and Objectives

Although the oncogenic Ras1 mating phenotype in *S.pombe* was observed over two decades ago, the molecular nature of this mutation remains to be explored. We aimed to assess the molecular reasoning behind the observation that constitutively active Ras1 (*ras1.val17*) and constitutively active MEK (*byr1.DD*) show distinctly different phenotypes upon the induction of mating as both mutations are constitutively active in nature. We hypothesise that each mutant is resulting in a unique MAPK output from the pheromone response pathway. We also wanted to provide a hypothesis as to why *ras1.val17* has little/no effect in mitosis but a prominent effect in meiosis. This work aimed to provide a better understanding of the coordination of the Ras1-MAPK pathway and Ras1-morphology pathway during meiosis to test the hypothesis that Ras1 is activating these two pathways independently upon pheromone stimulation. In order to do this we employ both genetic and biochemical methods of analysis. Specifically, we aimed to devise an highly synchronous mating assay to monitor the activation of the pheromone response pathway that would allow us to quantify the activation of Spk1 MAPK in various mutant strains via quantitative western blotting. The rounded morphology resulting from defective Ras1 indicates that Ras1 is an important protein in the control of cell morphology. Previously published work has reported that Ras1 localised to the endomembranes exclusively controls the Cdc42 morphology pathway via the Ras1 GEF Efc25 during mitosis, we aimed to investigate whether this statement is true in the context of meiosis with regards to the morphological changes associated with shmooing and the expression of the additional Ras1 GEF, Ste6. We further aimed to define the contribution of various components of the pathway to MAPK activation, particularly those of the negative regulators Sxa2, Rgs1 and Gap1 along with the G-protein, Gpa1, Ste4 and Ste6.

The aim of this work was to further our understanding of the coordination and regulation of Ras-protein signalling. In mammalian systems, Ras proteins play important roles in a number of fundamental cellular processes mainly those of cell proliferation and differentiation. Importantly, Ras proteins are found to be mutated in a high percentage of all human cancers as well as neurodegenerative diseases and a number of RASopathies making the understanding of their molecular biology of high importance. Specifically, we wanted to highlight key targets of Ras associated signalling pathways for potential therapeutic intervention by unveiling basic regulatory concepts.

CHAPTER 2 MATERIALS AND METHODS

2.1 Materials

2.1.1 Yeast Strains

To best described the origins of the *S.pombe* strains used in scientific research, I have taken a direct paragraph from the Genetic Overview section of the *Molecular biology of the fission yeast* book by P. Munz, K. woldf, J. Kohli, and U. Leupold, Academic press, INC, (1989):

"All strains are descendants of the strains, one homothallic (strain 968: h^{90}) and two heterothallic (strains 972 and 975: h^- and h^+ , respectively), which have all been derived from the same Delft culture and therefore from the same homothallic isolate of *S.pombe* strain *liquefaciens* originally described by Osterwalder (1924). This monolithic origin provides for a high degree of homogeneity in the genetic background of the mutant strains of *S.pombe* studied. This is an advantage that is lacking in some of the other yeasts and moulds used in genetic research where wild-type strains of widely different sources have contributed to the genetic makeup of the mutant strains used today" (Munz *et al.*, 1989). Genotypes of the strains used are listed in Table 2.1. Only the strains used in experimental analysis are described rather than the numerous strains produced during construction. Details of the methods by which particular alleles were introduced are given in the relevant chapters.

2.1.2 Oligonucleotides

The DNA sequences of the oligonucleotides used are given in Tables 2.2

2.1.3 Media

Fission yeast media and basic genetic manipulations are described in (Moreno *et al.*, 1991).

Liquid Media

Schizosaccharomyces pombe cells were routinely grown in YE+ade medium (Yeast Extract plus adenine) containing: Yeast Extract (Formedium, 5 g/L) and glucose (30 g/L) supplemented with adenine (200 mg/L).

Minimal medium minus nitrogen (MM-N) was used to induce meiotic differentiation. It was used to wash cells after culturing in YE medium before spotting onto sporulation agar (SPA, see below) to induce sporulation. It was also used as the medium to induce sporulation of liquid cultures for example when carrying out a mating time course.

MM-N contains: potassium hydrogen phthalate (SIGMA, 3.0 g/L), disodium hydrogen phosphate (Na₂HPO₄) (SIGMA, 2.2 g/L), 1% glucose (10 g/L), 50x Salt stock (see below) (20 ml/L), 1000x Vitamin stock (see below) (1 ml/L), 1000x Biotin stock (see below) (1 ml/L), 10,000x mineral stock (see below) (0.1 ml/L) and leucine (40 mg/L).

Minimal medium plus nitrogen (MM+N) was used to induce the expression of genes ligated into pREP plasmids. MM+N contains the same as MM-N but with the addition of 5g/L ammonium chloride, 2% glucose instead of 1% and adenine (200mg/L).

50x salt solution

MgCl ₂ 6H ₂ O	53.5 g/litre
CaCl ₂ 2H ₂ O	0.74 g/litre
KCL	50 g/litre
Na ₂ SO ₄	2.0 g/litre

Vitamins (x1000)

Sodium pantothenate	1.0 g/litre
Nicotinic acid	10 g/litre
Inositol	10 g/litre

Minerals (x10000)

H ₃ BO ₃	5.0 g/litre
MnSO ₄	4.0 g/litre

Solid Media

YE+ade agar plates were used for routine vegetative growth of yeast strains. They contain the same ingredients as YE+ade liquid media along with 20g/L agar (Formedium).

SD+ade agar plates were used for selection of strains carrying pREP plasmids. They contain: 6.7 g/L yeast nitrogen base without amino acids (formedium) and 10 g/L glucose and 30 g/L agar.

Sporulation agar (SPA) plates were used to induce meiotic differentiation of cells. They contain: 10 g/L glucose, 1 g/L KH₂PO₄, 1 ml/L biotin, 1 ml/L 3 vitamins, 30 g/L agar

For positive colony selection after transformation, agar plates containing geneticin G418 (Formedium) for kanamycin resistance, hygromycin B (Formedium) and nourseothricin (Werner BioAgents) for ClonNAT resistance were used, the appropriate amount of the respective drug (See below) was added to pre-poured YE+ade agar plates.

Antibiotic	Concentration in solid agar	Supplier
Geneticin (G418)	100 mg/L	Formedium
Hygromycin B	100 mg/L	Formedium
Nourseothricin	100 mg/L	Werner BioAgents

Escherichia coli cultures were grown in Luria-Bertani (LB) medium containing: tryptone (10 g/L), yeast extract (5 g/L) and sodium chloride (5 g/L). To ensure pREP plasmids were maintained during culturing, LB was supplemented with ampicillin (final concentration 100 mg/L). *E.coli* strains were routinely grown at 37°C and liquid

cultures were shaken at 200 rpm during incubation. *E.coli* strains were plated on LB agar plates after transformation (LB agar contains the same as LB media with the addition of 15 g/L agar).

Stocks of *Schizosaccharomyces pombe* strains were stored in YE +30% glycerol at -80 °C.

Table 2.1: Strain genotypes

Strain Number	Genotype
KT301	<i>JY450 h⁹⁰ ade6.M216 leu1.32</i>
KT2645	<i>h⁹⁰ ade6.M210 leu1.32 ras1.val17<<LEU2</i>
KT2673	<i>h⁹⁰ ade6.M216 leu1.32 Pnda3-GFP-atb2::aur1^R ras1.val17::hyg^R</i>
KT2734	<i>h⁹⁰ ade6.M210 leu1.32 ras1.val17<<LEU2 byr1.DD::hyg^R</i>
KT2852	<i>h⁹⁰ ade6.M216 leu1.32 Pnda3-GFP-atb2::aur1^R spk1::clonNAT^R</i>
KT2863	<i>h⁹⁰ ade6.M216 leu1.32 Pnda3-GFP-atb2::aur1^R spk1+::kan^R</i>
KT2864	<i>h⁹⁰ ade6.M216 leu1.32 Pnda3-GFP-atb2::aur1^R spk1+::kan^R</i>
KT2865	<i>h⁹⁰ ade6.M216 leu1.32 Pnda3-GFP-atb2::aur1^R spk1+::kan^R</i>
KT2875	<i>h⁹⁰ ade6.M216 leu1.32P-nda3-GFP-atb2::aur1^R spk1.Sho-A::kan^R</i>
KT2945	<i>h⁹⁰ ade6.M216 leu1.32 Pnda3-GFP-atb2::aur1^R spk1.V67I-ShoA::kan^R</i>
KT2946	<i>h⁹⁰ ade6.M216 leu1.32 Pnda3-GFP-atb2::aur1^R spk1.V67I-ShoA::kan^R</i>
KT2948	<i>h⁹⁰ ade6.M216 leu1.32 Pnda3-GFP-atb2::aur1^R spk1.ShoIA::kan^R</i>
KT2949	<i>h⁹⁰ ade6.M216 leu1.32 Pnda3-GFP-atb2::aur1^R spk1.ShoIA::kan^R</i>
KT2950	<i>h⁹⁰ ade6.M216 leu1.32 Pnda3-GFP-atb2::aur1^R spk1.ShoIA::kan^R</i>
KT3001	<i>h⁹⁰ ade6.M210 leu1.32:: Pnmt41-LA-GFP::leu1⁺ Pnda3-mCherry-atb2::aur1^R</i>
KT3005	<i>h⁹⁰ ade6.M210 leu1.32:: Pnmt41-LA-GFP::leu1⁺ Pnda3-mCherry-atb2-aur1^R ras1.val17::hyg^R</i>
KT3008	<i>h⁹⁰ ade6.M216 leu1.32 Pnda3-GFP-atb2::aur1^R byr1.DD::hyg^R spk1.V67I-ShoA::kan^R</i>
KT3009	<i>h⁹⁰ ade6.M216 leu1.32 Pnda3-GFP-atb2:: aur1^R byr1.DD::hyr^R spk1.V67I-ShoA::kan^R</i>
KT3010	<i>h⁹⁰ ade6.M216 leu1.32 Pnda3-GFP-atb2::aur1^R byr1.DD::hyg^R spk1.V67I-ShoA::kan^R</i>
KT3011	<i>h⁹⁰ ade6.M216 leu1.32 Pnda3-GFP-atb2::aur1^R byr1.DD::hyg^R spk1.V67I-ShoA::kan^R</i>
KT3017	<i>h⁹⁰ ade6.M210 leu1.32::Pnmt41-LA-GFP::leu1⁺ Pnda3-mCherry-atb2::aur1^R ras1.val17::hyg^R</i>
KT3035	<i>h⁹⁰ ade6.M210 leu1.32::Pnmt41-LA-GFP::leu1⁺ Pnda3-mCherry-atb2::aur1^R fus1::hyg^R</i>
KT3051	<i>h⁹⁰ ade6.M210 leu1.32::Pnmt41-LA-GFP::leu1⁺ Pnda3-mCherry-atb2::aur1^R byr1.DD::hyg^R</i>
KT3082	<i>h⁹⁰ ade6.M216 leu1.32 spk1-GFP-2xFLAG::kan^R</i>

Strain Number	Genotype
KT3084	<i>h⁹⁰ ade6.M210 leu1.32 ras1.val17<<LEU2 spk1-GFP-2xFLAG::kan^R</i>
KT3289	<i>h⁹⁰ ade6.M216 leu1.32 gap1::clonNAT^R</i>
KT3305	<i>KT2673 plus pRep1 empty</i>
KT3307	<i>KT2673 plus pRep41 empty</i>
KT3313	<i>KT2673 plus pRep1-gap1</i>
KT3316	<i>KT2673 plus pRep41-gap1</i>
KT3385	<i>h⁹⁰ ade6.M216 leu1.32 byr1.DD::hyg^R</i>
KT3435	<i>h⁹⁰ ade6.M216 leu1.32 byr1.DD::hyg^R spk1-GFP-2xFLAG::kan^R</i>
KT3439	<i>h⁹⁰ ade6.M210 leu1.32 ras1.val17<<LEU2 byr1.DD::hyg^R spk1-GFP-2xFLAG::kan^R</i>
KT3460	<i>h⁹⁰ ade6.M216 leu1.32 byr1.DD::hyg^R spk1.V67I-ShoA::kan^R</i>
KT3461	<i>h⁹⁰ ade6.M216 leu1.32 byr1.DD::hyg^R spk1.V67I-ShoA::kan^R</i>
KT3462	<i>h⁹⁰ ade6.M216 leu1.32 byr1.DD::hyg^R spk1.V67I-ShoA::kan^R</i>
KT3463	<i>h⁹⁰ ade6.M216 leu1.32 byr1.DD::hyg^R spk1.V67I-ShoA::kan^R</i>
KT3464	<i>h⁹⁰ ade6.M216 leu1.32 byr1.DD::hyg^R spk1.V67I-ShoA::kan^R</i>
KT3763	<i>h⁹⁰ ade6.M216 leu1.32 byr2::clonNAT^R spk1-GFP-2xFLAG::kan^R</i>
KT3875	<i>h⁹⁰ ade6.M216 leu1.32 spk1-GFP-2xFLAG::Kan^r sxa2::ClonNAT^r</i>
KT3992	<i>h⁹⁰ ade6.M210 leu1.3::Pnmt41-LA-GFP::leu1⁺ Pnda3-mCherry-atb2::aur1^R sxa2::clonNAT^R</i>
KT3997	<i>h⁹⁰ ade6.M216 leu1.32 spk1-GFP-2xFLAG::kan^R gap1::clonNAT^R</i>
KT4010	<i>h⁹⁰ ade6.M216 leu1.32 byr1.DD::hyg^R spk1-GFP-2xFLAG::kan^R byr2::clonNAT^R</i>
KT4047	<i>h⁹⁰ ade6.M216 leu1.32 byr1.DD::hyg^R spk1-GFP-2xFLAG::kan^R scd1::clonNAT^R</i>
KT4061	<i>h⁹⁰ ade6.M216 leu1.32 spk1-GFP-2xFLAG::Kan^r scd1::clonNAT^R</i>
KT4072	<i>KT3289 plus pREP1-gap1</i>
KT4076	<i>KT3289 plus pREP41-gap1</i>
KT4084	<i>KT3875 plus pREP41-gap1</i>
KT4098	<i>KT3875 plus pREP1-gap1</i>
KT4161	<i>h⁹⁰ ade6.M216 leu1.32 spk1-GFP-2xFLAG::kan^R rgs1::clonNAT^R</i>
KT4190	<i>h⁹⁰ ade6.M216 leu1.32 spk1-GFP-2xFLAG::kan^R</i>
KT4194	<i>h⁹⁰ ade6.M216 leu1.32 byr1.DD::hyg^R spk1-GFP-2xFLAG::kan^R</i>
KT4233	<i>h⁹⁰ ade6.M216 leu1.32 ras1.val17<<LEU2 spk1-GFP-2xFLAG::kan^R</i>
KT4300	<i>h⁹⁰ ade6.M216 leu1.32 spk1-GFP-2xFLAG::kan^R byr1::clonNAT^R</i>
KT4323	<i>h⁹⁰ ade6.M216 leu1.32 spk1-GFP-2xFLAG::kan^R ras1::clonNAT^R</i>

Strain Number	Genotype
KT4333	<i>h⁹⁰ ade6.M216 leu1.32 spk1-GFP-2xFLAG::kan^R ste6::clonNAT^R</i>
KT4335	<i>h⁹⁰ ade6.M216 leu1.32 spk1-GFP-2xFLAG::kan^R gpa1::clonNAT^R</i>
KT4346	<i>h⁻ ade6.M216 leu1.32 spk1-GFP-2xFLAG::kan^R gpa1::clonNAT^R</i>
KT4353	<i>h⁹⁰ ade6.M216 leu1.32 byr1.DD::hyg^R spk1-GFP-2xFLAG::kan^R gpa1::clonNAT^R</i>
KT4359	<i>h⁹⁰ ade6.M216 leu1.32 byr1.DD::hyg^R spk1-GFP-2xFLAG::kan^R ras1::clonNAT^R</i>
KT4376	<i>h⁹⁰ ade6.M216 leu1.32 spk1-GFP-2xFLAG::kan^R ste4::clonNAT^R</i>
KT4998	<i>h⁹⁰ ade6.M210 leu1.32 ras1.val17<<LEU2 spk1-GFP-2xFLAG::kan^R ste6::hyg^R</i>
KT5023	<i>h⁹⁰ ade6.M210 leu1.32 ras1.val17<<LEU2 spk1-GFP-2xFLAG::kan^R gpa1::clonNAT^R</i>
KT5030	<i>h⁹⁰ ade6.M210 leu1.32 ras1.val17<<LEU2 spk1-GFP-2xFLAG::kan^R byr1::clonNAT^R</i>
KT5035	<i>h⁹⁰ ade6.M210 leu1.32 ras1.val17<<LEU2 byr1.DD::hyg^R spk1-GFP-2xFLAG::kan^R gpa1::clonNAT^R</i>
KT5059	<i>h⁻ ade6.M216 leu1.32 ura4.d18 gpa1QL::ura4+ spk1-GFP-2xFLAG::kan^R</i>
KT5070	<i>h⁻ ade6.M216 leu1.32 ura4.d18 gpa1QL::ura4+ spk1-GFP-2xFLAG::kan^R ras1::clonNAT^R</i>
KT5136	<i>h⁹⁰ ade6.M216 leu1.32 byr1.DD::hyg^R ste4::clonNAT^R spk1-GFP-2xFLAG::kan^R</i>
KT5139	<i>h⁹⁰ ade6.M216 leu1.32 byr1.DD::hyg^R ste6::clonNAT^R spk1-GFP-2xFLAG::kan^R</i>
KT5143	<i>h⁹⁰ ade6.M210 leu1.32 ras1.val17<<LEU2 ste4::clonNAT^R spk1-GFP-2xFLAG::kan^R</i>

Table 2.2: Oligonucleotide sequences used in strain construction

Name	Sequence 5' to 3'
Spk1-F1	CTTAACAATTACCAACAGCTTTTCAA
Spk1-V67I-R	TGAAAGGATGTATTTTTTTAATAGCCACCTTTAG
Spk1-V67I-F	GCCTAAAGGTGGCTATTAATAAATACATCCT
Spk1-R1	GATGAAGCATTAAAAACAAGAAGATGA
Spk1-F1-mark	GGAAATCCTGGCTTTATGACTGAGTATGT
Spk1-CHK-R	AGAATAAGCGTAGAATAGGTTGAGGA
Spk1 -seq	ATTTAAAGCACAAAGGATTGCATAACAT
Spk1-gfp-f2	TTAATTAACCCGGGGATCCGTCTGAAATTTACTTCACGAAATATTAAGGCCTTCAATAC
Spk1-R2	GTTTAAACGAGCTCGAATTCAAAGCTTCAACTAGAATTCTCCTCATCAAG
Spk1-sho-IA-F	TTATATTATAGCAGAGCTTATGGAAACG
Spk1-sho-IA-R	CGTTTCATAAGCTCTGCTATAATATAA
Spk1-F2	TTAATTAACCCGGGGATCCGTAGACTACAAATTGAAAACTTGAAAGAAAT
Ras1-F1	CCTCTTCATGCATGTATTGCGAACACTTGAGC
Ras1-F2	TTAATTAACCCGGGGATCCGCTAACATATAACACAACATTTAGTTGAAACCTC
Ras1-R1	CTTACCATAGGTTACATTAAGGTTATCCC
Ras1-R2	GTTTAAACGAGCTCGAATTCCAAGTATTATTGCAGAATATTTGAGCTGTTTGGTG
Ras1-CHK-F	CCACFFTCGATAAAAACGCATGAAAGGAGTTTAAAC
Byr1-F1	AGTTTTATGTCGATAAAATTAGTCTCCCATAC
Byr1-F2	TTAATTAACCCGGGGATCCGTTCTAGCTATTGGCCAAATTCTCAAAGAAACCTG
Byr1-R1	TAATATTTGCAAACACTACGGGCTTTAAGC
Byr1-R2	GTTTAAACGAGCTCGAATTCATGTGCAAAGGACGCAATGGATACATAAATTATGTTAG
Byr1-CHK-R	CATTAAGCGAGCTAGTTAAAATACGTGATGCAG

Name	Sequence 5' to 3'
Gpa1-F1	CTCATTA AAA ACCCTGGTTTCTTTGTAAATTGTAC
Gpa1-F2	TTAATTAACCCGGGGATCCGGGTGAAAAGGCAGCTACAGATTCCAAATCC CCAC
Gpa1-R1	GGGTGGAGTGTGAAGCAGCTACATTAAATTGC
Gpa1-R2	GTTTAAACGAGCTCGAATTCATGAATTTTCTTAACTATCTTCATAATCTTTTCTG
Gpa1-CHK-R	CAAGGGGTAGTAGAATTATACAATGGTGAATCCTG
Scd1-F1	AATACATTTACGATACGCTATTCGATTCAA
Scd1-F2	TTAATTAACCCGGGGATCCGAACTGATAACTTCTTCTCGAGACTCCTCC
Scd1-R1	ATGGATCCTCGGTGAATGTAAATCATCAGG
Scd1-R2	GTTTAAACGAGCTCGAATTCCTAGCATTGTGCTAGCTGTACATTGTC
Scd1-CHK-R	TTTGAAACAAGCAATCGCTGAGATTCTCC
Ste4-F1	GCGGTATAT CTCGTTATGA TACATAAAAA CTTTTGCTCTC
Ste4-F2	TTAATTAACCCGGGGATCCGTAATTTTGCTTAGGATAGCAATGTAAAGGGCGTAG
Ste4-R1	GTAAACTACGTTTCGGGCATAATTTTGCGCC
Ste4-R2	GTTTAAACGAGCTCGAATTCCTAAGCTTTTTAAAAGCCATCTATTTATGAATTG
Ste4-CHK-R	CTCCTTCCAAATTTTCGGTATACCACCGTGTAC
Ste6-F1	TAGTCATCAAGTTTGGATCAATAGAAAAGAATTC
Ste6-F2	TTAATTAACCCGGGGATCCGTTTCGTAAGGGTCCATGAATGCTATCAATTCCAC
Ste6-R1	GACTTTCAAAGCCTCCATTTATCAAAGTTCAC
Ste6-R2	GTTTAAACGAGCTCGAATTCAGCGTGAACGTTAACAGTGATTTAAGTTTTTATG
Ste6-CHK-R	GCAGCGAACGGAAAGAAAGCATCAATGTTTC
Sxa2-F1	TAAGCATTAAGAATGCATAAATGATCGCTG
Sxa2-F2	TTAATTAACCCGGGGATCCGTGAAAAGAGAGACAATGATTTTGAGCCTATGAGAAAAGCG
Sxa2-R1	TGATCCTTACCGTCATATTGGCTGTACTGG

Name	Sequence 5' to 3'
Sxa2-R2	GTTTAAACGAGCTCGAATTCAAGTTTAATATCGGAAAATTTAAAATACAAGT
Sxa2-CHK-R	CACTGGTTTGGAACGATATGAACTTTTATC
F1-byr2	CTGAAACCGATTGAAACATTGAAATTG
F2-byr2	TTAATTAACCCGGGGATCCGAAATGCAGGAAAGTGGTTGTACAACGTATAACTTCTAAG
R1-byr2	TAGACAATTTATTTTATATCTACTATACC
R2-byr2	GTTTAAACGAGCTCGAATTCGCCGGCTAAGTTATGATGAAAACAGAAACATTATTTTAC
CHK-F-byr2	ATCTGTACGATCCGTCGTGATTGTGTTAC
Rgs1-F1	CTTTGTTCCGTTAAAGTTCCCATTTGTTCCGCC
Rgs1-F2	TTAATTAACCCGGGGATCCGCCAAAGCTGATTCTTACTTTTACGAATTTGTAGCC
Rgs1-R1	GATGCTGGTTAATGACTATGTTCTTTAGGCG
Rgs1-R2	GTTTAAACGAGCTCGAATTCGCATAGAAAACAATCGTGTTTTAAATCATTATTAGCAG
Rgs1-CHK	GGCAAGCGACTGCATATCCTTGTTTAAATG
Gap1-F1	CATCTACCTTCATATACAACACTCACTAG
Gap1-F2	TTAATTAACCCGGGGATCCGTATAAATTTCAATAGCTAA AAATTGCC TAA GTAGC
Gap1-R1	TTTAAAGACAGGTATGCCTTTTGATCCCGAGG
Gap1-R2	GTTTAAACGAGCTCGAATTCATGTTCTACCAAGCATCAGTGACAACACTG GCCATGC
Gap1-CHK	GCTT ATGCC GATG CTCTTT TGATAA TTCC
Gap1-5'-Sal1	TAGCTATTGAAAGTCGACATGACTAAGCGG
Gap1-3'-BamH1	TGATGCTTGGTAGGATCCTTACTTTTCGTAAAAAC
Gap1-C-trunc-BamH1	ATGTGTCTTCGTGGATCCTCAGCCATTGGCAACACTTTGA
Gap1-N-trunc-Sal1	ACCAATACGAGTGTGACATGCATCTTTTATTATC
Gap1-R340K-F	GTGGATTTTTCTTTCTTAAATTCGTTAATCCAGCTATT
Gap1-R340K-R	AATAGCTGGATTAACGAATTTAAGAAAGAAAAATCCAC

2.1.4 Antibodies

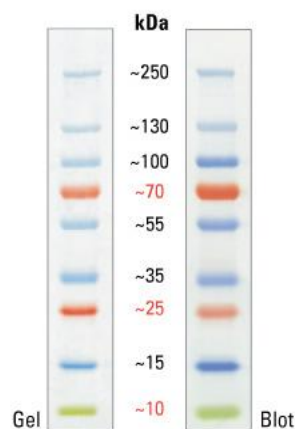
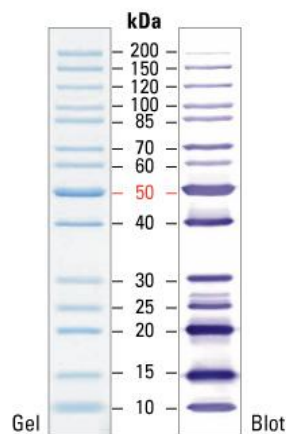
Antibodies used in this study are:

- Phospho-p44/42 MAPK (Erk1/2) (Thr202/Tyr204) Rabbit monoclonal antibody #4370 from Cell Signaling technology. Used at 1:2000 dilution for western blotting.
- TAT1 for the detection of α -tubulin which was a generous gift from Professor Keith Gull. It was provided as tissue culture supernatant of a hybridoma mouse cell line and used at a 1:3000 dilution for western blotting.
- Monoclonal GFP antibody (0.4 mg/ml), Roche Cat No 11814460001. Used at a 1:2000 dilution for western blotting.
- IRDye 680LT goat anti-mouse secondary antibody Li-cor 926-68020 (1.0 mg/ml). Used 1:16,000
- IRDye 800CW goat anti-rabbit secondary antibody Li-cor 926-32211 (1.0 mg/ml). Used 1:16,000

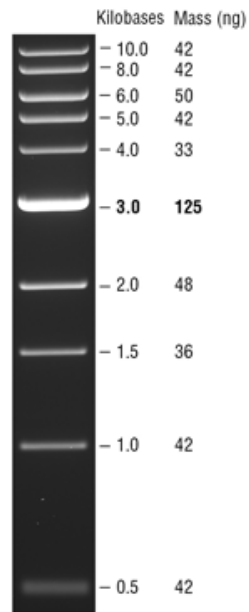
2.1.5 Molecular weight markers

Two types of protein ladders were used when carrying out SDS-PAGE, these were:

- Fermentas PageRuler Unstained Protein Ladder #26614 (below left)
- Fermentas PageRuler Plus prestained Protein Ladder #26619 (below right)



The 1kb DNA ladder from New England Biolabs (N3232L), shown below (total 500 ng DNA per 6 μ l), was routinely used during agarose gel electrophoresis to determine the size and approximate concentration of PCR products.



2.2 Methods

2.2.1 Agarose gel electrophoresis

PCR products were mixed with 6xloading buffer (10 mM Tris-HCl (pH 7.6) 0.03% bromophenol blue, 60% glycerol, 60 mM EDTA) prior to loading onto a 0.85% agarose gel containing ethidium bromide and subject to electrophoresis at 135mA until the DNA had run the length of the gel. Gel's were made by melting agarose (Formedium) in TAE buffer and the addition of ethidium bromide solution (final concentration 0.5 mg/ml)

2.2.2 Preparation of yeast genomic DNA

Yeast genomic DNA was prepared using the method outlined by (Alfa, C., Fantes, P., Hyams, J., McLeod, M. & Warwick, E., 1993). Cells were grown in 5 ml YE+ade overnight, centrifuged and resuspended in 500 µl of 1.2M Sorbitol, 0.1M EDTA (pH 7.5) and incubated with zymolase 20,000 (20T) (final 3mg/ml) at 37°C for 1-hour. Cells were centrifuged and the supernatant discarded. Cells were resuspended in 0.5 ml 50 mM Tris 20 mM EDTA (pH 7.4) and 50 µl of 10% SDS and incubated at 65°C for 30 minutes to inactivate DNase activities. 0.25 ml of 4M potassium acetate were added and tubes were thoroughly mixed before being placed on ice for 1-hour. Cells were centrifuged for 5 minutes at 13,000 rpm and the supernatant transferred to a fresh tube. 0.75 ml of isopropanol were added, tubes were mixed and left at room temperature for 5 minutes then centrifuged for 10 seconds. Supernatant was removed and the pellet left to air dry at 50°C. The pellet was resuspended in 0.3 ml of 10 mM Tris 1 mM EDTA (TE) (pH 7.5) - 0.3M sodium acetate and 2 µl of 1mg/ml solution of RNase was added and incubated at 37° for 30 minutes after which 1 volume (0.3 ml) phenol-chloroform was added and tubes centrifuged for 10 minutes at 13,000 rpm. About 175 µl of the top

layer was transferred to a fresh microfuge tube and about 3 volume (0.55 ml) of ethanol added at room temperature. This was mixed and left to sit for 5 minutes, then centrifuged for 5 minutes at 13,000 rpm and the supernatant removed. The pellet was rinsed with 0.3 ml of 70% ethanol and left to air dry at 50°C before being resuspended in 50 µl of 10mM Tris 1 mM EDTA pH 7.5 (TE) and stored at 4°C.

2.2.3 Plasmid preparation

The pREP series of plasmids have been used in this study. These plasmids allow the expression of genes under the thiamine repressible *nmt* promoter and variants of the *nmt* promoter which have altered expression levels (Maundrell, 1993).

Specifically used in this study were pREP1 and pREP41. pREP1 contains the wildtype *nmt1* promoter where the induced level of expression is around 80x greater than the repressed level. pREP41 is a variation of pREP1 that contains the *nmt41* promoter instead of the *nmt1* promoter. *nmt41* has around 6x lower induced expression compared to *nmt1*.

Plasmid digestion

pREP1/41

5' C A T A T G T C G A C T C T A G A G G A T C C C C G G G 3'
 Nde I Sal I (Xba I) BamH I Sma I

Above are the restriction sites in the pREP1 & pREP41 plasmids. pREP1 and pREP41 were digested with Fastdigest *Sal* I and Fastdigest *Bam* HI (Thermo Scientific) according to the manufacturer's instructions. This was followed by Antarctic phosphatase treatment (New England Biolabs). The purpose of adding this phosphatase is to remove 5' phosphoryl termini required by ligases so that the plasmids cannot self-

ligate. It is used to decrease the vector background in cloning strategies. The reaction conditions followed the manufacturer's instructions.

Insert generation

Primers were created that incorporated the *Sal* I site at the 5' end of the gene ORF & a *Bam* HI site at the 3' end of the gene open reading frame (ORF) of interest, this was achieved by replacing the six amino acids before the start codon and the six after the stop codon with the sequence of the relevant restriction sites.

The polymerase chain reaction (PCR) was used to create the DNA insert using 50 µl reactions and the Phusion DNA polymerase (ThermoScientific) (See 2.2.6.1). WT genomic DNA was used as a template along with the specific primers designed with the restriction enzyme sites at the 5' and 3' ends of the ORF of interest. Successful creation of insert was confirmed by running the PCR product on an agarose gel. The PCR product was purified (See 2.2.7) and stored at -20°C until required.

Insert digestion

Purified DNA insert was digested with Fastdigest *Sal* I and Fastdigest *Bam* HI (Thermo Scientific) according to the manufacturer's instructions. A few microlitres were run on an agarose gel with digested pREP1 & pREP41 to estimate the concentrations and therefore the amount for the ligation reactions, ideally would like 4:1 insert to vector ratio.

Ligation

Ligation reactions were set up in 20 µl volumes in PCR tubes. The ligation reaction was carried out using the T4 Ligase (NEB) and the appropriate buffer supplied with it. The reaction conditions were set up as specified in the manufacturer's instructions.

2.2.4 *E.coli* Transformation

The One Shot Mach1-T1 *E.coli* competent cells from Invitrogen were used during this study and the transformation reaction carried out as specified in the manufacturer's instructions. Cells were incubated with the ligated plasmids for 1 hour on ice before heat shocking at 42°C for 45 seconds. Cells were then plated on LB+ampicillin agar plates as the pREP plasmids have the ampicillin resistance marker for positive colony selection. Plates were incubated at 37°C overnight. Colonies were inoculated into LB + ampicillin & incubated overnight at 30°C 210 rpm for plasmid isolation.

2.2.5 *E.coli* Plasmid Isolation

Plasmid isolation was carried out using the QIAprep spin plasmid miniprep kit (Qiagen). Isolated plasmids were stored at -20°C.

To check if the isolated plasmid has the correct ORF ligated into it, a restriction enzyme digest was carried out.

Positive plasmids were used to transform *S.pombe* using the TRAF0 method outlined in 2.2.11. For each positive transformation reaction using a ligated plasmid, an empty plasmid was also transformed as a control.

The completed yeast transformations were plated on SD +ade plates & only positive colonies with the plasmid will grow as the host strains are *leu1.32* which is complemented by the budding yeast *LEU2* gene from the plasmid. Yeast strains containing the pREP plasmids were inoculated into 5ml MM+N (+ade) and incubated at 30°C shaking at 210 rpm for 20 hours to induce the *nmt1/41* promoter. This was followed by SPA spotting onto SPA plates as outlined in 2.2.12.1. The SPA plates were incubated at 30°C and the phenotypes of strains observed after 24 hours using a microscope.

2.2.6 Polymerase Chain reaction

2.2.6.1 Phusion DNA Polymerase

Phusion high-fidelity DNA polymerase (ThermoScientific) was routinely used for the generation of DNA fragments required for yeast transformations. See 2.2.9 for the methods to create specific types of fragments for gene disruption. Phusion was used according to the manufacturer's instructions. The High Fidelity (HF) buffer was routinely used when generating fragments containing the kanamycin and hygromycin resistance cassettes whereas the GC buffer was more effective when using the clonNAT cassette because of its high GC content. When GC buffer was used, 1 μ l of DMSO was also added to the reaction mixture and the annealing temperature was usually lowered from 58°C to 52°C. Typical reaction and cycling conditions are shown below:

Phusion reaction (25 μ l scale)

gDNA	1 μ l
5xPhusion HF buffer	5 μ l
dNTPs (10mM)	0.5 μ l
Primer-F (10 μ M)	1.25 μ l
Primer-R (10 μ M)	1.25 μ l
Phusion polymerase	0.5 μ l
Water	16 μ l

98°C	30secs	
98°C 58/52°C 72°C	5secs	x35
	20secs	
	30secs/kb	
72°C	10mins	
4°C (10°C)	hold	

2.2.6.2 Paq5000 DNA Polymerase

The Paq5000 DNA polymerase from Agilent technologies was routinely used for checking the genomic locus for successful integration of a DNA fragment and was used according to the manufacturer's instructions. Typical reaction conditions are shown below.

Reaction mixture (25 μ l scale)

gDNA(0.1-1 μ g)	1 μ l
10x Paq buffer	2.5 μ l
dNTPs (10mM)	0.5 μ l
Primer F (10 μ M)	0.5 μ l
Primer R (10 μ M)	0.5 μ l
Paq5000	0.25 μ l
Water	19.75 μ l

Cycling conditions:

95°C	2mins	
95°C 55°C 72°C	20secs	x35
	20secs	
	30secs/kb	
72°C	10mins	
4°C (10°C)	hold	

2.2.7 DNA Purification

Fermentas GeneJET PCR purification kit, (#K0701, #K0702) was used for routine DNA fragment purification after PCR reactions using the instructions provided by the manufacturer. Purified PCR products were routinely stored at -20°C.

2.2.8 DNA sequencing

DNA was sequenced using the BigDye V3.1 system (Applied Biosystems). Sequencing reactions were performed in a total of 10 μ l and contained 20-30ng/kb of purified DNA fragment as a template. The reaction mixture and PCR cycling conditions are outlined below and reagents were provided by the PNAFL facility at the University of Leicester:

Reaction:

Big Dye v3.1	0.5 μ l
5x Sequencing Buffer	1.75 μ l
Primer (10 μ M)	0.5 μ l
Template + water	7.25 μ l
Total	10 μ l

Cycle:

28 cycles
96°C 10 seconds

50°C 5 seconds

60°C 4 minutes

Clean up reaction:

Addition of 10 µl water and 2 µl 2.2% SDS followed by:

98°C 5 minutes

25°C 10 minutes

The reaction products were then purified using Performa Gel Filtration Cartridge (EdgeBio) to remove BigDye terminators. These reaction products were sent to the PNAFL facility (University of Leicester) for sequencing using the Applied Biosystems 3730 sequencer.

2.2.9 Gene disruption

2.2.9.1 Two-step gene replacement

Figure 2.1 shows a schematic to outline the process by which the ORF of a gene of interest can be deleted at its endogenous locus using a two-step PCR approach to replace the ORF with a antibiotic resistance cassette (Wach, 1996). Step 1 involves the amplification of the flanking regions upstream and downstream of the ORF of interest with a F1 x F2 and a R1 x R2 reaction, the F2 and R2 primers have “tails” which are complementary to the initial and final sequence regions of three resistance genes, kanamycin, hygromycin and clonNAT (Bahler *et al.*, 1998; Hentges *et al.*, 2005), (Sato *et al.*, 2005). The two PCR products from Step 1 are then amplified with the F1 and R1 primers in the presence of the deletion cassette of choice (Step 2) to create the final PCR product consisting of the deletion cassette surrounded by the upstream and downstream flanking regions of the ORF of interest. Once this PCR product is transformed into yeast, homologous recombination can take place and cells which are positive for the disruption cassette can be selected for.

Phusion DNA polymerase is used in all reactions to create transformation products. A

typical PCR reaction is outlined below:

Reactions 1 and 2 (25 μ l scale)

gDNA	1 μ l
5xPhusion HF buffer	5 μ l
dNTPs (10mM)	0.5 μ l
F1/R1 (10 μ M)	1.25 μ l
F2/R2 (10 μ M)	1.25 μ l
Phusion	0.5 μ l
Water	16 μ l

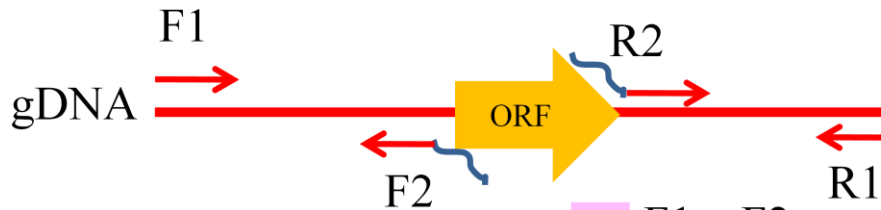
Reaction 3 (50 μ l scale):

selectable marker cassette	1 μ l
dNTPs (10mM)	1 μ l
product1	2.5 μ l
product2	2.5 μ l
F1 (10 μ M)	2.5 μ l
R1 (10 μ M)	2.5 μ l
5xHF/GC buffer	10 μ l
DMSO (if GC buffer used)	1 μ l
Phusion	1 μ l
Water	27.5 μ l

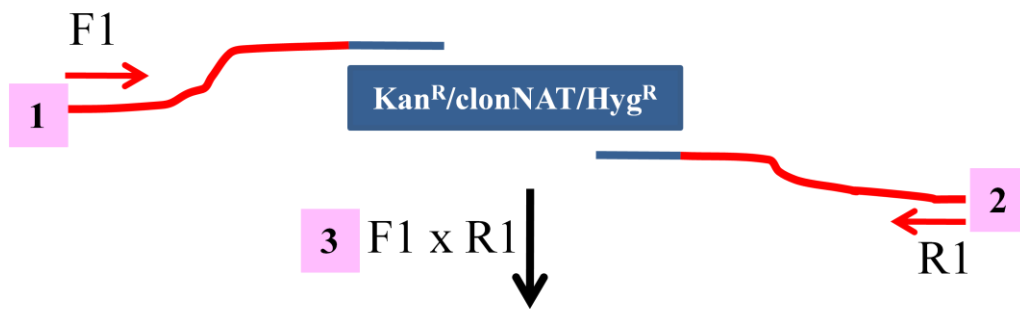
Cycling conditions:

98°C	30secs	
$\left[\begin{array}{l} 98^\circ\text{C} \\ 58^\circ\text{C} \\ 72^\circ\text{C} \end{array} \right.$	5secs	x35
	20secs	
	90secs	
72°C	10mins	
4°C (10°C)	hold	

Step 1 – Reactions 1 and 2:



Step 2 – Reaction 3:



Final PCR product:



Figure 2.1: Gene deletion at the endogenous locus.

Gene deletion at the endogenous locus involves the generation of a DNA fragment containing the flanking regions to the gene of interest which can be incorporated into the genome by homologous recombination. Step 1 creates two DNA fragments which can be sewn together in step 2 along with the sequence of a selectable marker of choice. The final DNA fragment is transformed into *S.pombe* using the TRAF0 method outlined in 2.2.11.

2.2.9.2 *GFP-tagging a gene of interest*

Figure 2.2 shows a schematic outlining the process by which a gene can be C-terminally tagged at its endogenous locus using a two-step PCR approach (in this case specifically with *GFP-2xFLAG-kan^R* (Tanaka *et al.*, 2005)). Step 1 involves the amplification of the flanking regions upstream and downstream of the STOP codon of the ORF of interest with a F1 x F2 and a R1 x R2 reaction, the F2 and R2 primers have “tails” which are complementary to the initial and final sequence regions of the tagging cassette. The two PCR products from Step 1 are then amplified with the F1 and R1 primers again in the presence of the tagging cassette of choice (Step 2) to create the final PCR product consisting of the tagging cassette surrounded by the complementary C-terminal ORF region and the complementary downstream region of the ORF of interest. Once this PCR product is transformed into yeast, homologous recombination can take place and cells which contain *GFP-2xFLAG-Kan^R* can be selected for.

DNA from positive colonies were isolated and the ORF of interest fully sequenced to confirm correct incorporation of the tag and to check that no additional mutations had been introduced.

The addition of a selectable marker to a gene of interest is accomplished in a similar manner but the R2 and F2 primers are designed so that they successfully incorporate the STOP codon of the gene whereas with tagging the gene of interest, we want the tag to be expressed as part of the protein therefore the gene for the tag is inserted just before the endogenous STOP codon.

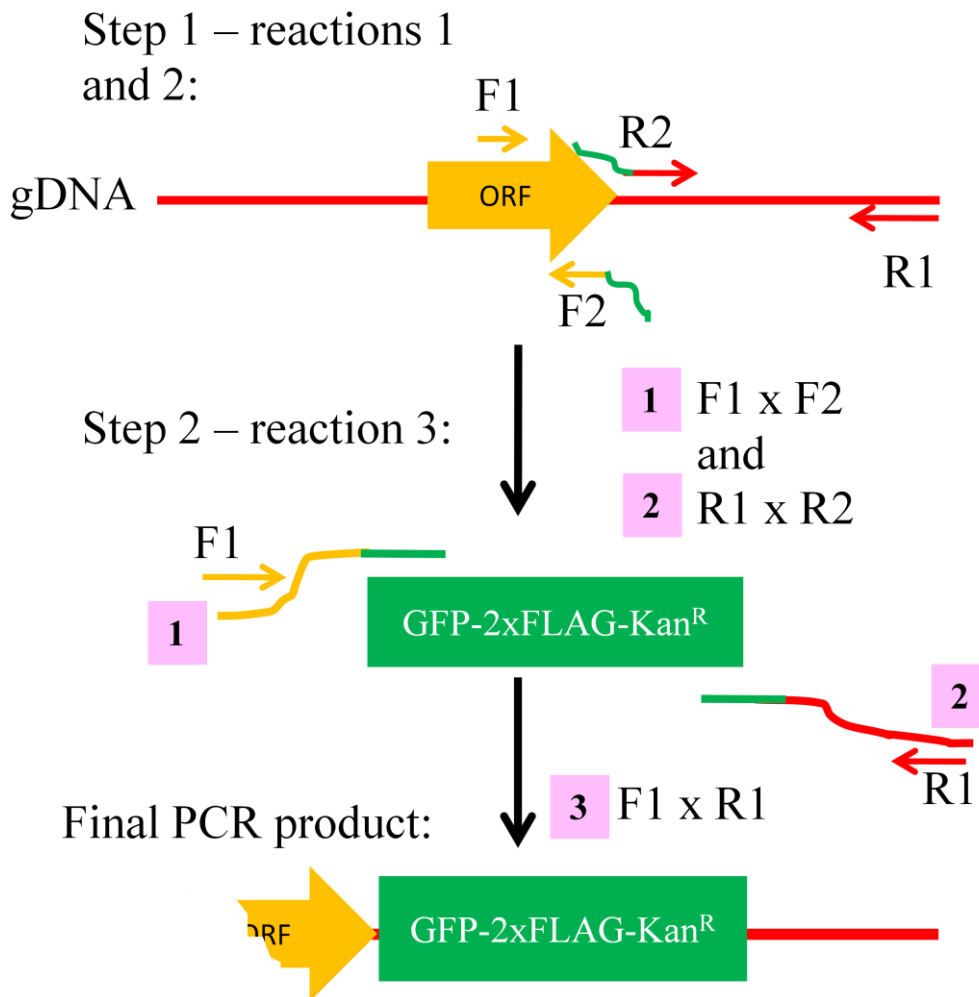


Figure 2.2 GFP-Tagging of a gene at the endogenous locus

A schematic to outline the process by which a gene can be C-terminally tagged with *GFP-2xFLAG-Kan^R* at its endogenous locus using a two-step PCR approach. Step 1 involves the amplification of the flanking regions upstream and downstream of the STOP codon of the ORF of interest, the F2 and R2 primers have “tails” which are complementary to the initial and final sequence regions of the tagging cassette. The two PCR products from Step 1 are then amplified with the F1 and R1 primers again in the presence of the tagging cassette of choice (Step 2) to create the final PCR product consisting of the tagging cassette surrounded by the complementary C-terminal ORF region and the complementary downstream region of the ORF of interest.

2.2.9.3 *Site-directed mutagenesis*

A DNA fragment containing the desired point mutation were generated using the 2-step PCR based approach outlined in **Figure 2.3**. Step 1 is the generation of two PCR products that contain the desired point mutation plus either part of the 5' or 3' flanking regions. Primers containing the desired point mutation - labelled as mutation-F and mutation-R - were designed and are complementary in sequence therefore allowing the first two PCR products generated in Step 1 to be "sewn" together in Step 2. The gDNA in Step 1 already contains the selectable marker downstream of the ORF. The final PCR product is purified (2.2.7) and contains the ORF with the desired point mutation plus a selectable marker cassette. This final PCR product is transformed (2.2.11) into a yeast strain in which the ORF of interest has already been deleted using the method outlined in **Figure 2.1**. Correct chromosomal integration was confirmed using the F1 and Chk-R primers as illustrated in **Figure 2.3** Step 1. Mutations were confirmed by DNA sequencing (2.2.8).

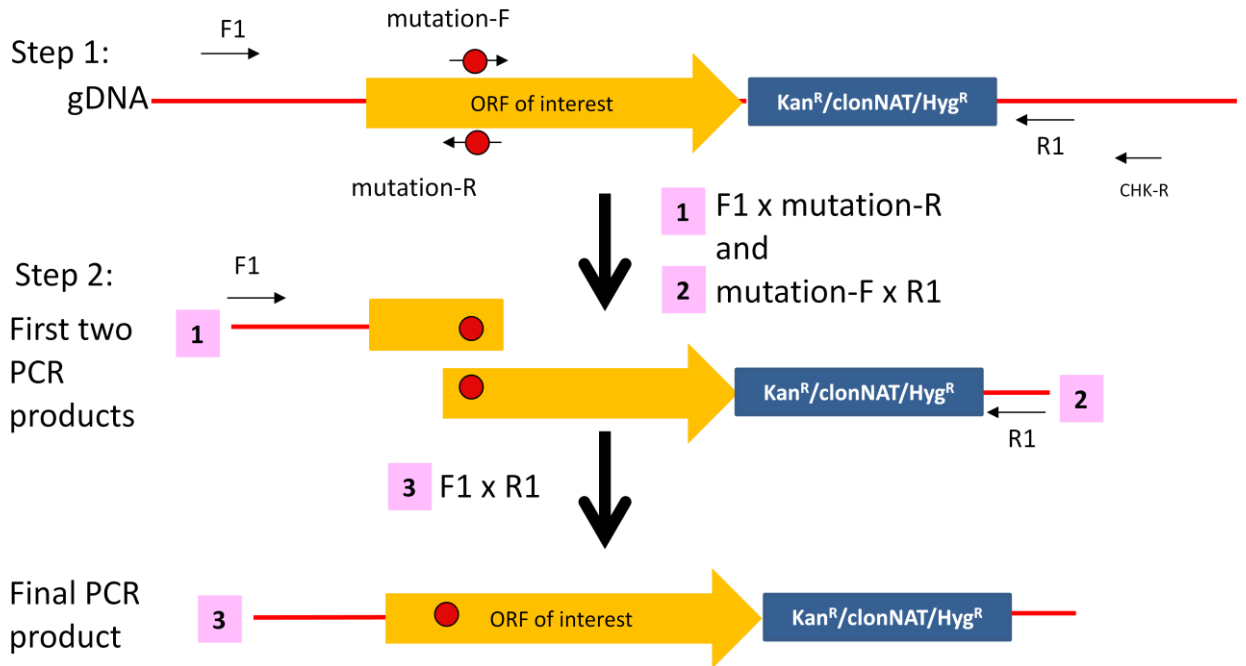


Figure 2.3 Site-directed mutagenesis

A two step PCR approach was used to generate a DNA fragment containing a specific point mutation. Step 1 amplified the 5' and 3' flanking regions of the ORF and also incorporates the sequence of the desired mutation from the specifically designed mutation primers (mutation-F and mutation-R). Step 2 "sews" the two products together using the F1 and R1 primers to create the final PCR product which is transformed into yeast, usually into a strain where the ORF of interest has already been replaced with a deletion cassette by the method illustrated in **Figure 2.1**.

2.2.10 Checking for correct chromosomal insertion

Correct chromosomal integration of fragments was carried out using PCR and the Paq5000 DNA polymerase. Genotyping was carried out using specifically designed CHK (check) primers. The location of the CHK primer is usually in the 3' flanking region of the gene of interest but further downstream than the R1 primer (**Figure 2.3** Step 1 right hand side for an example). If a PCR reaction consisting of F1 and the CHK-R primer gives a product of the expected size then the fragment is confirmed as correctly integrated into the genome at the endogenous locus.

2.2.11 Yeast Transformations

Yeast transformations followed the TRAF0 method outlined in (Daniel Gietz & Woods,). A small amount of the desired host strain were grown in 5 ml of YE+adenine media overnight. Most of the cells of the overnight culture were in a stationary phase and were diluted 1:10 and re-grown for another 3-4 hours to obtain an exponentially growing culture. Cells were centrifuged at 3000 rpm for 1 minute and resuspended in 1 ml 0.1M LiOAc. Roughly $2.5-5 \times 10^7$ cells were required for one transformation reaction therefore the resuspended cells were divided into the appropriate number of eppendorf tubes. Cells were pelleted at 3,000 rpm for 15 seconds and the LiOAc completely removed with a pipette.

The following were then added per reaction:

120 μ l PEG 3350 (50% w/v) (Sigma)

18 μ l 1M LiOAc (Sigma)

25 μ l freshly boiled and denatured salmon sperm DNA (SIGMA, 2mg/ml)

17-x μ l sterile water

X μ l plasmid DNA (usually 7-10 μ l of PCR product or 2 μ l of plasmid DNA, equivalent of 150-300 ng of DNA)

Total reaction volume is 180 μ l total

Cells were gently resuspended and incubated at 30°C for 1 hour (up to overnight).

Cells were then heat shocked at 42°C for 15 minutes, gently centrifuged, the

supernatant removed and resuspended in 100-200 µl of sterile water to aid plating and plated onto appropriate agar plates.

This method was used to transform yeast with both purified PCR fragments and plasmids isolated from *E.coli*. For gene disruption and selection using an antibiotic resistance marker, following the transformation and heat shock, cells were plated onto YE+ade plates and replica plated 24-hours later onto YE+ade plates supplemented with the appropriate antibiotic. Positive selection of clones following transformation of pREP plasmids (with LEU2 marker) was achieved by direct plating of cells onto SD+ade plates.

2.2.12 Induction of meiotic differentiation

2.2.12.1 SPA spot

To induce meiosis in cells for the purpose of visualising the meiotic phenotype of a strain, cells were grown overnight in 5 ml YE+ade, washed three times with MM-N, resuspended in 50x Leucine+Uracil (10 mg/ml) and densely spotted onto an SPA plate. Alternatively, cells were densely resuspended in MM-N and spotted onto an SPA plate containing Leucine (0.2 g/L). Cells were usually visualised after 24-hours using a microscope.

2.2.12.2 liquid assay system

The liquid mating assay system is described in detail in Chapter 3 Section 3.2.1 and depicted in **Figure 2.4**.

In order to obtain a large number of cells 5 ml YE+ade starter cultures of desired strains were inoculated 36 hours prior to the start of the assay, this culture was diluted around 16-hours later and then again a further 8-hours later to keep cells at a low density so

they do not start to starve. Cell cultures were routinely incubated at 30°C shaking at 210 rpm.

These cells were filtered and washed twice with minimal media containing no nitrogen (MM-N) to wash out all the nitrogen sources from cells as this inhibits the mating process. We chose to wash cells using filtration rather than centrifugation to limit the amount of stress the cells were subjected to. Cells were resuspended in MM-N to a defined cell density of 1×10^7 cells/ml. This represents time-point zero – the time that mating is induced. Cells were then placed back in a shaker with a shaking speed of 150 rpm. At the desired time-points, cells were collected, snap frozen in liquid nitrogen and stored at -80°C until all samples were collected after which cells were denatured and subject to western blotting.

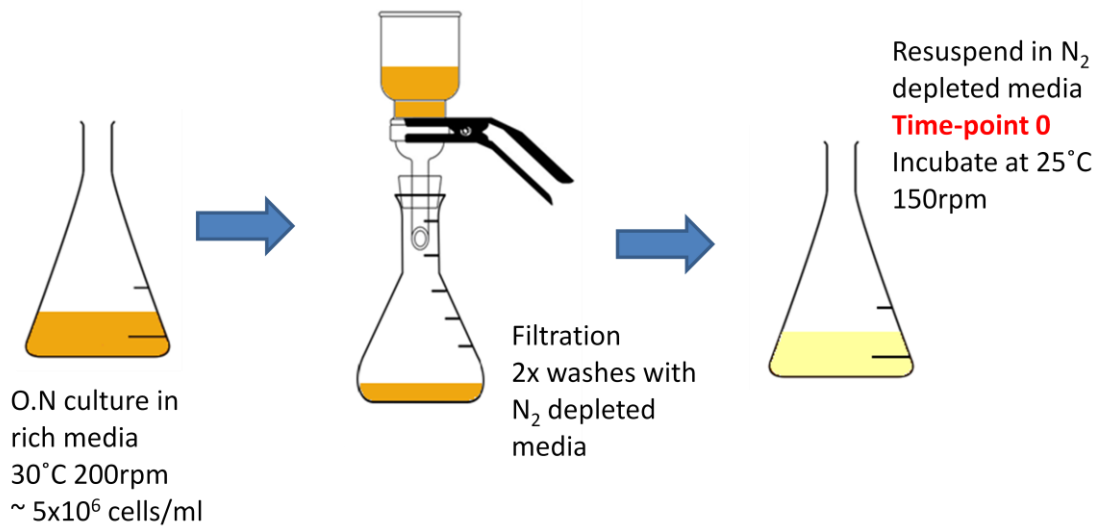


Figure 2.4 Liquid mating assay.

Illustrated here is the liquid mating assay system used to activate the MFSP and collect cells at desired time points to make whole cell protein extracts. The assay is set up as follows: cells are grown in rich media (YE+ade) to generate vegetatively growing cells. The culture is filtered and washed twice with minimal media containing no nitrogen (MM-N) to wash out all the nitrogen sources. The cells are resuspended in MM-N to a defined cell density of 1×10^7 cells/ml. This represents time-point zero – the time that mating process is induced. Cells are then collected at the desired time-points, a very small volume is taken for imaging (100 μ l) the rest is added with PMSF (1mM final), spun down, washed with Cdc2-Stop buffer with PMSF, spun down again, snap frozen in liquid nitrogen and stored at -80°C until required ready for preparation of whole cell extracts.

2.2.12.3 Plate assay system

The plate mating assay system is described in detail in Chapter 3 Section 3.2.2 and depicted in **Figure 2.5**. Large scale starter cultures of vegetatively growing cells were set up in the same way as for the liquid assay. Following the initial washes with MM-N, the cells were resuspended to roughly a cell density of 1×10^7 cells/ml. The cell density was calculated using a hemocytometer and a defined number of cells (8×10^7 cells) re-filtered onto a PDVF membrane (45 μ m diameter, Millipore). Filters were placed onto sporulation agar (SPA+Leucine 0.2 g/L) plates and at each time-point one membrane was removed, cells were collected and snap frozen ready for denaturation and western blotting.

2.2.13 Collection of Cells - The Cdc2 STOP buffer method vs. the Trichloroacetic acid (TCA) method

- Liquid Assay

A plus nitrogen (also known as time zero) sample of cells were harvested before the cells were washed and filtered to induce mating from the large mitotic cell cultures. During the optimisation of mating assay conditions using the liquid assay system, harvesting of cells at each time-point used the cdc2-STOP buffer method (Moreno *et al.*, 1991). We aimed for around 1.5×10^8 cells/tube, the required volume of cell culture was poured into a 50 ml tube, 100 mM PMSF (Sigma) was added while the culture was still at 30°C and cells were spun down (1 minute 3000 rpm). The supernatant was discarded, cells were resuspended in cdc2-stop buffer (50mM NaF, 10mM EDTA, 1mM NaN₃, 150mM NaCl, 1mM PMSF), transferred to tubes capable of storage at -80°C, spun down again, the supernatant completely removed and snap frozen in liquid nitrogen, Samples were stored at -80°C ready for denaturation by the RIPA buffer method - See "Preparation of total protein extracts" Section 2.2.15.

- Plate Assay

This harvesting method was quickly switched to that of the TCA method for the plate mating assay when it became apparent that there was a significant amount of protein degradation using the *cdc2* STOP-buffer method. At each time-point, one membrane was removed from the SPA plate and placed into a 50 ml tube containing 5 ml 20% TCA (Acros Organics), this was shaken by hand to remove cells from the membrane.

The tube was briefly centrifuged (~5 seconds) and the membrane removed from the tube. The tube was then centrifuged for 1 minute at 2000 rpm to pellet cells.

Supernatant was removed, cells were resuspended in 1 ml 20% TCA and transferred to a tube capable of storage at -80°C, cells were pelleted again using a bench top centrifuge, supernatant completely removed and the tube snap frozen in liquid nitrogen. Tubes were stored at -80°C ready for denaturation.

2.2.14 Calculating mating efficiency

Between 300-1400 cells were counted at each time-point and classified as either mating or non-mating. Percentage mating was calculated by dividing the number of cells mating by the total number of cells counted.

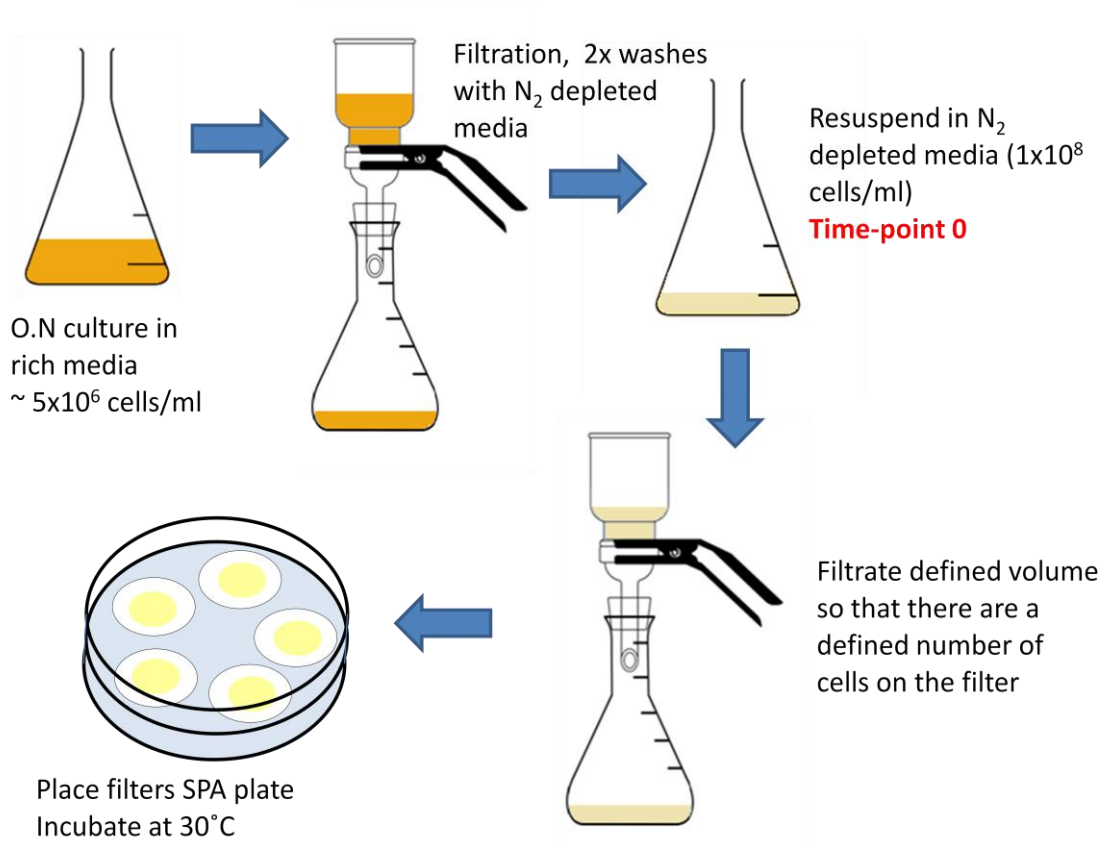


Figure 2.5 Plate mating assay

Illustrated here is the plate mating assay system established in Chapter 3. The assay was set up as follows: vegetative cells were prepared in rich media which are filtered and washed twice with minimal media containing no nitrogen (MM-N) to wash out all the nitrogen sources. The cells are resuspended in MM-N to a roughly a cell density of 1×10^7 cells/ml. This represents time-point zero – the time that mating is induced. The cell density is calculated using a hemocytometer and 8×10^7 cells re-filtered onto a PDVF membrane (Millipore). Filters were then placed onto sporulation agar (SPA) plates (50 ml SPA agar / 14cm diameter).

2.2.15 Preparation of total protein extracts (WCE)

Preparation of whole cell protein extracts was either by the RIPA method or TCA method outlined below. Both methods use 3x Laemmli Sample Buffer (Laemmli, 1970):

3x Laemmli sample buffer:

240 mM Tris-CL pH6.8
6% SDS
30% Glycerol
16% β -mercaptoethanol
0.0075% bromophenol blue

RIPA method

RIPA buffer :

10 mM Na-Phosphate pH7
1% Triton X-100
0.1% SDS
2 mM EDTA
150 mM NaCl
50 mM NaF

1 ml RIPA + 1 Protease inhibitor tablet (Roche complete, mini EDTA-free protease cocktail inhibitor tablets 04693159001) + 10 μ l PMSF (100mM)

Sample were taken from the -80°C freezer and 200 μ l of RIPA buffer added to each sample, these were heated for 6 minutes at 95°C before the addition of 500 μ l of acid washed glass beads (Sigma). Samples were lysed in a Fastprep24 machine (speed 6.5 x 20 seconds x 4 with 20 seconds intervals) in a 4°C room. Cell extracts were collected by piercing each tube with a needle, putting each tube into a collection tube, then placing both tubes into 50 ml tube and centrifuging at 4°C for 1 minute at 2000 rpm. 200 μ l of 3x Laemmli sample buffer were added to each sample which was then heated for 6 minutes at 95°C . Samples were stored at -20°C .

TCA method

This method is based on that described by Keogh lab Protocols (<https://sites.google.com/site/mckeogh2/protocols>)

All steps were performed on ice unless otherwise stated. Cell pellets were thawed on ice and resuspended in 250 µl 20% TCA. 250 µl of acid washed glass beads were added and samples chilled on ice for 5 minutes. Samples were lysed in a FastPrep24 cell beater (speed 6.5 x 1 minute x 3 with 1 minute intervals). Cell extracts were collected by piercing the bottom of tubes with a needle and placing them into collection tubes and centrifuged at 2000 rpm for 1 minute. Beads were washed with 300 µl of 5% TCA and centrifuged at 2000 rpm for 1 minute, this was repeated twice. The contents of the collection tube were transferred to an 1.5 ml tube and centrifuged at 14K rpm for 10 minutes at 4°C. The liquid was discarded and the cell pellet washed with 750 µl of 100% ethanol. Tubes were centrifuged briefly (~1min 14000rpm) again. Ethanol was completely removed with a pipette and the pellet resuspended in 100 µl 1M Tris pH8.0 and 100 µl 3x Laemmli sample buffer. Cell extracts were then heated for 5 minutes at 95°C, centrifuged for 5 minutes at 14K rpm and the supernatant transferred to a fresh 1.5 ml tube. Samples were stored at -20°C.

2.2.16 Western Blotting**2.2.16.1 SDS-PAGE**

Protein extracts were subject to SDS-PAGE using the BioRad Criterion Cell gel electrophoresis system and 26-well-10% BioRad precast gels (Criterion TGX). Before loading, the protein samples were heated at 95°C for 5 minutes and briefly centrifuged. Gels were routinely ran at 180V for around 1 hour until the protein samples had reached the bottom of the gel. Proteins were transferred from the gel to Immobilon-FL PVDF membrane (Millipore) using the BioRad Criterion Blotter, transferring at 0.35A for 1

hour. Membranes were routinely stained with Ponceau (Acros Organics) to determine whether protein transfer was successful and for trimming of the PVDF membrane.

Membranes were blocked for a minimum of 1-hour in Odyssey Blocking Buffer (Licor) diluted 1:1 in PBS. This was followed by primary and secondary antibody incubation as outlined in 2.2.17.

2.2.16.2 Western blotting buffers

1x Running buffer:

25 mM Tris (Melford)
192 mM Glycine (Fisher)
1% SDS

1x Transfer buffer:

48 mM Tris
39 mM Glycine

TBST:

154 mM NaCl
20 mM Tris-HCL pH 7.4
0.05% Tween 20

2.2.16.3 Detection and quantification

The Odyssey CLx infrared Imaging System was used for detection of protein bands on western blots. Quantitation of proteins was carried out using the Image Studio V2.1 supplied with the Odyssey CLx scanner. The background method used was median with a border of 3 pixels to the left and right of quantitation boxes.

2.2.17 Established protocol for measuring phospho-Spk1 by western blotting

Protein extracts were subject to western blotting using BioRad 10% precast gels and the Criterion electrophoresis and blotting systems as outlined above. Proteins were transferred to Immobilon-FL PVDF membranes (Millipore) at 0.35A for 1 hour. and

blocked using Odyssey Blocking Buffer (OBB) diluted 1:1 in PBS for a minimum of 1 hour. Primary antibody incubation was carried out over night with the anti phospho-ERK antibody (Cell signalling #4370, 1:2000), the monoclonal anti GFP antibody (Roche, 0.4 mg/ml, 1:2000) and the α -tubulin antibody, TAT1 (generous gift from Keith Gull, 1:3000) diluted in OBB 1:1 in PBS. Membranes were washed 3x 10 minutes with TBST whilst gently shaking followed by secondary antibody incubation (IRDye 680LT goat anti-mouse 1:16,000, IRDye 800CW goat anti-rabbit 1:16,000, 0.01% SDS, 0.1% Tween 20 in OBB 1:1 PBS) for 1 hour in the dark to prevent fluorophore bleaching. This was followed by 2x 10 minute TBST washes and a 1x 10 minute TBS wash before scanning on the Odyssey CLx infrared Imaging System and protein quantitation using the Image Studio V2.1 software.

2.2.18 Live Cell Imaging

The Nikon Eclipse Ti-E microscope stand equipped with CoolLED PreciSExcite High Power LED Fluorescent Excitation System was used for live cell imaging. Imaging was used to capture the morphology of cells and the localisation of the GFP-tagged Spk1 MAPK during mating time-courses. Images were taken at each time-point in both the brightfield and GFP channels in order to visualise Spk1-GFP. Each time point comprises 15-25 serial images of 0.4 μ m interval along the Z axis taken to span the full thickness of the cell. All of the Spk1-GFP images were deconvolved using the Huygens Essential Deconvolution. Deconvolved images were Z-projected, cropped and combined using ImageJ.

CHAPTER 3 ASSESSMENT OF MAPK ACTIVATION IN RESPONSE TO PHEROMONE

3.1 Introduction

Schizosaccharomyces pombe grow vegetatively in rich media by binary fission but can undergo sexual differentiation when starved of nutritional sources - the main source being nitrogen. The process of meiotic differentiation involves exchanges of parts of homologous chromosomes (meiotic recombination), that generate genetic diversity, and formation of four haploid spores which can remain dormant for prolonged periods of time and will only germinate once transferred to rich media. Activation of the mating factor signalling pathway (MFSP), which contains the Ras1-MAPK pathway, is one of the initial steps of meiosis in *S.pombe*.

A schematic representation of the MFSP is presented in **Figure 3.1**. The pathway is activated when mating pheromone binds to a G-protein coupled receptor (GPCR) at the cell surface. This binding activates the G-protein, Gpa1, which relays the signal to the Ras1 guanine nucleotide exchange factor (GEF), Ste6, which promotes the GDP for GTP exchange on Ras1. Activated Ras1 activates a MAPK cascade consisting of a MEKK (Byr2), a MEK (Byr1) and a MAPK, (Spk1). As with all MAPK cascades both the MEK (Byr1) and MAPK (Spk1) are activated by a series of dual phosphorylations by the upstream kinases. Once activated, Spk1, activates the major meiosis transcription factor (TF) Ste11, which translocates to the nucleus and activates a number of genes responsible for progression through meiosis. The pathway is subject to negative regulation by Sxa2 (mating factor protease), Rgs1 (regulation of Gpa1) and Gap1 (GTPase activating protein for Ras1). In addition, the MAPK phosphatases Pmp1 and Pyp1 may play a role in the dephosphorylation of Spk1 (Didmon *et al.*, 2002).

One of the major aims of this work was to decipher why *ras1.val17* and *byr1.DD* have different mating phenotypes. For this purpose we required a readout of the activity of the MFSP and proposed that direct quantitation of the activation of the MAPK Spk1 was an ideal system.

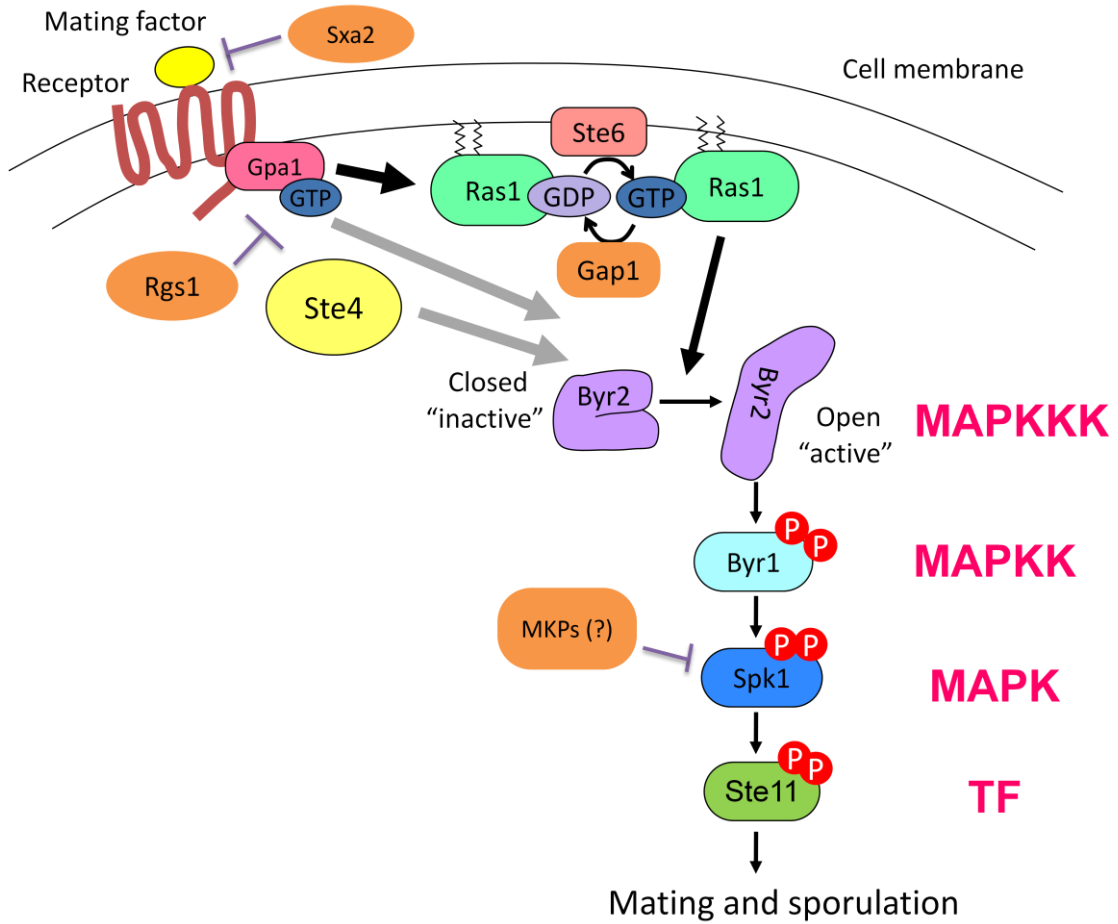


Figure 3.1 The mating factor signalling pathway

A outline of the structure of the pheromone response pathway in *S.pombe*. Activation of a GPCR leads to dissociation of the G-protein, Gpa1 which along with Ras1 activates the three-tiered MAPK cascade, Byr2-Byr1-Spk1. Spk1 directly phosphorylates the transcription factor Ste11. Full activation of Ste11 is required to activate the meiotic gene programme for successful meiosis.

Although quantitation of MAPK activity is important information to aid in our understanding of the RAS-MAPK cascade, no assay system to measure MAPK activation quantitatively was available. For that purpose, a highly synchronous cell population is required. When cells commit to meiotic differentiation, they firstly need to come to the G1 phase of the cell cycle from where they can differentiate. Previous studies show that after depleting the nitrogen source, cells complete an additional two cell cycles before arresting in G1 from where cells can start sexual differentiation (Nurse, 1985). When cells were forced to start meiotic differentiation from G2 phase of the cell cycle, using a *pat1* temperature sensitive mutant (see below), defects in meiotic recombination and chromosome segregation were observed and therefore, it is believed that starting meiotic differentiation from the G1 phase of the cell cycle is crucial for successful sexual differentiation (Nurse, 1985; Watanabe & Yamamoto, 1994). This means that when an asynchronous vegetative culture is sent into meiotic differentiation by simply depleting the nitrogen source from the culturing media, there will be a time delay of one cell cycle between the first cell and the last cell that commits to the meiotic differentiation. To circumvent this problem, *h⁺/h⁻ pat1.114/pat1.114* diploid cells have been used as a conventional tool (Beach *et al.*, 1985; Iino & Yamamoto, 1985). In this system, before letting cells start meiosis, cells are arrested (synchronised) in G1 by nitrogen starvation at 25°C. It is possible to arrest cells but not let them proceed into the sexual differentiation in this system as the mating type of the cells is *h⁺/h⁻* i.e. cells only carry the M-type mating cassette and therefore there is no Mat-pi expressed to work in collaboration with Mat-mi to induce *mei3* expression to inhibit Pat1 and Pat1 will remain active until cells are shifted to the restrictive temperature. Once cells are arrested in G1, the temperature is shifted up to 34°C to inactivate Pat1 and meiosis starts synchronously (**Figure 3.2**). Recently, this synchronous system was further

modified to employ *pat1.114 mat1-Pc* strain to have synchronous meiosis with pheromone signalling (Funaya *et al.*, 2012) which is required for normal chromosome segregation (Yamamoto *et al.*, 2004).

Unfortunately however, for the mating process between haploid cells, there is no such system and simply replacing the culture media means a time lag of the period that corresponds to the one cell cycle (about 2.3 hours at 30°C in YE+ade) will occur between a cell which is about to arrest at G1 and a cell that has just started DNA synthesis (S phase). Furthermore, most of the works looking at the transition from the vegetative cell cycle to meiotic differentiation, during which period the mating process occurs, employ liquid cultures that do not result in a high mating efficiency therefore we needed to establish a condition that allows us to reproducibly prepare highly synchronous mating cells with which we can measure the Spk1 MAPK activation status.

The first objective of this project was to establish a meiotic assay system in order to collect cells and make whole cell protein extracts with the purpose of quantification of the total amount of Spk1 MAPK and the amount of activated Spk1 MAPK through the technique of quantitative western blotting. We wanted to be able to use the activation status of the MAPK as a readout for the activity of the MFSP.

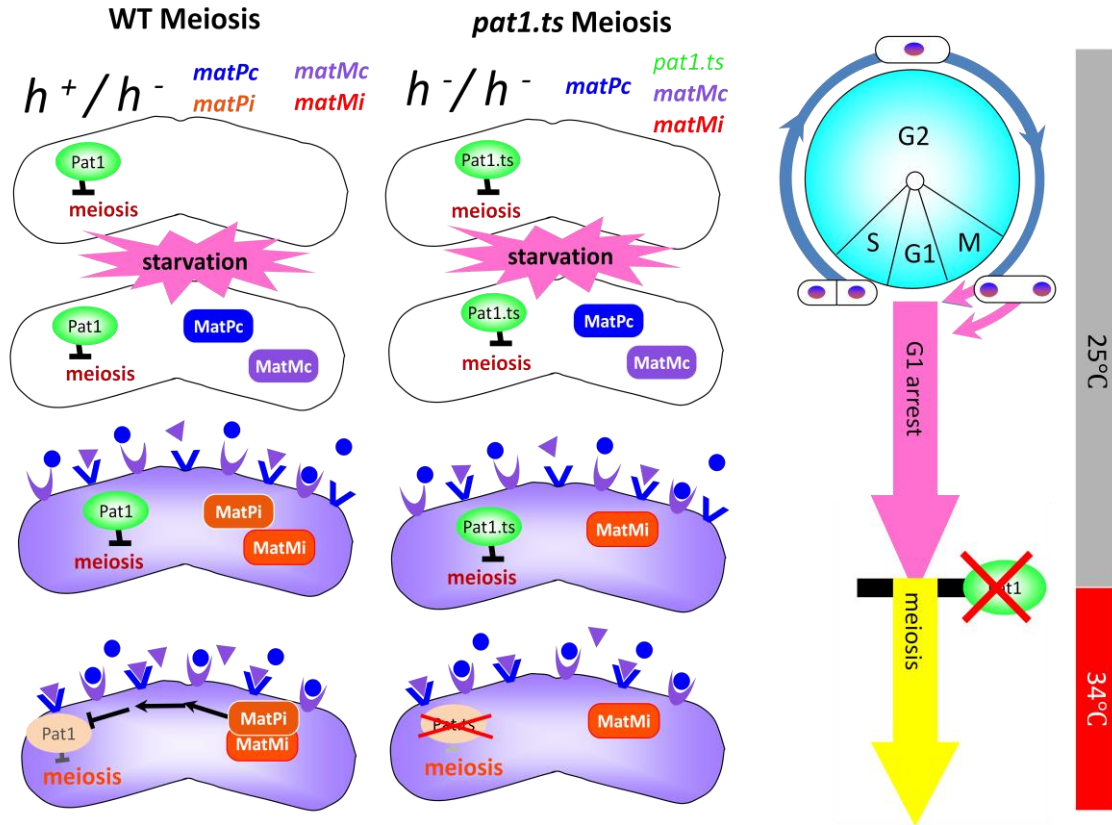


Figure 3.2 *pat1.114 (pat1.ts)* synchronous meiosis

Pat1 kinase inhibits meiosis in vegetatively growing diploid cells. The h^+/h^- diploid contains all four *mat* genes (*mat-Pc*, *mat-Pi*, *mat-Mc* and *mat-Mi*). Upon starvation, Mat-Pc and Mat-Mc induce the expression of both types of mating pheromone and receptor. Successful pheromone signalling allows expression of Mat-Pi and Mat-Mi which cooperate to inhibit Pat1 via Mei3, allowing entry into meiosis. In the h^-/h^- *pat1.ts* strain, cells are synchronised in G1 by starvation which allows the expression of Mat-Pc and Mat-Mc. Pheromone signalling is required for later stages of meiosis. Once cells are arrested in G1, a temperature shift from 25°C to 34°C inactivates Pat1 and cells enter into meiosis synchronously.

3.2 Establishing a mating assay system

3.2.1 Large scale liquid culture

The original aim was to establish a reproducible large scale synchronous sexual differentiation assay system in order to generate whole cell protein extracts from cells undergoing mating synchronously. Our first assay design was similar to that already established in the field to observe changes of gene expression profiles upon nitrogen starvation (outlined in **Figure 3.3**). Samples for the vegetatively growing cells were prepared from cells cultured in rich media (YE+ade). These cells were filtered and washed twice with minimal media containing no nitrogen (MM-N) to wash out all the nitrogen sources from cells as this inhibits the mating process. We chose to filter cells rather than centrifuge them in order to minimise the amount of stress to cells which could compromise mating efficiency. Cells were resuspended in MM-N to a defined cell density of 1×10^7 cells/ml. This represents time-point zero – the time that mating is induced. Cells were then placed back in a shaker with a shaking speed 150 rpm. At the desired time-points, cells were collected, snap frozen in liquid nitrogen and stored at -80°C until all samples were collected after which cells were denatured and subject to western blotting. It was quickly noted that the mating efficiency in a wild-type (WT) strain (KT301) was low (<10% after 24 hours). There are a few possible reasons for this. Firstly, as discussed earlier, the starting cells were completely asynchronous. Some cells that commit to the differentiation later than others may not be ready for mating while others were and others that were arresting at G1 without mating may have used up all the remaining energy/nutrition required for mating. Consequently, overall mating efficiency was low. Another reason may be due to the constant shaking of the culture which physically stopped cells from pairing up and diluted the pheromone gradients usually set up between mating pairs.

One of the challenges of mating assays was to make it reproducible between biological replicates. When cells were cultured in liquid media, cells started to get aggregated and generated clumps, which provide a widely variable micro-environment for those cells. This likely contributed to the high amount of variation seen between cultures in terms of mating efficiency and the variable levels of proteins in preliminary western blots (data not shown).

To define the signalling dynamics of the pathway to a high standard we had to optimise the mating assay to increase mating efficiency and synchronicity with the aim to mimic a more physiological condition and to minimise the variation seen between biological replicates.

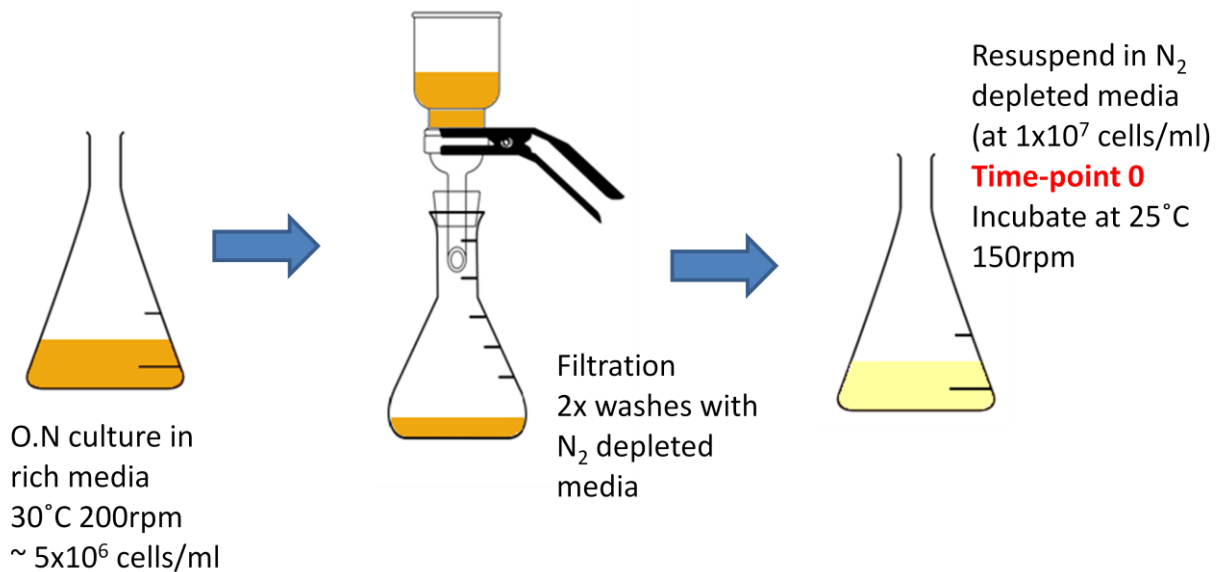


Figure 3.3 Liquid mating assay.

Illustrated here is the liquid mating assay system used to activate the MFSP and collect cells at desired time points to make whole cell protein extracts. The assay is set up as follows: cells are grown in rich media (YE+ade) to generate vegetatively growing cells. The culture is filtered and washed twice with minimal media containing no nitrogen (MM-N) to wash out all the nitrogen sources. The cells are resuspended in MM-N to a defined cell density of 1×10^7 cells/ml. This represents time-point zero – the time that mating process is induced. Cells are then collected at the desired time-points, a very small volume is taken for imaging (100 μ l) the rest is added with PMSF (1mM final), spun down, washed with Cdc2-STOP buffer with PMSF, spun down again, snap frozen in liquid nitrogen and stored at -80°C until required.

3.2.2 Agar Plate Assay

The liquid assay was modified as shown in **Figure 3.4**: following the initial washes with MM-N, WT cells (KT301) were resuspended to roughly a cell density of 1×10^8 cells/ml. The cell density was calculated using a hemocytometer and a defined number of cells re-filtered onto a PDVF membrane (Millipore). Filters were placed onto sporulation agar (SPA) plates and at each time-point one membrane was removed, cells were collected and snap frozen ready for denaturation and western blotting. Details of the cell collection process are outlined in Materials and Methods and in Section 3.3 of this Chapter. Mating efficiency of cells at specific time-points after the shift to minimal media was calculated by counting between 300-1400 cells and classifying them as either mating or non-mating. Percentage mating was calculated by dividing the number of cells mating by the total number of cells counted.

A number of optimal parameters had to be determined for optimal mating efficiency and whole cell extraction/denaturation. Firstly and most importantly an optimal density of cells on each membrane had to be determined. Different cell densities were tested ranging from 2.5×10^7 - 1×10^8 cells/membrane. Lower densities were quickly discarded as well as the highest density of 1×10^8 cells/membrane as the lower densities were not as efficient and at the highest density zygotes looked unhealthy and contained large vacuoles. An optimal cell density of 8×10^7 cells/ml was chosen as this density gave a high mating efficiency (see Table 3.1).

A preliminary experiment with cells spread directly onto an SPA plate with no leucine indicated that leucine was an important component of the SPA for these cells, that carry the leucine auxotroph (*leu1.32*), to undergo meiosis. Therefore two different concentrations of leucine, 0.2 g/L and 0.4 g/L, were tested. A concentration of 0.2 g/L, that has been used to supplement synthetic media for vegetative growth, was optimal

and the higher concentration such as 0.4 g/L reduced the mating efficiency although it did not apparently affect the vegetative cell growth. It has been reported that leucine stimulates the TORC1 complex, a signalling node that acts as a sensor for nutritional condition (Alvarez & Moreno, 2006). In fission yeast, TORC1 involves Tor2 that needs to be inactivated to allow sexual differentiation. Hence, it is possible that an excess amount of leucine activated Tor2 to slow down the onset of sexual differentiation.

Also noted during these optimisation experiments was the importance of the initial starter culture cell density to achieve an homogenous cell population that will respond to the environmental change in a similar manner leading to higher synchronicity. If the cell density is over the limit of the exponential growth, some cells start to arrest at G1 already while others still continue the vegetative cell cycle. Different starter culture cell densities were tested as shown in Table 3.1. The difference in mating efficiency between experiments 3 and 4 is likely due to the difference in the starter culture densities. Originally we predicted that the rich YE+ade media was capable of sustaining vegetative growth up to about 1.2×10^7 cells/ml, and the aim was to get the vegetative culture to a density of roughly 1×10^7 cell/ml. Following the preliminary experiments that showed a clear link between the cell density of the vegetative culture before sending them to sexual differentiation and the mating efficiency profile, great care was taken to control the starter culture density with the aim of achieving $5-7 \times 10^6$ cells/ml.

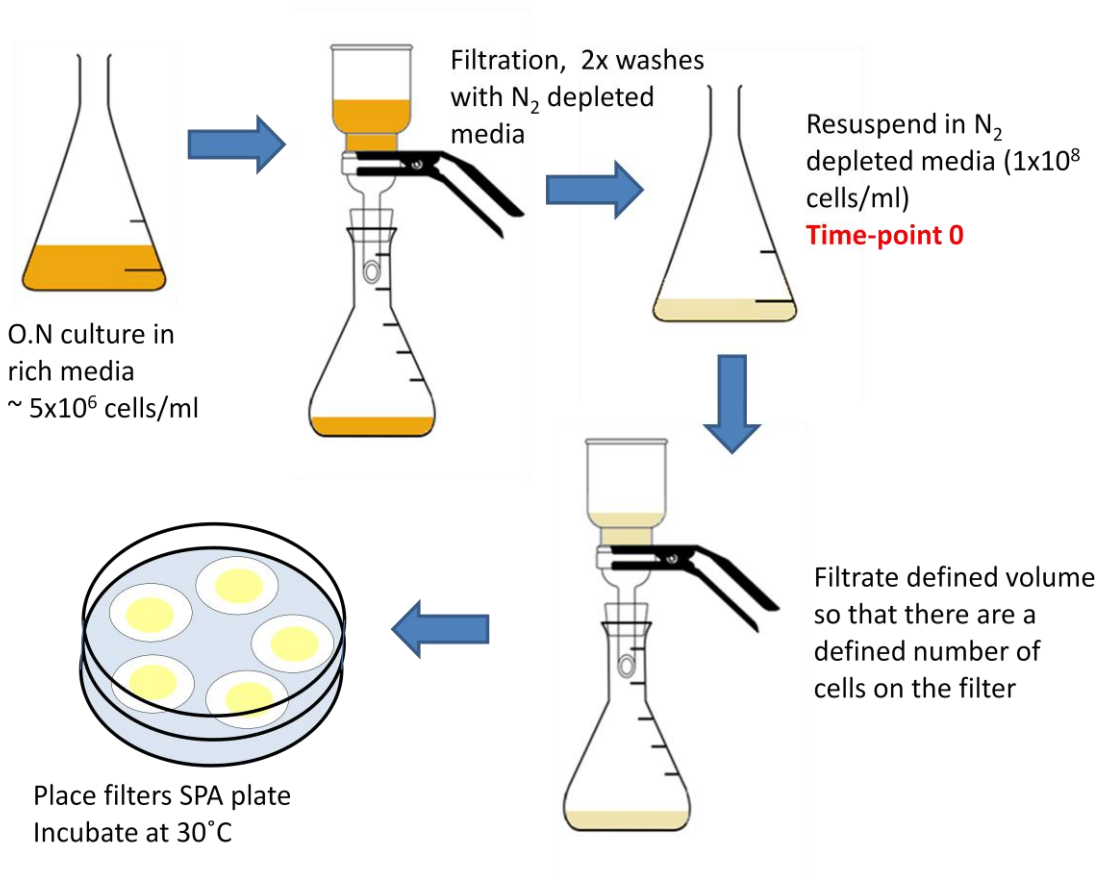


Figure 3.4 Plate mating assay

Illustrated here is the established plate mating assay system. The assay was set up as follows: vegetative cells were grown in rich media which are filtered and washed twice with minimal media containing no nitrogen (MM-N) to wash out all the nitrogen sources. The cells are resuspended in MM-N to a roughly a cell density of 1×10^8 cells/ml. This represents time-point zero – the time that mating is induced. The cell density is calculated using a hemocytometer and a defined number of cells re-filtered onto a PDVF membrane ($45 \mu m$ diameter, Millipore). Filters were placed onto sporulation agar (SPA) plates (50ml SPA agar / 14cm diameter) and incubated at $30^\circ C$.

Experiment	Cell density on PVDF filter on SPA plate (cells/ml)	% Mating at 16 hours post meiotic induction	Starter culture cell density (cells/ml)
1	7×10^7	65	1.7×10^7
2	8×10^7	75	5×10^6
3	8.5×10^7	82	4.5×10^6
4	8.5×10^7	70	1.3×10^7

Table 3.1. Summary of Cell density optimisation for the plate assay

A summary of the optimisation experiments for the plate mating assay. Outlining the major controllable variables; the cell density on the membranes was the main variable controlled in these experiments but starter culture density was also found to play an important role in the overall mating efficiency of a culture. Highlighted in pink are the conditions chosen for future time-courses.

A specific aim of this assay was to provide a system where this high mating efficiency was repeatable between biological replicates. To determine whether this was achievable, three biological replicates using the WT strain KT3082 (WT containing Spk1-GFP integrated at the Spk1 chromosomal locus - see 3.4.1) were undertaken and the mating efficiency determined every hour over a sixteen hour period. This data is presented in **Figure 3.5**.

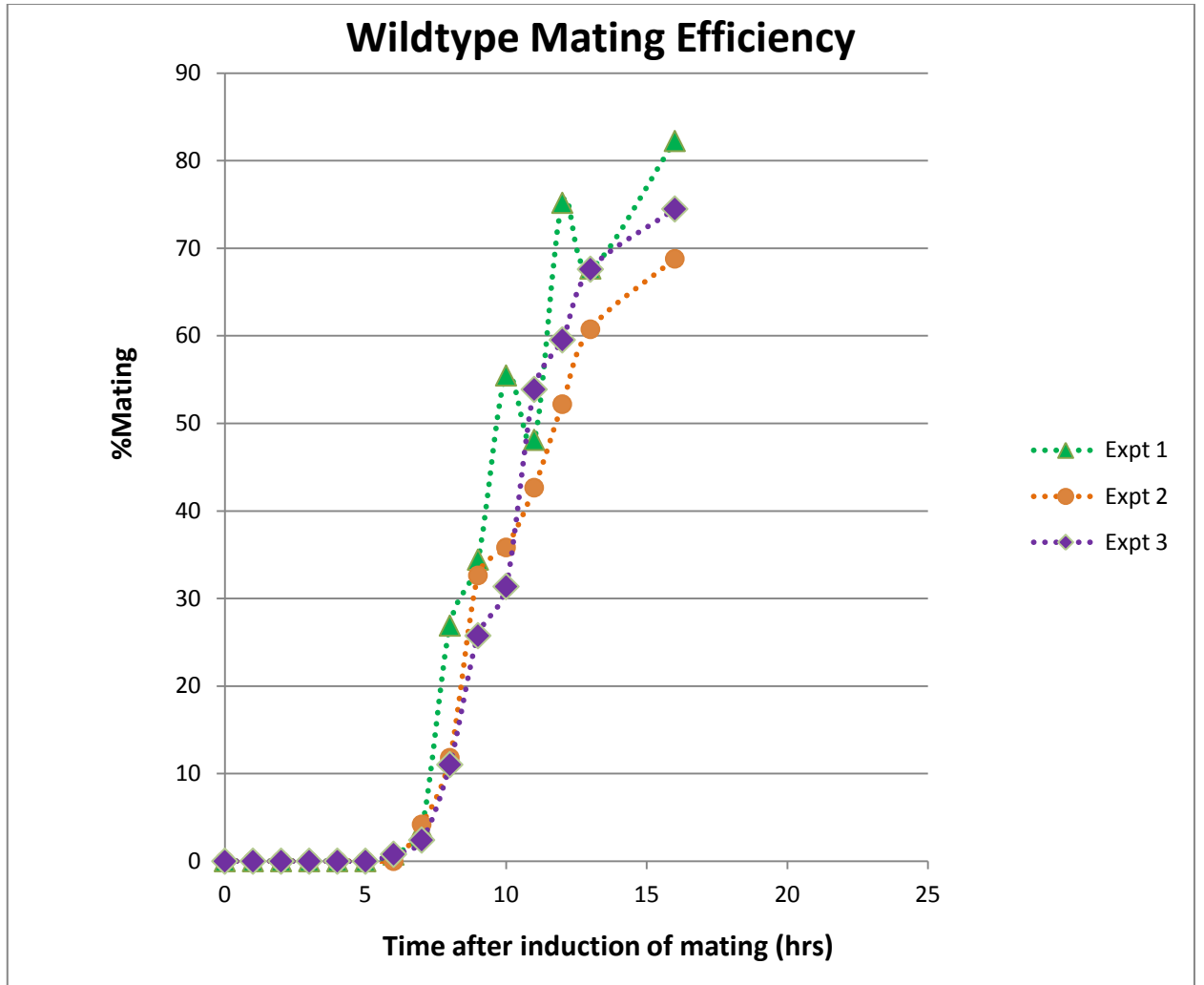


Figure 3.5 Quantification of WT mating efficiency using the Plate assay

A graphical representation of mating efficiency for three wild-type biological replicates (strain KT3082). The percentage of cells mating was calculated as described in the text.

We conclude that the plate assay is highly repeatable in terms of mating efficiency (70-80%) (**Figure 3.5**) and timing of mating is highly synchronised. Therefore the plate assay was used for all further experiments as our mating assay system.

3.3 Denaturation of Cell Extracts

Following the establishment of the plate assay there were two potential methods of removing the cells from the membranes and preparing whole cell protein extracts. The first involved the pre-treatment of cells with excess amount of PMSF (1.5mM final concentration) at the physiological culturing condition (30°C) for 2 minutes to inhibit autophagy activity followed by rinsing the cells with Cdc2-STOP buffer containing PMSF (50 mM NaF, 10 mM EDTA, 1 mM NaN₃, 150 mM NaCl, 1 mM PMSF), cells were collected by centrifugation and snap frozen in liquid nitrogen. Denaturation was by the RIPA buffer method outlined in Materials and Methods (2.2.13). The second option was to use the trichloroacetic acid (TCA) method which is also outlined in Materials and Methods (2.2.13). In a number of preliminary experiments, we observed that there was a substantial amount of protein degradation seen when using the RIPA buffer method - which is used routinely in the lab for mitotic whole cell protein extraction. This protein degradation was not seen when using the TCA method. A possible explanation for this is that during meiosis, the autophagy (bulk protein degradation) and regulated proteasome degradation machinery within the cells is hyper-activated as the cell is undergoing a dramatic change in protein expression that involves highly regulated degradation and recycling of amino acids. Therefore, once the cell is disrupted and contents of cellular organelles, full of protease activities, are released, bulk protein degradation is expected to occur even in the presence of PMSF whereas TCA instantly denatures all the proteins preserving the protein state. A disadvantage of using TCA is that all protein activity is terminated instantly so the cell extracts cannot

be used to observe native protein function. Due to the vast amount of protein degradation seen using Cdc2-STOP buffer followed by RIPA buffer this was clearly not an option for preparing good quality protein extracts for these cells and the TCA method was used instead. An overview of the entire established protocol can be seen in **Figure 3.6**.

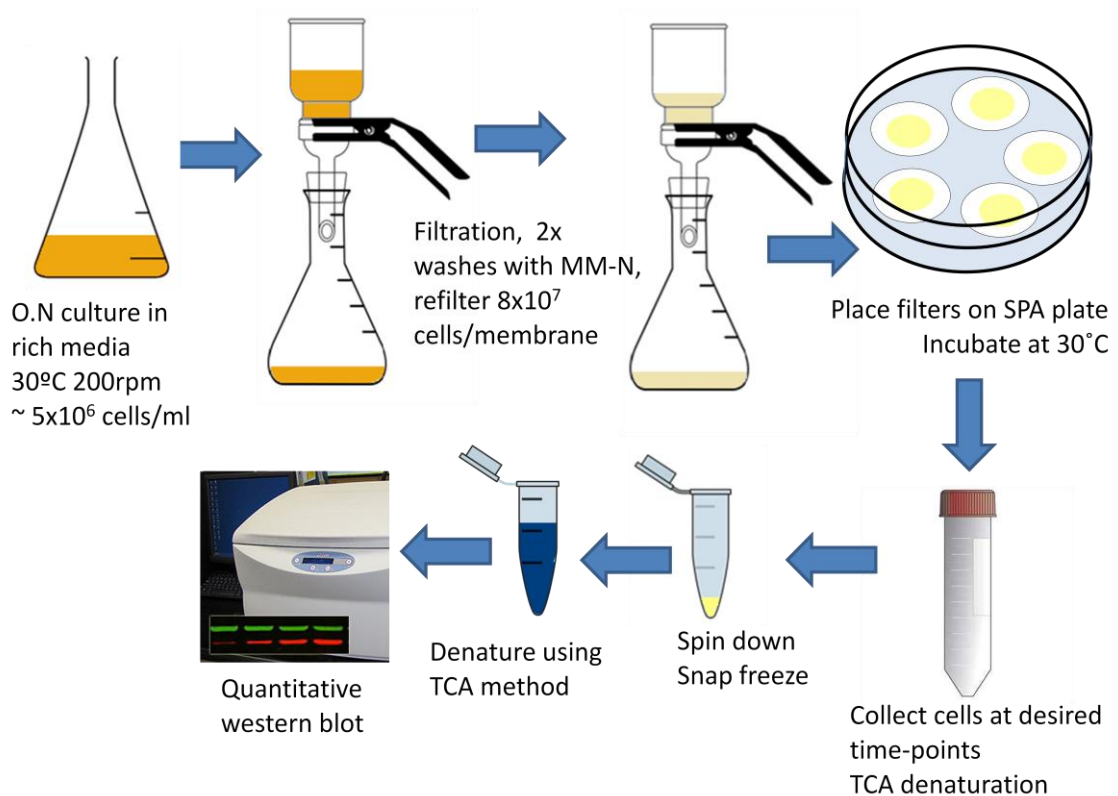


Figure 3.6 Experimental design for quantitative mating assay and protein extraction

A summary of the plate mating assay system used to activate the MFSP and collect cells at desired time points to make whole cell protein extracts to assess the activation status of the MAPK. The assay is set up as follows: vegetatively growing cells are prepared in rich media (YE+ade) which is filtered and washed twice with minimal media containing no nitrogen. The cells are resuspended in minimal media to a cell density of roughly 1×10^8 cells/ml. This represents time-point zero – the time that sexual differentiation is induced. The density of the cell culture is calculated using a hemocytometer and 8×10^7 cells are filtered onto a PVDF membrane (45 μm diameter, Millipore) using the filtration apparatus. Cells are then collected at the desired time-points. Cells are washed off the membrane in the presence of 20% TCA, spun down, snap frozen and stored at -80°C until required. Cells are denatured via the TCA method and subject to quantitative western blotting using the Licor Odyssey system.

In conclusion, the SPA plate mating assay provides us with an excellent tool to induce highly synchronous and efficient sexual differentiation in fission yeast cells. The density of the rich media culture is exceptionally important in influencing the overall mating efficiency, therefore for future experiments this was closely monitored and accurately calculated for each culture with the aim of achieving a density of no more than 7×10^6 cells/ml at the time of filtration. The number of cells on each membrane is defined as 8×10^7 cells and overall these conditions have given us a highly reproducible assay system to induce mating (**Figure 3.5**). The TCA method is used to denature the cells to make whole cell protein extracts as we found this gave us extracts with no obvious degradation in comparison to using the RIPA method.

Once the assay was established the next step was to validate the tools required to detect the amount of phosphorylated Spk1 MAPK as a readout for the activity of the MFSP.

3.4 Validation of the use of a phospho-ERK antibody to detect phospho-Spk1

3.4.1 Detection of Spk1 MAPK

There is currently no antibody available against Spk1. Generating Spk1 specific antibodies may allow us to use them as versatile tools in western blotting as well as immune-fluorescent microscopy to detect Spk1 in any fission yeast strains. However, it may be a labour intensive process if a recombinant Spk1 protein is not readily prepared and there is no guarantee that high affinity Spk1 antibodies would be generated.

Another approach for protein detection is protein tagging, provided that the tagging does not impair the protein function. Tagging may also be useful especially when the target protein is tagged with green fluorescent protein (GFP) as this may enable us to observe the cellular behaviour of the protein by live cell imaging.

For this purpose the *spk1* gene was tagged with GFP at the C-terminus, in order to use it both for western blotting and live cell imaging. The tag also contains 2xFLAG which may be useful for western blotting and Spk1 biochemical purification. The GFP-2xFLAG tag is marked with a kanamycin resistance cassette for selection purposes (GFP-2xFLAG:Kan^R). The method for C-terminally tagging a protein is outlined in Materials and Methods 2.2.9.2. Specifically for *spk1* tagging with GFP-2xFLAG:Kan^R the following PCR reactions were set up (See Oligonucleotide Table 2.2 for primer sequences):

1. Spk1-F1-Mark x Spk1-F2-gfp
2. Spk1-R1 x Spk1-R2
3. Spk1-F1-Mark x Spk1-R1

The generated PCR product was purified and transformed into the WT host strain KT301 using the TRAF0 method. DNA was extracted from positive colonies and the entire *spk1* gene fully sequenced to confirm no mutations had been introduced during the tagging process. Spk1-GFP-2xFLAG:Kan^R will be described as Spk1-GFP throughout the rest of this thesis. A 24 hour time-course was carried out using the WT strain KT301 and the WT strain containing Spk1-GFP, KT3082 (**Figure 3.7**). A monoclonal anti-GFP antibody (Roche) detected a band of the expected molecular weight of the Spk1-GFP-2xFLAG (69kDa) exclusively in the tagged strain (**Figure 3.7C**). Levels of α -tubulin were blotted for using the TAT1 antibody (1:3000) and are used as a loading control for protein quantitation. This blot confirmed that the Spk1-GFP protein is detected by the anti-GFP antibody and is induced upon nitrogen starvation.

3.4.2 Detection of phosphorylated Spk1 MAPK

We wanted to be able to detect the biologically active form of Spk1 MAPK. The reasoning behind trying a commercially available phospho-ERK1/2 antibody (Cell Signalling #4370), which is routinely used to detect the dually phosphorylated form of the mammalian ERK1/2 proteins, is illustrated in **Figure 3.7A**. MAPKs requires dual phosphorylation by the upstream MEK for activation, for ERK1, this dual phosphorylation is on the residues threonine 202 and tyrosine 204 of the conserved "TEY" motif (shown in orange in **Figure 3.7B**). The epitope for the phospho-ERK antibody is the dually phosphorylated residues and residues surrounding the motif. From the sequence alignment between ERK1, ERK2 and our MAPK of interest, Spk1, (**Figure 3.7B**) it appears likely that the mammalian designed antibody would detect the *S.pombe* Spk1 MAPK because of the number of conserved residues surrounding the TEY motif - shown in green. The western blot in **Figure 3.7C** was incubated with the

phospho-ERK1/2 (pERK) antibody which is a rabbit monoclonal antibody. Due to the nature of the Licor Odyssey scanning system multiple primary antibodies can be incubated on the same western blot at the same time and accurate detection of proteins of the same molecular weight can be achieved by using primary antibodies raised in different animals and secondary antibodies conjugated to different IRDyes detectable at different wavelengths (700 and 800 nm). **Figure 3.7D** shows a strong corresponding band at expected molecular weight of untagged Spk1 (42kDa) exclusively in the untagged protein extracts. There is also an exclusive band detected at the expected molecular weight of Spk1-GFP (69kDa) in lanes containing cell extracts from the tagged strain. This is evidence that the phospho-ERK antibody is detecting the fission yeast MAPK Spk1 and this is further confirmed when the blots scanned at the two wavelengths are overlaid (**Figure 3.7E**). There is a direct overlap between the protein detected with the GFP antibody and the protein detected with the phospho-ERK antibody. However, this does not validate that the phospho-ERK antibody is exclusively detecting the phosphorylated species of Spk1 and could be binding to unphosphorylated Spk1.

Figure 3.7F is a western blot to confirm that the phospho-ERK antibody is specifically detecting phospho-Spk1 and not just binding to the Spk1 protein in an unphospho-specific manner. Protein extracts were prepared from a time course experiment with a WT strain (KT3082) and a strain where the upstream kinase of Spk1 is deleted (*byr1Δ*, KT4300). Total Spk1 and Phospho-Spk1 have been blotted for at the same time using anti-GFP and anti-phospho-ERK antibodies. The WT time-course shows overlapping of both the green signal, which is the phospho-ERK antibody, and the red signal, which is the GFP antibody. Comparing this to the *byr1Δ* time-course, it is clear that there is no phosphorylation signal (i.e. no green signal is detected) yet there is still the GFP

signal in red which represents total Spk1 protein, therefore the pERK antibody is exclusively detecting the phosphorylated species of Spk1. The total amount of Spk1 is much lower in this strain mainly because expression of the MAPK is induced by positive feedback of the pathway which is missing in this strain.

To conclude, the commercially available phospho-ERK1/2 antibody (Cell Signalling #4370) has been validated as a tool for the detection of phosphorylated Spk1 MAPK. There are additional bands detected in **Figure 3.7D** possibly corresponding to other MAPKs present in fission yeast. One evident background band in **Figure 3.7D, E** and **F** is marked with a red asterisk and runs just below the band corresponding to Spk1-GFP but there is enough evidence provided to validate that the phospho-ERK antibody can specifically detect a quantifiable band corresponding to phosphorylated Spk1. This antibody was used as a tool for the detection of phosphorylated MAPK and therefore a direct readout for the activity of the MFSP at the level of the MAPK.

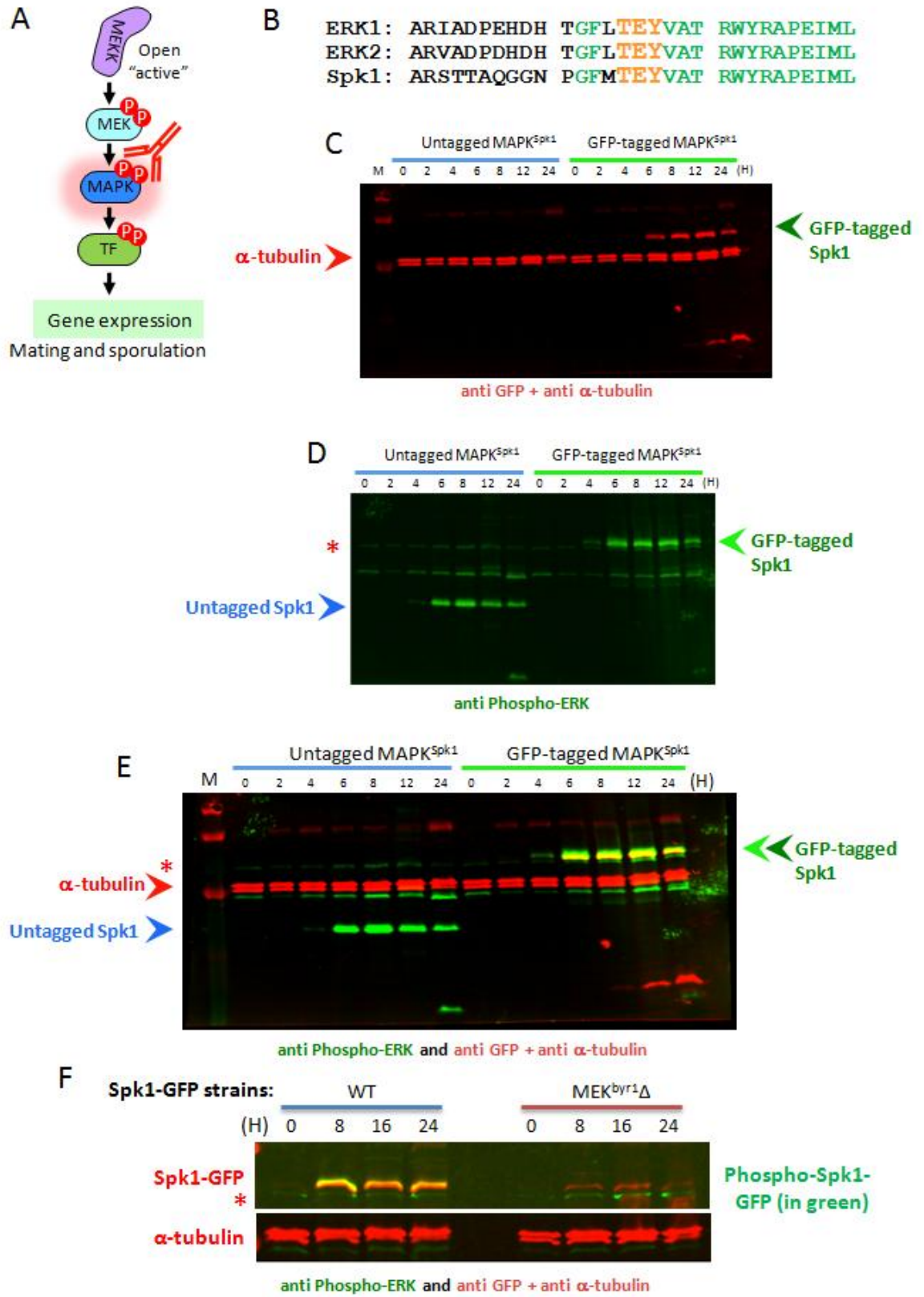


Figure 3.7: Validation of the use of a commercially available anti-GFP and anti-phospho-MAPK specific antibody.

(A) Schematic outlining the principal of a phospho-specific MAPK antibody. (B) Sequence alignment between mammalian ERK1, ERK2 and *S.pombe* Spk1 at the region of the dual phosphorylation required for activation (TEY in orange) and surrounding residues, conserved residues are highlighted in green. (C) Western blot of a time-course of a WT and a Spk1-GFP strain (KT301 and KT3082) over 24 hours and incubated with a primary monoclonal mouse anti-GFP antibody and the primary anti α -tubulin antibody TAT1, followed by the IRDye 680LT (goat anti-mouse) secondary antibody. α -tubulin was used as an internal loading control. (D) The same blot as in (C) but showing the 800 nm wavelength scan to detect signals from a phospho-ERK antibody (Cell Signalling #4370) visualised by the IRDye 800CW goat anti-rabbit secondary antibody. (E) An overlay of the 700 and 800 nm channels. (F) The phospho-ERK antibody is phospho-specific. Cell extracts were prepared from the time-course of Spk1-GFP tagged WT and *byr1* Δ strains (KT3082 and KT4300 respectively) and Spk1-GFP was detected by anti-GFP (red) while phospho-Spk1 was detected by anti-pERK antibody (green). The asterisk (*) indicates a green background band that exists in both non-tagged and tagged Spk1 strains seen in (D) and in both wildtype and MEK-del strains in (F). Although this band runs very close to Spk1-GFP, it does not exactly overlap with the Spk1-GFP signal in red in (E) and (F). M is the protein marker lane, (H) corresponds to the number of hours after mating was induced.

3.5 MAPK dynamics in WT and Ras1-MAPK mutants

3.5.1 WT cells; changes in MAPK activation and cellular localisation during meiosis

By using the meiotic assay system introduced in 3.1 and the quantification of phosphorylated and total Spk1 MAPK via western blotting, the activity of the MFSP may be quantified at the level of the MAPK. This was done to address the question of how MAPK activation changes during meiotic differentiation. The mitotic and meiotic morphological phenotypes of a WT strain are shown in **Figure 3.8A**. Mitotic cultures contain cells which are rod shaped and cells showing septa. Using the plate assay, at 24-hours post mating induction around 70% of cells have successfully undergone mating and formed asci containing four haploid spores (See **Table 3.1**).

3.5.1.1 *Quantitative Western Blotting for a Wildtype strain*

The WT strain KT3082, containing Spk1-GFP, was subject to an intense 24-hour sexual differentiation time-course using the SPA plate assay. Cells were collected every hour for 13-hours and again at 16 and 24-hours post induction to be used for protein extraction. Changes in cell morphology and the localisation of Spk1-GFP were followed at each time-point using fluorescence microscopy (**Figure 3.9**). Western blots were used to quantify the amount of phospho- and total- Spk1 MAPK (**Figure 3.8**), α -tubulin was used as a loading control. Mating efficiency was also monitored at each time-point. After all the time-points were collected, cells were subject to denaturation via the TCA method and Western blotting with the anti-GFP, anti-phosphor-ERK antibody and the anti α -tubulin antibody (TAT1) as described in 2.2.16. Membranes were scanned using the Odyssey CLx. A typical western blot is shown in **Figure 3.8B**. Protein bands were quantified using Image Studio v2.1 software. Activation of the

MAPK was calculated by dividing the intensity of the phospho-ERK signal by the α -tubulin signal as this is assumed to be constant throughout the differentiation stages (**Figure 3.8C**). Total MAPK signal is represented as the anti-GFP signal divided by the α -tubulin signal (**Figure 3.8D**). The ratio of phospho to total MAPK was also calculated and for the WT is shown in **Figure 3.8C**. Data represented in **Figure 3.8** is from three technical replicates of one biological replicate. Two biological replicate time-courses were collected and subject to quantitative western blotting. Both biological replicates showed similar data therefore quantitation of only one biological replicate is shown.

Figure 3.8C shows the quantified amount of phosphorylated MAPK increasing steeply over the first 7-hours post induction and peaks after 7-8 hours, this is followed by a slow decrease in the amount of phosphorylated MAPK which levels off but still remains in significant quantities after 24-hours. By plotting the percentage of cells mating at each time-point on the same graph it can be seen that cells first start to mate after the MAPK phosphorylation has peaked and this percentage increases rapidly up until 16-hours post induction where it levels out after around 70% of cells having undergone successful mating.

The changes in the levels of total MAPK are represented in **Figure 3.8D**. Spk1 MAPK is induced upon nitrogen starvation with the levels of protein mirroring that of the phosphorylated species. The amount of Spk1 peaks and remains high for a prolonged period of time (between 6-13 hours post mating induction) and then slowly decreases probably due to protein degradation. We assume that by that time spores have formed there is no longer any requirement for the MAPK.

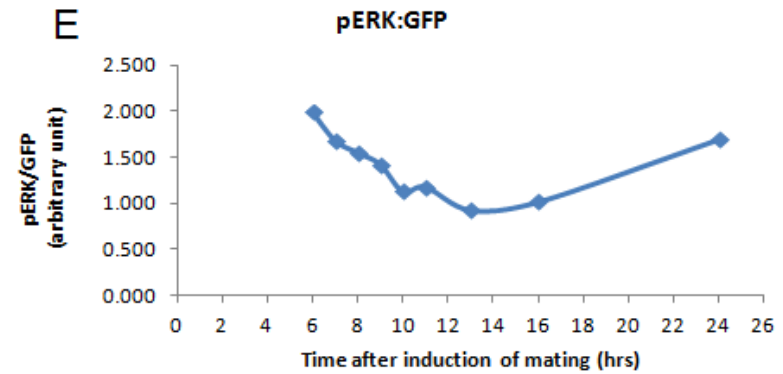
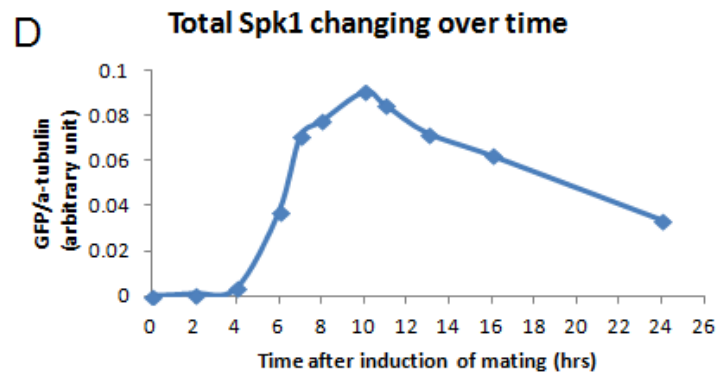
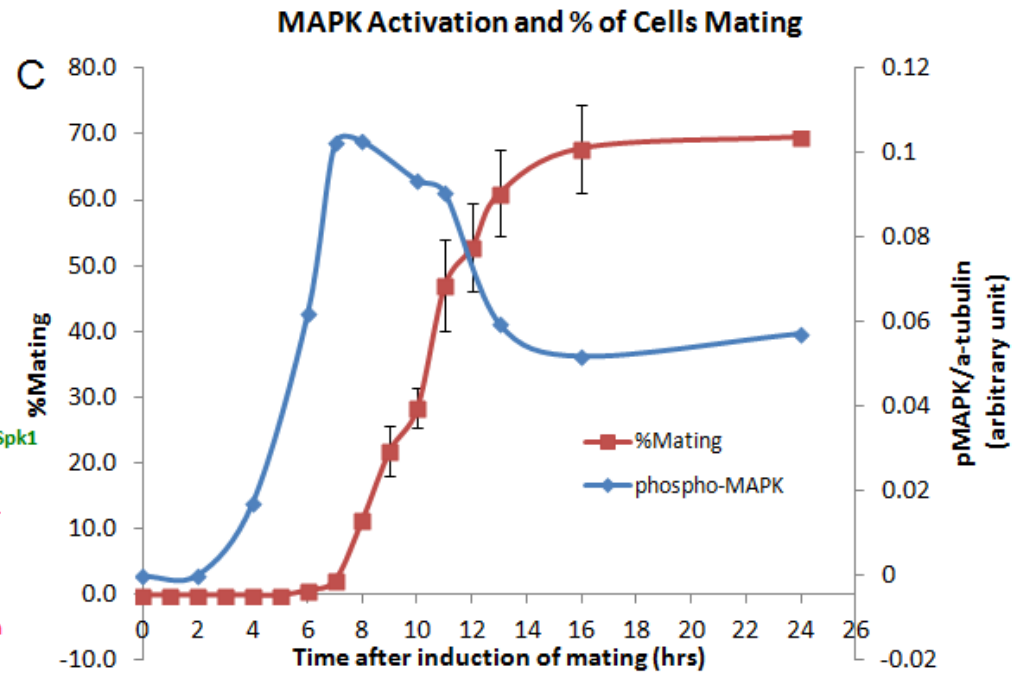
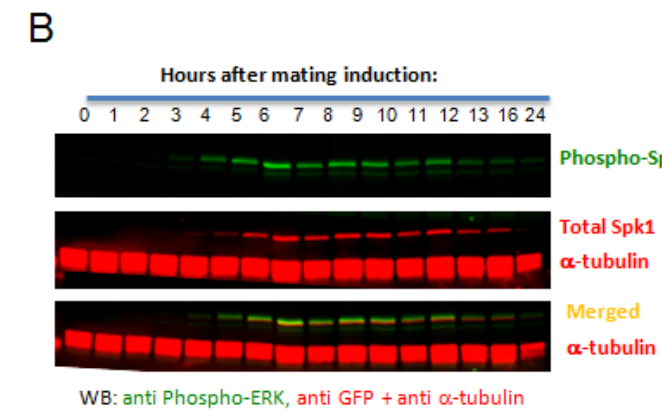
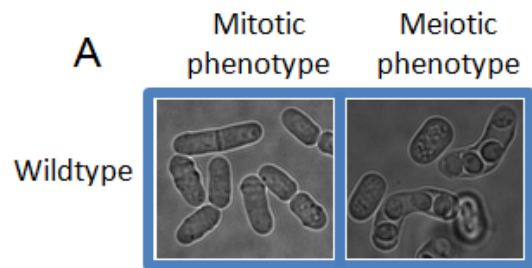


Figure 3.8 Wildtype MAPK dynamics during sexual differentiation

Cells of WT strain KT3082 were collected as described by the plate assay system. (A) Brightfield images of WT cells either growing mitotically in rich media (left hand panel) or cells which have successfully mated and sporulated (right hand panel) (B) Western blot of phospho-Spk1 (upper panel - scanned at a wavelength of 800 nm). The middle panel shows the total amount of Spk1 protein over the time-course by blotting with anti-GFP and α -tubulin as a loading control which is used to normalise the amount of phospho-Spk1 signal to the total amount of protein in the extract (scanned at 700 nm). The lower panel shows the merged 800 and 700 nm channels (C) Quantitation of one biological replicate time course for each set of data is represented here. Two biological replicates comprising of three technical replicate blots were carried out. Quantitation was carried out using the Image Studio ver2.1 software supplied with the Licor Odyssey CLx Scanner. This graph also shows the % of cells mating at each time-point, details of how this was calculated are in **Figure 3.5** and Materials and Methods 2.2.14 and comprises of three biological replicates, error bars are \pm SEM. . (D) Changes in the levels of MAPK over the time-course, quantified as in (C) but using the GFP signal normalised against α -tubulin. (E) The ratio of phospho to total MAPK, data only shown from 6-hours onwards due to there being very little GFP signal before that point therefore the ratios were unrealistically massive and subject to vast variation due to the minute numbers.

The ratio of phospho to total MAPK is shown in **Figure 3.8E**. This ratio appears to slightly decrease over time, this could be due to increasing activity/activation of MAPK phosphatases and/or a decrease in the activity of the upstream kinase, Byr1, both of which are likely regulatory mechanisms. The decrease we see is minor showing that down-regulation of the phospho-MAPK could mainly be due to decreases in the amount of Spk1 MAPK protein rather than dephosphorylation. The quantitation of phospho- to total-MAPK is limited by the quality of the anti-GFP signal, therefore data is only shown from 6-hours onwards because before that the detection on a western blot is limited and therefore ratios were exceptionally high and varied as the phospho signal was being divided by very small numbers. In future, more protein could be loaded onto the gel to get a stronger signal of anti-GFP at the earlier time-points.

To summarise, quantification highlights key features of the Spk1 MAPK signalling dynamics in a wildtype strain, there is an initial time delay in the phosphorylation of Spk1 which is likely to be due to the lack of Spk1 protein expression at the early time-points. Once Spk1 is expressed the phospho-Spk1 signal increases up until 7-hours post mating induction then gradually decreases mirroring the decrease in the total amount Spk1 protein.

3.5.1.2 Visualisation of the dynamics of Spk1-GFP using fluorescence microscopy

The intracellular location of Spk1-GFP was visualised during a 24-hour time-course at the same time as cells were collected to make protein extracts to directly link the dynamics seen during imaging and western blotting - practically, a small amount of cells were scraped off a PVDF membrane with a pipette tip and images taken using the Nikon Ti Eclipse microscope. Both brightfield and green fluorescence images were taken. Representative pictures of cells are each time-point for the WT strain (KT3082) are shown in **Figure 3.9**. All images in this thesis captured during mating time-courses

were taken by Dr Kayoko Tanaka, representative images and image deconvolution was carried out by myself.

During the first three hours post induction there is very little signal in the GFP channel which corresponds to the Spk1-GFP signal. This is in agreement with the Spk1 protein expression level observed in the western blotting (**Figure 3.8B and D**). At the early time-points (0-4 hours) there are barely detectable levels of Spk1-GFP in the cell extracts. At 4-5 hours there is a clear increase in the Spk1-GFP signal and it is distinctly non-nuclear, the cells are also arresting in G1 as they appear smaller and more rounded than at the earlier time-points. Spk1-GFP may form some patchy foci on the plasma membrane at early time-points (**Figure 3.9** at 5- and 6-hours post induction) indicating it may directly be involved in the mating site selection. This is further discussed in the Discussion 3.6.1.

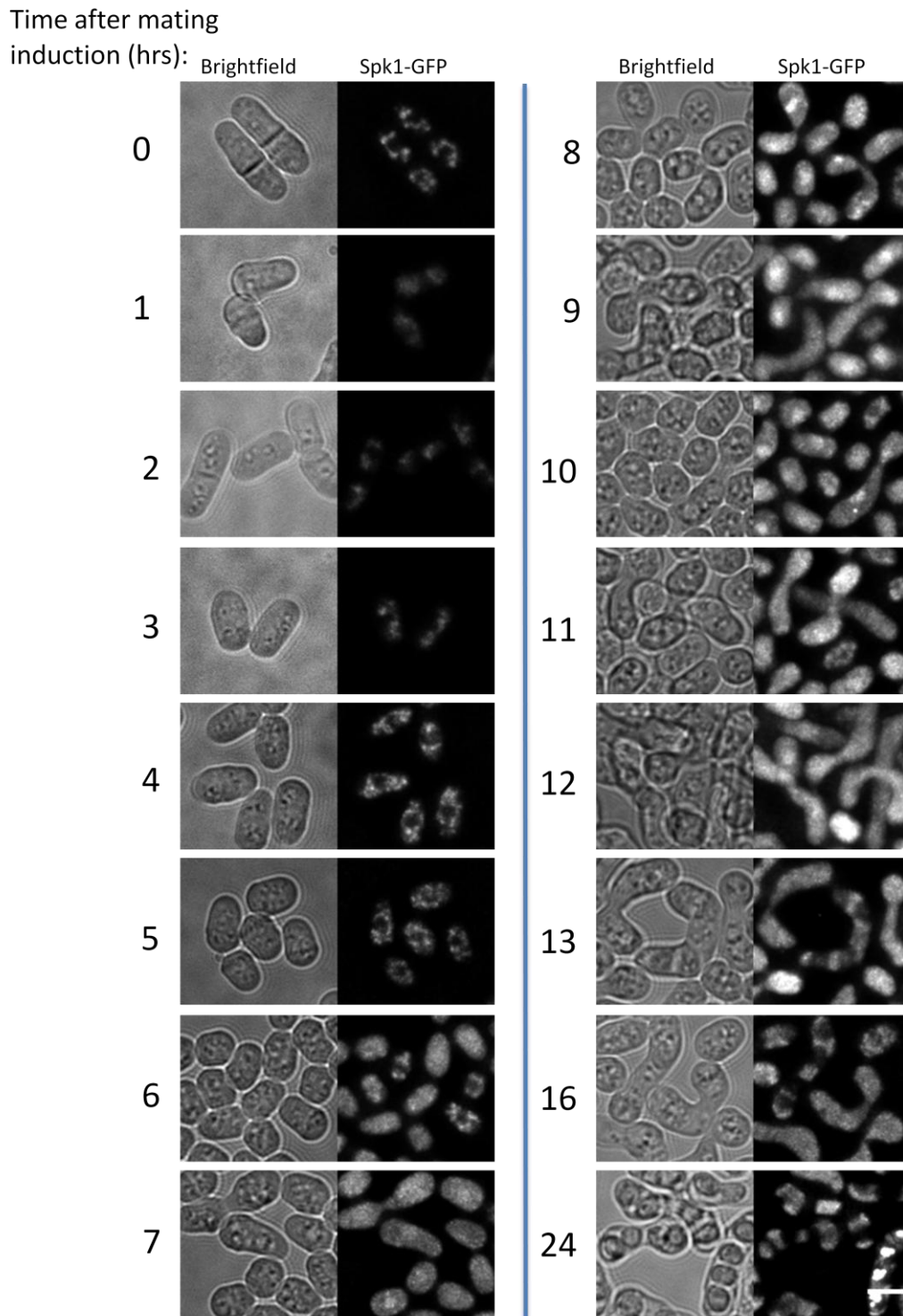


Figure 3.9 Imaging of Spk1-GFP over a 24 hour time-course in WT cells.

Images were taken at each time-point in both the brightfield and GFP channels in order to visualise Spk1-GFP. Each time point comprises 15-25 serial images of 0.4 μm interval along the Z axis taken to span the full thickness of the cell. All of the Spk1-GFP images were deconvolved using the Huygens Essential Deconvolution. Deconvolved images were Z-projected, cropped and combined using ImageJ. Scale bar is 5 μm .

After 6-7 hours post induction the GFP signal becomes more dispersed throughout the whole cell within the cytoplasm and the nucleus and there is evidence of Spk1-GFP nuclear signal in a minority of cells. The first mating pairs are also seen at this time. Between 7-10 hours there is strong nuclear signal in the majority of cells, independent of whether they have mated or not. From 11-hours onwards the nuclear signal is no longer visible in mated cells and a high percentage of cells (around 50% - **Figure 3.8C**) have mated by this time-point. Sporulated zygotes first appear at around 13-hours with the majority of mating pairs forming spores by 24-hours. The image taken at 24-hours shows spores having high levels of autofluorescence.

In summary, the imaging reflects the Spk1 protein levels seen using western blotting (**Figure 3.8B** and **D**). The Spk1 nuclear signal appears in G1 arrested cells, persists in the nucleus until after cells have undergone mating and then disappears. It is noted, however, that cells which do not undergo mating do not appear to have Spk1-GFP in the nucleus at 13- and 16- hours post induction. This could be because the cell has become desensitised to pheromone signalling after a prolonged starvation period and cells are highly unlikely to mate after such a long period as mating efficiency plateaus between 16 and 24-hours (**Figure 3.8C**)

Nuclear localisation of MAPKs upon activation is an important characteristic seen in other MAPK homologues - especially mammalian MAPKs - where nuclear relocation upon stimulation is essential for their function to phosphorylate nuclear targets especially those involved in gene regulation (Plotnikov *et al.*, 2011). This result shows that this characteristic is preserved in *S.pombe* with respect to the MFSP MAPK Spk1.

3.5.2 Meiotic phenotype of a constitutively active MEK mutant

To dissect the regulation of the MFSP, a phospho-mimetic MEK mutant was generated by a previous Masters student in the lab, Shubhchintan Randhawa. This mutant has been mentioned by Ozoe *et al* 2002 previously but its phenotype has not been analysed extensively. In their paper they generate and express *byr1.DD* from its chromosomal locus and describe the meiotic phenotype as exhibiting "elongated conjugation tubes" (Ozoe *et al.*, 2002). In our lab, the phospho-mimetic mutations were introduced using PCR site directed mutagenesis. The molecular concept of these mutations is represented in **Figure 3.10A**. MEKs require dual phosphorylation by the upstream MEK Kinase for activation (Zheng & Guan, 1994), Byr1 is phosphorylated on Serine 214 and Threonine 218 by Byr2 (Ozoe *et al.*, 2002), if these two residues are mutated to a negative amino acids, in this case aspartic acids, this mimics the negative charge of the covalently added phosphorylation modifications thereby mimicking the phosphorylated state and creating a protein which is constitutively activated and resistant to the action of phosphatases.

The mitotic and meiotic phenotypes of the *byr1.DD* (KT3435) mutant are shown in **Figure 3.10B** along with the WT phenotypes as a comparison. There are no obvious differences between the WT and *byr1.DD* mitotic phenotypes. The Byr1 protein has been found to be expressed constitutively in *S.pombe* and its mRNA levels do not appear to change during the mitotic cell cycle (Nadin-Davis & Nasim, 1990) but it is dispensable for the vegetative growth (Nadin-Davis & Nasim, 1988). The difference between WT and *byr1.DD* is evident from the meiotic phenotypes; WT cells successfully conjugate and sporulate on a SPA plate whereas the *byr1.DD* cells show a "prezygotic" phenotype (**Figure 3.10B**) (Ozoe *et al.*, 2002)(S Randhawa, MSc Thesis, University of Leicester, 2009). Even though the work of Ozoe *et al* 2002 referred to the

meiotic phenotype of this mutant as exhibiting elongated conjugation tubes, looking back at their microscopy figure, it is clear that the mutant is making the prezygotic phenotype but we assume they overlooked the significance of this pairing and concentrated on the obvious shmooing. We observed that the *byr1.DD* homothallic strain form mating pairs but fusion between the two cells does not happen and the cell walls between the two cells remains intact (data not shown). These cells remain at this stage and therefore do no progress any further through the differentiation stages. In order to obtain further insights as to the cellular signalling status of this mutant the dynamics of the MAPK, Spk1, were again visualised via cell imaging and quantitative western blotting.

3.5.2.1 MAPK phosphorylation in the *byr1.DD* mutant

The *byr1.DD spk1-GFP* strain, KT3435, was generated by the transformation of the *byr1.DD* strain KT3385 with the *Spk1-GFP-2xFLAG-Kan^R* PCR fragment via the TRAF0 method. Chromosomal integration was confirmed by PCR. This strain was subjected to a 24-hour mating time-course using the same method outlined in 3.5.1.1 as was previously used for the WT strain. A representative western blot using protein extracts from this strain can be seen in **Figure 3.10C**. Data represented in **Figure 3.10** is from two technical replicates of one biological replicate. Two biological replicate time-courses were collected and subject to quantitative western blotting. Both biological replicates showed similar data therefore quantitation of only one biological replicate is shown. **Figure 3.10D** shows that Spk1 MAPK phosphorylation happens much slower compared to WT which could be because the kinase activity of *byr1.DD* is not as effective as the fully phosphorylated WT version. The most striking but predicted feature of the MAPK phosphorylation in this mutant is the constitutive signal which remains high and does not seem subject to effective down-regulation compared to the

WT strain. It also indicated that whatever down regulation is happening at the level of the MAPK - i.e. the action of potential MAPK phosphatases - is not effective if the direct upstream kinase remains active.

In summary, if the MEK is constitutively activated the MAPK is constitutively phosphorylated. In terms of the total amount of MAPK in the *byr1.DD* mutant, this seems to follow the trend of MAPK phosphorylation - slower increase than WT but then levels remains high **Figure 3.10E**. The expression of Spk1 is under a positive feedback mechanism through activation of the MFSP, initially expression of Spk1 is activated by nitrogen starvation through the activation of Ste11, this would explain the slower increase in the amount of protein as the positive feedback loop is delayed in being switched on as we predict that the Byr1.DD protein is working obliviously to pheromone stimulation and is functioning independently of anything upstream of itself in the MFSP therefore activation of Spk1 would be dependent on the relative expression of both Byr1 and Spk1 and the colocalisation of these two proteins within the cell. There is very limited information about the expression of *byr1* upon mating induction and it does not appear to be a Ste11 target gene (Mata & Bahler, 2006).

The ratio of phospho to total MAPK (**Figure 3.10F**) shows no significant difference between WT and *byr1.DD*, both profiles show the a slightly higher ratio to begin with compared to 24-hours post induction.

Why do the levels of phospho- and total-Spk1 reach a plateau and do not continue to increase indefinitely? A possible explanation for this is that if Spk1 protein is being actively degraded via a proteosome pathway then for the levels to stay constantly elevated, expression and degradation must be happening at a similar rate as there is no further increases in the total amount of protein. Control of gene expression over the

entire meiotic differentiation process is highly complex and transcriptional regulation appears to occur in waves with each wave controlled by specific transcription factors with Ste11 being the major transcription factor for starvation and pheromone induced genes (Mata *et al.*, 2007). We predict that because Spk1 is constitutively phosphorylated, as a direct consequence, the activity of Ste11 is also likely to be constitutive along with the expression of Spk1 and other Ste11 target genes and that Spk1 and/or Ste11 activity needs to be down-regulated in order for cell fusion and continued differentiation. The mechanism by which cells sense that they are ready to activate the next set of genes - required for pre-meiotic S-phase and recombination - is currently unknown.

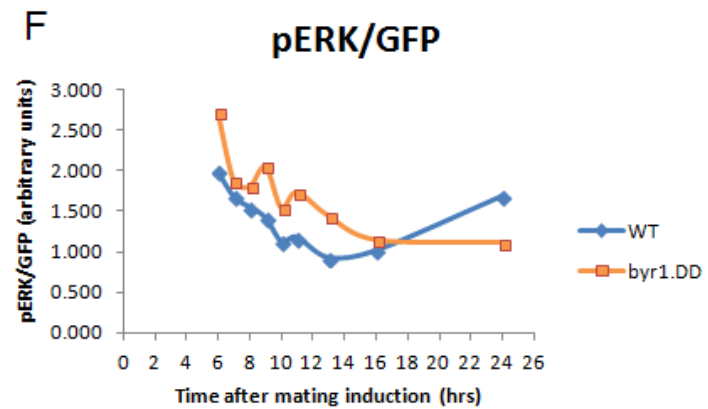
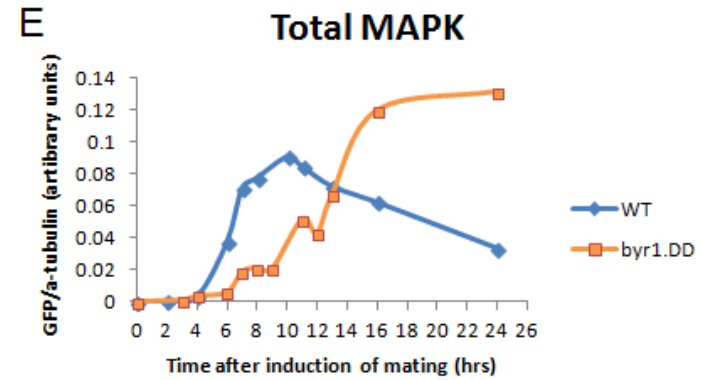
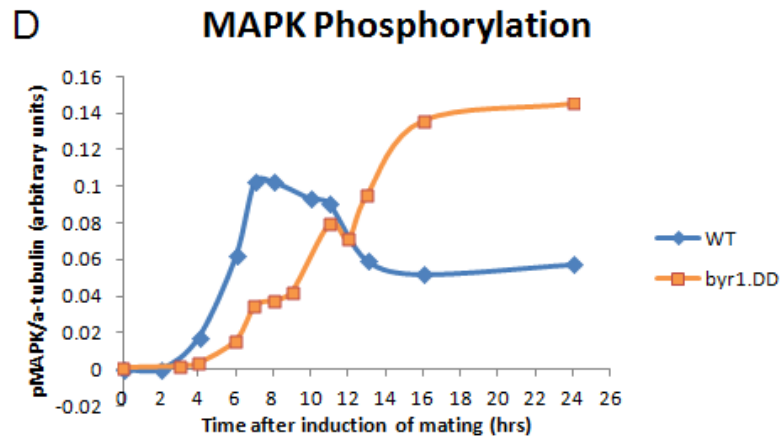
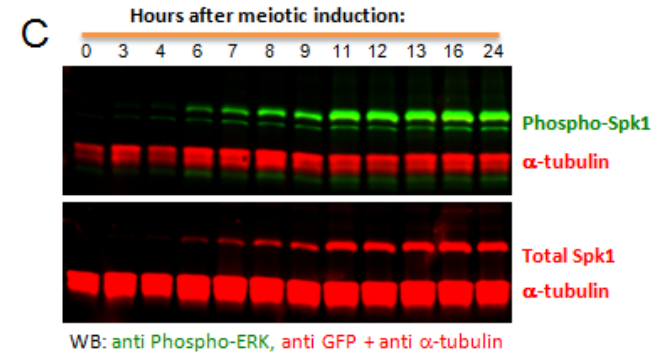
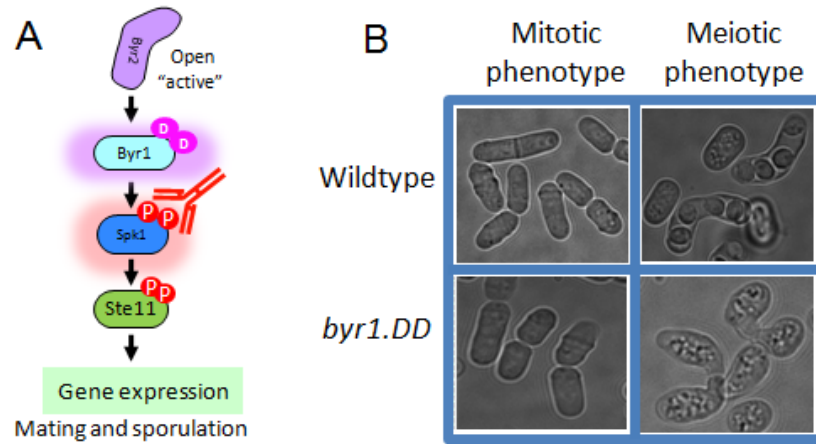


Figure 3.10 A direct comparison of Spk1 MAPK dynamics in WT and *byr1.DD* strains during a mating time-course.

A wildtype strain (KT3082) and *byr1.DD* strain (KT3435) were subject to a mating time-course over 24 hours. (A) Schematic showing the basis of the phosphomimetic *byr1.DD* mutations to create a constitutively active mutant. (B) Microscope images of WT cells and *byr1.DD* cells either growing mitotically in rich media (left hand panels) or cells which have been on an SPA plate for 24-hours and are showing their terminal phenotype (right hand panel) (C) Western blot of phospho-Spk1 and α -tubulin (upper panel) as a loading control. The lower panel shows the total amount of Spk1 protein over the time-course by blotting with anti-GFP. (D) Quantitation of one biological replicate is represented. Two biological replicate time courses were carried out and each set of biological replicate data comprises two technical replicate blots. Quantitation was carried out using the Image Studio ver2.1 software supplied with the Licor Odyssey CLx Scanner. (E) Changes in the levels of MAPK over the mating time-course, quantified as in (C) but using the GFP signal. (F) The ratio of phospho to total MAPK.

3.5.2.2 *MAPK localisation in byr1.DD*

Live cell imaging of the *byr1.DD* strain, KT3435, over the 24-hour mating time-course (**Figure 3.11**) shows that the expression of Spk1-GFP in these cells is delayed compared to WT with very little protein detected in the first 9-hours, this corresponds with the levels of total MAPK in the western blots shown in **Figure 3.10C** and **E**. At this time, Spk1-GFP is exclusively cytoplasmic. Cells arrest in G1 in a similar manner to WT as shown by the smaller more rounded cell morphology from 4-5 hours onwards. Nuclear Spk1-GFP is not evident until 10-12 hours after induction and the first cells to show any shmooing appear at 13-hours, this is the same time when the first prezygotes - which are paired but not fused cells - can be seen and the majority of cells have a nuclear Spk1-GFP signal. This nuclear signal remains strong in cells showing the distinctive "prezygotic" phenotype even after 24-hours. In this mutant, Spk1-GFP expression appears to be delayed/happening on a slower timescale and it is delayed in moving into the nucleus compared to WT (**Figure 3.9** and **Figure 3.11**), the shmooing response is delayed and the Spk1 nuclear signal remains in the cells for a prolonged period of time.

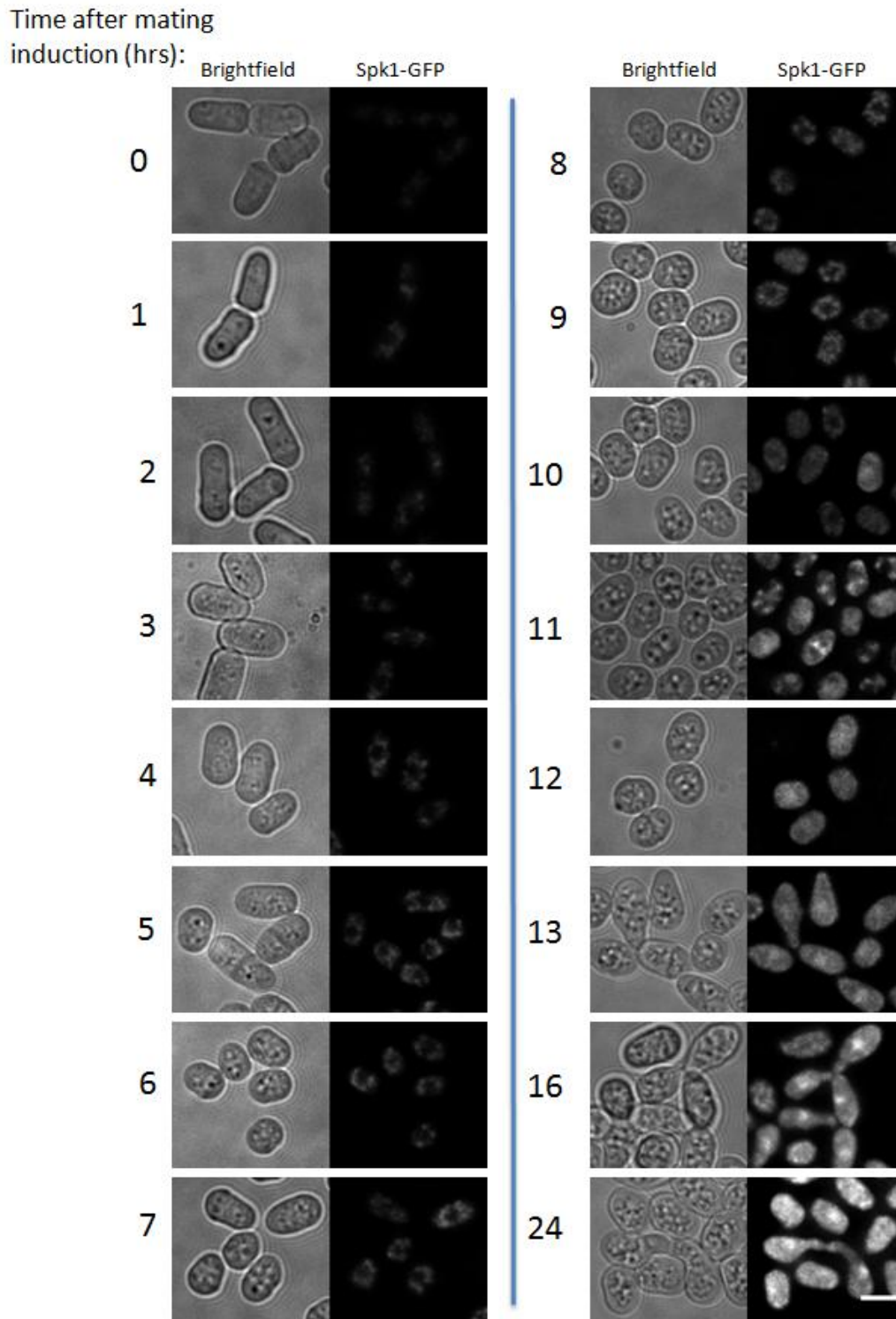


Figure 3.11 Imaging of Spk1-GFP over a 24 hour time-course in *byr1.DD* cells.

Images were taken at each time-point in both the brightfield and GFP channels in order to visualise Spk1-GFP. Each time point comprises 15-25 serial images of 0.4 μm interval along the Z axis taken to span the full thickness of the cell. All of the Spk1-GFP images were deconvolved using the Huygens Essential Deconvolution. Deconvolved images were Z-projected, cropped and combined using ImageJ. Scale bar is 5 μm .

From these data we hypothesize that down-regulation of the MFSP is essential for conjugation and therefore further progression through sexual differentiation. This hypothesis is examined in Chapter 7. We predict that the down-regulation of the MAPK signal could act as an indicator that cells have successfully connected with a cell of opposite mating type or that MAPK is keeping key conjugation components/machinery inactive via inhibitory phosphorylation.

In summary, cells expressing a constitutively active MEK show constitutive phosphorylation and nuclear localisation of the MAPK, again this leads us to believe that down-regulation of the MAPK is essential for further progression through sexual differentiation.

3.5.3 MAPK dynamics in an oncogenic Ras mutant

RAS proteins are found to be mutated in a high proportion of all human cancers making their mechanisms of regulation of increasingly high interest. One of the most common cancer mutations found in human K-*ras* is a glycine 12 to valine substitution which prevents the binding of GAPs and therefore the Ras protein stays in a GTP-bound activated form. The homologous mutation in *S.pombe*, a glycine 17 to valine substitution, was introduced into the unique Ras homologue in *S.pombe*, Ras1, in the late 1980's by Nadin-Davis *et al.* This mutant, which will be referred to as Ras1.val17, encoded by the mutant allele *ras1.val17*, generates excessively elongated conjugation tubes upon nutrient starvation but its mitotic phenotype is indistinguishable from WT (**Figure 3.13B**) (Nadin-Davis *et al.*, 1986a). *ras1Δ* cells are viable but have a rounded/lemon shaped morphology therefore Ras1 is important for maintaining the elongated cell shape during mitosis. We predict that the reason *ras1.val17* shows no obvious phenotype during mitosis is that Ras1 is continuously activated in mitotically growing cells therefore constitutive activation make little or no difference to cell morphology. Ras1.val17 mutant cells cannot mate and are therefore sterile although diploid cells carrying the *ras1.val17* mutation can sporulate, indicating that the problem associated with the *ras1.val17* mutation is specific to the mating process (Nadin-Davis *et al.*, 1986a). *ras1Δ/ras1Δ* diploids can also sporulate at low efficiency.

Although *S.pombe* contains only one Ras homologue, Ras1, it is reported to play a role in both the MFSP where it is coupled to the activation of the MAPK and the Cdc42 morphology pathway which is responsible for actin cytoskeleton rearrangements (**Figure 3.12**). This is further examined in Chapter 4. Our aim was to uncover the molecular basis of this "elongated" oncogenic Ras phenotype by specifically investigating the signalling dynamics of Spk1 MAPK.

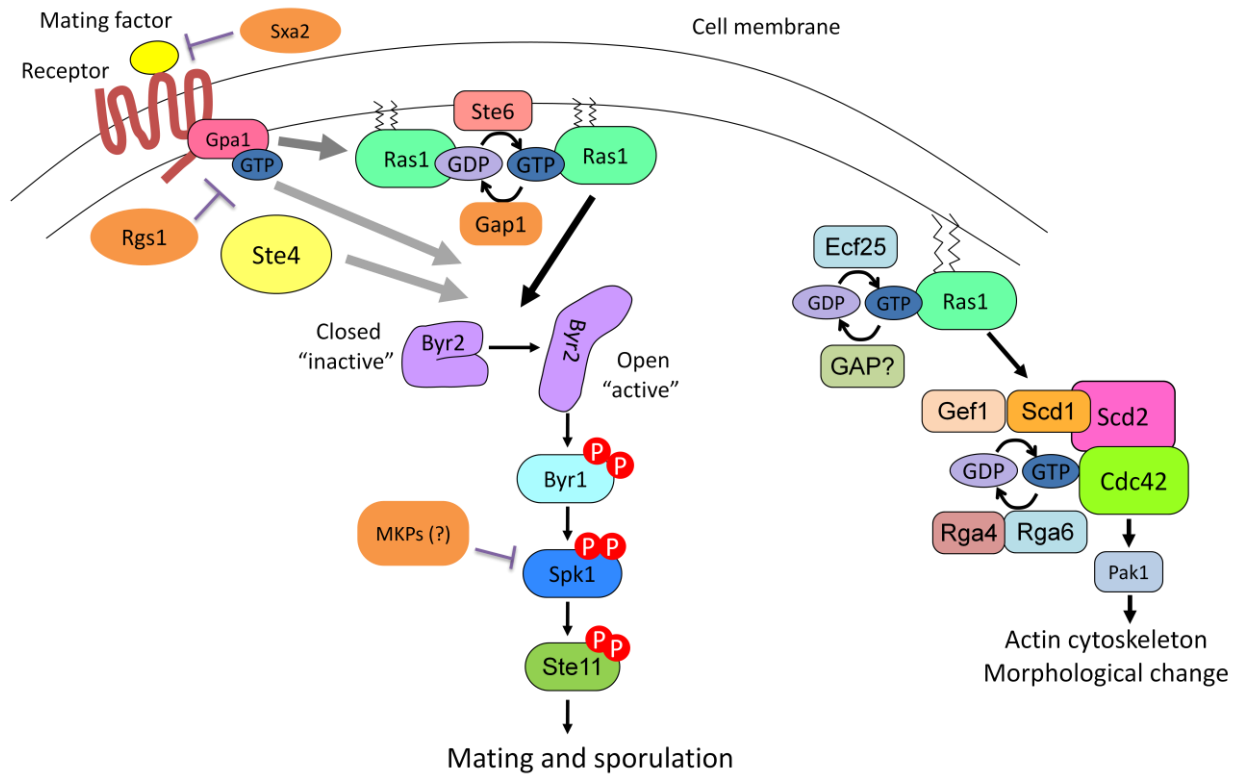


Figure 3.12 Ras1 plays roles in both the MFSP and the Cdc42 morphology pathway.

Ras1 is reported to be a key component of both the MFSP where it is coupled to the activation of a MAPK cascade and the Cdc42-morphology pathway which is responsible for actin cytoskeleton rearrangements.

3.5.3.1 MAPK phosphorylation in an oncogenic *Ras1* mutant

The oncogenic *ras1.val17* strain KT3084 containing *spk1-GFP* was generated by transforming the *ras1.val17* strain, KT2645 with the *Spk1-GFP-2xFLAG-Kan^R* PCR fragment and integration was confirmed by PCR. This strain was subject to 24-hour time-courses as outlined previously for the WT strain. A typical western blot for phospho-Spk1, Spk1-GFP and α -tubulin from this strain is shown in **Figure 3.13C**. Quantification of MAPK phosphorylation, total protein and the phospho to total ratio was calculated using the same method as for the WT described in 3.5.1.1. Data represented in **Figure 3.13** is from two technical replicates of one biological replicate. Two biological replicate time-courses were collected and subject to quantitative western blotting. Both biological replicates showed similar data therefore quantitation of only one biological replicate is shown.

MAPK phosphorylation is significantly quicker in this strain with the peak activation occurring after 4-hours compared to 7-8 hours in the WT (**Figure 3.13D**). Importantly, the signal is then quickly down-regulated to a level similar to that of the WT between 7-13 hours after which the signal fails to decrease any further. Thus, in striking contrast to the *byr1.DD* case, the *ras1.val17* mutation does not cause constitutive MAPK phosphorylation. There is also an increased level of Spk1 protein in these *ras1.val17* cells. The positive feedback for protein expression appears stronger as the Spk1 protein is detected earlier (**Figure 3.13E**) but there is no Spk1-GFP detected at time zero (+N sample) therefore *ras1.val17* does not appear to be activating the MAPK cascade in the absence of pheromone probably as there is no Spk1 protein present and signalling components are not localised correctly. The total amount of Spk1-GFP is increased in this mutant compared to WT across the entire 24-hour mating time-course but more significantly at the later time-points (later than 12-hours post induction), this could be

due to a stronger positive feedback as a consequence of initial hypersensitive activation of the MFSP or a decrease in Spk1 degradation. The phospho to total Spk1 ratio in **Figure 3.13F** for *ras1.val17* appears relatively constant at around 1:1 over the 24-hours and appears to be slightly lower to that of WT although this may not be significant and more replicates would be required to determine this.

One of the major limiting factors for MAPK phosphorylation is that Spk1 is only expressed upon nitrogen starvation therefore the acute phosphorylation of the MAPK in *ras1.val17* could be happening because the MFSP is responding earlier probably to a lower concentration of pheromone in a hypersensitive manner, setting the positive feedback for Spk1 expression in motion earlier. There is also likely to be a higher basal level of the GTP-bound form of Ras1 in these cells, due to the predicted nature of the *ras1.val17* mutation, which is ready to contribute to the activation of the MAPK cascade once the correct components are in place. The cells appear to be hypersensitive to pheromone so the MFSP is getting activated prematurely as a consequence of *ras1.val17*. Once activated, *ras1.val17* cannot be switched off, therefore regulation of Ras1 by GAPs is essential to stop this hypersensitive activation of the pathway. The essential role of Gap1 is investigated in Chapters 6 and 7.

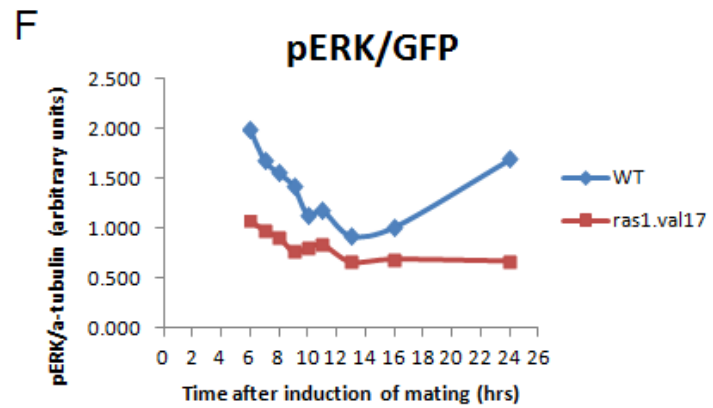
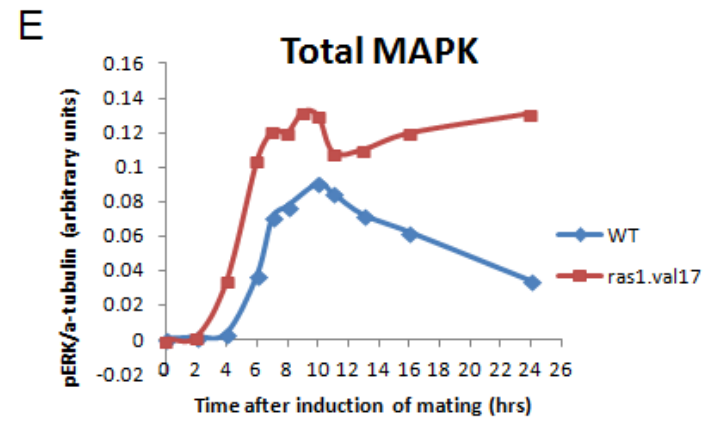
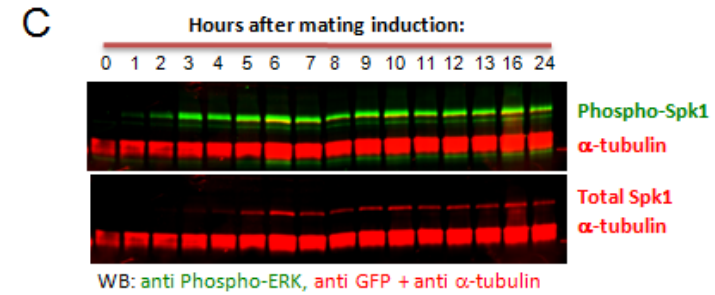
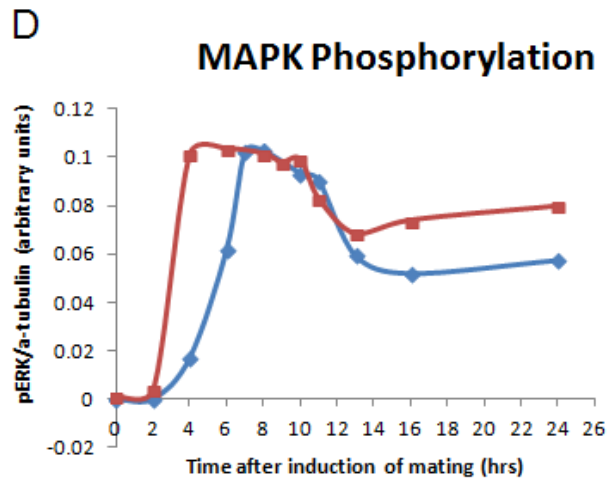
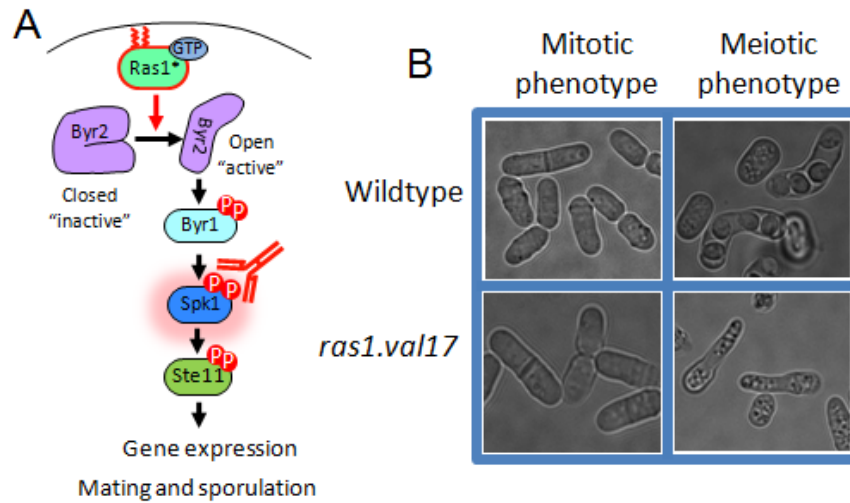


Figure 3.13 A direct comparison of the MAPK signalling dynamics in WT and *ras1.val17* during a mating time-course.

A wildtype strain (KT3082) and *ras1.val17* strain (KT3084) were subject to a mating time-courses over 24-hours. (A) Schematic showing the principle of the *ras1.val17* oncogenic mutation.(B) Brightfield images of WT cells and *ras1.val17* cells either growing mitotically in rich media (left hand panels) or cells which have been on an SPA plate for 24-hours and are showing their terminal phenotype (right hand panel) (C) Western blot of phospho-Spk1 and α -tubulin (upper panel) as a loading control which is used to normalise the amount of phospho-Spk1 signal to the total amount of protein in the extracts. The lower panel shows the total amount of Spk1-GFP protein over the time-course by blotting with anti-GFP. (D) Quantitation of phospho-ERK normalised against α -tubulin to represent changes in the amount of phospho-Spk1 during the time-course. Data is representative of one biological replicate time courses each set of biological replicate data comprises two technical replicate blots. Overall two biological replicates were carried out of each strain Quantitation was carried out using the Image Studio ver2.1 software supplied with the Licor Odyssey CLx Scanner. (E) Changes in the levels of MAPK over the mating time-course, quantified as in (C) but using the GFP signal. (F) The ratio of phospho to total MAPK.

3.5.3.2 *MAPK localisation in ras1.val17*

The *ras1.val17* strain KT3084 was subject to live cell imaging using the same cells that were collected for protein extraction as outlined for WT. Representative images are shown in **Figure 3.14**. As soon as the Spk1-GFP is detected it is clearly seen in the nucleus at 4-hours post induction compared to 6-7 hours for the WT. The timing of nuclear localisation mirrors the timings of phospho-Spk1 detection in **Figure 3.13** which corresponds with the literature in that phosphorylation of ERKs appears to be the signal for translocate to the nucleus (Seger & Krebs, 1995) therefore the accelerated appearance of phospho-Spk1 (**Figure 3.13D**) correlates with an accelerated appearance of Spk1-GFP in the nucleus.

Polarised growth also starts at much earlier time points compared to WT with the first shmoo visible at between 4-5 hours. The nuclear Spk1-GFP signal remains nuclear in the elongated cells and is still relatively strong after 24-hours. There is also potentially Spk1-GFP signal at the shmooing cell tips (See images for time-points 11, 12,13 and 24-hours in **Figure 3.14**, yellow arrows) but this could be due to autofluorescence as these cells are unhealthy looking and contain a large number of vacuoles which can be seen clearly in the corresponding brightfield images and therefore this requires further investigation. If Spk1 localisation to the shmoo tip is indeed real, it fits well with our hypothesis that Spk1 is required at the site of polarised growth and coordinates this growth with the site of pheromone stimulation on the cell cortex.

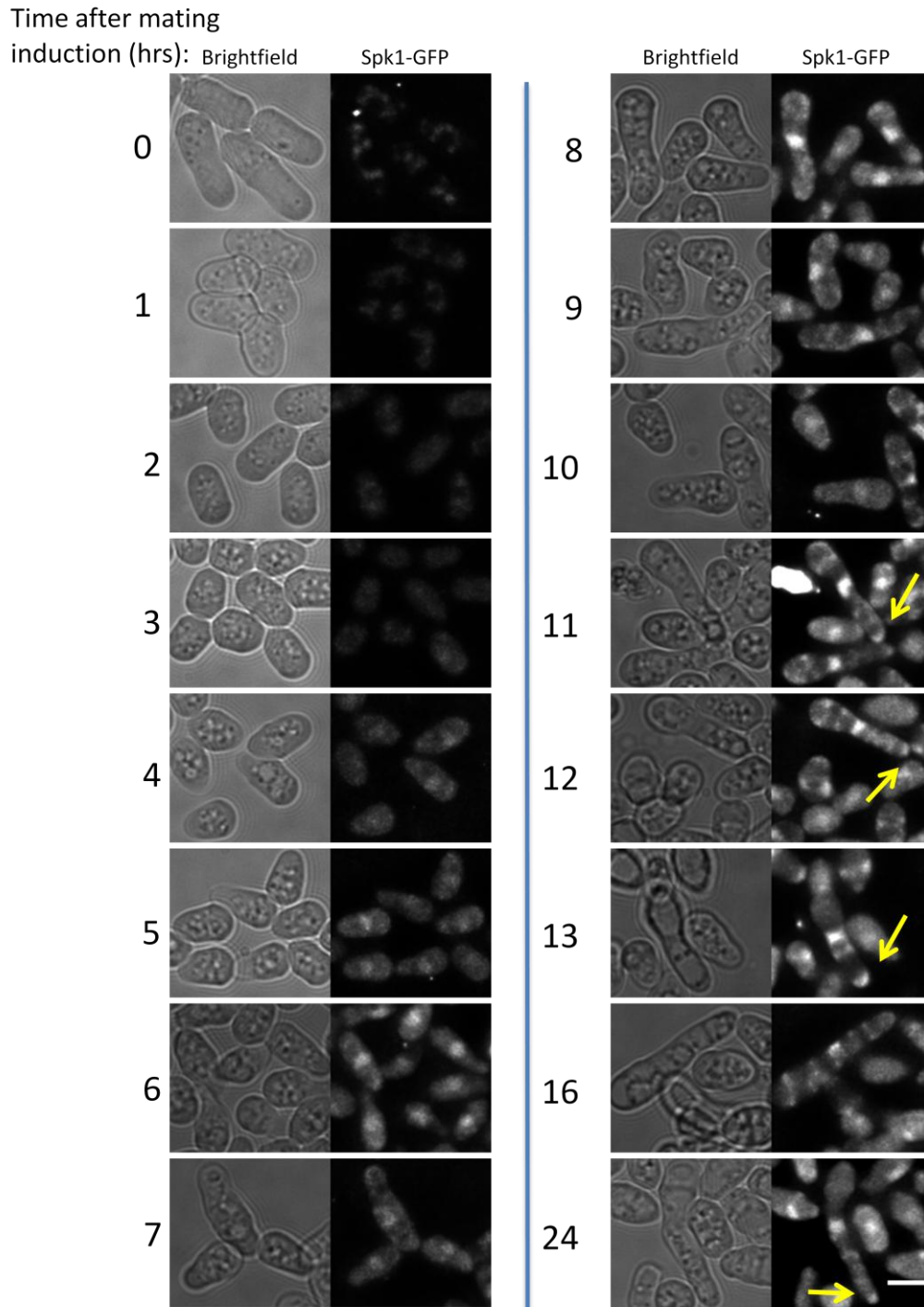


Figure 3.14 Imaging of Spk1-GFP over a 24 hour time-course in *ras1.val17* cells.

Images were taken at each time-point in both the brightfield and GFP channels in order to visualise Spk1-GFP. Each time point comprises 15-25 serial images of 0.4 μm interval along the Z axis taken to span the full thickness of the cell. All of the Spk1-GFP images were deconvolved using the Huygens Essential Deconvolution. Deconvolved images were then z-projected, cropped and combined using ImageJ. Scale bar is 5 μm .

3.6 Discussion

3.6.1 WT MAPK dynamics

To conclude, the successful creation of the SPA plate mating assay and validation of the tools for quantification of MAPK dynamics during mating have highlighted key features about the control of Spk1 MAPK phosphorylation. Using this plate mating assay, we observed in WT cells, Spk1 phosphorylation is relatively transient with a peak phosphorylation occurring 7-8 hours post induction and this coordinates well with the timing of mating. The levels of phospho-Spk1 decrease thereafter and plateau at a level around 50% of the maximum from 13-hours post induction onwards.

Spk1-GFP may form some patchy foci on the plasma membrane at early time-points indicating Spk1 may directly be involved in the mating site selection. The imaging in **Figure 3.9** is not conclusive of this and therefore, a future experiment would be the extensive live imaging of Spk1- GFP to potentially show that it also appears at the cell cortex as distinctive foci. It is likely that Spk1 is activated at the cell cortex by the MFSP and following activation it translocates to the nucleus to carry out its function in the activation of the mating transcriptional programme as seen in the conserved mammalian ERK1/2 growth factor stimulated pathways (Plotnikov *et al.*, 2011). To prove that this Spk1-GFP signal is definitely nuclear, DAPI staining could also be used but as we wanted to take images as soon as possible at the correct time-point we did not use it - potentially we could have fixed cells at the desired time-points and imaged them at a later point. In *S.cerevisiae*, the Spk1 homologue, Fus3 is localised to the site of mating factor stimulation to coordinate polarised growth. Pheromone activated MAPK, FUS3, is localised to the shmoo via $G\alpha$ (Methodiev *et al.*, 2002) and is important for polarised growth as it phosphorylates an important formin protein required for actin

assembly, Bni1 (Matheos *et al.*, 2004) and Fus3 phosphorylates G β to stabilise the Cdc42-Far1- G β complex and keep it at the cell cortex (Metodiev *et al.*, 2002). Spk1 could be playing a similar role to FUS3 via the formin Fus1 which is essential for cell-cell conjugation in *S.pombe* (Petersen *et al.*, 1995).

3.6.2 The *byr1.DD* phenotype

In a mutant where the MEK, Byr1, is constitutively activated by phospho-mimetic mutations, MAPK phosphorylation is constitutive and appears resistant to down-regulation. Combine this observation with the "prezygotic" mating phenotype seen in this mutant highlights an essential role for down-regulation of the MAPK signal for mating progression specifically the process of cell fusion between mating partners.

Using quantitative western blotting we have observed that the MAPK signalling dynamics are drastically altered in *byr1.DD*. The duration of MAPK phosphorylation is exceptionally important for concerted signalling as reported previously in the literature (Ebisuya *et al.*, 2005; Chalmers *et al.*, 2007; Murphy *et al.*, 2004; Murphy *et al.*, 2002; Dikic *et al.*, 1994; Traverse *et al.*, 1994). The decision for PC12 cells to either undergo proliferation or differentiation - two contrasting cellular outcomes - directly depends on the duration of ERK activation which in this case is either classed as transient or sustained. The reason behind this is due to the induction of early response genes whose gene products can be phosphorylated by ERK stabilising them once they are expressed. Many early response genes are transcription factors which will set in motion a different genetic programme. If ERK is only transiently activated then it will not be able to phosphorylate and stabilise these proteins thereby promoting a different cellular outcome/gene expression profile.

We were concerned with the finding that timing of Spk1 phosphorylation is severely delayed in *byr1.DD* which brings in to question the activity of the phospho-mimetic mutations and it is likely that Byr1.DD has compromised kinase activity or a decreased affinity of Spk1 compared to the WT phosphorylated Byr1 protein. Despite this delay in signalling, cells can orientate polarised growth and recognise a mating partner. Shmooing of this mutant is delayed in a similar manner to the delay in the appearance of phospho-Spk1 highlighting a potential link between MAPK activation and a morphological response - this is further investigated in Chapter 4 Section 4.4.3. The significant delay in Spk1 expression (and therefore phosphorylation) is likely to be causing a delay in all functions dependent on the activity of the MFSP during mating including the expression and activation of the transcription factor Ste11 therefore we cannot rule out that the *byr1.DD* paired phenotype is a direct consequence of a decrease in MFSP output over the first 10 to 13-hours post mating induction rather than the constitutive MAPK phosphorylation we observed after 13-hours, this possibility is further discussed in Chapter 7 Section 7.4.

Apart from the finding that Ste11 is a direct Spk1 target (Kjaerulff *et al.*, 2005) there have been no other published investigations into other Spk1 target proteins of which there are likely to be many. We can predict that initially Spk1 translocates to the nucleus where it activates the mating transcriptional programme but a pool of Spk1 may be required outside of the nucleus to phosphorylate/regulate proteins required for cell fusion. Live imaging of *byr1.DD* cells showed constitutive Spk1-GFP localisation in the nucleus. Upon phosphorylation ERKs translocate to the nucleus and this translocation is not dependent on MAPK activity (Seger & Krebs, 1995) therefore it is likely that if Spk1 was successfully translocated out of the nucleus, because of the constitutive nature of Byr1.DD, Spk1 would be phosphorylate again resulting in nuclear

relocation. There is also evidence in mammalian cells that MEK plays a role in the translocation of ERK out of the nucleus (Adachi *et al.*, 2000). If a similar mechanism is happening in *S.pombe* then perhaps Byr1.DD is not capable of this function due to the phospho-mimetic mutations. Overall, the MAPK spatial-temporal dynamics are significantly different in the presence of Byr1.DD compared to WT.

3.6.3 The *ras1.val17* phenotype

Investigations into the MAPK dynamics in the oncogenic *ras1.val17* mutant found that there is acute phosphorylation of the MAPK followed by effective down-regulation. The MFSP appears to be hypersensitive in this mutant causing premature MAPK phosphorylation and hyper-activation of the shmooing response resulting in cells exhibiting single elongated conjugation tubes. These two observations may be linked i.e. the acute MAPK activation could be directly causing the "elongated" mating phenotype. The next objective of this work was to investigate this potential link and investigate the role Ras1 plays in both the MFSP and the Cdc42-morphology pathway during mating.

How can *ras1.val17* cause Spk1 to be expressed more quickly compared to WT? We've already shown in the WT case that the phospho-Spk1 profile strongly follows the Spk1 total protein profile therefore the amount of phospho-Spk1 is limited by the amount of Spk1 present in the cell. The induction of Spk1 protein expression must be faster in *ras1.val17* cells which we can see clearly in **Figure 3.13E**. It is also likely that the Ras1-Byr2-Byr1 components of the pathway are primed in this mutant thereby accelerating the positive feedback for Spk1 expression. Once a small amount of Spk1 is expressed due to nitrogen starvation it can be phosphorylated straight away thereby setting the transcriptional programme into motion on a much faster timescale which includes further induction of the *spk1* gene.

The hypersensitive nature of the *ras1.val17* mutant may help to explain the elongated phenotype when combined with the findings of (Bendezu & Martin, 2013) in which hyperactivated pheromone mutants (*map3.dn9* and *rgs1Δ*) elongate from a default cell tip as the morphology machinery has not had time to orientate polarised growth towards a pheromone gradient and sample the membrane for most favourable location to initiate polarised growth. In this case the polarised growth is unlikely to be coordinated with the specific location of the cell membrane which is receiving the strongest pheromone induced stimulation.

Why don't *ras1.val17* cells stick to a mating partner? When this work was initially started we were using large liquid mating cultures as described in 3.2.1 and it was quickly noted that cultures of *ras1.val17* get very clumpy over 24-hours of shaking in the incubator to a much greater extent than a WT culture running in parallel. It is the role of agglutinins to help cells stick together but little is known about how they function. we could predict that the levels of agglutinins correlates to activity of the MFSP and that there is an increased level of agglutinins excreted in the hypersensitive *ras1.val17* mutant. Even with this increase in the "clumpyness" of the liquid cell culture and the high density of cells on the PVDF membrane for the agar assay, the shmoos of these cells never stick together to form the "prezygotic" phenotype of *byr1.DD*. This is rather unexpected as we would predict that shmoos would meet based purely on spatial dynamics even if they were elongating in a random direction independent of the pheromone gradient. This calls in to question whether these cells are completely defective in partner recognition therefore if shmoos do meet by random they do not recognise that they are shmoos and therefore do not stick together and initiate cell fusion.

A striking feature of MAPK phosphorylation profile in *ras1.val17* cells is the presence of effective down-regulation in the form of attenuation of the phospho-Spk1 signal (**Figure 3.13D**). For a long time, in mammalian cells, it was thought that the mechanism by which this mutation was oncogenic and causing enhanced proliferation was by constitutive activation of the downstream growth factor transcriptional programme brought about by constitutive ERK activation. More recently it was shown that expression of oncogenic Ras from its endogenous locus does not cause constitutive MAPK activation (Tuveson *et al.*, 2004). Our result clearly shows that there is effective down regulation of the phospho-MAPK signal, acting downstream of Ras1 which does not appear to be effective in the *byr1.DD* mutant. There is potentially an unidentified down-regulator acting at the level of MEKK or MEK itself which are yet to be identified for the *S.pombe* MFSP. This down-regulation, seen in *ras1.val17* cells, could be due to a number of other down-regulatory mechanisms including the negative regulation of the G-protein, Gpa1 and the binding of 14-3-3 proteins to Byr2 to influence its activity/localisation (Ozoe *et al.*, 2002; Pereira & Jones, 2001) The overall conclusion is that whatever down-regulation mechanisms are in place in the WT situation, they are no longer effective in the presence of Byr1.DD due to its constitutive nature and that it is important to terminate Byr1 activity to attenuate the phospho-Spk1 MAPK signal.

In the *ras1.val17* mutant there is potentially Spk1-GFP signal at the shmooing cell tips (**Figure 3.14**) but this could be due to autofluorescence as these cells are unhealthy looking and contain a large number of vacuoles therefore this requires further investigation. If Spk1 localisation to the shmoo tip is indeed real, it fits well with our hypothesis that Spk1 is required at the site of polarised growth and coordinates this growth with the site of pheromone stimulation on the cell cortex. Continual live cell

imaging of this mutant forming the elongated phenotype would be informative in this respect although preliminary experiments to try and capture shmoo formation in this mutant have been unsuccessful probably as a high density of cells is required to produce this phenotype which is not ideal for live cell imaging as we need a flat layer of cells.

The next objective was to investigate the role of Ras1 in the activation of both the MFSP and the Cdc42-pathway in response to pheromone signalling and if there is potential cross-talk between them. The coordinated activation of the pheromone MAPK pathway and polarised growth has been well studied in *S.cerevisiae* and is detailed in Chapter 1 Section 1.3.8.3. As mentioned, there are fundamental difference between *S.pombe* and *S.cerevisiae* in terms of the presence of the Ste5 and Far1 scaffolds which play essential roles in this coordination and this process remains largely undefined in *S.pombe*.

CHAPTER 4 RAS1 ACTIVATES TWO INDEPENDENT PATHWAYS DURING MEIOTIC DIFFERENTIATION

4.1 Introduction

The MAPKKK, Byr2 is a known effector of Ras1 (Wang *et al.*, 1991) and overexpression of *byr2* or *byr1* on multicopy plasmids in *ras1Δ* diploids can partially suppress the meiotic defect which lead to the hypothesis that Ras1, Byr2 and Byr1 are in a linear pathway activated by pheromones (Wang *et al.*, 1991). The observations that *byr2Δ* does not cause the same rounded phenotype in mitotic cells as *ras1Δ* predicted that Ras1 was also involved in the control of cell morphogenesis and a screen for mutants showing the same rounded mitotic phenotype as *ras1Δ* isolated four "ras-like" genes, *ral1-4* (Fukui & Yamamoto, 1988). Investigations into the functions of these identified genes lead to the conclusion that Ras1 forms a complex with two of these *ral* genes - *ral1* and *ral3* - which were renamed *scd1* and *scd2* respectively along with the rho-GTPase, Cdc42 which is involved in a number of processes including cell polarisation and actin organisation (Chang *et al.*, 1994). Single deletion mutants of the MAPK components *byr2*, *byr1* and *spk1* are sterile and so are single deletion mutants of *scd1* and *scd2* from the morphology pathway. Curiously, the single deletion mutants of the MAPK components show no shmooing response upon nitrogen starvation, this gave us our first indication that MAPK activation is required for a polarised growth response, this is explored in **Section 4.4**.

Our hypothesis is that Ras1 is playing an essential role in activation of both the mating factor signalling pathway (MFSP) and the Cdc42-morphology pathway upon pheromone stimulation to control activation of the MAPK cascade and the polarised growth response - referred to as the "MAPK branch" and the "morphology branch" -

both of which are required for successful mating (**Figure 4.1**). We predict that MAPK activation and polarised growth will be highly coordinated at the site of pheromone stimulation resulting in shmooing in the direction of a mating partner and that this coordination is dependent on Ras1.

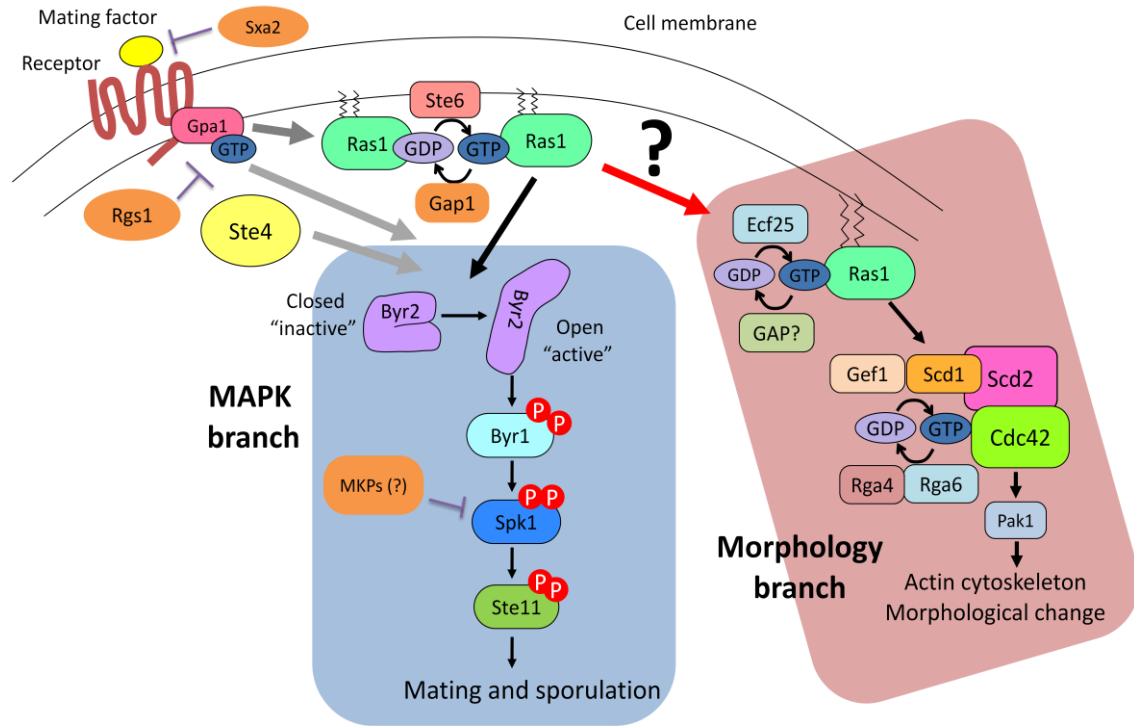


Figure 4.1 Hypothesis: Ras1 activates two independent pathways upon pheromone signalling.

The MFSP is activated when mating factor (either M or P factor) binds to its cognate GPCR on the cell surface. Once activated the GPCR activates the G-protein, Gpa1, which relays the signal to the RasGEF, Ste6, which activates Ras1. The hypothesis is that Ras1 activates both the MAPK branch and the morphological branch leading to the activation of the Cdc42 pathway in direct response to pheromone signalling to coordinate both the pheromone dependent transcriptional programme and the morphological changes required for mating.

4.2 Constitutively active MEK can bypass the requirement of Ras1 for MAPK phosphorylation but not the morphological defect

To investigate the role of Ras1 in MAPK activation and whether its role in the Cdc42 pathway is essential for the mating process, the MAPK activation and morphology of the following mutants were examined; *ras1Δ* (KT4323), *byr1.DD* (KT3435) and *ras1Δbyr1.DD* (KT4359). All strains contained Spk1-GFP expressed from its endogenous locus and were generated by transforming the relevant host strains with the *Spk1-GFP-2xFLAG-Kan^R* PCR fragment. Cells were subject to the SPA plate mating assay (as outlined in Chapter 3 and Materials and Methods) and cells collected at four time-points; 0, 8, 16 and 24 hours post induction. Cells were denatured by the TCA method and subject to western blotting to investigate levels of phospho- and total-Spk1. Live cell imaging was used to observe the cell morphology and localisation of Spk1-GFP over the time-course.

The deletion of *ras1* in *S.pombe* cells causes them to become rounded during mitotic growth and haploid *ras1Δ* cells are completely defective in mating process. Diploid *ras1Δ/ras1Δ* strains are capable of sporulation at a very low frequency indicating that Ras1 is important for both the mating process and sporulation. The prediction is that if *ras1Δ* cells are sterile because the MAPK is not fully activated then the addition of the Byr1.DD constitutively active protein would overcome this defect and as a consequence the *ras1Δbyr1.DD* double mutant would show the characteristic "prezygotic" phenotype of *byr1.DD* cells introduced in Chapter 3.

The western blot in **Figure 4.2A** shows that Ras1 is important for full MAPK phosphorylation as there is a significant reduction in the amount of phospho-Spk1 detected in a *ras1Δ* (the lower green band is an undefined background band - See

Chapter 3 Section 3.4 Phospho-antibody validation). As expected, when the *ras1Δ* was combined with the *byr1.DD* to generate the *ras1Δ byr1.DD* double mutant strain, it showed restored levels of phospho- and total-Spk1 protein comparable to those of the *byr1.DD* single mutant. However, the live cell imaging in **Figure 4.2B** shows that there was no morphological conversion associated with this restoration of *byr1.DD*-type MAPK output in the *ras1Δbyr1.DD* mutant. Once expressed, Spk1-GFP does not show obvious translocation to the nucleus in the *ras1Δ* strain and this nuclear relocation is restored somewhat in the *ras1Δbyr1.DD*, yet there is no morphological changes which mirror that of the single *byr1.DD* single mutant. This concludes that restoring MAPK phosphorylation via the addition of a constitutively active MEK can bypass the requirement of Ras1 for MAPK phosphorylation but not the morphological defect which we associate with a defective Cdc42-pathway in the absence of Ras1.

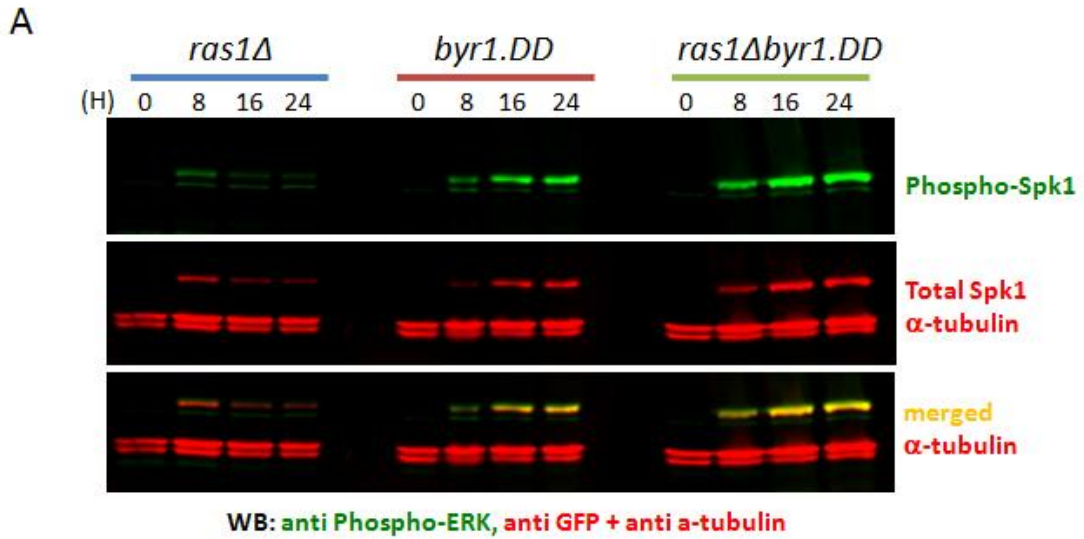


Figure 4.2 *byr1.DD* can bypass the requirement of Ras1 for MAPK activation but not the morphological defect.

(A) Western blot of *ras1Δ* (KT4323), *byr1.DD* (KT3435) and *ras1Δbyr1.DD* (KT4359) cell extracts, membrane was blotted with anti-phospho-ERK, anti-GFP and anti- α -tubulin at times-points 0, 8, 16 and 24 after mating induction represented by (H). (B) Live cell imaging of the mentioned strains in the brightfield and GFP channels. Each time point comprises 15-25 serial images of 0.4 μ m interval along the Z axis taken to span the full thickness of the cell. All of the Spk1-GFP images were deconvolved using the Huygens Essential Deconvolution. Deconvolved images were Z-projected, cropped and combined using ImageJ. Scale bar is 5 μ m.

4.3 MAPK activation does not define the morphological phenotype

To determine whether the MAPK phosphorylation profile is indicative of the final mating phenotype in a strain where all the components of the Cdc42 pathway are present, unlike in *ras1Δ*, we went about altering the Spk1 phosphorylation profile in the *ras1.val17* mutant by combining it with the *byr1.DD* mutant, and directly comparing the MAPK phosphorylation profiles of the *byr1.DD* single mutant (KT3435) and the *ras1.val17 byr1.DD* double mutant (KT3439) on the same western blot membrane. The *ras1.val17 byr1.DD spk1-GFP* strain (KT3439) was generated by the transformation of a previously generated double mutant strain, KT2734, with the *Spk1-GFP-2xFLAG-Kan^R* PCR product as outlined previously.

Direct comparison of the MAPK dynamics in *byr1.DD* and *ras1.val17 byr1.DD* were carried out by comparing two biological replicates time-courses from each strain. Data represented in **Figure 4.3** is from one technical replicate of one biological replicate. Two biological replicate time-courses were collected and subject to quantitative western blotting. Both biological replicates showed similar data therefore quantitation of only one biological replicate is shown.

A western blot directly comparing the phospho- and total- Spk1-GFP levels is represented in **Figure 4.3A**. Considering the direct comparisons of *byr1.DD* and *ras1.val17 byr1.DD* the MAPK a levels are comparable in both, as shown in **Figure 4.3B**, therefore the presence of the *ras1.val17* mutation has not altered the MAPK activation to resemble that of the *ras1.val17* single mutant (**Chapter 3 Figure 3.13**). In other words, in terms of the MAPK phosphorylation profile, the *byr1.DD* mutation is epistatic to the *ras1.val17* mutation because the activation of Spk1 goes exclusively through Byr1.

There may be a decrease in the maximal level of MAPK phosphorylation as the double mutant does not appear to reach the same level as *byr1.DD* alone. This may be because there is more degradation of Spk1 in the double mutant as there is a possible decrease in the total amount of Spk1 in the double mutant compared to *byr1.DD* single (**Figure 4.3C**). A stronger degradation may occur due to a more hyper-activated proteasome as a consequence of the presence of Ras1.val17 in these cells as the Ras1-Scd1-Cdc42 pathway has been shown to play a role in proteasome translocation and assembly during mitosis (Yen *et al.*, 2003).

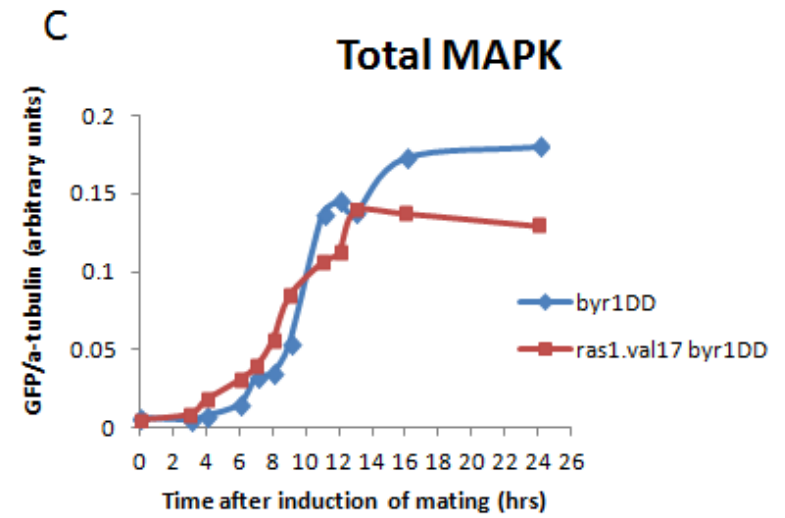
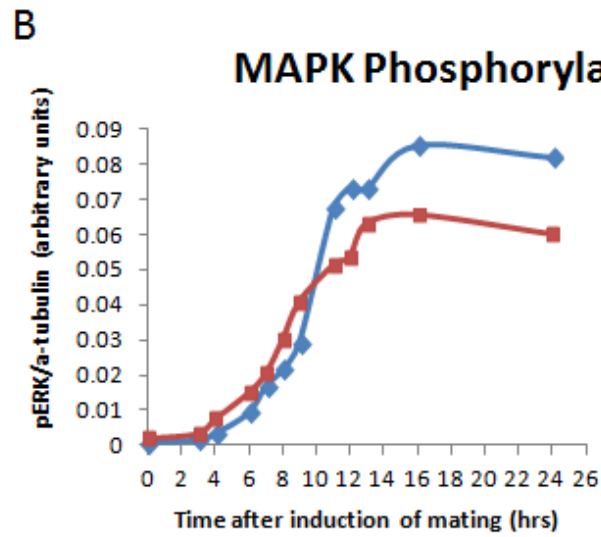
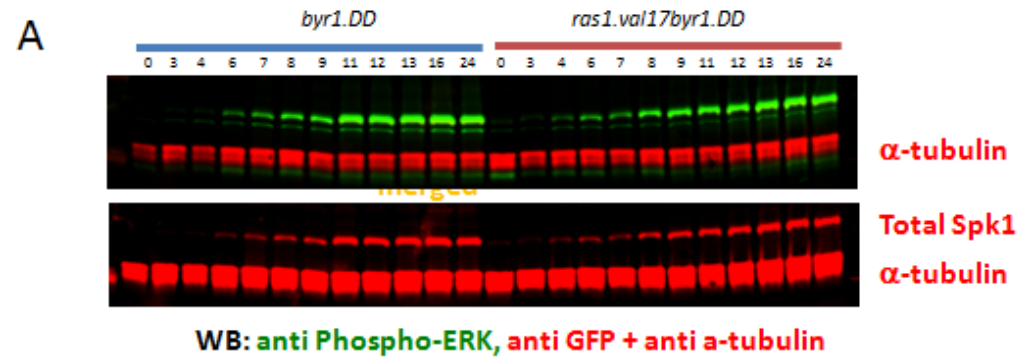


Figure 4.3 Direct comparison of MAPK phosphorylation in *byr1.DD* and *ras1.val17 byr1.DD* by quantitative western blot.

(A) Western blots of direct comparisons of *byr1.DD* (KT3435) and *ras1.val17 byr1.DD* (KT3439). Membrane was blotted with anti-phospho-ERK, anti-GFP and anti- α -tubulin. (B) Quantitation of the phospho-MAPK signal normalised against α -tubulin as a loading control. Quantitation is of one biological replicate comprising one technical replicate. Two biological replicate time courses were carried out for each mutant. (C) Quantitation of GFP/ α -tubulin to represent the changes in total Spk1-GFP levels over a mating timecourse. Quantitation is representative of one biological replicate.

In conclusion, the MAPK phosphorylation profile in the *ras1.val17 byr1.DD* double mutant mirrors that of the *byr1.DD* single mutant, and the presence of oncogenic Ras1.val17 mutant protein does not appear to alter MAPK output in the presence of Byr1.DD i.e. it does not appear to cause any additional MAPK phosphorylation. If *ras1.val17* was having no effect on a separate morphology pathway and was solely working in the activation of the MAPK then this double mutant MAPK phosphorylation profile would indicate that the double mutant would have the same "prezygotic" phenotype as the single *byr1.DD* mutant. This prediction was examined using live cell imaging with the results shown in **Figure 4.4**.

Live cell imaging clearly showed that the terminal mating phenotype of the *ras1.val17 byr1.DD* double mutant (observed from 16-hours onwards) is the elongated phenotype of the *ras1.val17* single mutant in contrast to the paired prezygotic phenotype of the *byr1.DD* single mutant. The dynamics of Spk1-GFP in the double mutant are more reflective of the *byr1.DD* single mutant as there is an evident delay in the nuclear translocation of Spk1-GFP compared to the *ras1.val17* single mutant, the nuclear localisation doesn't appear in the nucleus until 9-hours post induction compared to 6-hours in the images presented in **Figure 4.4**— this is much more reflective of *byr1.DD* but it is interesting to note that the nuclear localisation seems to be happening at earlier time-points in the double mutant compared to *byr1.DD* alone (compare images to 9-hours in **Figure 4.4** and maybe MAPK phosphorylation is not the only factor which influences MAPK relocation to the nucleus. It is however clear that the elongated phenotype doesn't start to appear until much later in the *ras1.val17 byr1.DD* double mutant compared to *ras1.val17* alone and there is a dramatic change in the morphology of the double mutant observed between 13 and 16 hours post induction. We conclude

that the terminal mating phenotype of *ras1.val17 byr1.DD* is a phenocopy of *ras1.val17*.

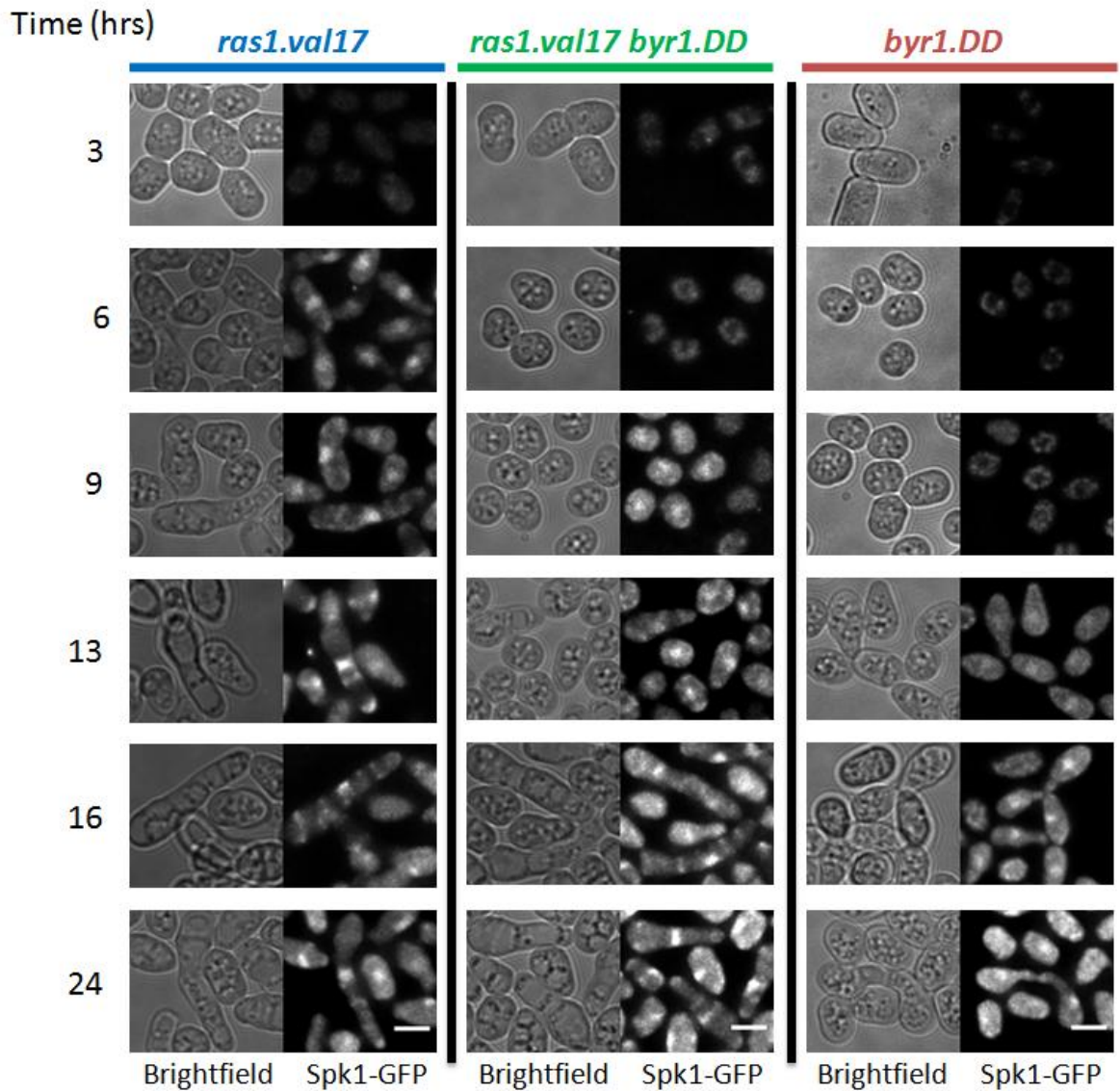


Figure 4.4 The terminal mating phenotype of *ras1.val17 byr1.DD* is a phenocopy of *ras1.val17*.

Images were taken of the strains *ras1.val17* (KT3084), *ras1.val17 byr1.DD* (KT3439) and *byr1.DD* (KT3435) at specific times post mating induction in both the brightfield and GFP channels in order to visualise Spk1-GFP. Each time point comprises 15-25 serial images of 0.4 μm interval along the Z axis taken to span the full thickness of the cell. All of the Spk1-GFP images were deconvolved using the Huygens Essential Deconvolution. Deconvolved images were Z-projected, cropped and combined using ImageJ. Scale bar is 5 μm .

In conclusion, the Spk1 phosphorylation profile is very similar in the single *byr1.DD* mutant and *ras1.val17 byr1.DD* double mutant but the morphology is a direct phenocopy of the *ras1.val17* single mutant therefore the MAPK phosphorylation profile is not indicative of morphological phenotype. This is summarised in **Table 4.1**. This result proves that *ras.val17* is activating at least two pathways in specific response to pheromone signalling: the MAPK cascade and the shmooing response.

The triple mutant, *ras1.val17 byr2Δ byr1.DD* also shows the elongated phenotype (data not shown). This result begins to separate out the signalling components, for example Ras1 must be signalling to a Byr1 independent pathway simultaneously in order for the double and triple mutants to have the elongated phenotype. The most likely candidate pathway is the Ras1-Cdc42 pathway. This lead us to the hypothesis that premature/hyper-activation of the Cdc42 pathway is responsible for the elongated mutant mating phenotype in the presence of an unregulated Ras1 protein. In conclusion, Ras1 regulates morphology independently of the MAPK activation. In terms of phenotype, *ras1.val17* is epistatic to *byr1.DD* and it is the activation status of Ras1 which governs the mating phenotype. This hypothesis is supported by a finding reported in (Marcus *et al.*, 1995) where they saw an attenuation of the hypersensitive response of *ras1.val17* by the overexpression of the N-terminal regulatory domain of Pak1/Shk1 and therefore the elongation of *ras1.val17* is working through Pak1 which is a known Cdc42- effector (Otilie *et al.*, 1995; Marcus *et al.*, 1995).

Genotype	Phenotypes	
	MAPK profile	Morphology
<i>byr1.DD</i>	<i>byr1.DD</i> type	<i>byr1.DD</i> type
<i>ras1.val17</i>	<i>ras1.val17</i> type	<i>ras1.val17</i> type
<i>ras1.val17</i> <i>byr1.DD</i>	<i>byr1.DD</i> type	<i>ras1.val17</i> type

Table 4.1 Summary MAPK activation and morphology observations:

- (1) MAPK phosphorylation profile, defined by the MEK*(*byr1.DD*), is not linked to the morphological phenotype
- (2) Morphological phenotype is defined by the *ras1.val17* mutation

4.4 MAPK activation is essential for a morphological response

Ras1 is playing a key role in MAPK phosphorylation and the morphological response during the mating process. The following section outlines experiments used to dissect whether there is further cooperation between these two pathways other than at the level of Ras1.

4.4.1 Byr2 is exclusive to the activation of the MAPK cascade

The MAPK phosphorylation and morphological responses were examined and directly compared in the following mutants: *byr2Δ* (KT3763), *byr1.DD* (KT3435) and *byr2Δ byr1.DD* (KT4010) for the purpose of uncovering whether Byr2 is required in both the MAPK response and the morphology response. All mutants were created via the two-step PCR method outlined previously and all contain *Spk1-GFP-2xFLAG-Kan^R*.

Figure 4.5 shows that there is no MAPK phosphorylation in the *byr2Δ* mutant but Spk1-GFP protein present, therefore Byr2 is an essential protein for MAPK activation, along with Byr1 (this was shown in Chapter 3 with the validation of the phospho-specific antibody where there is no phospho-Spk1 in the *byr1Δ* strain, KT4300, **Figure 3.7F**). In conclusion, Byr2 exclusively activates Byr1 which exclusively phosphorylates Spk1 and there is no additional input into the pathway from additional pathways at the level of Byr1 or Spk1. MAPK phosphorylation is restored in cells containing *byr2Δ* by the addition of *byr1.DD* as shown by the restoration of the phospho-MAPK signal in **Figure 4.5A and B**. Is this restoration in MAPK activation enough to influence the mating morphology phenotype? Live cell imaging of the *byr2Δ byr1.DD* mutant revealed that the morphological phenotype of this strain is indeed that of the *byr1.DD* where cells are paired but not fused (**Figure 4.6**). Therefore, we conclude that Byr2 acts exclusively to activate the MAPK and is not required in the morphology pathway. This highlights that MAPK output is essential for any morphological change as the single

byr2Δ mutant is completely sterile and cells remain G1-arrested with no shmoo formation (**Figure 4.6**). This also confirms that Byr1.DD signals independently of any upstream signalling because the *byr1.DD* MAPK phosphorylation profile is not significantly different to the *byr2Δ byr1.DD* MAPK phosphorylation profile (**Figure 4.5B**).

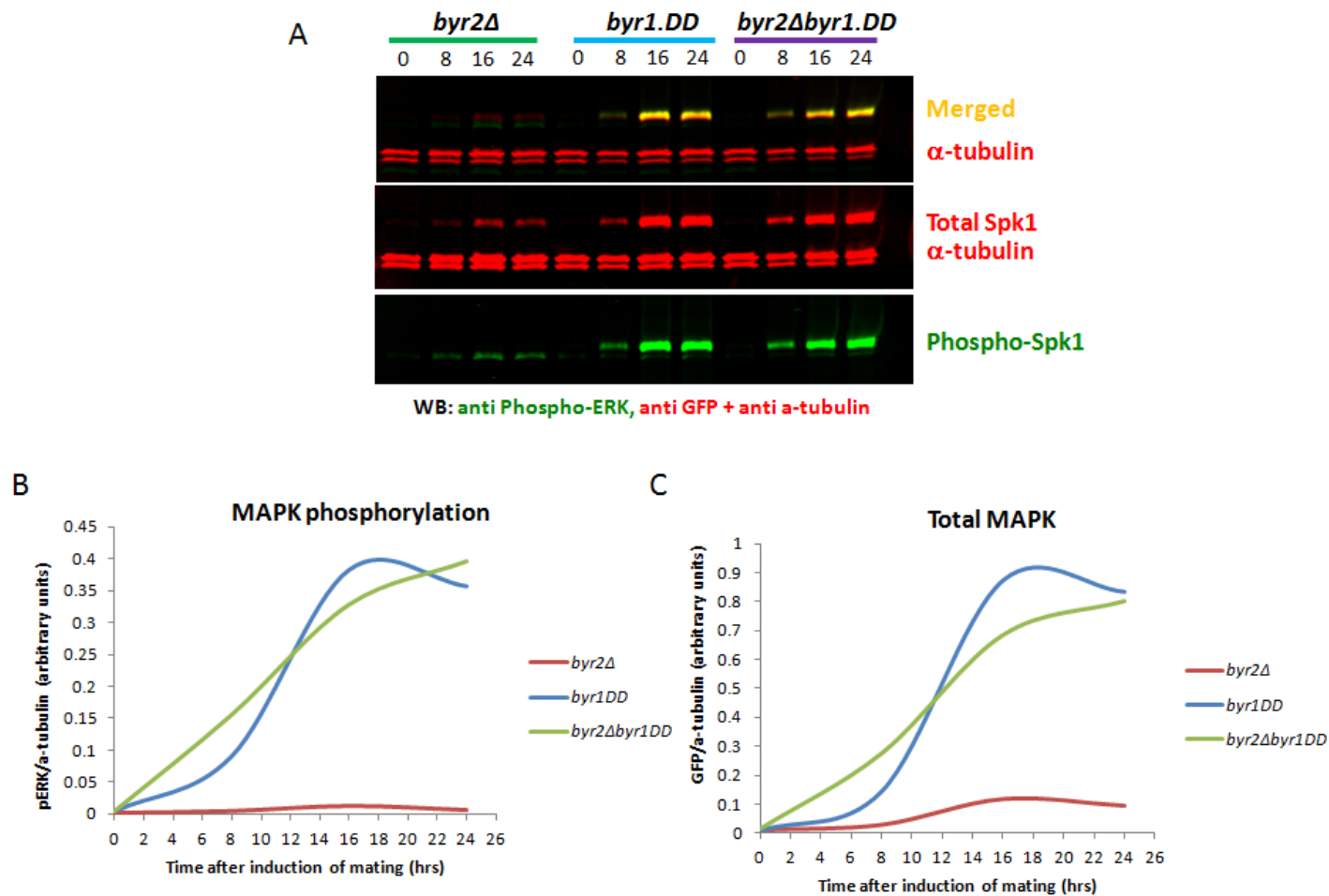


Figure 4.5 *Byr1.DD* signals independently of *Byr2*

(A) Western blot of *byr2Δ* (KT3763), *byr1.DD* (KT3435) and *byr2Δ byr1.DD* (KT4010) cell extracts, membrane was blotted for phospho-ERK, GFP and α -tubulin. (B) Quantification of MAPK phosphorylation (C) Quantification of total Spk1-GFP. Quantification was carried out using the Image Studio ver2.1 for both phospho-Spk1 and total Spk1-GFP and normalised against α -tubulin as a loading control.

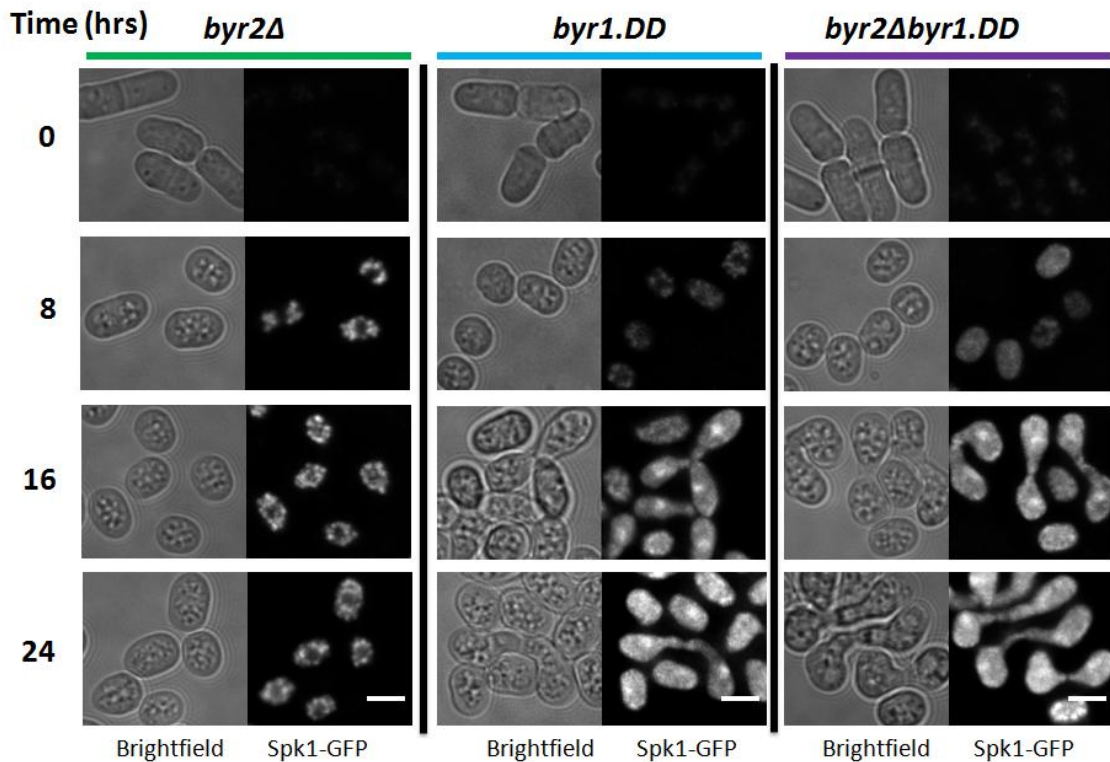


Figure 4.6. The *byr1.DD* "paired" phenotype is independent of Byr2

Live cell imaging of *byr2Δ* (KT3763), *byr1.DD* (KT3435) and *byr2Δ byr1.DD* (KT4010) strains in the brightfield and GFP channels. Each time point comprises 15-25 serial images of 0.4 μm interval along the Z axis taken to span the full thickness of the cell. All of the Spk1-GFP images were deconvolved using the Huygens Essential Deconvolution. Deconvolved images were Z-projected, cropped and combined using ImageJ. Scale bar is 5 μm .

4.4.2 Scd1 is exclusive to activation of the morphology branch

Scd1 is a guanine nucleotide exchange factor (GEF) for Cdc42 (Chang *et al.*, 1994) (**Figure 4.1**). *scd1Δ* cells are rounded just like *ras1Δ* during the vegetative cell cycle and incapable of mating although diploid *scd1Δ/scd1Δ* cells are able to sporulate, indicating that its deficiency is largely limited to cell morphology and not to defective MAPK signalling (Fukui & Yamamoto, 1988). Indeed, by comparing Spk1 MAPK phosphorylation in *scd1Δ* (KT4061), *byr1.DD* (KT3435) and *scd1Δ byr1.DD* (KT4047) as shown in **Figure 4.7**. All strains contain *Spk1-GFP-2xFLAG-Kan^R*. We conclude that unlike *ras1Δ* cells (**Figure 4.2A**) MAPK phosphorylation in *scd1Δ* is detectable in significant amount over a 24-hour mating time-course (**Figure 4.7A**) and nuclear localisation of Spk1-GFP is evident at 8-hours post induction (**Figure 4.7B**) and yet there is no morphological changes in this mutant. The addition of *byr1.DD* fails to change the morphology of cells containing *scd1Δ* even though the MAPK phosphorylation is converted to that of the *byr1.DD* mutant (**Figure 4.7A** - not quantified). In conclusion, Scd1 is an essential part of the morphology pathway and manipulating the MAPK phosphorylation in these cells cannot suppress the morphological defect of *scd1Δ*. MAPK phosphorylation in *scd1Δ* compared to WT is examined in detail in **Section 4.6 (Figure 4.10)**.

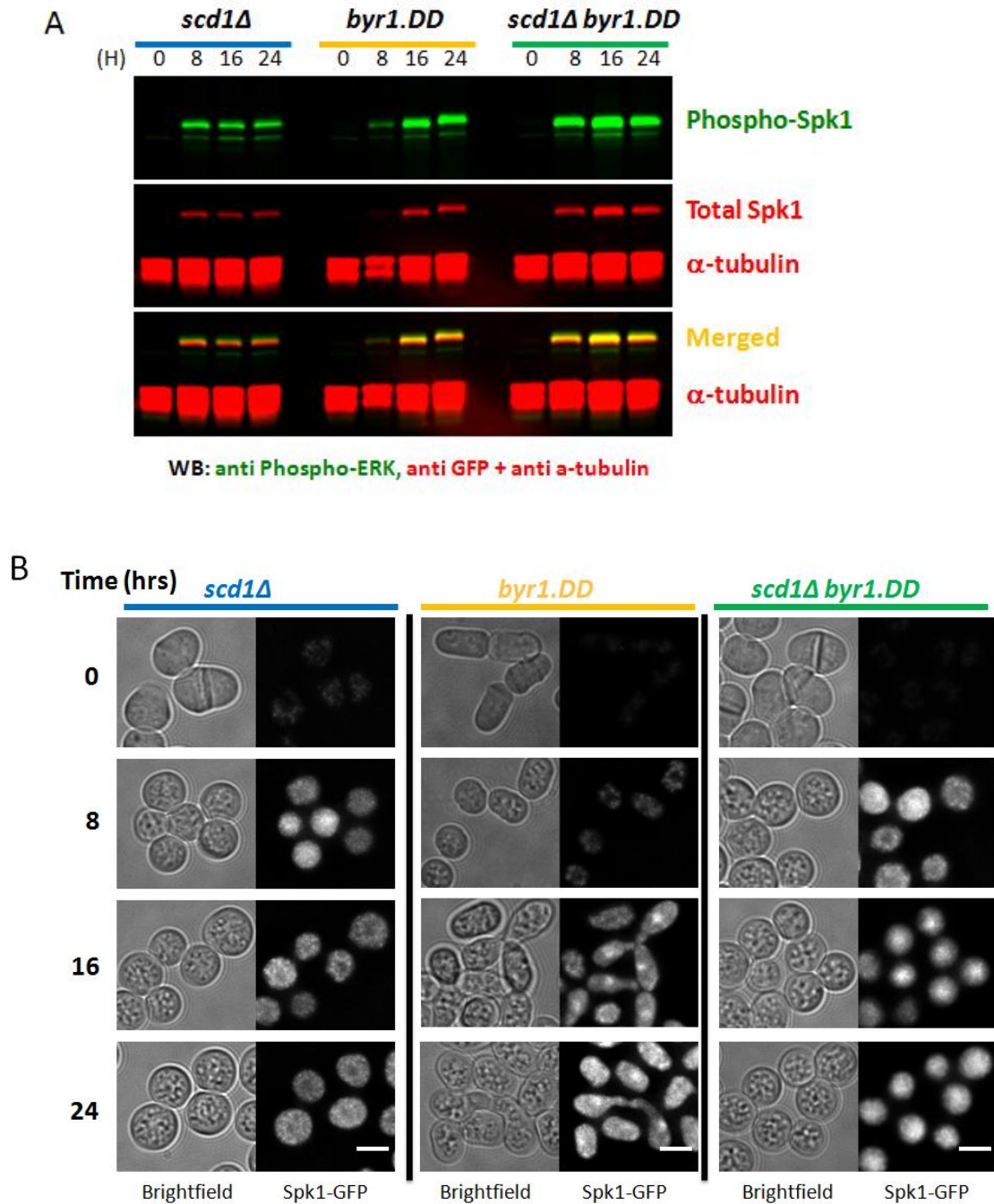


Figure 4.7 Scd1 is an essential part of the morphology branch

(A) Western blot of *scd1Δ* (KT4061), *byr1.DD* (KT3435) and *scd1Δbyr1.DD* (KT4047) cell extracts, the membrane was blotted with anti-phospho-ERK, anti-GFP and anti- α -tubulin at times-points 0, 8, 16 and 24 after mating induction represented by (H).. (B) Live cell imaging of the mentioned strains in the brightfield and GFP channels. Each time point comprises 15-25 serial images of 0.4 μ m interval along the Z axis taken to span the full thickness of the cell. All of the Spk1-GFP images were deconvolved using the Huygens Essential Deconvolution. Deconvolved images were Z-projected, cropped and combined using ImageJ. Scale bar is 5 μ m.

4.4.3 Activation of the morphology branch still requires MAPK activation in the presence of oncogenic Ras1.

To determine the nature of how MAPK is feeding into activation of the morphology branch we wanted to determine whether MAPK was acting upstream of Ras1 for the morphology branch. If this was indeed the case then we would predict in the absence of a MAPK output (in this case, *byr1Δ*) but in the presence of the oncogenic *ras1* mutation (which we predict would constitutively activate the Cdc42 pathway) then cells would show the elongated *ras1.val17* single mutant phenotype.

Live cell imaging of *ras1.val17 byr1Δ* in **Figure 4.8** reveals that actually *ras1.val17* is not enough to promote a morphological response on its own, it requires intact MAPK signalling. This is also the case in a *ras1.val17 byr2Δ* mutant (data not shown), therefore the contribution of MAPK signalling towards the morphology pathway is unlikely to be via the upstream activation of Ras1 seeing as Ras1 is already activated in these mutants.

Timing of a morphological change links with timings of MAPK phosphorylation/nuclear translocation

Looking at the timings of morphological response and the timings of the translocation of Spk1-GFP to the nucleus in the *ras1.val17* and *ras1.val17 byr1.DD* double strains highlights that the change in morphology links well with the timing of MAPK phosphorylation which is dramatically delayed in the *ras1.val17 byr1.DD* double compared to the *ras1.val17* single mutant (**Figure 4.9**). *ras1.val17* cells start to show polarised growth by 6-hours post mating induction with cells showing the elongated phenotype by 9-hours. In contrast to the *ras1.val17 byr1.DD* cells where small shmoos are starting to become evident at 13-hours and are highly prominent by 16-hours. These

data confirm that the timings of a morphological response correlate well with the timings of MAPK phosphorylation and that by changing the MAPK phosphorylation profile in *ras1.val17* by the addition of *byr1.DD* we significantly delay the morphological response linking MAPK activation directly to shmoo formation.

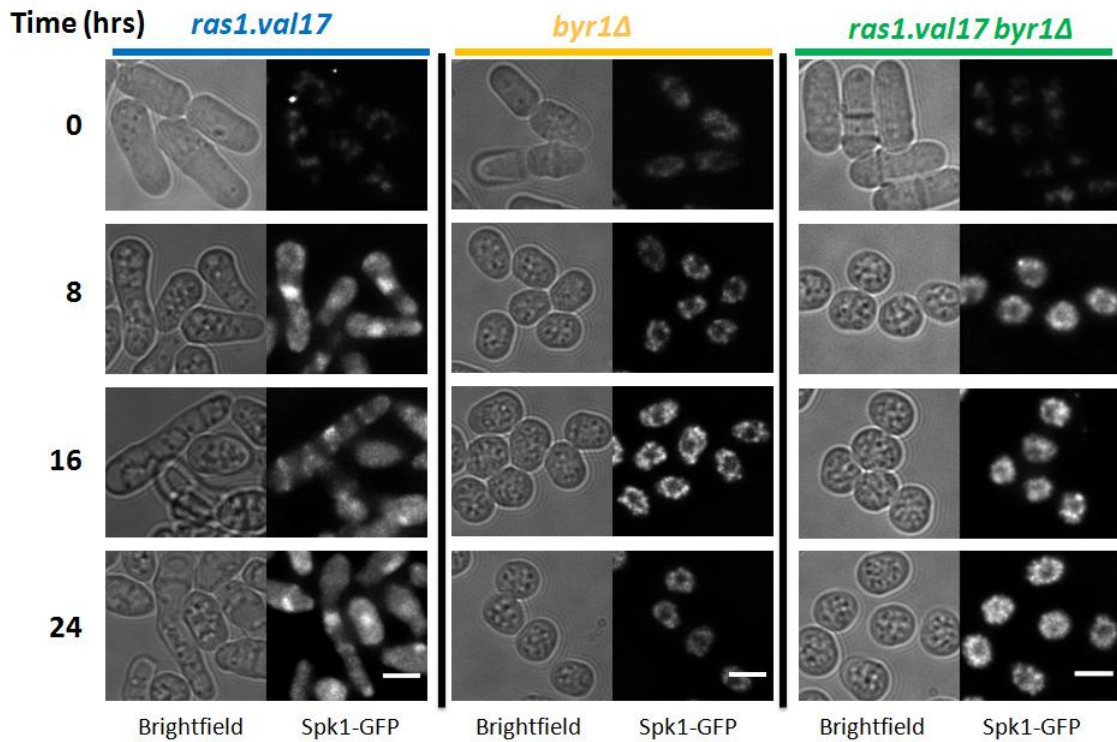


Figure 4.8 No morphological change in the absence of MAPK signalling

Live cell imaging of *ras1.val17*(KT3084), *byr1Δ* (KT4700) and *ras1.val17 byr1Δ* (KT5030) in the brightfield and GFP channels. All strains contain *spk1-GFP-2xFLAG-Kan^R* integrated at the *spk1* chromosomal locus. Each time point comprises 15-25 serial images of 0.4 μm interval along the Z axis taken to span the full thickness of the cell. All of the Spk1-GFP images were deconvolved using the Huygens Essential Deconvolution. Deconvolved images were Z-projected, cropped and combined using ImageJ. Scale bar is 5 μm .

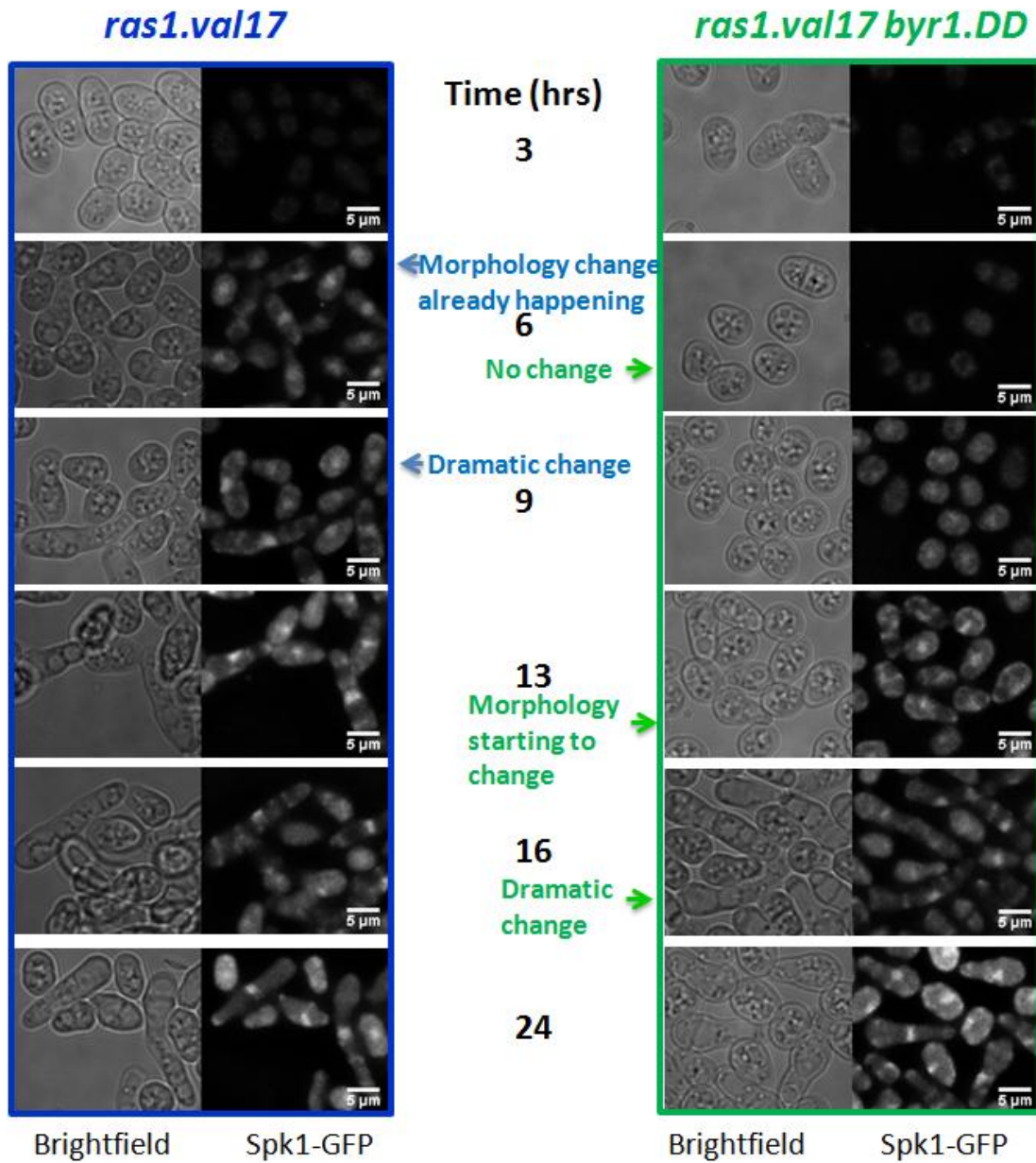


Figure 4.9 Morphological change associated with the *ras1.val17* occurs at later time points in the *byr1.DD* mutant

Live cell imaging of *ras1.val17*(KT3084), and *ras1.val17 byr1.DD* (KT3439) in the brightfield and GFP channels. Each time point comprises 15-25 serial images of 0.4 μm interval along the Z axis taken to span the full thickness of the cell. All of the Spk1-GFP images were deconvolved using the Huygens Essential Deconvolution. Deconvolved images were Z-projected, cropped and combined using ImageJ.

4.5 Does the morphology pathway feeding into MAPK activation?

We've shown that the MAPK pathway cross-talks with the Cdc42 pathway as phosphorylation of the MAPK, Spk1, is essential for a morphological response. Our next aim was to establish whether the Cdc42 pathway can feed into the activation of the MAPK pathway possibly via the activation of Pak1/Shk1 which is a kinase activated by Cdc42. Work by Tu *et al* 1997 showed that Pak1 was capable of promoting the "open" form of Byr2 MAPKKK and it has been shown that the Pak1 homologue in *S.cerevisiae*, Ste20, is directly involved in the activation of the MAPKKK, Ste11 (Tu *et al.*, 1997; Elion, 2001).

To investigate this possibility, WT (KT3082) and *scd1Δ* (KT4061) strains were subject to intense 24-hour mating time-courses with cells collected at various time-points followed by western blotting and quantification of the phospho- and total- MAPK signals (**Figure 4.10**). In the absence of Scd1, activation of Cdc42 is expected to be impaired and the downstream events are likely to be affected. A western blot directly comparing the levels of phospho- and total- Spk1 in WT and *scd1Δ* cells extracts are shown in **Figure 4.10A**. Quantification of the phospho-and total-MAPK signal was carried out as described previously and is representative of three biological replicates. **Figure 4.10B** shows that MAPK phosphorylation peaks at around 4-hours post induction in *scd1Δ* compared to 8-hours in WT. After 4-hours the phospho-signal decreases to the level of WT by 24-hours. There is an increase in the total amount of Spk1 in *scd1Δ* (**Figure 4.10C**) probably due to the increased positive feedback on Spk1 expression through pathway activation. The ratio of phospho- to total- Spk1 remains fairly constant in *scd1Δ* at 1:1 in a similar manner to WT (**Figure 4.10D**).

Live cell imaging of WT and *scd1Δ* at 0, 4, 8 and 12-hours post induction can be seen in **Figure 4.11** and shows that the Spk1-GFP signal is present in the nucleus of some cells at 4-hours in *scd1Δ* but not in WT showing that the nuclear dynamics of Spk1-GFP are again mirroring the MAPK phosphorylation timings. *scd1Δ* cells show no morphological change upon mating induction over the 24-hour time-course.

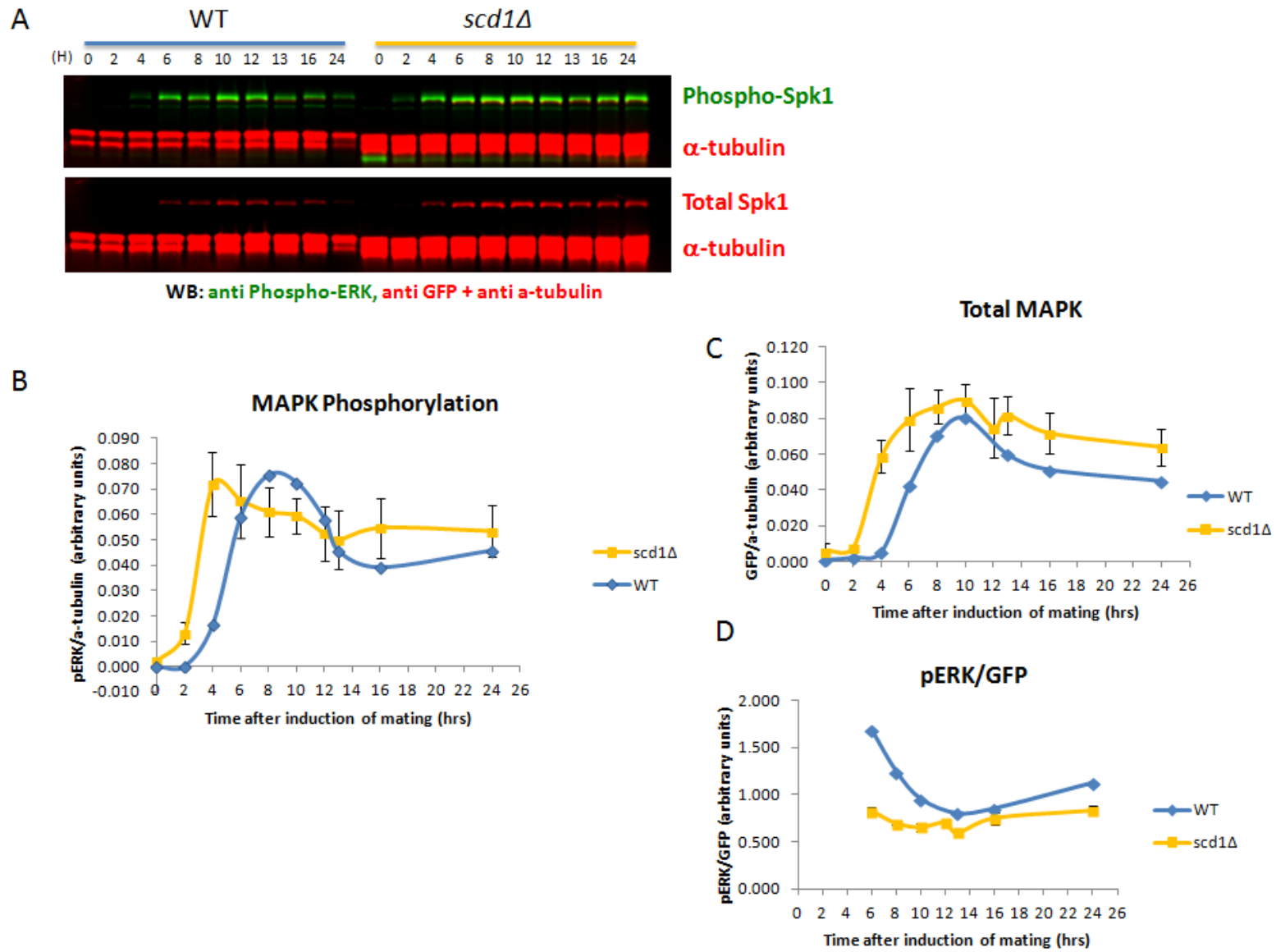


Figure 4.10 Does the morphology pathway influence MAPK activation?

(A) Western blot of WT (KT3082) and *scd1Δ* (KT4061) cell extracts, membrane was blotted with anti-phospho-ERK, anti-GFP and anti- α -tubulin at times-points after mating induction represented by (H).. (B) Quantitative of the western blot in (A) carried out using the Image Studio ver2.1 for both phospho-Spk1 (B) and total Spk1 (C) normalised against α -tubulin as a loading control. (D) The ratio of phospho- to total- Spk1. (H) indicates the number of hours post mating induction. Quantitation was carried out using three biological replicates and one technical replicate for *scd1Δ*. Quantitation of WT is using one biological replicate only. Error bars are \pm SEM.

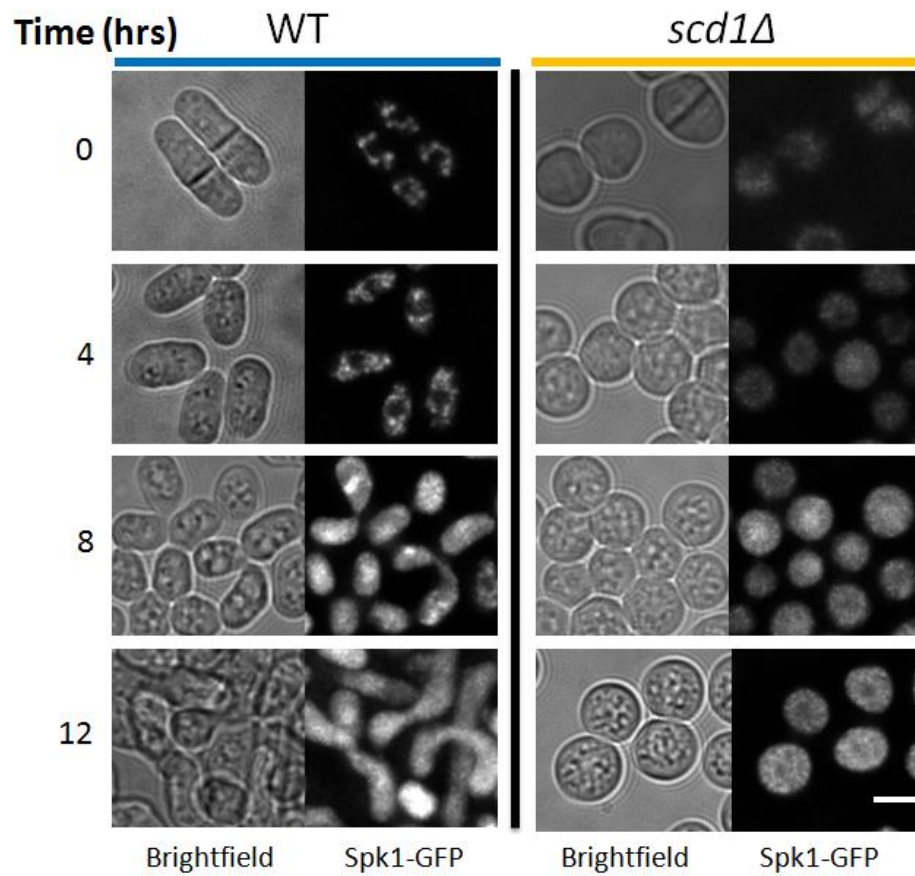


Figure 4.11 *scd1Δ* morphology

Live cell imaging of WT (KT3082), and *scd1Δ* (KT4061) in the brightfield and GFP channels. Each time point comprises 15-25 serial images of 0.4 μm interval along the Z axis taken to span the full thickness of the cell. All of the Spk1-GFP images were deconvolved using the Huygens Essential Deconvolution. Deconvolved images were Z-projected, cropped and combined using ImageJ. Scale bar is 5 μm .

4.6 Discussion

In summary, Ras1 has been proven to be important for both MAPK activation and activation of the Cdc42-morphology pathway upon pheromone signalling (**Figure 4.12**). These pathways diverge at the level of Ras1 as a defect in Byr2 has can be rescued by restoration of MAPK signalling and therefore the morphology branch is fully functional in a *byr2Δ* mutant. As a consequence of these results we predict that the elongated phenotype associated with the oncogenic Ras1 mutation, *ras1.val17*, is dependent on the hypersensitive activation of the Cdc42 branch directly through Ras1 activation and crosstalk with activated MAPK cascade.

We found that in the absence of Ras1 (**Figure 4.2A**) there is a small amount of MAPK phosphorylation although it is severely depleted compared to WT. This confirms previously reported findings that the MAPK cascade can be partially activated independently of Ras1 (Xu *et al.*, 1994) even though it is only to a small extent compared to WT - quantified data comparing phospho-MAPK levels in WT and *ras1Δ* is shown in Chapter 5 **Figure 5.10**. We have not checked whether this small amount of MAPK phosphorylation translates into a transcriptional response and our *ras1Δ* imaging (**Figure 4.2B**) shows no obvious Spk1-GFP in the nucleus.

MAPK activation is essential for a morphological response as shown by the rounded phenotype of the *ras1.val17 byr1Δ* strain. We predict that Spk1 may be phosphorylating a key component of the Cdc42 complex which could lead to stabilisation and correct localisation which are required for the specific polarised growth associated with mating.

If the Cdc42 pathway is defective, as is the case with *ras1Δ* and *scd1Δ*, then there can be no morphological response to mating pheromone even in the presence of a fully activated MAPK pathway. These data reconfirms that the Cdc42 pathway is the major

regulator of cell morphology during mating and even though we've seen that MAPK phosphorylation is essential for a morphological response in **Figure 4.8**, the restoration of MAPK phosphorylation via the addition of *byr1.DD* in both *ras1Δ* and *scd1Δ* cells is not enough to overcome the morphological defect, therefore the contribution of Spk1 is not effective in the absence of the Ras1 or Scd1.

There are a number of hypotheses for the actions of Spk1 towards the Cdc42-morphology pathway. There is evidence that the components of the morphology pathway form a multi-protein complex and act in a cooperative manner (Chang *et al.*, 1994) therefore Spk1 could be stabilising this complex at the site of pheromone stimulation via phosphorylation of one of the components and concentrating the complex at the site of pheromone stimulation. In *S.cerevisiae*, Fus3 phosphorylates Gβ to stabilise the Gβ-Far1-Cdc24 complex and keep it localised at the cell cortex at the site of pheromone stimulation (Metodiev *et al.*, 2002). Phospho-Spk1 could be acting as a marker on the cell cortex to signify the area of highest pheromone stimulation. The lack of a morphological response in the absence of MAPK phosphorylation might not be due to a lack of activation of the morphology complex but more due to that it is not localised specifically as a prominent foci. This is perhaps unlikely as (Bendezu & Martin, 2013) predict that without proper orientational information, cells tend to default the location of the shmoo to one of the cell poles. Three main possibilities are:

- The morphology complex is not active without Spk1-activation
- The morphology complex cannot form a stable complex without Spk1-phosphorylation
- The morphology complex is active but mislocalised without Spk1-phosphorylation

Further investigations into the activity and localisation of Cdc42 and components of the morphology complex and potential colocalisation with MFSP components (Ras1, Scd1 and Scd2 along with Gap1, Ste4 and Ste6) in the absence of MAPK activation will help to distinguish between these options. In mammalian cells, Ras and Cdc42 have been shown to colocalise (Cheng *et al.*, 2011) but this has yet to be reported in *S.pombe*. The activity of the morphology complex can be assessed using CRIB-GFP which has been used to observe the localisation of Cdc42-GTP (Das *et al.*, 2012; Bendezu & Martin, 2013).

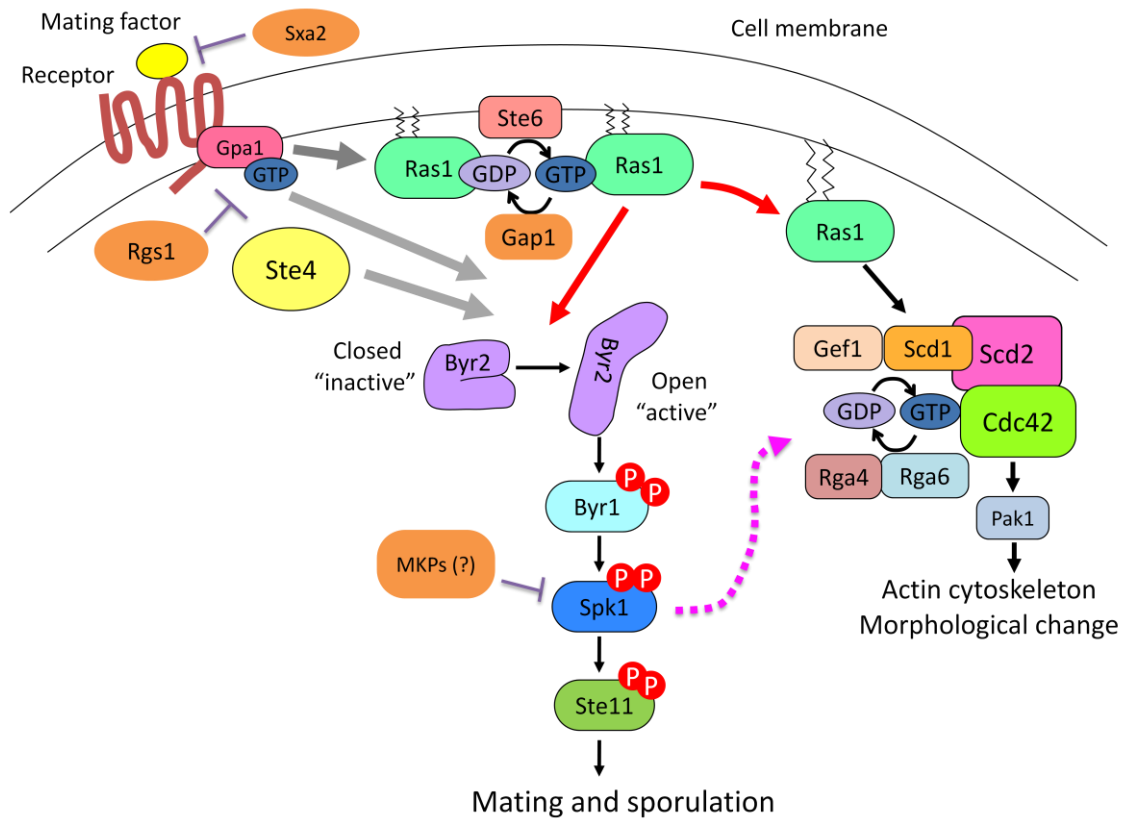


Figure 4.12 Conclusion: Ras1 activates two independent pathways and activated MAPK feeds into the morphology branch

MAPK may potentially phosphorylate a component of the Cdc42-morphology pathway to coordinate the polarised cell growth required for mating and the binding of mating pheromone to its receptor on the cell membrane. There are a number of potential candidate for the MAPK target protein including Scd2 and Rga4. MAPK activation is required for the polarised growth associated with meiotic differentiation as *ras1.val17* alone cannot activate a morphological response without intact MAPK signalling.

4.6.1 The potential Spk1 MAPK target of the morphology branch

Unidirectional polarised growth - as exhibited during shmooing - requires Cdc42 to cease its role in mitotic cell growth and localise to the single site of highest pheromone stimulation on the cell cortex. During mitosis, Cdc42 oscillates between the two growing cell tips (Das *et al.*, 2012). This paper highlights interesting mechanisms of Cdc42 dynamics; Cdc42 has been shown to be subject to autocatalytic activation (Chang *et al.*, 1994; Endo *et al.*, 2003; Wheatley & Rittinger, 2005; Chang *et al.*, 1999) which aids in positive feedback, to achieve its oscillatory effect there must be a negative feedback in place. This is thought to be through the actions of Pak1 because the *orb2-34* mutant allele of *pak1* - which has decreased activity (Verde, 1998) - caused a delay in the timings of oscillations and a retention of Cdc42-GTP, Scd1 and Scd2 exclusively at one cell tip (Das *et al.*, 2012), therefore the dissociation of the Cdc42 complex is hypothesised to be dependent on Pak1 activity possibly via the phosphorylation of Scd2 which has been shown to be a Pak1 substrate *in vitro* (Chang *et al.*, 1999). If we translate these observations over to the mating response, we require active Cdc42 to cluster at the site of pheromone stimulation to promote shmoo formation and we don't want the complex to dissociate until after mating has been successful therefore we propose that Spk1 could be directly phosphorylating a component of the Cdc42 complex stabilising the complex and preventing the negative feedback potentially promoted by Pak1. We have formulated two hypotheses as to how MAPK activation could be contributing to control of the Cdc42-response to try and explain how the activity of Cdc42 can be altered between mitosis and mating and the switch from cell tip elongation to shmooing.

- The Scd2 hypothesis

A potential target for Spk1 is the scaffold protein, Scd2 (**Figure 4.12**) and that phosphorylation of Scd2 causes it to relocate to the plasma membrane at the site of pheromone stimulation where it coordinates the activation of Cdc42 via the binding of Ras1 and Scd1. Another possibility is that Spk1 phosphorylation of Scd2 stabilised the morphology complex at the cell cortex and phosphorylation of Scd2 at specific MAPK phosphorylation sites may prevent negative feedback phosphorylation by Pak1 thereby sustaining the morphology complex at the site of pheromone stimulation.

A proposed future experiment to investigate this further is to use recombinant Scd2 protein, provided by collaborators Dr Mikako Shirouzu and Prof. Shigeyuki Yokoyama, as an *in vitro* substrate for Spk1 which will be immunoprecipitated from *byr1.DD* cells to hopefully obtain a good amount of the phosphorylated (and therefore activated) form of Spk1 MAPK and carry out a *in vitro* kinase assay. This can be further investigated with the identification and mutation of MAPK phosphorylation sites. In *S.cerevisiae*, the coordinated process of MAPK cascade activation and shmoo formation is reliant on the Far1 and Ste5 scaffolds which do not have obvious homologues in *S.pombe*, however, the importance of scaffold proteins in this process provides an excellent basis for the switch between the control of polarised growth for mitosis and mating.

- Rga4/Rga6 hypothesis

Another potential hypothesis is based on the Rga4 protein. Rga4 is a GAP for Cdc42 thereby promoting Cdc42 inactivation. The localisation of Rga4 is extremely important in dictating the localisation of activated Cdc42 at the cell tips in mitotic cells (Tatebe *et al.*, 2008; Kelly & Nurse, 2011; Das *et al.*, 2007). Potentially Spk1 could play a role in controlling the location of active Cdc42 at the shmoo site by indirectly regulating the activity of Rga4. Recently, Rga6 was also shown to be a Cdc42 GAP (Perez lab, Pombe

2013 - International Fission Yeast conference 2013). Both *rga4Δ* and *rga6Δ* strains have been generated in the lab but are still fully able to mate and sporulate at high efficiency when induced for meiosis. Interestingly, when *rga4Δ* was introduced into the *ras1.val17* background (KT3084) the cells became large and rounded in morphology during vegetative growth compared to the WT phenotype usually observed in *ras1.val17* (data not shown). This concludes that during mitosis the activation of Cdc42 is very tightly regulated at the level of Cdc42 itself and not at the level of Ras1. We hypothesize that during mating, Spk1 could be phosphorylating and thereby inactivating Rga4 which would allow a concentrated level of Cdc42-GTP to accumulate at the site of pheromone stimulation. The experimental design to investigate this hypothesis is outlined in Chapter 8 Section 8.1.8.

4.6.2 Does the Cdc42 pathway contribute to MAPK activation?

This increase in phospho- and total- MAPK in *scd1Δ* was unexpected as we predicted that activation would be lower in this mutant if the actions of the Cdc42 pathway were involved in Byr2 activation as has been suggested by (Tu *et al.*, 1997). However this result could be due to the actions of Cdc42 input being of a more inhibitory nature, in that case, it could be working to prevent acute MAPK activation and without Scd1 this inhibition is lost. In the *scd1Δ* mutant the peak activation is seen around 4-hours earlier compared to WT, and a time delay in MAPK activation may be essential for cells to orientate polarised growth in the direction of a mating partner. This proposed idea is supported by findings in (Bendezu & Martin, 2013) that showed that mutants with increased levels of pheromone signalling (*map1.dn9* and *rgs1Δ*) failed to show the Cdc42 complex exploring the periphery of the cell which they show to be important for correct shmoo orientation towards the strongest pheromone signal and a cell of opposite mating type therefore the timing of MAPK activation plays a crucial role in correct

orientation of polarised growth. However, this inhibitory hypothesis of Scd1-Cdc42 does not fit with the findings that Pak1 promotes the open "active" conformation of Byr2 (Tu *et al.*, 1997) and therefore positively contributes to MAPK cascade activation. It has also been reported that Scd1 is not required for MAPK signalling because the expression of *mam2* (the P-factor receptor) was unchanged compared to WT in *scd1Δ* cells (Chang *et al.*, 1994). Looking back at their data, there may be an increase in *mam2* expression in their *scd1-null* cells but without quantitation this is not clear and their main priority was to compare *mam2* expression in *scd1-null* to *ras1-null* cells to conclude that Scd1 is exclusively involved in the control of morphology and not MAPK activation - *ras1-null* cells showed no *mam2* expression. Therefore they may have overlooked a subtle increase in the amounts of *mam2* expression in their *scd1-null* strains compared to WT. These data bring into question whether Cdc42 signalling positively contributes to MAPK activation.

Another and perhaps more likely explanation for the acute MAPK phosphorylation in *scd1Δ* could also be because there is more "free" Ras1 protein available in the cell as it is not being used in the activation of Scd1 and that the Cdc42-morphology complex containing Ras1-Scd1-Scd2-Cdc42 and Pak1 could be dissociated in the absence of Scd1. Therefore the proportion of the total amount of Ras1 protein in the cell usually tied up in the activation of Scd1 is now free to be incorporated into activation of the MAPK cascade instead. Both the phospho- and total-MAPK profiles are strikingly similar to those of *ras1.val17* (Chapter 3 **Figure 3.13**) and we associate these "hypersensitive" MAPK dynamics with a hyperactive Ras1. This favours the hypothesis that there is an increase in the amount of Ras1 signalling through the MAPK cascade in the absence of Scd1. This can be tested by investigating the MAPK dynamics in the presence of overexpressed Ras1 and whether this too causes the hypersensitive effect.

Ideally to distinguish between if this hypersensitive MAPK phosphorylation in *scd1Δ* is due to an inhibitory nature of Scd1-dependent signalling or the case of more "free" Ras1 to signal via the MAPK cascade we require a morphology complex that has the correct stoichiometry of components but has compromised activity. Pak1 is an essential gene therefore it is not possible to investigate MAPK phosphorylation after the deletion of the *pak1* gene but there are Pak1 mutants with altered activities; a K415R is kinase deficient (Chang *et al.*, 1999) and G517E (also known as *orb2-34*) has decreased activity (Das *et al.*, 2012) which can also be used to further investigate if the activation of the morphology pathway feeds into the activation of the MAPK cascade. A Cdc42 mutant with compromised activity (Cdc42-L160S) (Estravis *et al.*, 2012) could also be used to evaluate the contribution of Cdc42 to MAPK activation.

In conclusion, the morphology pathway may be involved in subtle coordination of MAPK activation and the morphological response or the effect seen in **Figure 4.10** could be as a indirect consequence of the availability of more Ras1 in the absence of Scd1. These possibilities are not mutually exclusive. It is inconclusive to say whether the effect seen is due to direct or indirect morphology pathway disruption. Anyhow, the current data suggests an intimate link between the morphology pathway and the MAPK pathway.

4.6.3 Targeting Cdc42 in Ras-induced transformation

In terms of translating the key observations from this chapter over to mammalian research, we conclude that it is the activation status of Ras that is indicative of the final cellular phenotype independently of the duration of MAPK phosphorylation and that this oncogenic phenotype can only be prevented if MAPK phosphorylation is abolished completely as is the case of *ras1.val17 byr1Δ*. The complete inhibition of ERK MAPKs in Ras-transformed tumour cells is potentially unachievable and unrealistic in

terms of a treatment strategy. Recently the contribution of the ERK effector pathway to Ras induced oncogenesis has been called into question (Luo *et al.*, 2009) especially as MEK inhibition has had variable success in Ras malignancies compared with B-Raf driven malignancies which is probably because of the diverse number of Ras effector pathways. The work by (Tuveson *et al.*, 2004) showed that endogenously expressed oncogenic Ras did not cause aberrant ERK activation in MEFs and was therefore unlikely to be causing the partial transformation phenotype seen in these cells. This has led to the quest for a more relevant and effective target for Ras-driven tumours. Published work by (Stengel & Zheng, 2012) has shown that gene targeting of Cdc42 impaired oncogenic H-Ras to drive tumour formation in mice and that this effect was partially dependent on Akt but not MEK and ERK therefore highlighting that Cdc42 is an attractive therapeutic target. This ties in with our work which suggests that targeting of the morphology pathway is likely to be more successful in preventing the oncogenic Ras phenotype compared to targeting the MAPK pathway.

CHAPTER 5 SIGNAL TRANSDUCTION UPSTREAM OF RAS1: COORDINATION OF MAPK AND MORPHOLOGY ACTIVATION

5.1 Introduction

The findings of Chapter 4 have concluded that Ras1 plays a role in the activation of both the MAPK signalling pathway and the morphology pathway. The next objective was to investigate if activation of the two pathways is directly dependent on common upstream MFSP components. Our aim is proposed in pictorial form in **Figure 5.1**.

The roles of Ras1 and Gpa1 for Byr2 activation are partially independent of each other (Xu *et al.*, 1994) as expression of *gpa1* from a multi-copy plasmid can induce *mam2* expression in the absence of *ras1* and the expression of *ras1.val17* from a multi-copy plasmid can induce *mam2* expression in the absence of *gpa1*. This work also found that in *h* cells there is an additive affective on the decrease in *mam2* expression if both *ras1* and *gpa1* are deleted compared to if they are singly deleted (Xu *et al.*, 1994). Ste4 is proposed to link Gpa1 with Byr2 and Ste4 and Byr2 have been shown to interact directly via their SAM domains (Ramachander *et al.*, 2002).

This Chapter will focus on dissection of the links between the G-protein, Gpa1, the activation of Ras1 and the MAPK cascade and how they may act to coordinate the pheromone response and polarised growth. Our specific aims were to investigate the roles of Gpa1, Ste4 and Ste6 in MAPK phosphorylation and morphology pathway activation.

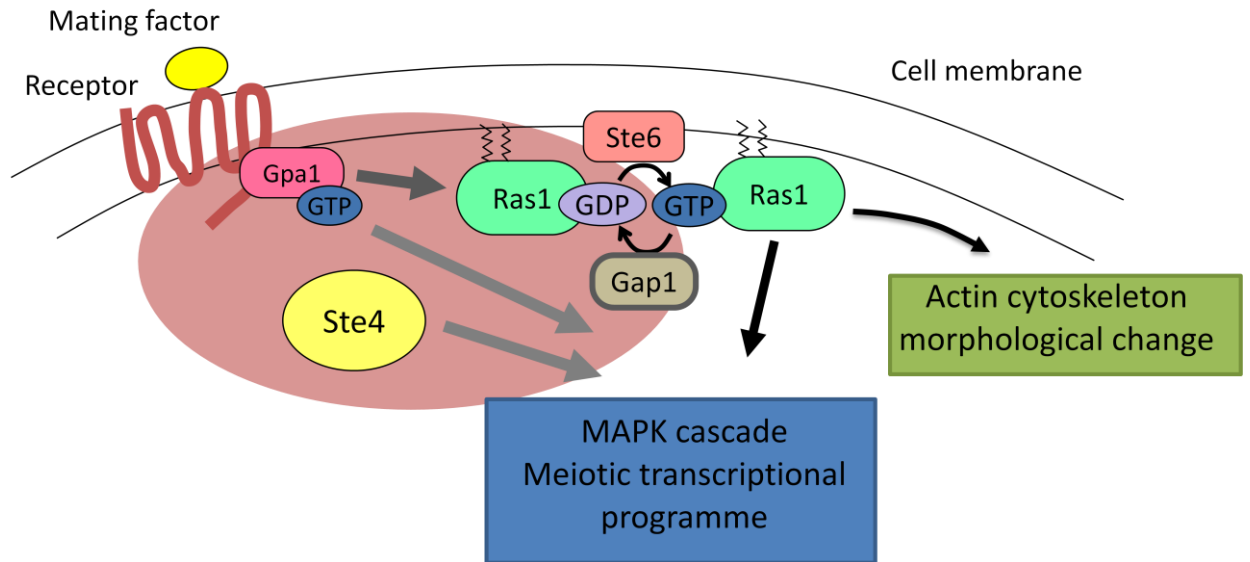


Figure 5.1 Aim of Chapter 5.

Previous Chapters have concentrated on the actions downstream of Ras1 and its dual role in the activation of both the MAPK cascade and the morphology pathway. This Chapter will focus on dissection of the links between the G-protein, Gpa1, and the activation of Ras1 (highlighted by the pink oval) and how they may act to coordinate the pheromone response and polarised growth.

5.2 Gpa1 plays a key role in activation of both the pheromone and morphology pathways

5.2.1 Role of Gpa1

Gpa1 is the G-protein activated by the mating factor receptor - either Mam2 or Map3 depending on the mating type of the cell. Gpa1 has been identified as a G α subunit and it is unknown whether this combines with a yet unidentified G $\beta\gamma$ subunit to form a heterotrimeric G-protein as present in other homologous systems. A potential candidate for the G β subunit is Gnr1 which interacts with Gpa1 in a two hybrid assay (Goddard *et al.*, 2006). Importantly, very little is known about how activation of Gpa1 leads to activation of Ste6 and Ras1 and the role of Gpa1 to aid in the activation of Byr2 which is predicted to be via Ste4 and is at least partially independent of Ras1 (Xu *et al.*, 1994; Barr *et al.*, 1996).

A number of *gpa1* Δ mutants all containing *Spk1-GFP-2xFLAG::Kan^R*, were created to investigate how this may be happening and to uncover the role Gpa1 plays in the activation of sexual differentiation. The MAPK phosphorylation and morphological phenotypes were examined in *gpa1* Δ (KT4335), *gpa1* Δ *ras1.val17* (KT5023), *gpa1* Δ *byr1.DD* (KT4353) and *gpa1* Δ *ras1.val17 byr1.DD* (KT5035) at 0, 8, 12, 16, and 24 hours after mating induction using the SPA plate assay, quantitative western blotting and live cell imaging as described previously and the results are shown in **Figure 5.2**.

It is clear from the western blot and phospho-MAPK quantification, that in the absence of Gpa1 there is no phospho-Spk1 detected but the Spk1 protein is present, revealing Gpa1 to be an essential signal transducer, linking the binding of pheromone to its receptor and the activation of the MAPK. In the *gpa1* Δ *ras1.val17* double mutant there is also no phospho-MAPK detected even though Spk1 protein is expressed, concluding

that, activated Ras1 requires the presence of the G-protein to activate the MAPK cascade. The addition of *byr1.DD* into the *gpa1Δ* mutant strain restores the MAPK phosphorylation as expected because Byr1.DD needs no upstream input for activation and signals independently of upstream events (Shown in Chapter 4 Section 4.4.1). A triple mutant of *gpa1Δ ras1.val17 byr1.DD* also has the MAPK phosphorylation level restored to that of a similar level to the *gpa1Δ byr1.DD* mutant (**Figure 5.2B**).

Live cell imaging of these mutants at the 0, 8, 12, 16 and 24-hours post mating induction are presented in **Figure 5.3**. We already confirmed that MAPK phosphorylation is essential for a morphological response therefore we predicted that the *gpa1Δ* and *gpa1Δ ras1.val17* mutants would show no morphological phenotype as there is no phospho-MAPK detected in these mutants. This is confirmed in **Figure 5.3** and even though Spk1-GFP is expressed there is no obvious nuclear localisation probably due to the lack of any phospho-Spk1 in these strains.

The phenotype of *gpa1Δ byr1.DD* is striking because the cells show no change in morphology over the 24-hour time-course. Spk1-GFP is clearly visible within the nucleus therefore there must be a defect in activation of the morphology branch. This leads us to predict that Gpa1 is essential for activation of the Cdc42-pathway as well as the MAPK branch and we predict that this signal is going through Ras1. To confirm that Gpa1 is essential for activation of both the MAPK cascade and Cdc42-pathway independently of each other we artificially activated both of these signalling pathways in the absence of Gpa1 by generating a triple mutant of *gpa1Δ ras1.val17 byr1.DD*. This mutant shows the elongated phenotype (**Figure 5.3**) as predicted by the hypothesis and this shows we have successfully reactivated the morphology pathway via the addition of *ras1.val17* which we predicted was missing in the *gpa1 byr1.DD* double mutant. To conclude, activation of both of the two pathways is required and sufficient

to mimic the pheromone signalling in the absence of the receptor coupled G-protein, Gpa1.

The elongated phenotype of *gpa1Δ ras1.val17 byr1.DD* is subtle compared to the single *ras1.val17* mutant, we predict that this is because these cells are lacking any orientational information about where pheromone is binding on the membrane as Gpa1 is absent and therefore cannot transduce the pheromone signal from the receptor therefore there is no strong anchoring point on the membrane to signify a shmoo site.

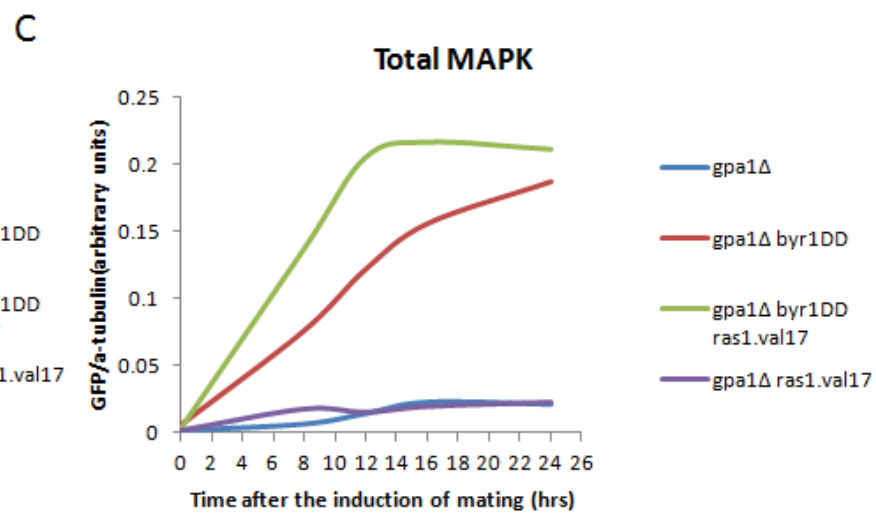
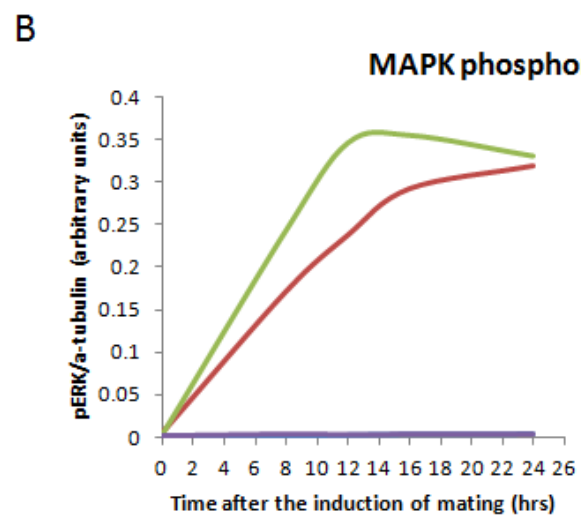
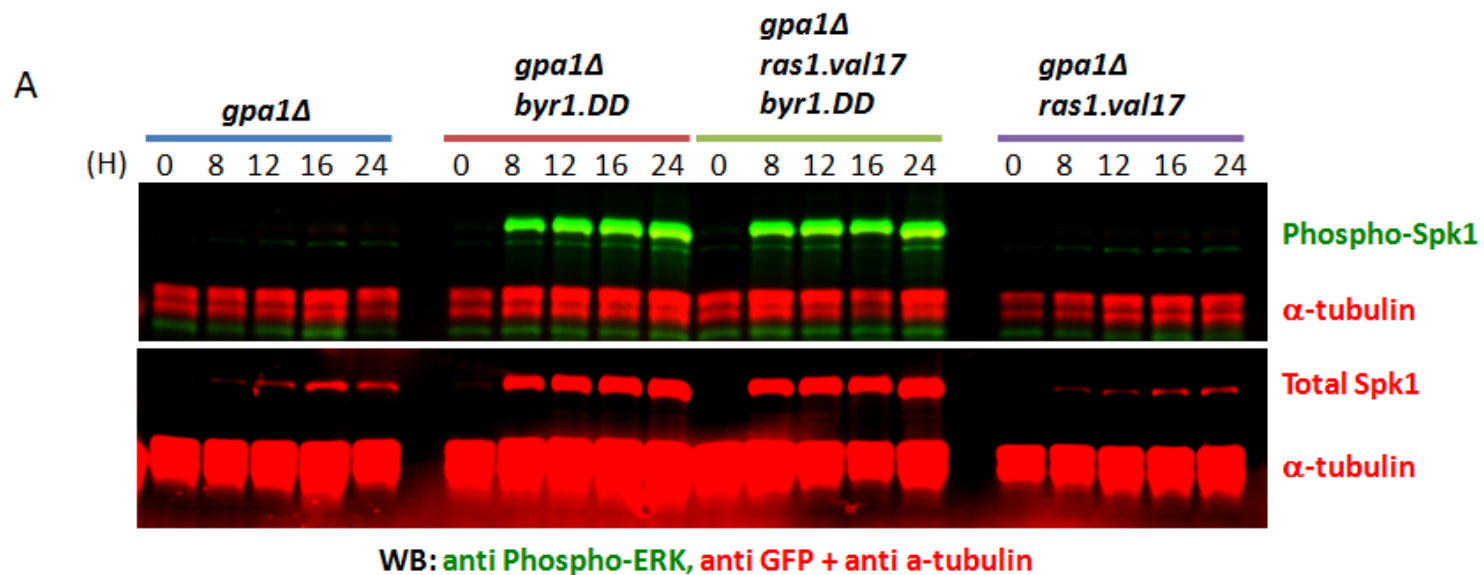


Figure 5.2 Gpa1 is an essential component for MAPK phosphorylation.

(A) Western blot of *gpa1Δ* (KT4335), *gpa1Δ ras1.val17* (KT5023), *gpa1Δ byr1.DD* (KT4353) and *gpa1Δ ras1.val17 byr1.DD* (KT5035) at 0, 8, 12, 16, and 24 hours after mating induction using the SPA plate assay. Membranes blotted with anti-phospho-ERK, anti-GFP and anti- α -tubulin at times-points 0, 8, 12, 16 and 24 after mating induction represented by (H).

(B) Quantification of the Phospho-Spk1 signal as a ratio of the α -tubulin signal to represent MAPK phosphorylation over 24-hours.

(C) Quantification of the Spk1-GFP signal as a ratio of the α -tubulin signal to represent MAPK expression over 24-hours. All quantification in (B) and (C) was carried out using Image Studio ver2.1.

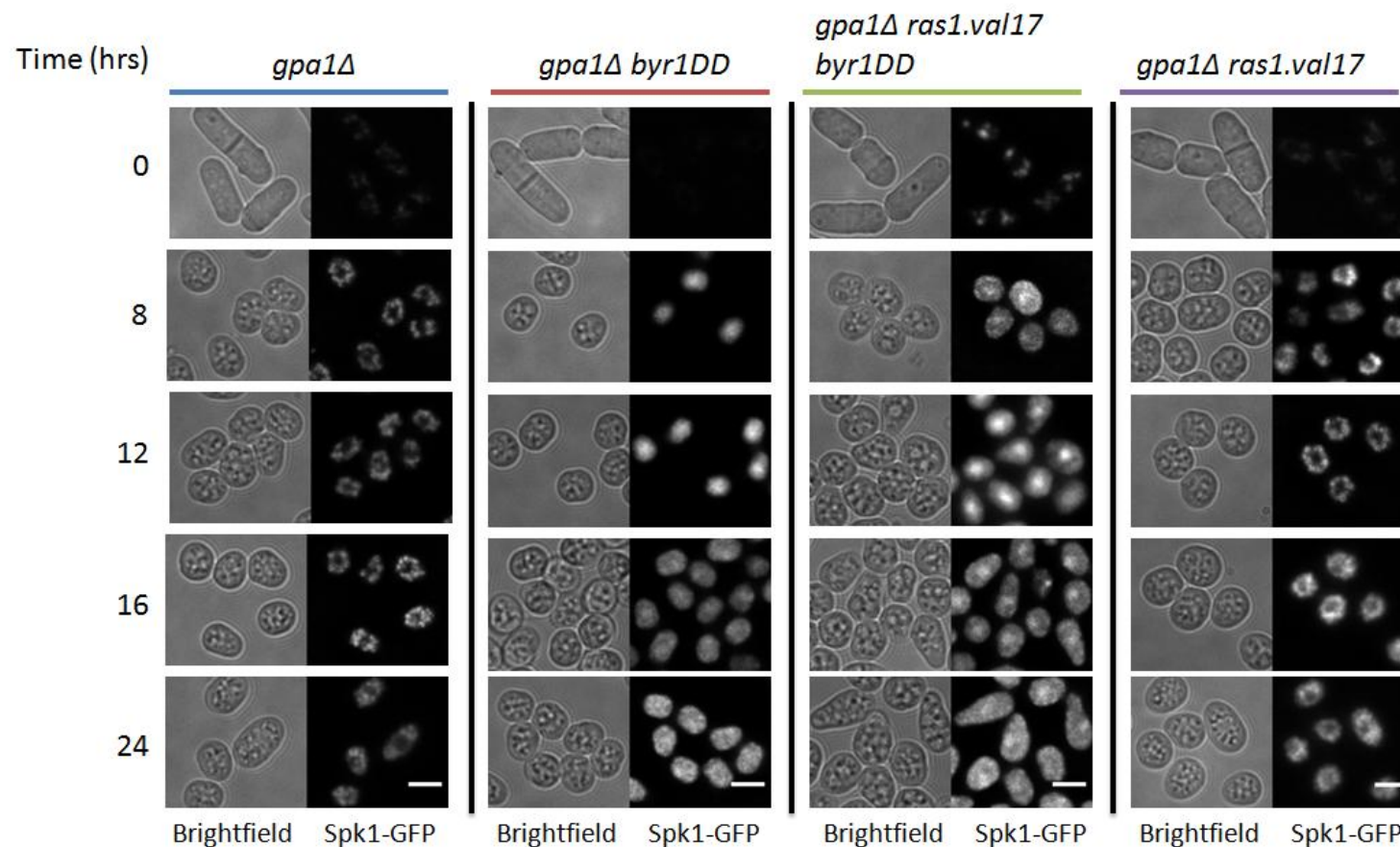


Figure 5.3 Rescue of the *gpa1Δ* phenotype is dependent on reactivation of both the morphology pathway and MAPK pathway

Live cell imaging of *gpa1Δ* (KT4335), *gpa1Δ byr1.DD* (KT4353), *gpa1Δ ras1.val17 byr1.DD* (KT5035) and *gpa1Δ ras1.val17* (KT5023) at 0, 8, 12, 16, and 24 hours after mating induction using the SPA plate assay. Images were taken at each time-point in both the brightfield and GFP in order to visualise Spk1-GFP. Each time point comprises 15-25 serial images of 0.4 μm interval along the Z axis taken to span the full thickness of the cell. All of the Spk1-GFP images were deconvolved using the Huygens Essential Deconvolution. Deconvolved images were Z-projected, cropped and combined using ImageJ. Scale bar is 5 μm .

These results shows that Ras1.val17 itself is an active protein, that does not rely on Gpa1 for activation of the Cdc42 pathway, but interestingly, in the absence of Gpa1, Ras1.val17 is not able to activate Byr2 and therefore the MAPK cascade.

In the absence of Gpa1, simultaneous activation of both the MAPK pathway and the morphology pathway was achieved by combining *byr1.DD* and *ras1.val17* and this was enough to promote a mating specific morphological phenotype, therefore the role of Gpa1 has been revealed as the coordinated activation of both branches which is enough to reproduce the full response mediated by pheromone signalling. A schematic of this observation is shown in **Figure 5.4**.

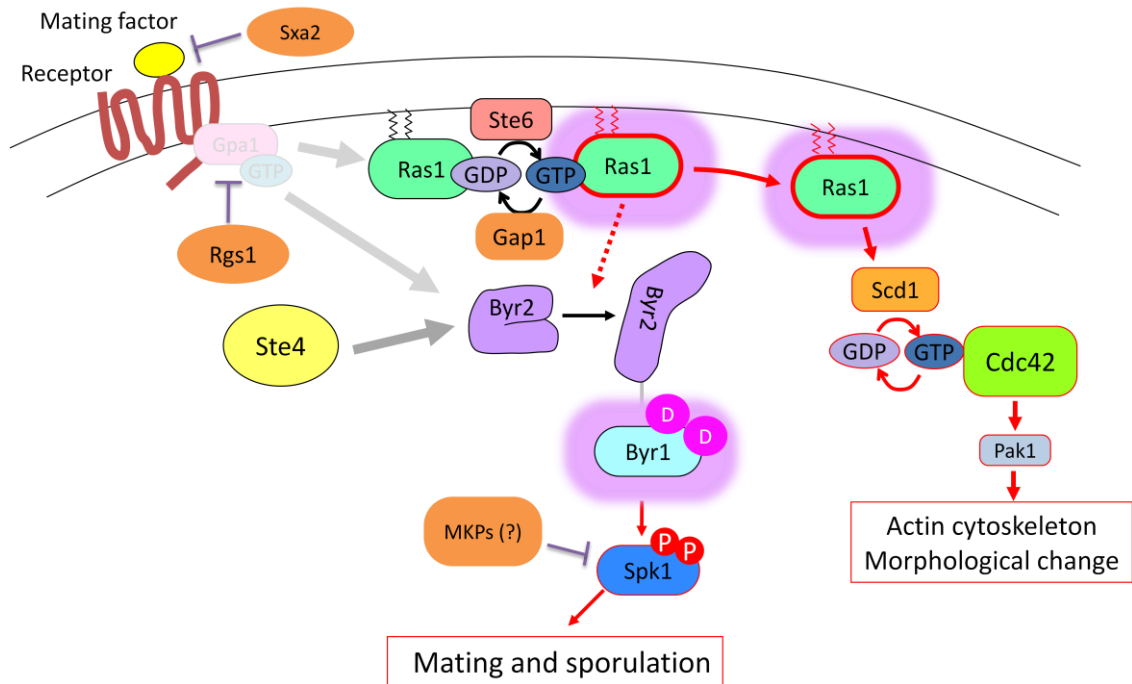


Figure 5.4 Activation of both of the two pathways is required and sufficient to mimic the pheromone signal

In the absence of Gpa1, simultaneous activation of both the MAPK pathway and the morphology pathway was achieved by combining *byr1.DD* and *ras1.val17* and this was enough to promote a mating specific morphological phenotype, therefore the role of Gpa1 has been revealed as the coordinated activation of both branches upon pheromone signalling.

5.2.2 Gpa1.QL

To further confirm that activation of Gpa1 is enough to activate both pathways for the mating response we used the previously described constitutively active Gpa1.QL protein (Obara *et al.*, 1991) which we requested from the National BioResource project in Japan.

The *gpa1.QL* mutant was provided in a h^- heterothallic cell type background and we decided to continue using this mutation in the h^- background instead of transforming it into a h^{90} background as theoretically a culture of h^- cells cannot activate the MFSP because of lack of P-factor in the media which is excreted by h^+ cells and seeing as Gpa1.QL is constitutively active there was no need to transfer it into h^{90} .

It has been believed that h^- cells should not activate the MFSP upon starvation because even though these cells express the P-factor receptor they only excrete M-factor therefore in a culture of h^- cells there should be no P-factor secreted into the media to bind the P-factor receptor and therefore no Gpa1 activation can occur. Indeed, extensive gene expression studies have supported this view. For example, expression of *sxa2*, a prototype mating-pheromone-induced gene, is not detectable in either heterothallic h^- or h^+ cells and is only seen in the homothallic h^{90} cells where cells exchange mating pheromones and transduce the signalling in the cells (Imai & Yamamoto, 1992).

However, it has to be noted that in the h^- cells, although tightly repressed, genes that encode P-factor and M-factor receptor are still in the genome. Similarly, in the h^+ cells, genes that encode M-factor and P-factor receptor are intact in the genome although they are tightly repressed.

5.2.2.1 *The h⁻ autocrine effect*

Western blotting with cell extracts from a *h⁻* WT (KT4190) strain containing Spk1-GFP revealed a small amount of phospho-Spk1 signal in this strain upon nitrogen starvation (**Figure 5.5A**). This phospho-Spk1 signal in *h⁻* is much weaker than in its *h⁹⁰* counterpart (See Appendix Figure 1). We predicted that this signal in *h⁻* strains was due to an autocrine response due to an incomplete inhibition of expression of the genes encoding P-factor and M-factor receptor. To assess whether this phospho-MAPK signal was being transduced via the MFSP, *gpa1* was deleted in cells of a *h⁻* WT background to create *h⁻ gpa1Δ* (KT4346), **Figure 5.5** shows that this indeed seems to be the case as there is no phospho-MAPK signal detected in the *h⁻ gpa1Δ* strain therefore the activation seen in *h⁻ WT* is happening exclusively through the MFSP. To further confirm that this activation is occurring via the mating factor receptors in an autocrine fashion, future work includes the generation of a *h⁻* strain where both *mam2* and *map3*, that encodes P-factor receptor and M-factor receptor respectively, are deleted. In conclusion, activation of Spk1 is exclusive to the MFSP and not subject to activation by any other pathways activated upon nitrogen starvation.

5.2.2.2 *Gpa1.QL can activate the MAPK branch and morphology branch upon nitrogen starvation*

The *h⁻ gpa1.QL* mutant (KT5059) and *h⁻ gpa1.QL ras1Δ* (KT5070), both containing Spk1-GFP, were subject to the SPA mating assay, *h⁻ gpa1.QL* shows substantial MAPK phosphorylation in response to nitrogen starvation compared to *h⁻ WT* and reaches similar levels to that of *h⁻ byr1.DD* (**Figure 5.5B**). This MAPK phosphorylation is heavily dependent on Ras1 as the *h⁻ gpa1.QL ras1Δ* mutant shows a significantly lower level of phosphorylation (**Figure 5.5B**). This supports that Gpa1 is responsible for activation of Ras1 which provides the major route for MAPK cascade

activation. The phospho-MAPK signal in *h⁻ gpa1.QL ras1Δ* proves that Gpa1 can also transduce a small amount of signal in the absence of Ras1 confirming that Gpa1 has a partially independent role in Byr2 activation as already shown in the literature (Xu *et al.*, 1994). Live cell imaging of the *h⁻ gpa1.QL* mutant in **Figure 5.6** shows these cells subtle elongating exclusively in response to induction of mating (i.e. nitrogen starvation) with a clear nuclear Spk1-GFP signal at 8 and 12-hours on the SPA plate. This concludes that nitrogen starvation plus activation of Gpa1 are the only things required to successfully activate MAPK cascade and morphology pathway. We propose that the elongated phenotype of *h⁻ gpa1.QL* cells only occurs upon nitrogen starvation and it not evident in the mitotically growing cells because Gpa1 is a known Ste11-target gene (Mata & Bahler, 2006) and along with a number of key components of the MFSP, including Spk1, are not expressed during mitosis.

To conclude, the *h⁻ gpa1.QL* strain is capable of activating both the MAPK and morphology pathways in response to nitrogen starvation. The major route for MAPK cascade activation is via Gpa1-Ras1 because *h⁻ gpa1.QL ras1Δ* shows a severely attenuated phospho-MAPK signal compared to *h⁻ gpa1.QL* alone, although MAPK phosphorylation is still evident in the *h⁻ gpa1.QL ras1Δ* strain therefore there is still MAPK cascade activation through a more minor route activated solely through Gpa1. We assume that as a constitutively activated protein, Gpa1.QL is not further activated by the minimal autocrine response identified in *h⁻* cells however this can be confirmed by deletion of the pheromone receptors in this strain to prove that indeed Gpa1.QL is insensitive to pheromone signal input. We hypothesis that the subtle elongation associated with *h⁻ gpa1.QL* is due to lack of orientation information on the membrane as in the *h⁻* heterothallic strain there should be no P-factor present in the media to activate the P-factor receptor on the cell membrane.

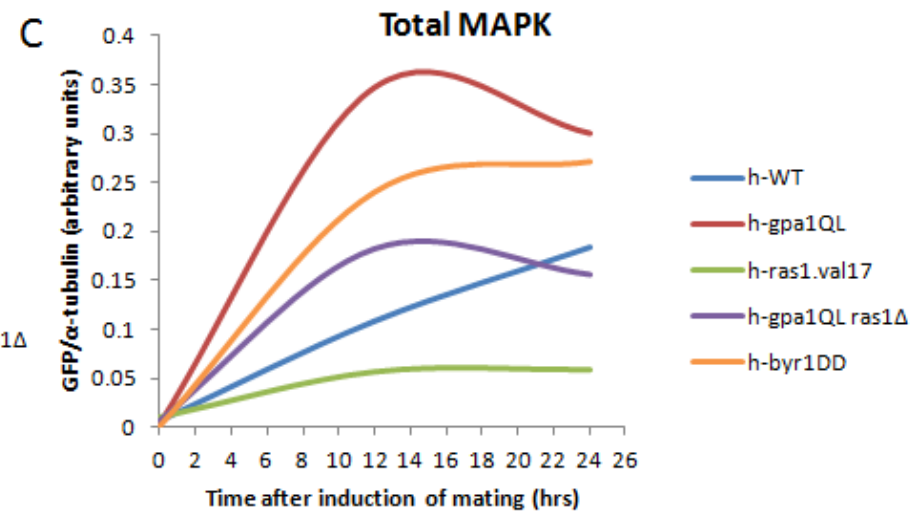
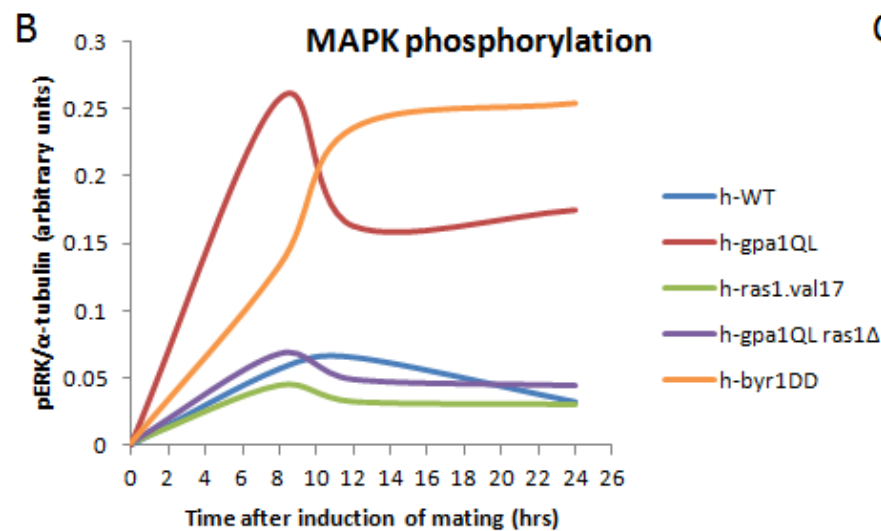
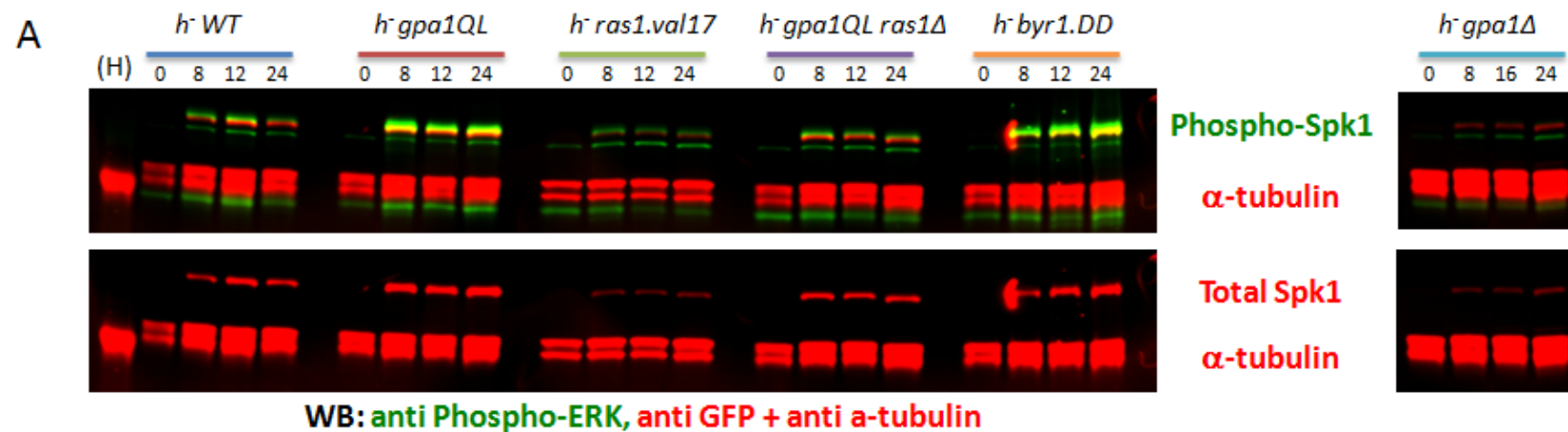


Figure 5.5 Gpa1.QL causes MAPK phosphorylation upon nitrogen starvation

(A) Western blot of *h⁻* WT (KT4190), *h⁻ gpa1.QL* (KT5059), *h⁻ ras1.val17* (KT4233), *h⁻ gpa1.QL ras1Δ* (KT5070), *h⁻ byr1.DD* (KT4194) and *h⁻ gpa1Δ* (KT4346) - shown separately. Membranes were blotted with anti-phospho-ERK, anti-GFP and anti- α -tubulin at times-points 0, 8, 12 and 24 after mating induction represented by (H).

(B) Quantification of the Phospho-Spk1 signal as a ratio of the α -tubulin signal to represent MAPK activation over 24-hours.

(C) Quantification of the Spk1-GFP signal as a ratio of the α -tubulin signal to represent MAPK activation over 24-hours. All quantification in (B) and (C) was carried out using Image Studio ver2.1.

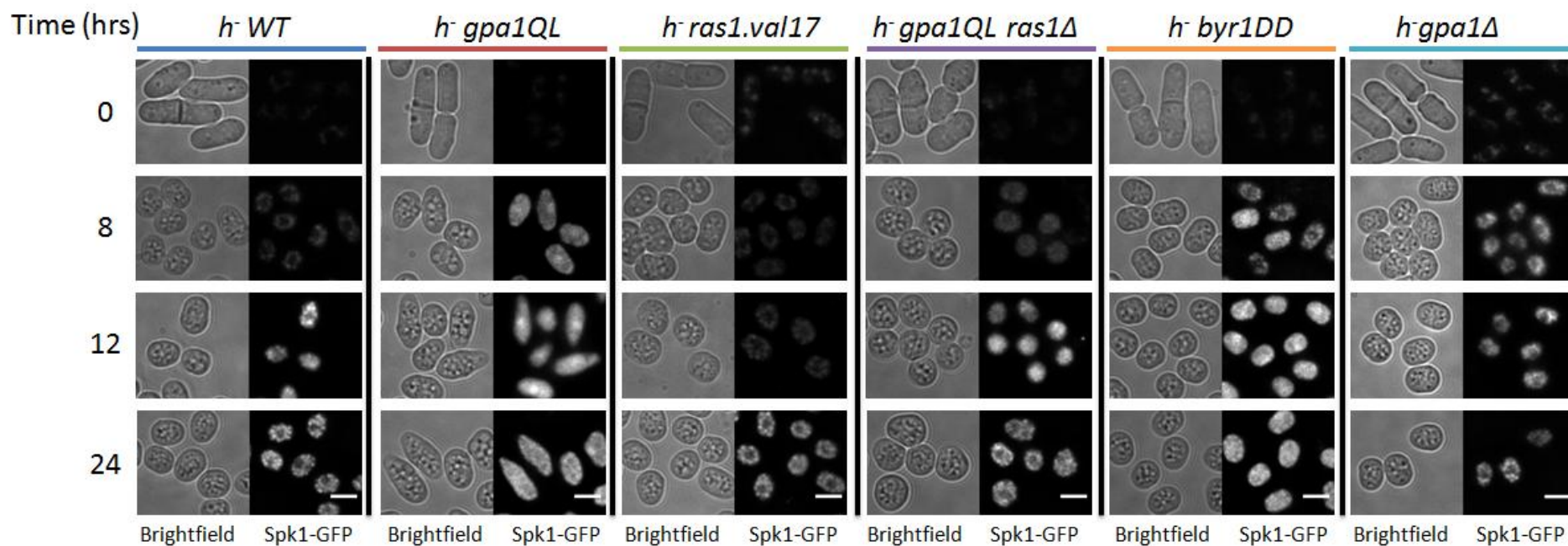


Figure 5.6 Gpa1.QL causes the elongated phenotype in response to nitrogen starvation

Live cell imaging of *h⁻ WT* (KT4190), *h⁻ gpa1.QL* (KT5059), *h⁻ ras1.val17* (KT4233), *h⁻ gpa1.QL ras1Δ* (KT5070), *h⁻ byr1.DD* (KT4194) and *h⁻ gpa1Δ* (KT4346). Images were taken at each time-point in both the brightfield and GFP channels in order to visualise Sp1k-GFP. Each time point comprises 15-25 serial images of 0.4 μm interval along the Z axis taken to span the full thickness of the cell. All of the Sp1k-GFP images were deconvolved using the Huygens Essential Deconvolution. Deconvolved images were Z-projected, cropped and combined using ImageJ. Scale bar is 5 μm .

In summary, Gpa1 is essential for activation of both the MAPK and morphology pathways, without it there is no MAPK phosphorylation and MAPK phosphorylation cannot be rescued by the presence of Ras1.val17 therefore without Gpa1, Ras1 is unable to activate Byr2. We have already seen that oncogenic Ras.val17 cannot activate a morphological response without MAPK activation and the lack of a morphological response in *gpa1Δ ras1.val17* is rescued by the addition of MAPK phosphorylation via Byr1.DD. Byr1.DD alone is not enough to rescue the *gpa1Δ* morphology defect due to the deficient activation of the morphology branch which is a direct consequence of lack of Ras1 activation in the absence of Gpa1 which is restored via the addition of activated Ras1 (*ras1.val17*).

The result that the morphological defect of *gpa1Δ byr1.DD* is rescued by the addition of *ras1.val17* shows that Ras1.val17 itself is an active molecule, that does not require Gpa1 for activation of the morphology pathway, but strikingly *ras1.val17* is not able to activate Byr2 and therefore the downstream MAPK cascade in the absence of the G-protein. This lead to the hypothesis that Gpa1 is essential for Byr2 activation on the plasma membrane. It has been shown that Byr2 localises to the membrane in a Ras1 dependent manner (Bauman *et al.*, 1998) and that Gpa1 can activate Byr2 in a Ras1 dependent manner (Xu *et al.*, 1994). We predicted that Ste4 may be involved in the interaction between Gpa1 and Byr2 as it is already reported that Ste4 interacts with Byr2 and is essential for mating (Barr *et al.*, 1996). We've shown that there is no MAPK phosphorylation in *gpa1Δ* and predict that Ste4 has a role as a potential scaffold linking Gpa1 and Byr2. This hypothesis is represented in pictorial form in **Figure 5.7**.

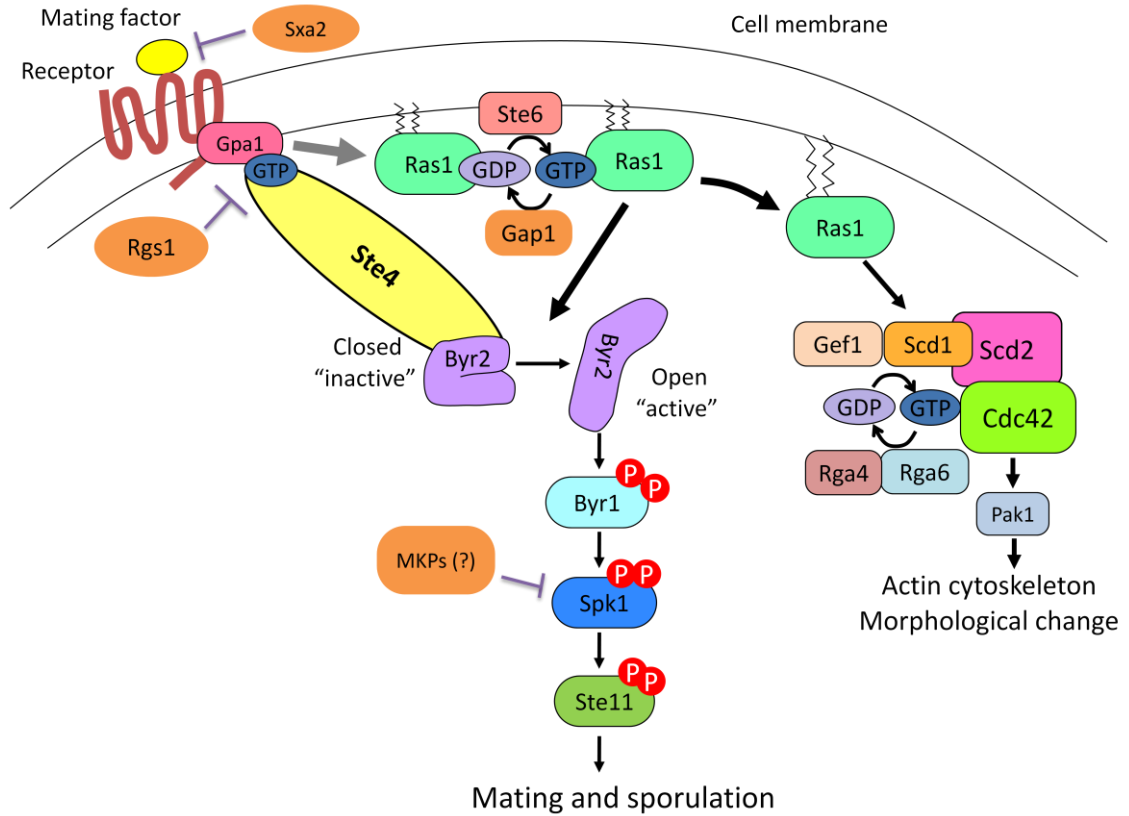


Figure 5.7 Hypothesis: Ste4 links Byr2 and Ras1

We predict that Ste4 is able to link Gpa1 and the activation of Byr2 via Ras1 as we've observed that *ras1.val17* cannot activate the MAPK cascade in the absence of Gpa1. We hypothesize that Ras1 recruits Byr2 to the membrane and Gpa1-Ste4 activate Byr2 possible via dimerisation and the promotion of autophosphorylation.

5.3 The role of Ste4 in mating signal transduction

The following mutants were generated and subject to mating assays to investigate MAPK and morphology pathway activation via western blotting and live cell imaging as described previously; *ste4Δ* (KT4376), *ste4Δ ras1.val17* (KT5143) and *ste4Δ byr1.DD* (KT5136). All strains contain *spk1-GFP-2xFLAG-Kan^R* integrated at the *spk1* chromosomal locus. Results for these strains are presented in **Figure 5.8**.

As is the case in the absence of Gpa1, there is no MAPK activation or morphological change in the *ste4Δ* or in the *ste4Δ ras1.val17* double mutant. This phenotype can be explained by our hypothesis that upon Gpa1 activation, Ras1-GTP brings Byr2 into close proximity of Ste4 which is essential for Byr2 activation - probably through dimerisation and autophosphorylation/phosphorylation from an additional kinase. The hypothesis predicts that when Ste4 is missing, Byr2 cannot be activated even though Ras1 is activated and Byr2 is predicted to be localised to the membrane via Ras1, leading to a failure of MAPK cascade activation. The *ste4Δ ras1.val17* mutant shows no morphological change which is explained by no detectable level of MAPK phosphorylation in the absence of Ste4. It could however be the case that Ste4 could also be required for Ras1 activation just like Gpa1 and the lack of a morphological response is due to deficient Ras1 activation of the morphology branch. However, the *ste4Δ byr1.DD* mutant has *byr1.DD* phenotype (**Figure 5.8B**) therefore the morphology pathway activation is intact in the *ste4Δ* and when MAPK signalling is restored, via *byr1.DD*, cells can respond to the pheromone signal. We conclude that Ste4 is not required for activation of the morphology pathway and is exclusively required for MAPK phosphorylation. We propose that Ste4 is essential for coordinated activation of Byr2 which has been localised to the plasma membrane at the site of pheromone stimulation by activated Ras1.

We assume from previous works that Byr2 localisation to the plasma membrane is solely dependent on Ras1 but the reason there is no MAPK phosphorylation in *ras1.val17 gpa1Δ* or *ras1.val17 ste4Δ* is that additional inputs are required for Byr2 activation. A crucial further experiment is to investigate the localisation of Byr2 in *ras1Δ* and *ras1.val17* along with *gpa1Δ* and *ste4Δ* strains to check if Byr2 localisation to the membrane is dependent on Ras1 only.

These results help to explain the role Ste4 is playing in pheromone signalling but fail to reveal how Ras1 activation is linked to Gpa1, therefore another identified component of the pathway, Ste6, which is known to be a Ras1 GEF (Hughes *et al.*, 1994) was investigated.

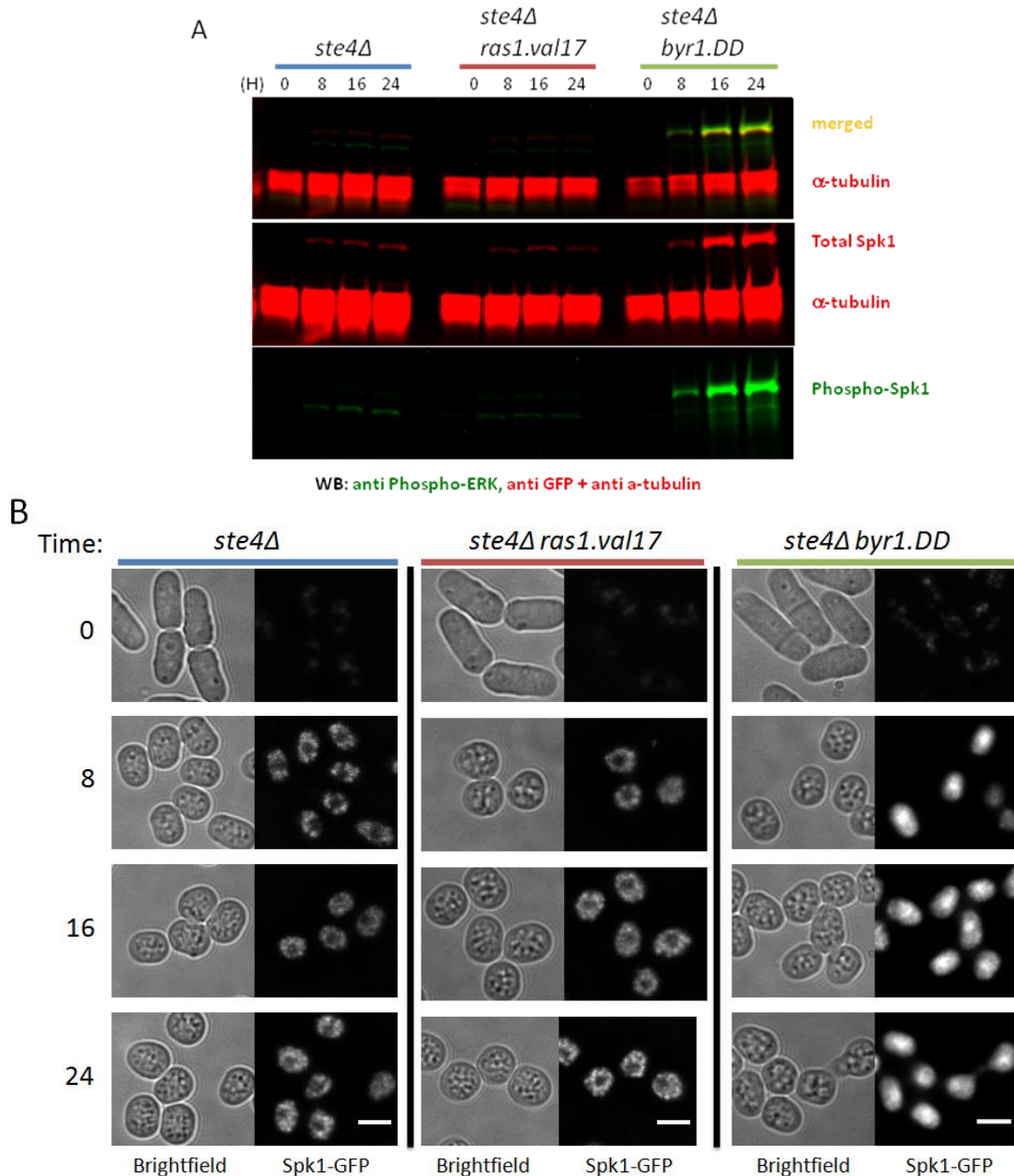


Figure 5.8 The role of Ste4 as an exclusive MAPK pathway activator

(A) Western blot of *ste4Δ* (KT4376), *ste4Δ ras1.val17* (KT5143) and *ste4Δ byr1.DD* (KT5136) blotted with anti-phospho-ERK, anti-GFP and anti- α -tubulin at time-points 0, 8, 16 and 24 after mating induction represented by (H).

(B) Live cell images of the above strains. Images were taken at each time-point in both the brightfield and GFP channels in order to visualise Spk1-GFP. Each time point comprises 15-25 serial images of 0.4 μ m interval along the Z axis taken to span the full thickness of the cell. All of the Spk1-GFP images were deconvolved using the Huygens Essential Deconvolution. Deconvolved images were Z-projected, cropped and combined using ImageJ. Scale bar is 5 μ m.

5.4 Role of Ste6 for Ras1 activation

Ste6 is a GEF for Ras1 (Hughes *et al.*, 1990), deletion of *ste6* does not show an obvious morphological defect during the vegetative growth unlike *ras1Δ* cells that show round morphology phenotype. Efc25, another *S.pombe* protein that shows homology to Ras-GEFs, is required for maintenance of cell morphology during the vegetative cell cycle and when deleted, the cells become round like *ras1Δ* cells (Tratner *et al.*, 1997).

Interestingly, whilst Ste6 is required for the mating process, deletion of *efc25* does not affect mating, therefore, it has been proposed that Ste6 activates Ras1 to prime the MAPK pathway whilst Efc25 activates Ras1 to regulate the Cdc42 pathway (Papadaki *et al.*, 2002) This is hypothesis 1 - there are two separate pools of Ras1 which are regulated by the two GEFs. The functions of the two GEFs are not interchangeable i.e. overexpression of *efc25* cannot rescue the mating defect of *ste6Δ* and *ste6* overexpression cannot rescue the rounded morphological phenotype of *efc25Δ* (Papadaki *et al.*, 2002). Alternatively, Ste6 could control the activation of Ras1 during mating for both pathways and Efc25 acts exclusively for Ras1 activation during vegetative growth, this is hypothesis 2. The two hypothesis are outlined in **Figure 5.9**. If failure of mating in *ste6Δ* cells comes from lack of MAPK activation, as hypothesis 1 predicts, providing Byr1.DD should restore the mating ability as it does to the *ste4Δ* mutant.

Quantitative western blotting and live cell imaging of *ste6Δ* (KT4333) alongside WT (KT3082), *gpa1Δ* (KT4335), *ras1Δ* (KT4323), *gpa1Δ ras1.val17* (KT5023) and *byr2Δ* (KT3763) (all containing *spk1-GFP-2xFLAG::kan^R*) are shown in **Figure 5.10** and **Figure 5.11**. Western blotting and live cell imaging revealed that both Ste6 and Ras1 are not essential for MAPK phosphorylation but are essential for activation of morphology. There is a substantial amount of phospho-Spk1 detected in the *ste6Δ*

mutant as confirmed by quantitation of the western blot; MAPK phosphorylation in the *ste6Δ* strain seems only slightly decreased compared to WT (**Figure 5.10B**). Spk1-GFP successfully translocates to the nucleus in the *ste6Δ* strain unlike in *ras1Δ* where even though Spk1 is phosphorylated to a limited extent there is no clear nuclear localisation during the 24-hour time-course (**Figure 5.11**). In *ste6Δ*, this amount of MAPK phosphorylation is therefore not able to promote a morphological response hinting that, unlike Ste4, Ste6 is linked strongly to activation of the morphology pathway. We would have expected the phospho-Spk1 levels to be similar in *ste6Δ* to *ras1Δ* if Ste6 was the only GEF controlling Ras1 activity during mating. From the data presented in **Figure 5.10** this doesn't appear to be true as the levels are higher after quantitation in *ste6Δ* compared to *ras1Δ*. It is important to note that these results represent only one technical replicate of one biological replicate therefore to confirm the levels of phospho-Spk1 in *ste6Δ* compared to *ras1Δ* and WT more biological replicates are required at more frequent time-points. The main conclusion is that MAPK phosphorylation is compromised in *ste6Δ*. The extent to which it is compromised remains to be investigated.

If the levels of phospho-MAPK in *ste6Δ* are dependent on Ras1 it means that Ras1 is still activated in the absence of Ste6 and we predict this would be through the actions of the other Ras1 GEF, Efc25. This can be confirmed in the future by investigating the levels of phospho-MAPK in a *ste6Δ ras1Δ* double and a *ste6Δefc25Δ* double mutant.

To investigate this further *ste6Δ* was introduced into the *ras1.val17* and *byr1.DD* single mutants (KT3084 and KT3435 respectively) using the method outlined in 2.2.11. If Byr1.DD can promote the prezygotic phenotype in the absence of *ste6* we can conclude that Ste6 is dispensable for activation of the Ras1-Cdc42 pathway as is the case with

Ste4 and that Ste6 is the Ras1 GEF exclusively for the Byr2-Byr1-Spk1 MAPK cascade

- hypothesis 1 .

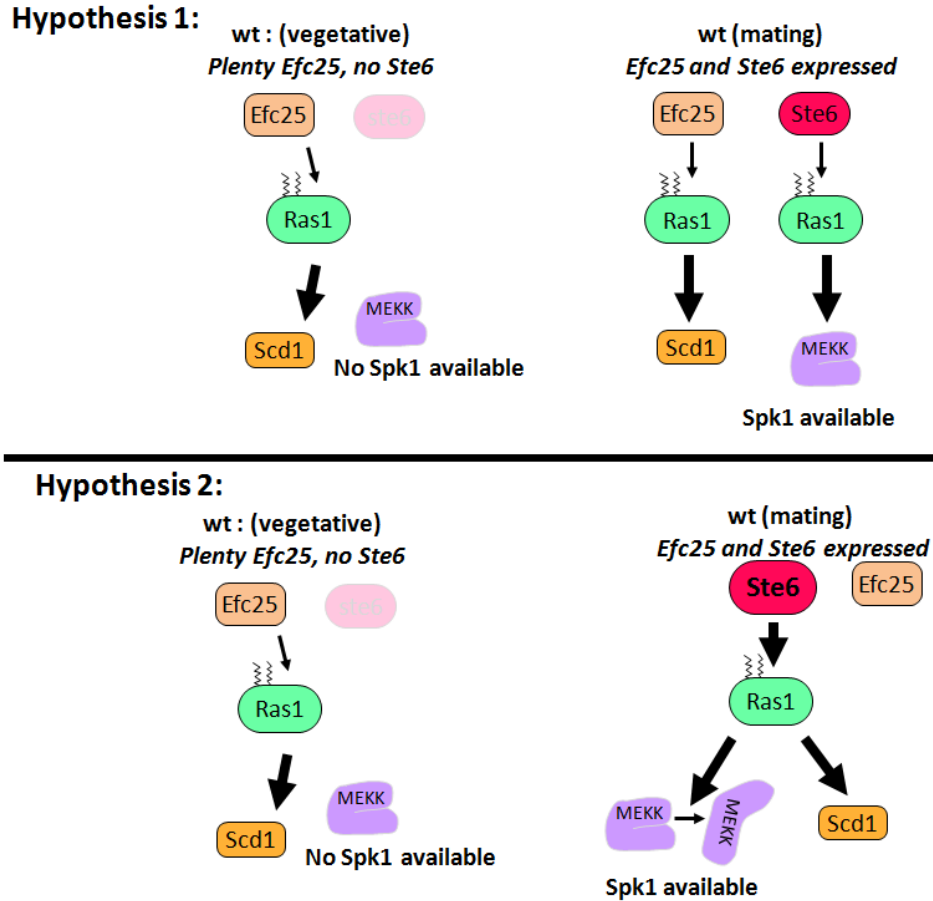


Figure 5.9 The control of Ras1 activation during mating.

Hypothesis 1: There are two separate pools of Ras1 which are regulated by the two GEFs. During vegetative growth *ste6* mRNA is barely detectable whereas *efc25* is constitutively expressed. *Byr2* is expressed during vegetative growth but expression increases upon mating induction (Papadaki *et al.*, 2002).

Hypothesis 2: *Ste6* could control the activation of Ras1 during mating for both pathways and *Efc25* acts exclusively for Ras1 activation during vegetative growth.

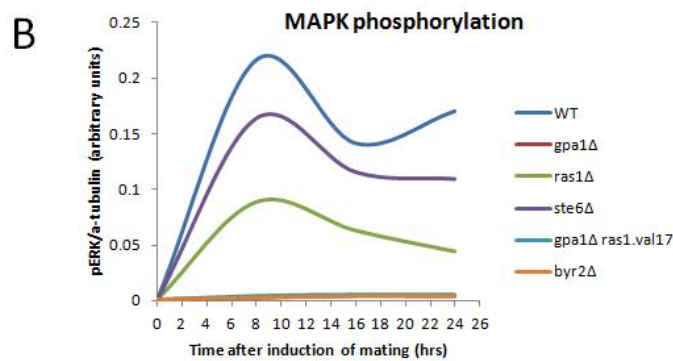
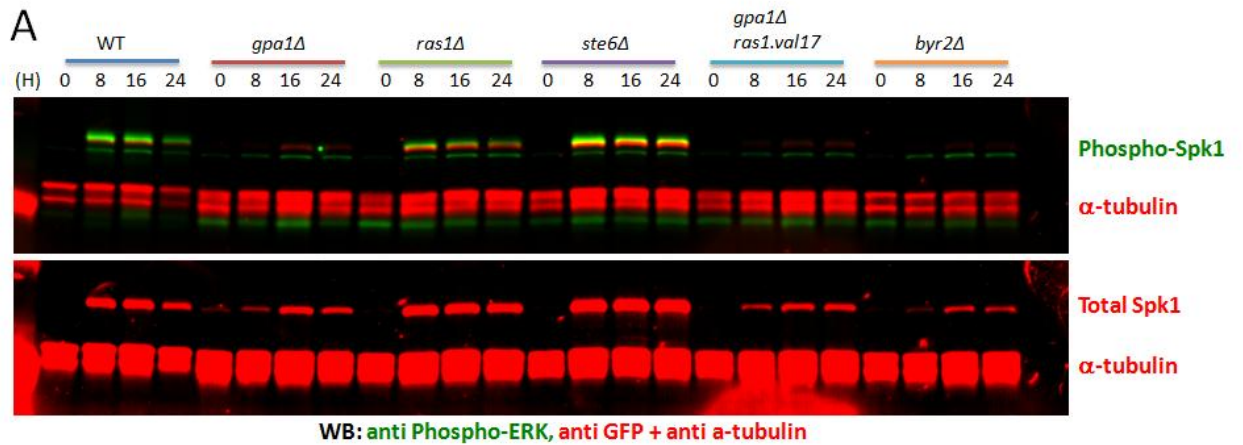


Figure 5.10 Ras1 and Ste6 are not essential for MAPK activation.

(A) Western blot of WT (KT3082), *gpa1Δ* (KT4335), *ras1Δ* (KT4323), *ste6Δ* (KT4333), *gpa1Δ ras1.val17* (KT5023) and *byr2Δ* (KT3763). (H) represents the number of hours post mating induction. Membrane was blotted with anti-phospho-ERK, anti-GFP and anti- α -tubulin.

(B) Quantification of the phospho-ERK signal as a ratio of the α -tubulin signal to represent MAPK phosphorylation of the strains specified in (A). Quantification was carried out using Image Studio Ver2.1.

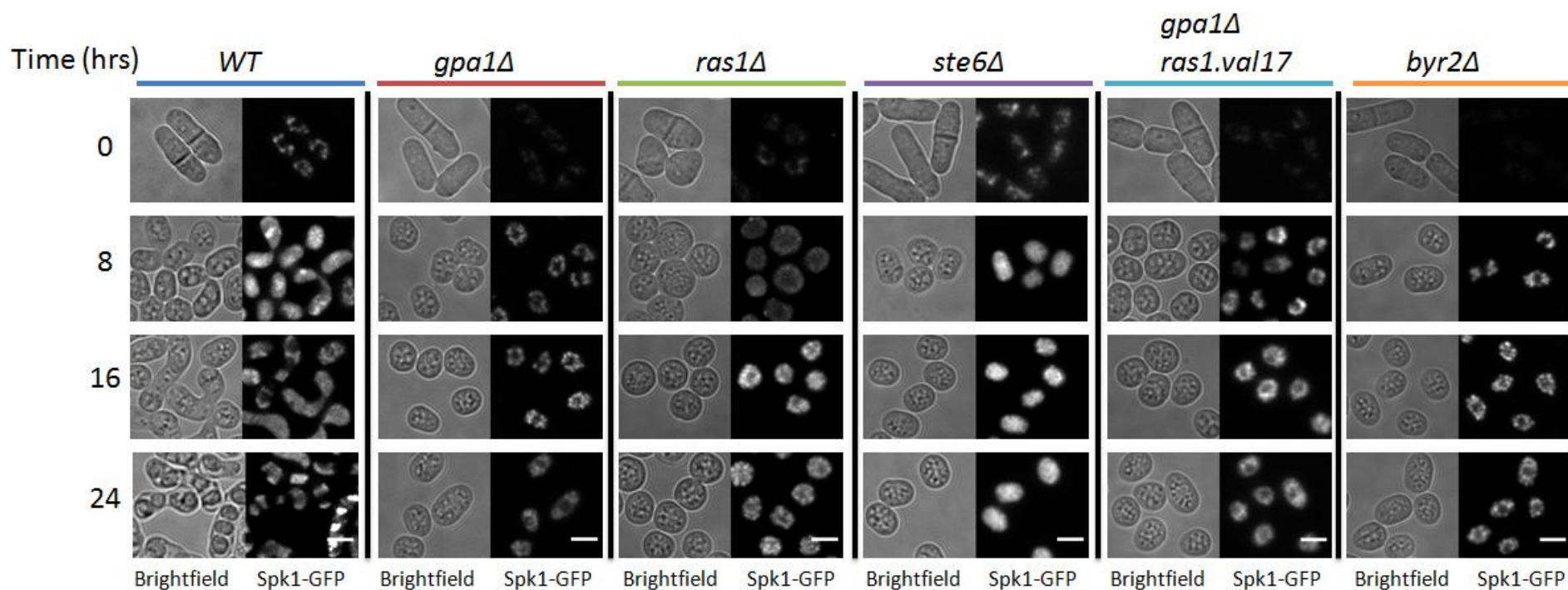


Figure 5.11 Comparison of morphology between various MFSP mutants

Live cell imaging of WT (KT3082), *gpa1Δ* (KT4335), *ras1Δ* (KT4323), *ste6Δ* (KT4333), *gpa1Δ ras1.val17* (KT5023) and *byr2Δ* (KT3763). Images were taken at each time-point in both the brightfield and GFP channels in order to visualise Spk1-GFP. Each time point comprises 15-25 serial images of 0.4 μm interval along the Z axis taken to span the full thickness of the cell. All of the Spk1-GFP images were deconvolved using the Huygens Essential Deconvolution. Deconvolved images were Z-projected, cropped and combined using ImageJ. Scale bar is 5 μm .

The MAPK phosphorylation and morphological phenotypes of *ste6Δ* (KT4333), *ste6Δ ras1.val17* (KT4998) and *ste6Δ byr1.DD* (KT5139) are presented in **Figure 5.12**.

Introduction of the activated Ras1 protein, Ras1.val17 can rescue the sterile phenotype of *ste6Δ*, whereas *ste6Δ byr1.DD* shows no morphological change. Therefore the reason that cells show no morphological change in *ste6Δ* is because of a lack of activation of Ras1 and not due to a lack of phospho-MAPK. The morphology pathway is still defective in *ste6Δ byr1.DD* and we already know that Byr1.DD can cause enough MAPK activation for a morphological response on its own as long as Ras1 is successfully activated and working through the morphology pathway as is the case with *ste4Δ* and *byr2Δ*.

Our hypothesis is that Ste6 activates Ras1 that activates both the MAPK and morphological pathways in response to pheromone stimulation - depicted as hypothesis 2 in **Figure 5.9**. This is based on the observation that if Ste6 is missing, there is a decrease in the amount of phospho-MAPK present and the morphology pathway does not function even when MAPK phosphorylation is manipulated to that of *byr1.DD*. Restoration of ras1 activity via *ras1.val17* can promote the elongated phenotype characteristic of *ras1.val17* single mutant (**Figure 5.12**). Therefore it is likely that the reason *ste6Δ* is sterile is because of a compromised activation of Ras1 for both pathways.

In order to conclude whether the phospho-MAPK signal is not significantly different between *ste6Δ* and *ste6Δ ras1.val17* requires more biological replicates at more frequent time-points as it is unclear in **Figure 5.12A** if the amount of phospho-MAPK is different between the two mutants.

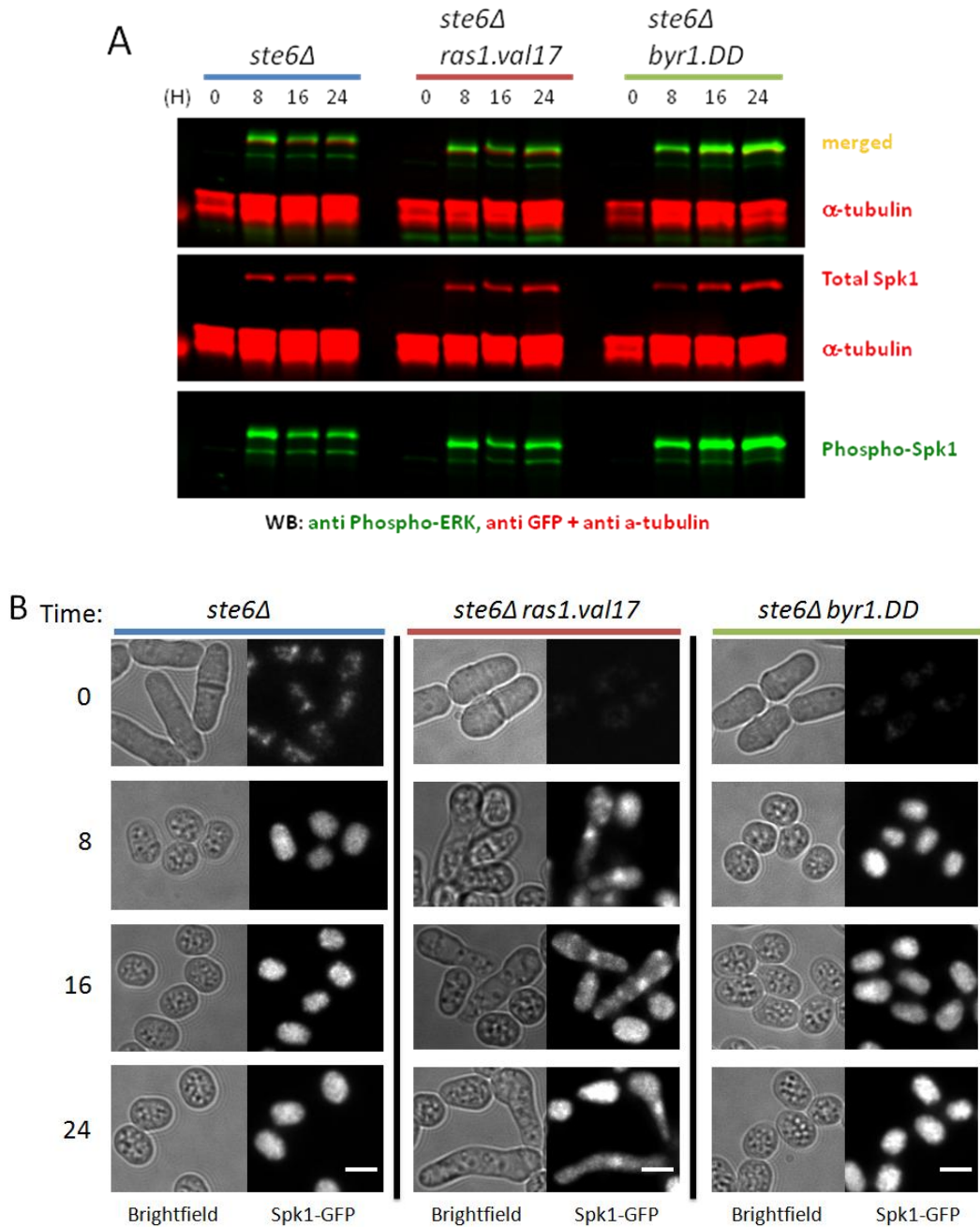


Figure 5.12 Ste6 is required for both MAPK activation and a morphological response

(A) western blot of *ste6Δ* (KT4333), *ste6Δ ras1.val17* (KT4998) and *ste6Δ byr1.DD* (KT5139) at 0, 8, 16 and 24 hours post mating induction. Membrane was blotted with anti-phospho-ERK, anti-GFP and anti- α -tubulin.

(B) Images were taken at each time-point in both the brightfield and GFP channels in order to visualise Spk1-GFP. Each time point comprises 15-25 serial images of 0.4 μ m interval along the Z axis taken to span the full thickness of the cell. All of the Spk1-GFP images were deconvolved using the Huygens Essential Deconvolution. Deconvolved images were Z-projected, cropped and combined using ImageJ. Scale bar is 5 μ m.

Compartmentalised signalling of Ras1, along with the two non-functionally interchangeable GEFs for Ras1 in *S.pombe* has been proposed as the mechanism by which Ras1 can separately control the mating process and morphology (Papadaki *et al.*, 2002; Onken *et al.*, 2006) although we believe that actually, Ste6 is playing a vital role in activation of the Ras1-Scd1 pathway during mating as the morphological defect of *ste6Δ* is rescued by *ras1.val17*. There is a significant amount of phospho-MAPK signal detected in the absence of Ste6, this could either be because of Ras1-independent Byr2 activation - which is seen in the absence of Ras1 (**Figure 5.10**) - which can be investigated using a *ste6Δ ras1Δ* double mutant, or Ras1 is being activated by another GEF, presumably Efc25 which can be investigated using a *ste6Δ efc25Δ* double mutant, therefore highlighting that the function of the two GEFs is not completely non-interchangeable and the regulation of Ras1 is not as black and white as proposed by (Papadaki *et al.*, 2002) in terms of mutually exclusive pools of Ras1 which are controlled entirely separately via localisation to different cellular compartments and the functions of the two Ras1GEFs, Ste6 and Efc25.

5.5 Discussion

In conclusion, we explored the mechanisms by which Ras1 can coordinate activation of the pheromone responsive MAPK cascade and the Cdc42-morphology pathway during mating. We found that the G-protein, Gpa1, is absolutely essential for MAPK phosphorylation unlike Ras1, which is responsible for activation of a substantial amount of the MAPK phosphorylation but some phosphorylation still occurs without it. Also, Gpa1 must be involved in activation of Ras1 for the Cdc42 pathway as restoration of MAPK signalling in the *gpa1Δ* mutant could not restore the morphological defect. Activated Ras1 requires Gpa1 and Ste4 for MAPK cascade activation, which we propose, is through a Gpa1-Ste4 complex which may function to bring Byr2 in close proximity to Ras1 for full activation of MAPK cascade. Ste6 plays a role in Ras1 activation which leads to successful activation of both the MAPK cascade and Cdc42-pathway. It is important to quantify the MAPK phosphorylation in the *ste6Δ* and determine if it is dependent on Ras1 as this will help us determine whether Ras1 is being activated via another protein in the absence of Ste6 - presumably by the second Ras1GEF Efc25. This can be done by creation of a *ste6Δ ras1Δ* double mutant and quantitation of the MAPK phosphorylation compared to the *ste6Δ* single mutant. It will also be interesting to determine whether Efc25 has any effect on MAPK phosphorylation in this context as it is proposed to have a mitotic specific function (Papadaki *et al.*, 2002).

Our proposed model for coordinated MAPK and Cdc42 pathway activation via Gpa1 and Ras1 is outlined in **Figure 5.13**. Activation of Gpa1 causes activation of Ras1 via Ste6 and is also responsible for Byr2 activation via Ste4. Activation of the Cdc42-morphology pathway is directly linked to activation of the pheromone receptor via Gpa1 which activates Ras1, therefore Gpa1 plays a vital role in coordinating the

activation of both the Ras1-MAPK transcriptional branch and the Ras1-Scd1-Cdc42 morphology branch.

The mechanism by which Gpa1 is activating Ras1 is unknown but from the literature we can make a prediction that this activation could involve the protein, Ral2 (Fukui *et al.*, 1989). The *ral2* gene was isolated in the same screen as *scd1* and *scd2* when (Fukui & Yamamoto, 1988) were screening for mutants which have the same rounded mitotic phenotype as *ras1^{null}* cells. Not a lot is known about the function of Ral2 although interestingly (Fukui *et al.*, 1989) showed that the sterility and rounded mitotic morphology of *ral2^{null}* cells could be rescued by *ras1.val17* indicating that Ral2 plays an important function in Ras1 activation although it is not thought to be a RasGEF due to the fact that its sequence shows no homology to that of known RasGEFs. We therefore predict that it may play a role in Ras1 activation indirectly perhaps by influencing the activity or localisation/activity of Ste6. The function of Ral2 in Ras1 activation should be assessed to further our understanding of how Ras1 is activated upon pheromone stimulation, it would be interesting to investigate whether Ral2 interacts with Gpa1, Ste4 and/or Ste6 as well as Ras1 itself to further support our hypothesis.

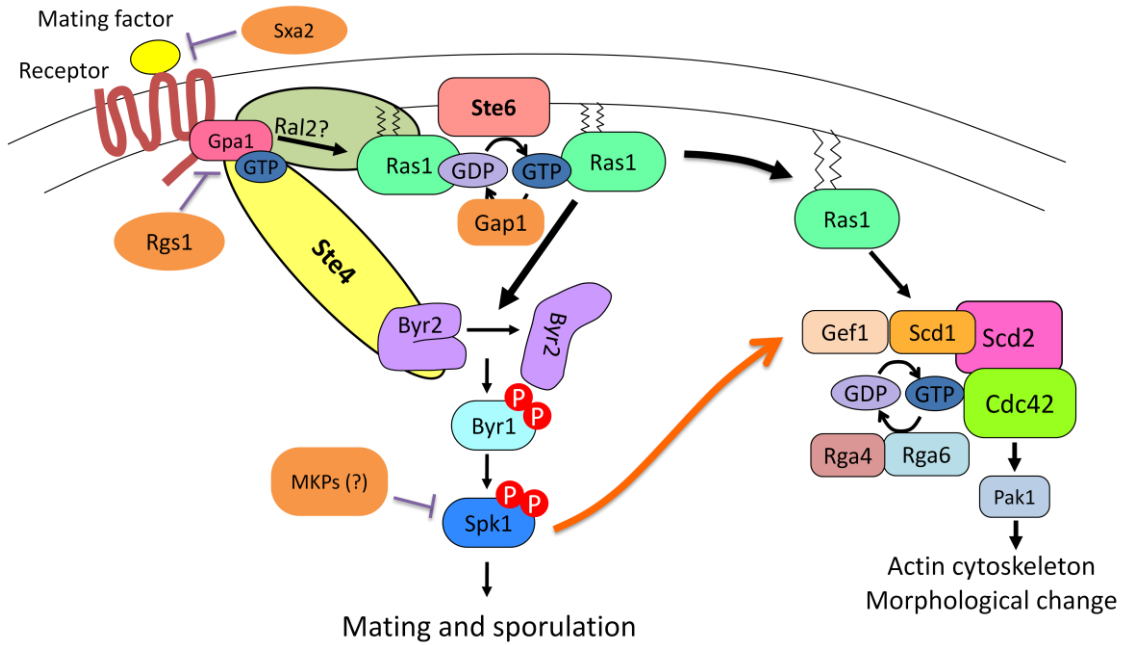


Figure 5.13 Proposed model for coordination of MAPK activation and morphology pathway activation

Ras1 plays a central role in the activation of both the MAPK pathway and the Cdc42-pathway. Activation of both pathways is dependent on Gpa1 activation thereby localising activation of the morphology pathway to the site of pheromone signalling at the cell membrane.

5.5.1 The role of Ste4 in Byr2 activation

Ste4 is essential for mating and sporulation, it is a Ste11 target gene and is strongly induced upon nitrogen starvation (Okazaki *et al.*, 1991). Ste4 has been shown to interact with itself and the regulatory domain of Byr2 at a different site to which Ras1 binds (Barr *et al.*, 1996). The Byr2-N28I mutant, which can bind to Ras1 but not to Ste4 cannot rescue a *byr2-null* mutant therefore the interaction between Byr2 and Ste4 is essential for Byr2 activation, also disruption of *ste4* abolishes the hypersensitivity of *ras1.val17* and *gpa1.E244L* just as disruption of *byr2* does (Barr *et al.*, 1996). We have shown that in the absence of *ste4* there is absolutely no phosphorylation of Spk1 even in the presence of *ras1.val17* which explains why disruption of *ste4* abolishes the hypersensitivity of *ras1.val17* as mentioned above and it is exceptionally likely that this is also the same reason for *gpa1.E244L* as well although we have not shown this directly. Regions of Ste4 show homology to the *S.cerevisiae* protein Ste50 which has been shown to bind to the regulatory region of Ste11 (the MAPKKK of the pheromone response pathway). Yeast-2-hybrid studies showed that Ste50 cannot bind Byr2 and Ste4 cannot bind STE11 and that the region of Ste4 required for the interactions between another Ste4 protein and Byr2 are not conserved between Ste4 and Ste50 (Barr *et al.*, 1996) therefore it is difficult to draw similarities about the function of *S.pombe* Ste4 when comparing to *S.cerevisiae* Ste50.

A significant conclusion from our data is that *ras1.val17* cannot activate Byr2 without Ste4. It has already been shown that Byr2 translocates to the plasma membrane in a Ras1-dependent manner by (Bauman *et al.*, 1998) and this is conserved in the mammalian system where Raf-1 binds to activated Ras and translocates from the cytoplasm to the plasma membrane (Bauman *et al.*, 1998). To relate this to our results, in the absence of Gpa1 or Ste4 but in the presence of Ras1.val17, Byr2 is probably

recruited to the membrane and may even adopt the "opened up" conformation ready for further post-translational modifications/protein-protein interactions but has no catalytic activity. We can relate these findings to the model proposed by (Tu *et al.*, 1997) illustrated in **Figure 5.14**, although this model is far from clarified they propose that in mitotic cells Ras1 is in its inactive form (Ras1-GDP) and Byr2 is in its closed inactive conformation located in the cytoplasm. Activated Ras1 (Ras1-GTP) promotes Byr2 membrane localisation where it is in close proximity to Shk1/Pak1 which is activated through the Ras1-Cdc42 pathway. Shk1/Pak1 somehow promotes the open conformation of Byr2 possibly through phosphorylation. Ste4 acts to dimerise Byr2 allowing autophosphorylation of the catalytic domains. Ras1 may have a role in the opening up of Byr2 as the Ras1 binding domain and the Byr2-catalytic domain overlap in the regulatory region as shown in **Figure 1.8**. From Chapter 4 we could not confirm the role of the Cdc42 pathway in Byr2 activation and therefore MAPK activation through disabling this pathway by deletion of *scd1*. This however does not disprove the theory as Shk1/Pak1 could have activity in the absence of Scd1 or through the actions of the other Cdc42 GEF, Gef1, therefore using Shk1/Pak1 mutants with altered activity would be a more appropriate experiment to confirm this - see Chapter 4 discussion. Also, presently there is no evidence that Shk1 phosphorylates Byr2 or that Byr2 can autophosphorylate itself, experiments to investigate this would be *in vitro* kinase assays and mutagenesis of phosphorylation sites to prove phosphorylation is important for activation. We also see MAPK phosphorylation in *ras1Δ* therefore if Shk1/Pak1 is essential for Byr2 activation then there must be basal activation of Cdc42- Shk1/Pak1 in the absence of Ras1. However, without Ras1 this basal activation of the Cdc42 pathway is not enough for shmooing as we predict that there has to be a strong very localised activation of Cdc42 to promote a shmooing response. Another theory to fit with these

observations is that the Cdc42-complex is active in the absence of Ras1 but mislocalised. It would be interesting to see if the "probing" behaviour of the Cdc42-morphology complex reported in (Bendezu & Martin, 2013) is dependent on Ras1. CRIB-GFP could be used to investigate the amount and localisation of Cdc42-GTP in *ras1Δ* and *ras1.val17* to conclude if Ras1 has a role in activation and/or localisation of the Cdc42-morphology complex.

One potential observation that doesn't fit with the model proposed in **Figure 5.14** is that Ras1 is in a GDP bound state in mitotic cells. It is highly likely that there is a substantial amount of Ras1-GTP in mitotic cells which helps to explain why *ras1.val17* has no obvious mitotic phenotype. If this is true then perhaps the sequestration of Byr2 away from the plasma membrane by proteins such as Rad24 and Rad25 (Ozoe *et al.*, 2002) during mitosis would be of major importance. Localisation experiments of Byr2/Rad24/Rad25 during mitosis and meiosis would further this observation. In mammalian cells 14-3-3 proteins bind to CRAF in unstimulated cells and sequester it in the cytoplasm, this localisation changes upon growth factor stimulation and Ras displaces the 14-3-3 protein (Freed *et al.*, 1994) and it is tempting to speculate that a similar mechanism is employed in *S.pombe*.

Does there have to be a priming kinase? Potentially no, even though this is the case in mammalian systems and *S.cerevisiae*, the proposed dimerisation of Byr2 via Ste4 may be enough to promote autophosphorylation and activation as we know that Ste4 is absolutely essential for Byr2 activation. One amendment to the model proposed in **Figure 5.14** would be that perhaps Ste4 is required for the opening up of Byr2 because if the conformation in Step 3 is correct there would be a chance that two Byr2 molecules would come together by chance and activate each other purely as they are in close proximity on the membrane at the site of activated Ras1.

We have shown that Ras1-GTP alone cannot activate Byr2 but in the absence of Ras1 Byr2 can be activated to a limited extent, this is probably due to there being an increase in the amount of *byr2* mRNA in cells upon nitrogen starvation (Papadaki *et al.*, 2002) and therefore presumably an increase in the amount of Byr2 protein. If Byr2 happens to be close enough to the membrane it will bind Ste4 and if two or more come together there can be activation via a Gpa1-Ste4 and possibly Shk1/Pak1 complex. To summarise, the proposed reason there is no MAPK phosphorylation in *gpa1Δ ras1.val17* and *ste4Δ ras1.val17* is that Byr2 is probably localised correctly by Ras1-GTP but it cannot be activated. Future experiments into the localisation of Byr2 in these mutants will be essential for further clarification.

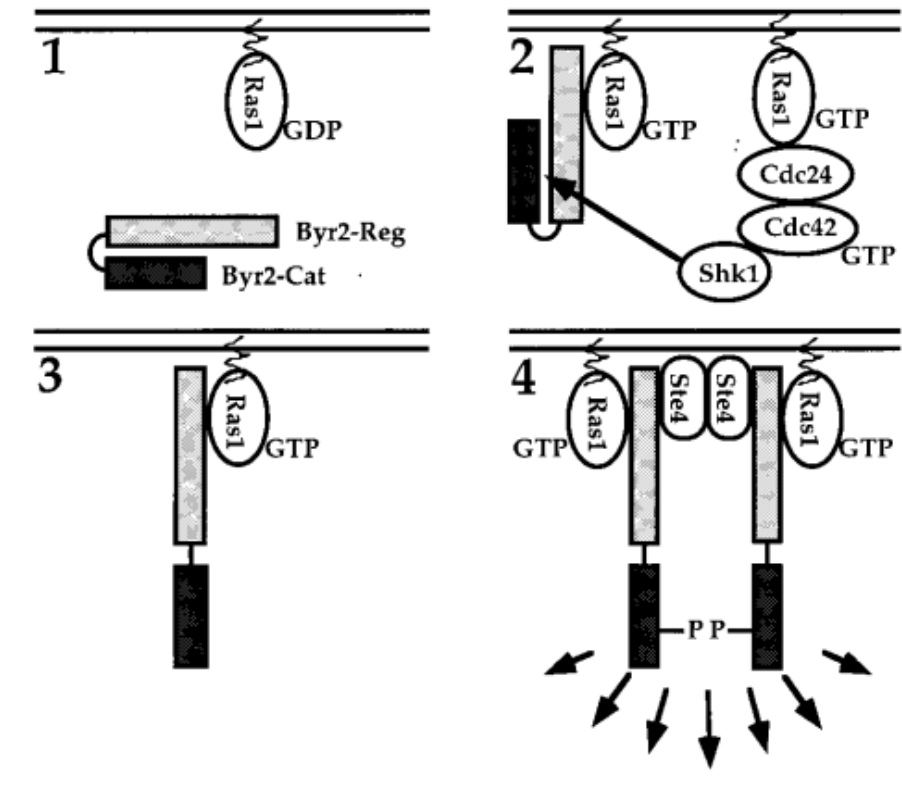


Figure 5.14 Proposed model for Byr2 activation.

Reproduced from Tu *et al.*, 1997. In mitotic cells Ras1 is in its inactive form (Ras1-GDP) and Byr2 is in its closed inactive conformation (1). Activated Ras1 (Ras1-GTP) promotes Byr2 membrane localisation where it is in close proximity to Shk1(2) which is activated through the Ras1-Cdc42 pathway. Shk1 somehow promotes the open conformation of Byr2 possible through phosphorylation (3). Ste4 acts to dimerise Byr2 allowing autophosphorylation of the catalytic domains (4).

5.5.2 Ste6 and the activation of Ras1 during mating

A morphological change does not occur in the *ste6Δ byr1.DD* double mutant even though nuclear Spk1-GFP is evident (**Figure 5.12**). Therefore, providing more phospho-MAPK signal to that seen in *ste6Δ*, via the addition of *byr1.DD*, does not help to provoke a morphological response in the absence of Ste6. However, a morphological change occurs in the *ste6Δ ras1.val17* double mutant which phenocopies the *ras1.val17* single mutant concluding that the role of Ste6 is Ras1 activation for both MAPK activation and Cdc42 activation. Collectively, these findings contradict the previous prediction of Ste6 function proposed in the paper by (Papadaki *et al.*, 2002) and outlined in hypothesis 1 (**Figure 5.9**). They predicted two distinctive pools of the activated Ras1 protein and that each pool requires the specific GEF molecule i.e. Ste6 was exclusively activating Ras1 for Byr2 activation and Efc25 was exclusively activating Ras1 for Cdc42 activation. We observed that in the absence of Ste6, the MAPK phosphorylation still occurs to but at a compromised level and that the addition of *byr1.DD* did not result in a phenotype different to that of single *ste6Δ* mutant. On the other hand, we showed that the *ste6Δ ras1.val17* double mutant shows the *ras1.val17* single mutant phenotype therefore, the sterile phenotype of the *ste6Δ* is caused by failure to activate the morphological pathway as well as compromised MAPK activation.

Through these observations we propose that hypothesis 2 is more representative of Ras1 activation (**Figure 5.15**). It is reasonable to conclude that Ste6 activates Ras1 that activates both the MAPK and morphological pathways upon pheromone stimulation. The quantitative role of Ste6 in MAPK phosphorylation remains to be investigated as the data presented is only representative of one biological replicate but this preliminary data may suggest the levels of phospho-Spk1 are higher in *ste6Δ* compared to *ras1Δ* and

perhaps Ras1 activation can also be occurring by the Ras1GEF Efc25 in the absence of Ste6 but that would not explain why therefore there is no morphological response in *ste6Δ byr1.DD*. The activation status of Ras proteins is a balance between the activity of GEFs and GAPs and therefore, the higher than expected phospho-MAPK signal in *ste6Δ* could also be because of a decrease in the activity of Gap1 as a potential negative feedback loop. Ste6 may somehow influence the activity of Gap1 to limit the extent of Ras1 activation therefore there is a higher basal level of activated Ras1 carried over from mitosis in the absence of Ste6 due to less Gap1 activity and this basal activity is amplified by the MAPK cascade causing the higher than expected phospho-MAPK signal. This is supported by the previous findings of (Wang *et al.*, 1991) which showed that the *ste6Δ gap1Δ* mutant shows the characteristic *ras1.val17* elongated phenotype upon nitrogen starvation therefore even in the absence of Ste6 Ras1 is probably hyperactivated due to the loss of Gap1, whether this phenotype is dependent on Efc25 is unknown but it would be interesting to see if Efc25 is having a role in Ras1 activation in the context of fission yeast mating.

Future work would be to examine whether MAPK activation is impaired in the *ste6Δ efc25Δ* double mutant during a mating time-course. At the moment we assume that the phospho-MAPK signal in *ste6Δ* is dependent on Ras1 and in the future this can be checked via the creation of a double deletion strain.

Our concluding hypothesis is that in mitotically growing cells, Ste6 and Spk1 are not expressed so Ras1 is exclusively signalling via the Scd1-Cdc42 pathway under the control of the Ras1GEF, Efc25 but during mating Ras1 plays a dual role in the activation of both the pheromone activated MAPK cascade (Byr2-Byr1-Spk1) and the Cdc42-morphology pathway which is controlled by Ste6 (**Figure 5.15**).

The works of (Papadaki *et al.*, 2002) showed that the functions of Efc25 and Ste6 are not interchangeable as Ste6 overproduction cannot rescue the rounded phenotype of *efc25Δ* and Efc25 overproduction cannot rescue the sterility of *ste6Δ*. This again raises the question of how the Cdc42-morphology complex is specifically being controlled during mating in contrast to mitosis and the switch between cell tip extension and shmooing. It is thought that the binding of different Ras GEFs promotes Ras to bind and activate different effector pathways but in this case, if our hypothesis is true, both Efc25 and Ste6 can activate Ras1 that signals down the Scd1 path, Efc25 during mitosis and Ste6 during meiosis. It is likely that Ste6 is part of the multiprotein morphology complex along with Gap1 as these have both been seen to colocalise with Scd2 - personal communication with Sophie Martin's lab - perhaps forming a meiosis specific morphology complex that can be stabilised and concentrated at the site of pheromone stimulation at the cell cortex by the actions of Spk1 MAPK as proposed in the Chapter 4 Discussion.

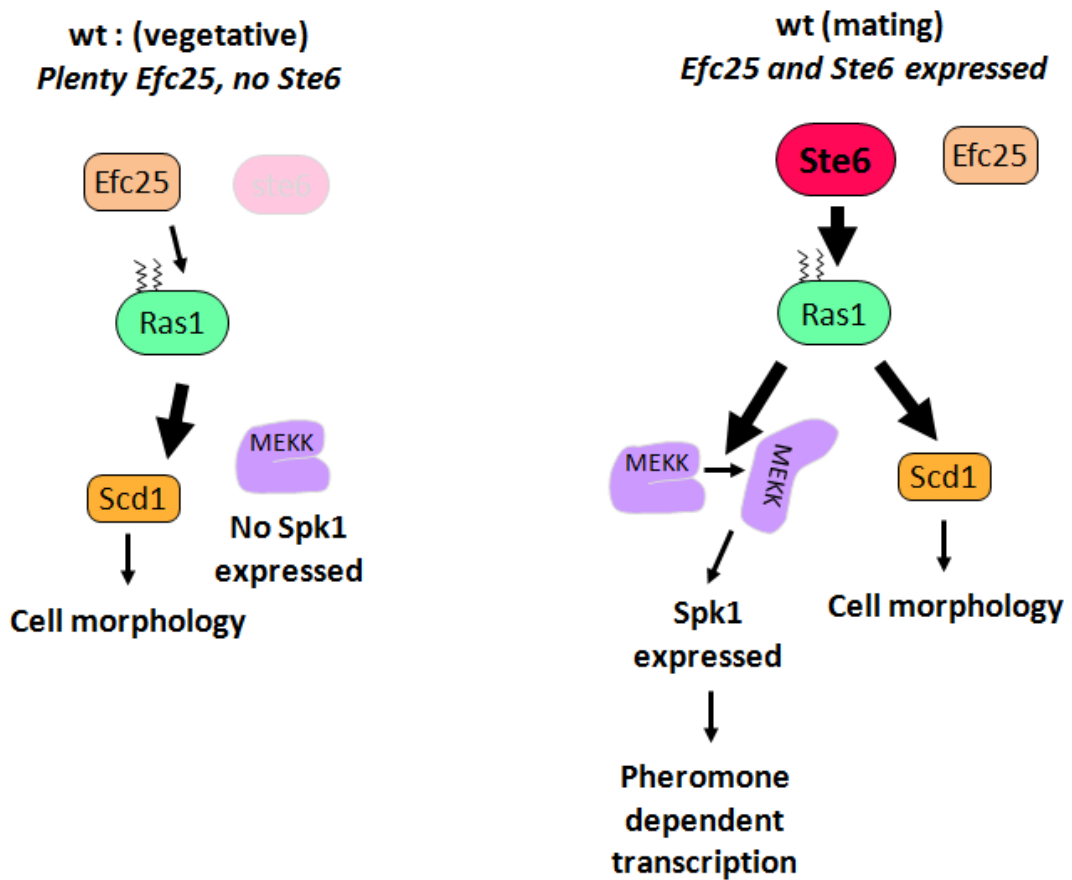


Figure 5.15 The proposed model for activation of Ras1

Our current model for Ras1 activation. During vegetative growth, Efc25 is expressed and controls the activity of Ras1 for the activation of the Scd1-Cdc42 pathway. Upon nitrogen starvation both Ste6 and Efc25 are expressed but Ste6 is the major activator of Ras1 for both the MAPK branch and the Cdc42 branch.

5.5.3 Coordinated activation of the MAPK cascade and the morphology pathway

Potentially, proteins of the MAPK branch and the morphology branch may form a large multi-protein complex at the plasma membrane to coordinate activation. Ste4, Ras1, Gap1 and Ste6 all colocalise with Scd2 (unpublished - communications with Sophie Martin's lab) and we've shown that Ste4 has a role exclusively in MAPK activation and not morphology pathway activation therefore its role in this complex has to be MAPK activation. Further experiments to identify Ste4 interacting partners is of high interest as it is currently unknown whether Ste4 directly interacts with Gpa1 which is an essential part of our hypothesis for Byr2 activation. Drawing on what is currently known of the Ste4 homologue in *S.cerevisiae*, Ste50, it has been shown that Ste50 and Ste11 MAPKKK constitutively interact via their SAM domains and that Ste50 interacts with the heterotrimeric G-protein of the mating response pathway as well as Cdc42, Ras1 and Ras2 (Ramezani-Rad, 2003). Ste50 interacts with Cdc42 and Ras1 and Ras2 via its Ras-associated domain (RAD) which is amino acids 235-327. Barr *et al.*, 1996 concluded that the amino acids 204-262 of Ste4 showed 32% identity and 64% homology to amino acids 267-325 of Ste50 which directly coincides with the RAD therefore Ste4 may interact with other crucial signalling components of the MAPK and morphology pathways. However, using yeast-2-hybrid (Barr *et al.*, 1996) could not show an interaction between Ste4 and Gpa1 or Ras1, this could be due to the difficulty of using G-proteins in Y2H experiments as the interactions are usually dependent on the binding of GTP, Cdc42 was not tested in these experiments and I think it would be an interesting area to go back and revisit. In *S.cerevisiae*, pheromone activated MAPK, Fus3 is localised to the shmoo via $G\alpha$ (Metodiev *et al.*, 2002) and is important for polarised growth as it phosphorylates an important formin protein required for actin

assembly, Bni1 (Matheos *et al.*, 2004) and Fus3 phosphorylates G β to stabilise the Far1- G β complex and keep it at the cell cortex (Metodiev *et al.*, 2002). Far1 is a scaffold which localises activated Cdc42 to the site of polarised growth via Cdc24. During mitosis, Far1 sequesters Cdc24 in the nucleus and is released upon Far1 phosphorylation and degradation (Shimada *et al.*, 2000; Nern & Arkowitz, 2000) but during meiosis the Far1-Cdc24 complex relocates to the cell cortex and recruits Cdc42 and Bem1 away from the bud site to activate a shmoo site (Valtz *et al.*, 1995; Wiget *et al.*, 2004). Relating this to the *S.pombe* system, perhaps the G-protein (Gpa1 and possibly Gnr1) can interact with a number of components in order to coordinate the MFSP response and therefore the identification of Gpa1 interacting proteins is of great interest.

CHAPTER 6 THE ROLE OF NEGATIVE REGULATORS IN SHAPING MAPK ACTIVATION

6.1 Introduction

We wanted to investigate the role of known negative regulators of the MFSP pathway and how they contribute to shaping the MAPK signalling profile to highlight the important and potential individual roles that each negative regulator plays.

The Gap1, Sxa2 and Rgs1 proteins are confirmed negative regulators of the MFSP and these are highlighted in red in **Figure 6.1**. Gap1 (also known as Sar1) was originally identified by two separate groups at similar times, Imai *et al* isolated the *gap1* gene by screening for mutants which exhibited the elongated conjugation tube phenotype of *ras1.val17* which was identified a few years earlier (Nadin-Davis *et al.*, 1986b; Imai *et al.*, 1991) whereas Wang *et al* isolated the same gene but called it *sar1* (Suppressor of Activated Ras1) by screening for high-copy vectors that suppress the conjugation defect of *ras1.val17* (Wang *et al.*, 1991). This observation is important as it shows that Ras1.val17 is still sensitive to the actions of Gap1 even though the oncogenic nature of the *ras1.val17* mutation is constitutive activation due to an insensitivity to GAPs (Trahey & McCormick, 1987; Gibbs *et al.*, 1988). This observation is further investigated in Chapter 7.

The P-factor protease, Sxa2, was also isolated from a screen for phenocopy mutants of *ras1.val17* (Imai & Yamamoto, 1992) and was characterised as a secreted P-factor protease by (Ladds *et al.*, 1996). Rgs1 is a member of the "Regulators of G-protein Signalling" (RGS) family of proteins and was originally identified through the *S.pombe* genome sequencing project and was predicted to be an RGS family protein (Tesmer *et*

al., 1997). Characterisation of Rgs1 confirmed it as a negative regulator of the MFSP as an *rgs1Δ* shows signs of enhanced MAPK activation in the form of quicker G1 arrest and increased expression of *mam2* (P-factor receptor) (Pereira & Jones, 2001). Deletion of *rgs1* also results in the elongated phenotype similar to *gpa1.QL*, an activated *gpa1* mutation (Obara *et al.*, 1991). In this sense, the *rgs1* deletion phenotype is similar to the *ras1.val17* phenotype where elongation of the cells occurs only when the mating pheromone is around (Pereira & Jones, 2001). Rgs1 is closely related to Sst2 of *S.cerevisiae* which was the first RGS protein to be discovered (Chan & Otte, 1982). Sst2 can suppress *rgs1Δ* in *S.pombe* highlighting the close functional relationship between the two proteins (Watson *et al.*, 1999).

Mitotic and meiotic phenotypes of *ras1.val17*, *gap1Δ*, *sxa2Δ* and *rgs1Δ* are shown in **Figure 6.2**.

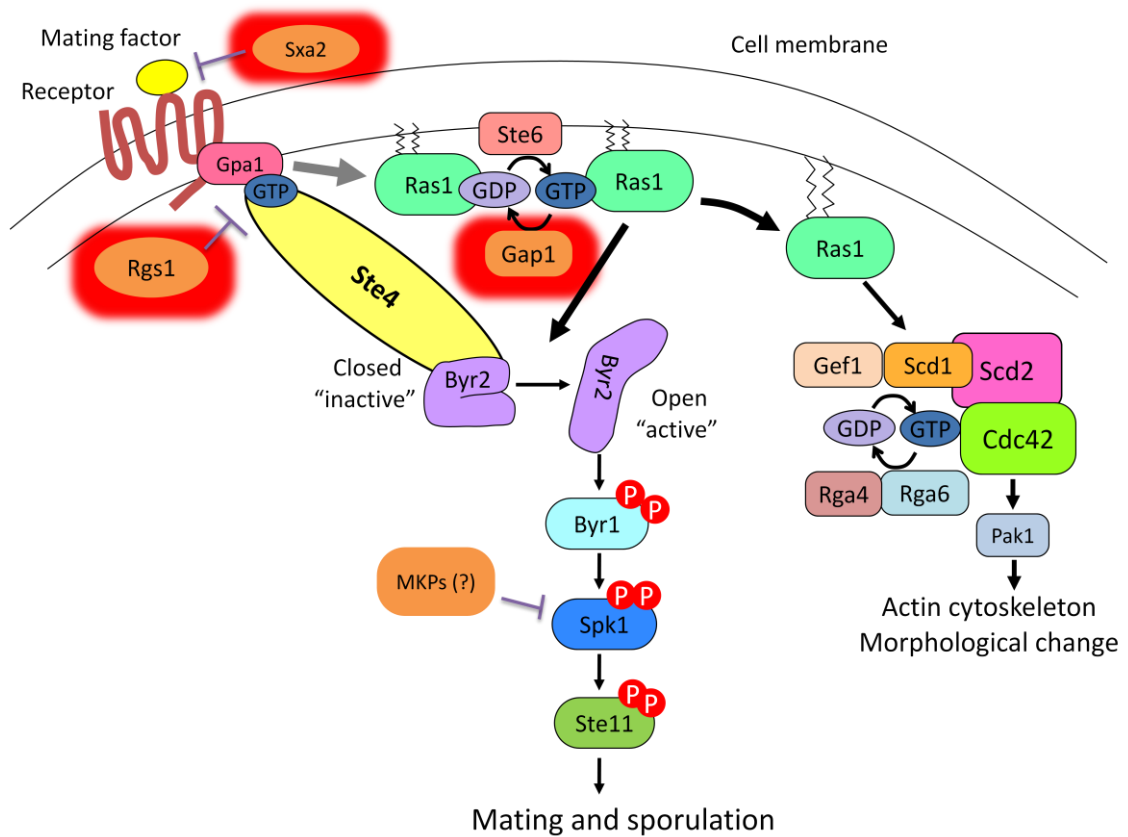


Figure 6.1 Identified negative regulators of the MFSP

The three negative regulators of the pathway, Gap1, Sxa2 and Rgs1 are highlighted in red, each one was addressed individually for MAPK dynamics and cell imaging by creating deletion mutants via two-step PCR method followed by transformation using the TRAF0 method.

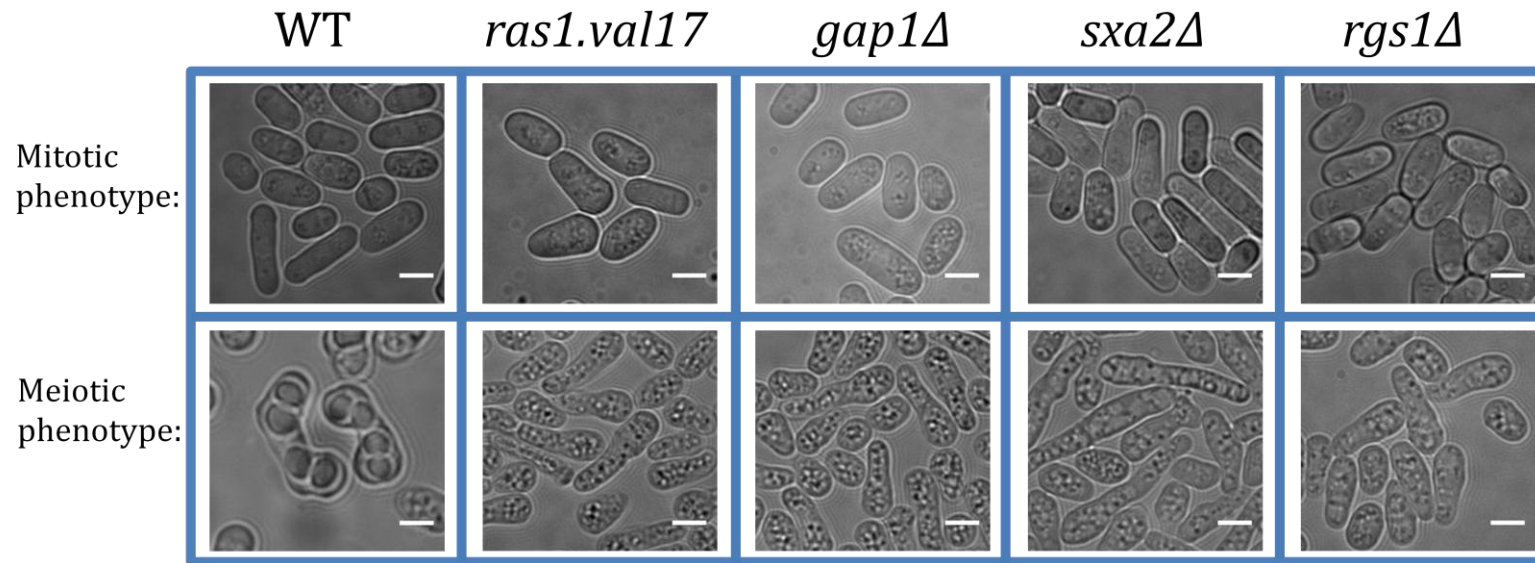


Figure 6.2 Mutants that phenocopy *ras1.val17*

Single deletion mutants that show the characteristic elongated phenotype first associated with *ras1.val17* in comparison to WT (KT3082); *ras1.val17* (KT3084), *gap1Δ* (KT3997), *sxa2Δ* (KT3875) and *rgs1Δ* (KT4161). Scale bar is 5 μm .

6.2 Role of Gap1

Gap1 is the GTPase activating protein for Ras1. *gap1*⁻ haploid strains show no morphological defects in mitotic cells and disruption of *gap1* has no effect on the growth rate therefore *gap1* is not an essential gene (Wang *et al.*, 1991). It has also been identified as a Ste11 target gene (Mata & Bahler, 2006). Gap1 is the only identified RasGAP in *S.pombe* but is strongly linked with the pheromone pathway rather than the Cdc42-pathway as *gap1Δ* shows no change in cell shape in mitotic cells unlike *ras1Δ*, *scd1Δ*, *scd2Δ* and *efc25Δ*.

To monitor the MAPK phosphorylation profile in the absence of Gap1, the *gap1* gene was replaced by the ClonNAT cassette at its chromosomal gene locus using PCR based techniques in a WT strain harbouring the *spk1-GFP* to create the *gap1Δ* mutant (KT3997). This mutant was subject to a 24-hour mating time-course, cells were collected for protein extraction and images were taken every hour for 13-hours then again at 16- and 24-hours post mating induction. Whole cell protein extracts were made via the TCA method, followed by SDS-PAGE and quantitative western blotting of two biological replicates and directly compared to WT (KT3082). Data represented in **Figure 6.3** is from two technical replicates of one biological replicate. Two biological replicate time-courses were collected and subject to quantitative western blotting. Both biological replicates showed similar data therefore quantitation of only one biological replicate is shown. **Figure 6.3A** shows a western blot of WT and *gap1Δ* extracts and blotted for phospho-Spk1, total-Spk1 and α -tubulin. Quantification of MAPK phosphorylation (pERK/ α -tubulin) shows an phosphorylation profile similar to that of *ras1.val17* (**Figure 6.3B** and **C**) with the phospho-MAPK signal peaking earlier in both mutants compared to WT. The total amount of Spk1 is indistinguishable in WT compared to the *gap1Δ* mutant (**Figure 6.3D**) up until 12-13-hours post induction when

the levels of Spk1 continue to increase in the mutant. This could be as a consequence of a prolonged positive feedback of Spk1 expression due to there being increased amounts of phospho-Spk1 after 10-12 hours when the phospho-signal usually decreases as seen in the WT. It appears likely that the earlier presence of phospho-Spk1 is linked to an uncoupling of Ras1 and Gap1 and that Gap1 plays a role to modulate the MAPK output via Ras1 throughout the entire duration of pheromone signalling as without it we see acute initial MAPK phosphorylation.

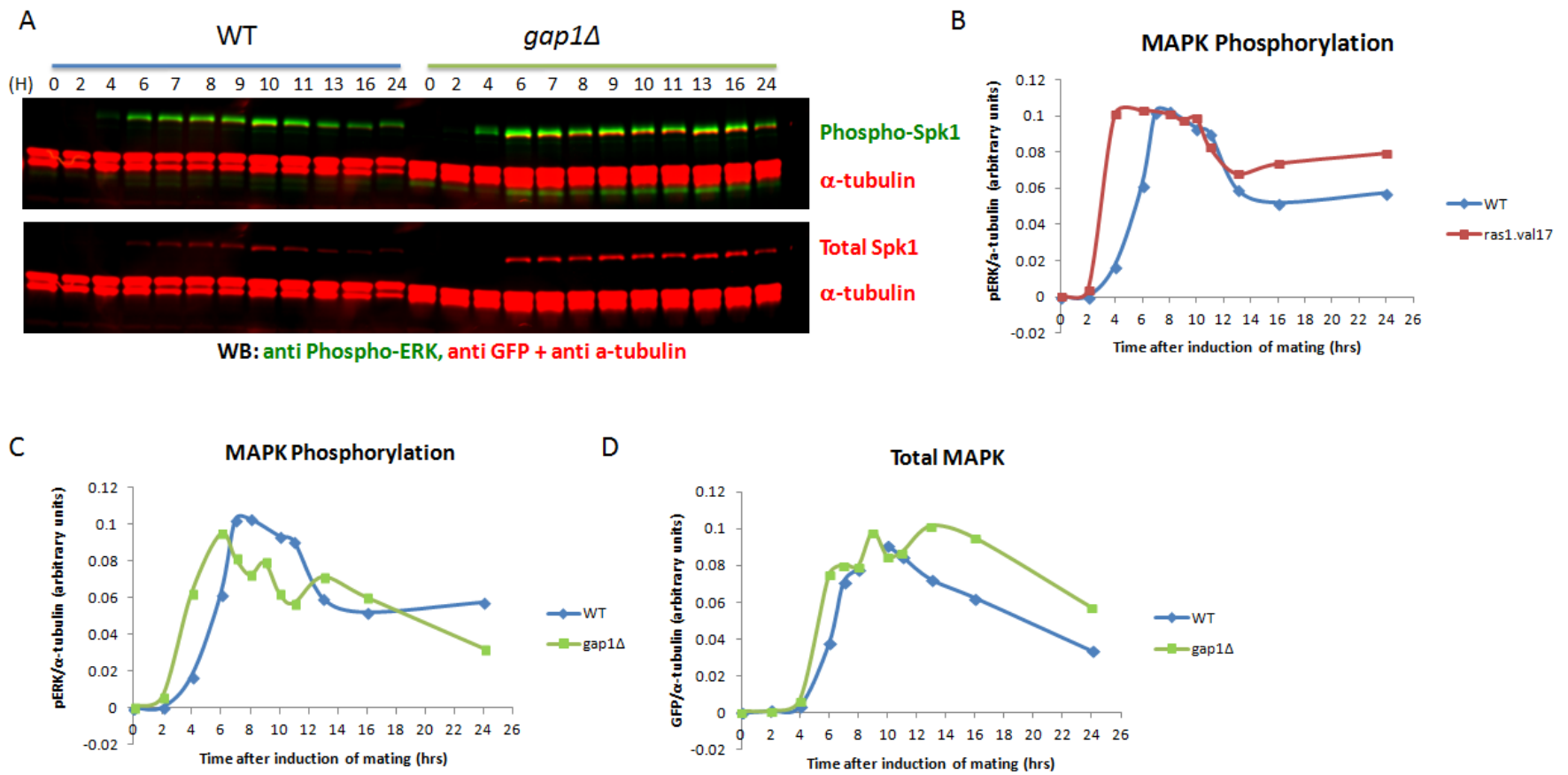


Figure 6.3 A direct comparison of the MAPK dynamics during aWT and *gap1Δ* mating time-course.

A wildtype strain (KT3082) and *gap1Δ* strain (KT3997) were subject to a time-course over 24 hours. (A) Western blot comparing a WT time-course with a *gap1Δ* time-course. Membrane was blotted for phospho-Spk1 and α -tubulin (upper panel) as a loading control which is used to normalise the amount of phospho-Spk1 signal to the total amount of protein in the extracts. The lower panel shows the total amount of Spk1 protein over the time-course by blotting with anti-GFP. (B) represents quantitation of the WT vs. *ras1.val17* phospho-MAPK/tubulin data from **Figure 3.13** (C) and (D) Quantitation of one biological replicate time courses comprising two technical replicate blots. Quantitation was carried out using the Image Studio ver2.1 software supplied with the Licor Odyssey CLx Scanner and (C) represents changes in the phospho-MAPK/tubulin signal in WT vs. *gap1Δ* WCE (D) represents changes in the levels of MAPK over the time-course for WT and *gap1Δ*, quantified as in (C) but using the GFP signal. (H) represents the number of hours post mating induction.

Imaging of *gap1Δ* cells during the time-course is shown in **Figure 6.4** for selected time-points directly compared to the *ras1.val17* cells. The Spk1-GFP dynamics and timings of morphological changes are very similar in both these strains; there is strong nuclear signal and the starting of shmoo formation at 6-hours onwards and nuclear signal is still present in elongated cells at 24-hours post induction. This confirms that the MAPK activation dynamics and timing of shmooing are mirrored in these two mutants and is therefore characteristic of an unregulated Ras1 protein.

In conclusion, it appears likely that the characteristic elongated mating phenotype associated with *ras1.val17* is linked to premature activation of the pheromone response which we hypothesis leads to a hypersensitive activation of the Cdc42-pathway directly through the activation of Ras1 and indirectly through the contribution of the MAPK towards the morphology pathway. In the case of the *gap1Δ* mutant this is due to an uncoupling of Ras1 and its GAP which leads to a hyperactivated Ras1 protein.

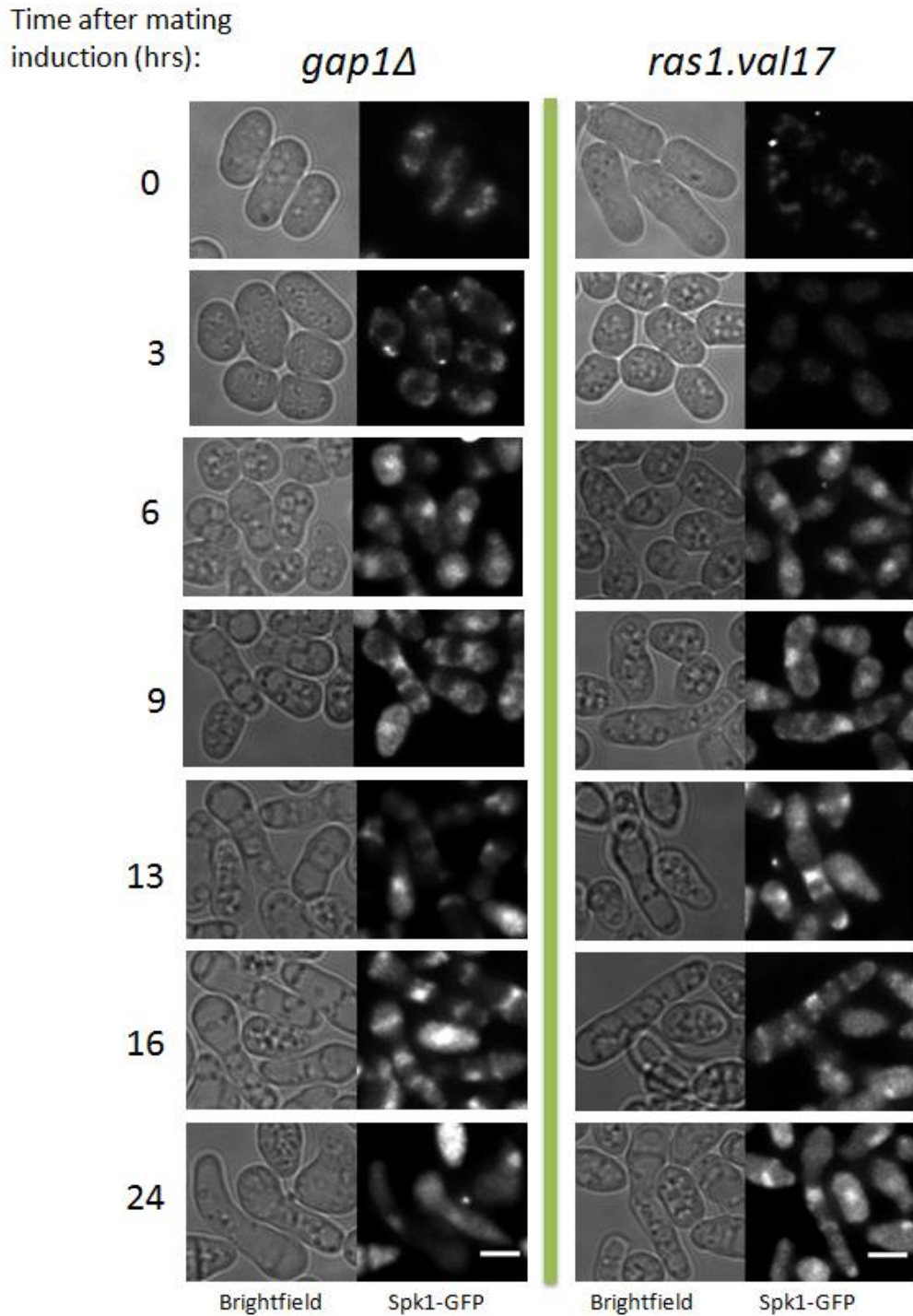


Figure 6.4 Imaging of Spk1-GFP over a 24 hour time-course in *gap1Δ* cells compared to *ras1.val17* cells.

Live cell imaging in the brightfield and GFP channels. Each time point comprises 15-25 serial images of 0.4 μm interval along the Z axis taken to span the full thickness of the cell. All of the Spk1-GFP images were deconvolved using the Huygens Essential Deconvolution. Deconvolved images were Z-projected, cropped and combined using ImageJ. Scale bar is 5 μm .

6.3 Role of Sxa2

Sxa2 is a P-factor protease whose expression is induced upon activation of the MFSP, the gene for Sxa2 was replaced by the ClonNAT cassette at its chromosomal locus using PCR and recombination techniques as used previously. The *sxa2Δ* fragment was transformed into the WT *spk1-GFP* host strain (KT3082) to create the *sxa2Δ* mutant containing *spk1-GFP* (KT3875). MAPK dynamics and morphology were examined using quantitative western blotting and live cell imaging. **Figure 6.5A** shows a western blot of WT and *sxa2Δ* protein extracts collected over a 24-hour time-course. Data represented in **Figure 6.5** is from two technical replicates of one biological replicate. Two biological replicate time-courses were collected and subject to quantitative western blotting. Both biological replicates showed similar data therefore quantitation of only one biological replicate is shown. Following quantification of the phospho-MAPK signal it is clear to see that the levels are extremely high compared to WT (**Figure 6.5C**). This is also the case for the total levels of MAPK (**Figure 6.5D**). The *sxa2Δ* MAPK phosphorylation and total MAPK profiles show an abrupt increase in the amount of activated and total Spk1 which remains significantly higher than WT across the entire 24-hour time-course. This shows that Sxa2 is exceptionally important in regulating the activity of the MFSP over the entire period of signalling. Down regulation of the phospho-MAPK signal is evident in the *sxa2Δ* mutant which is likely to be the result of the actions of other down regulators of the MFSP (for example Gap1 and Rgs1) and receptor internalisation which will act to terminate signalling at the level of the receptor which is the same molecular level of the pathway that Sxa2 is acting.

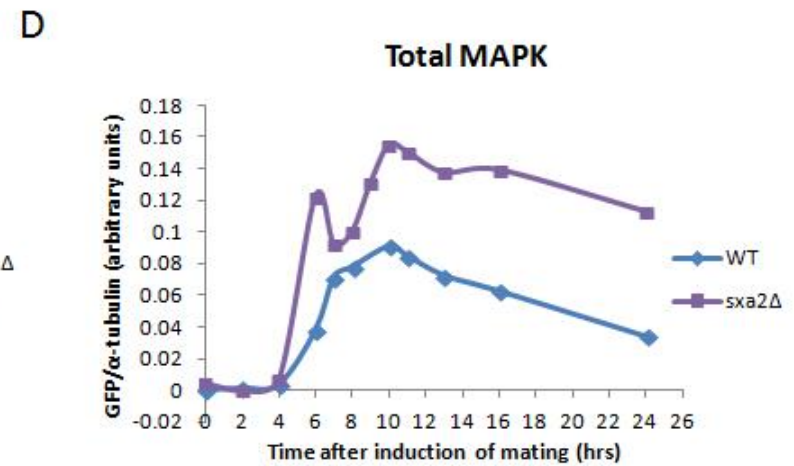
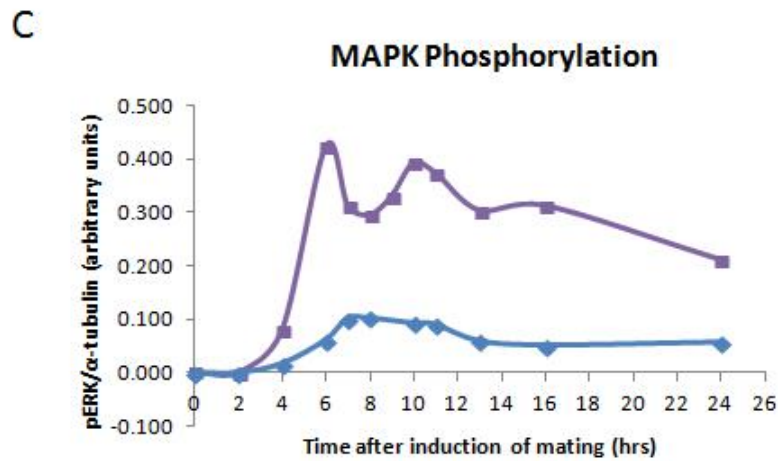
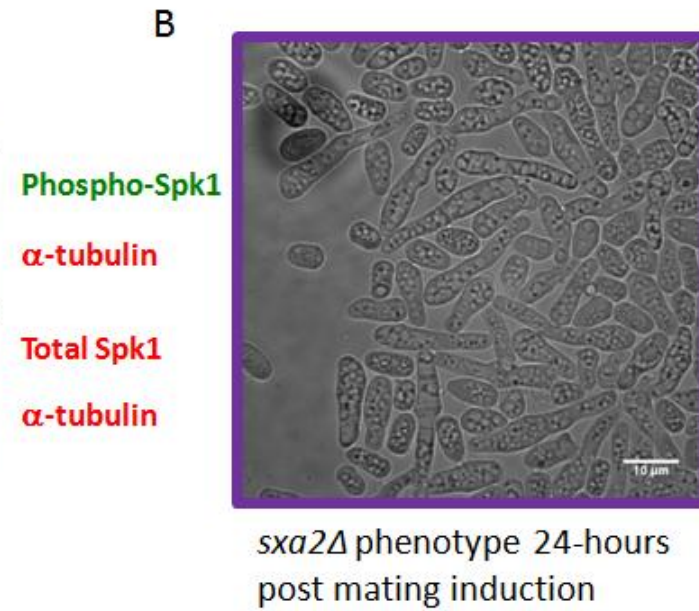
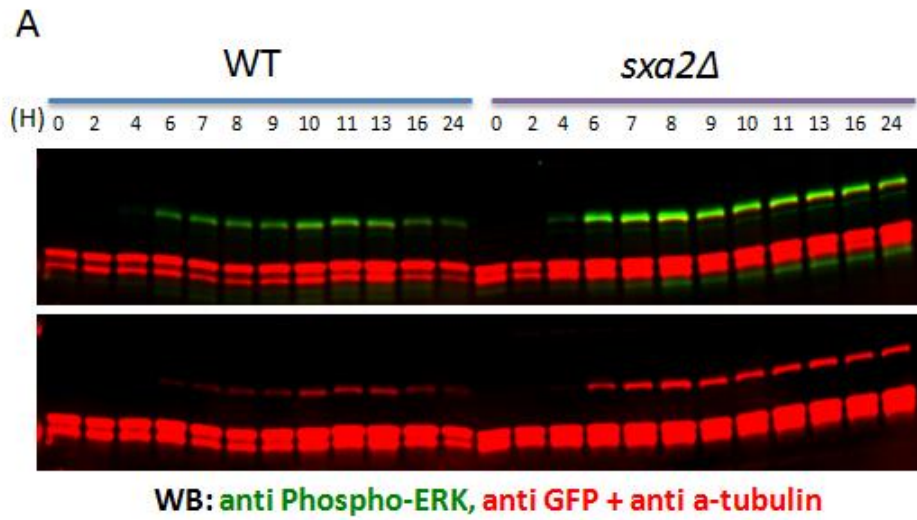


Figure 6.5 A direct comparison of the MAPK dynamics during a WT and *sxa2Δ* mating time-course.

A wildtype strain (KT3082) and *sxa2Δ* strain (KT3875) were subject to a meiotic time-course over 24 hours. (A) Western blot comparing a WT time-course with a *sxa2Δ* time-course. Membrane was blotted for phospho-Spk1 and α -tubulin (upper panel) as a loading control which is used to normalise the amount of phospho-Spk1 signal to the total amount of protein in the extracts. The lower panel shows the total amount of Spk1 protein over the time-course by blotting with anti-GFP. (B) *sxa2Δ* cells after 24-hours post mating induction (C) and (D) Quantitation of one biological replicate time courses comprises one technical replicate blot. Quantitation was carried out using the Image Studio ver2.1 software supplied with the Licor Odyssey CLx Scanner. (C) represents WT vs. *sxa2Δ* MAPK activation (D) Changes in the levels of MAPK over the meiotic time-course for WT and *sxa2Δ*, quantified as in (C) but using the GFP signal. In (A) H represents the number of hours post mating induction. Scale bar is 10 μ m.

Cell imaging in **Figure 6.6** show the cell morphology and Spk1-GFP signal in *sxa2Δ* compared to *ras1.val17* cells at the same time-points post mating induction. The *sxa2Δ* cells are full of vacuoles from 9-hours onwards. The Spk1-GFP localisation tends to follow that of the *ras1.val17* cells with a strong nuclear signal from 6-hours onwards which remains present for the entire time-course.

Sxa2 was originally isolated by a screen for mutants which cause the same elongated phenotype as *ras1.val17*. Following these experiments it is clear that the cell morphology is severely affected by the absence of Sxa2 and cells show extremely long conjugation tubes upon pheromone signalling as shown in **Figure 6.5B**. The shmooing response appears to be more severe in *sxa2Δ* cells with the elongation tubes reaching much longer lengths than *ras1.val17*, *gap1Δ* and *rgs1Δ* (**Figure 6.2**). This elongation is likely due to a combination of both a dramatic amount of MAPK activation feeding into the Cdc42-pathway and direct over stimulation of that pathway via Ras1 which we assume would be over activated in the absence of Sxa2 due to the prolonged activation of the mating factor receptor by mating factor.

In conclusion, in *sxa2Δ* cells there is no Sxa2 protease to terminate the signal at the level of the pheromone/receptor at the cell cortex and other regulators downstream are too weak to control the level of the activated MAPK signal alone in the prolonged presence of pheromone. Therefore the contribution of Sxa2 to down regulation is of great importance to prevent the excessive increases in phospho-MAPK levels shown in **Figure 6.5**.

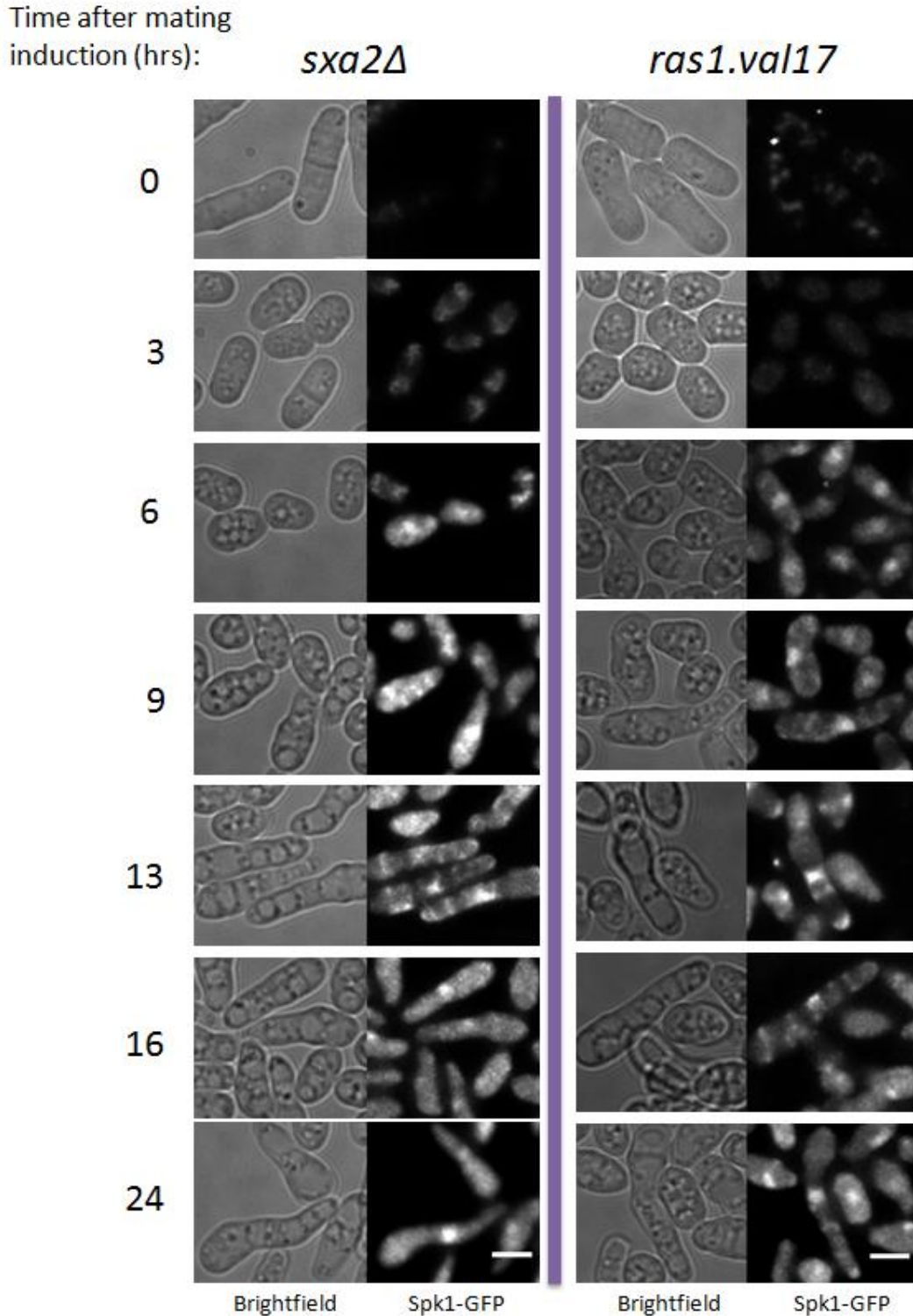


Figure 6.6 Imaging of Spk1-GFP over a 24 hour time-course in *sxa2Δ* cells compared to *ras1.val17* cells.

Live cell imaging of *sxa2Δ* (KT3875) and *ras1.val17* (KT3084) in the brightfield and GFP channels. Each time point comprises 15-25 serial images of 0.4 μm interval along the Z axis taken to span the full thickness of the cell. All of the Spk1-GFP images were deconvolved using the Huygens Essential Deconvolution. Deconvolved images were Z-projected, cropped and combined using ImageJ. Scale bar is 5 μm .

6.4 Role of Rgs1

Chapter 5 concluded that the G-protein, Gpa1 plays an essential role in transducing pheromone signalling to both the MAPK and morphology pathways, therefore regulation of Gpa1 would be predicted to be exceptionally important as well. Rgs1 is a member of the "Regulator of G-protein Signalling" family of proteins which are a conserved family of proteins that promote GTP hydrolysis specifically on G α -proteins (Dohlman & Thorner, 1997). The deletion of *rgs1* in *S.pombe* causes the elongated conjugation tube phenotype upon pheromone stimulation (Pereira & Jones, 2001) (**Figure 6.2**).

The MAPK protein dynamics were investigated by quantitative western blotting and live cell imaging in a *rgs1Δ* strain generated by replacing the *rgs1* gene at its chromosomal locus with the ClonNAT cassette in a strain already containing *spk1-GFP* (KT3082). Results of the quantification of phospho- and total-MAPK are in **Figure 6.7**. Data represented in **Figure 6.7** is from two technical replicates of one biological replicate. Two biological replicate time-courses were collected and subject to quantitative western blotting. Both biological replicates showed similar data therefore quantitation of only one biological replicate is shown. The phospho-MAPK signal appears to peak marginally earlier than WT (**Figure 6.7B**) at around 6-hours instead of 7-hours post induction, and this is around 2-hours later compared to *gap1Δ* and *ras1.val17*. This may reflect the difference in the nature of *rgs1* expression in that the expression requires both nutrient starvation and pheromone signalling for expression whereas *gap1* is expressed constitutively (Mata *et al.*, 2002). Along with a marginal, yet reproducible shift in the timing of peak phospho-MAPK signal there is a prolonged duration of the signal which may be mainly explained by the increases in the total amount of MAPK seen in this mutant compared to WT (**Figure 6.7C**). Overall, the

premature MAPK phosphorylation, which may be the cause of the hypersensitivity, seen in *ras1.val17/gap1Δ* does not appear to be as evident in *rgs1Δ*. *rgs1Δ* cells look reasonably similar to *ras1.val17/gap1Δ* mutants (**Figure 6.8**) although the elongation doesn't seem to be as prominent. It may be that in the *rgs1Δ* cells, a prolonged activation of Ras1 via Gpa1 is happening because, in the absence of Rgs1, we assume that Gpa1 will be active for a longer period. This fits with our hypothesis that it is hyperactivation of Ras1, but not MAPK, is responsible for the hyperactive shmooing observed upon mating induction.

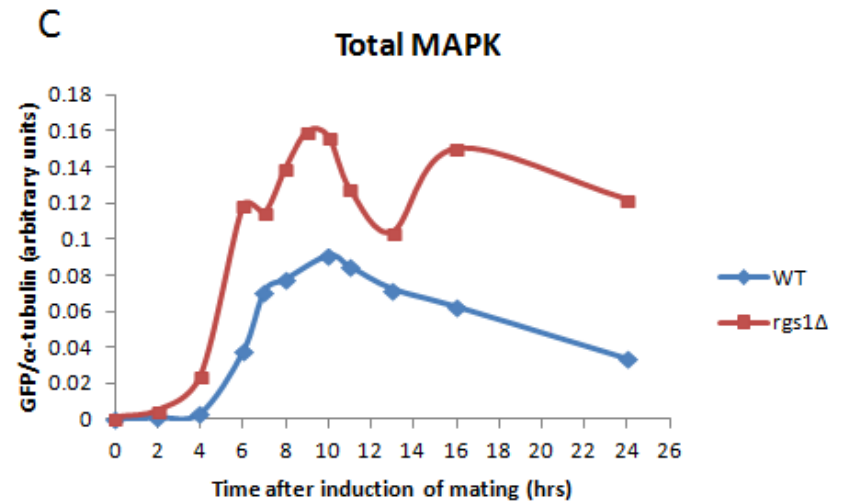
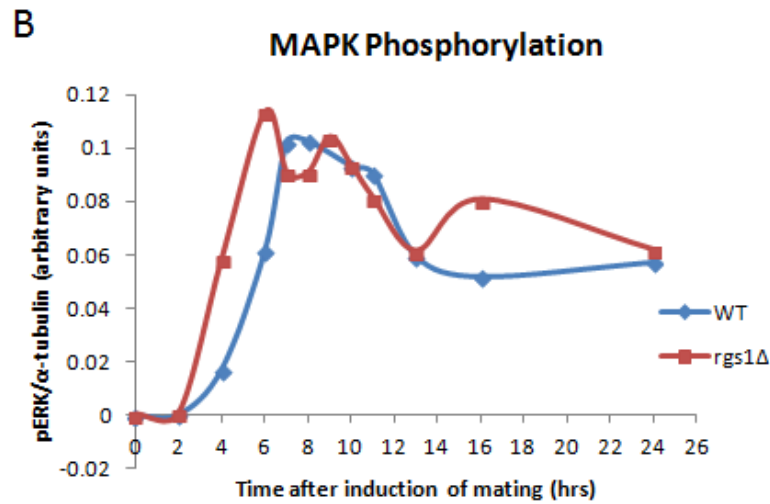
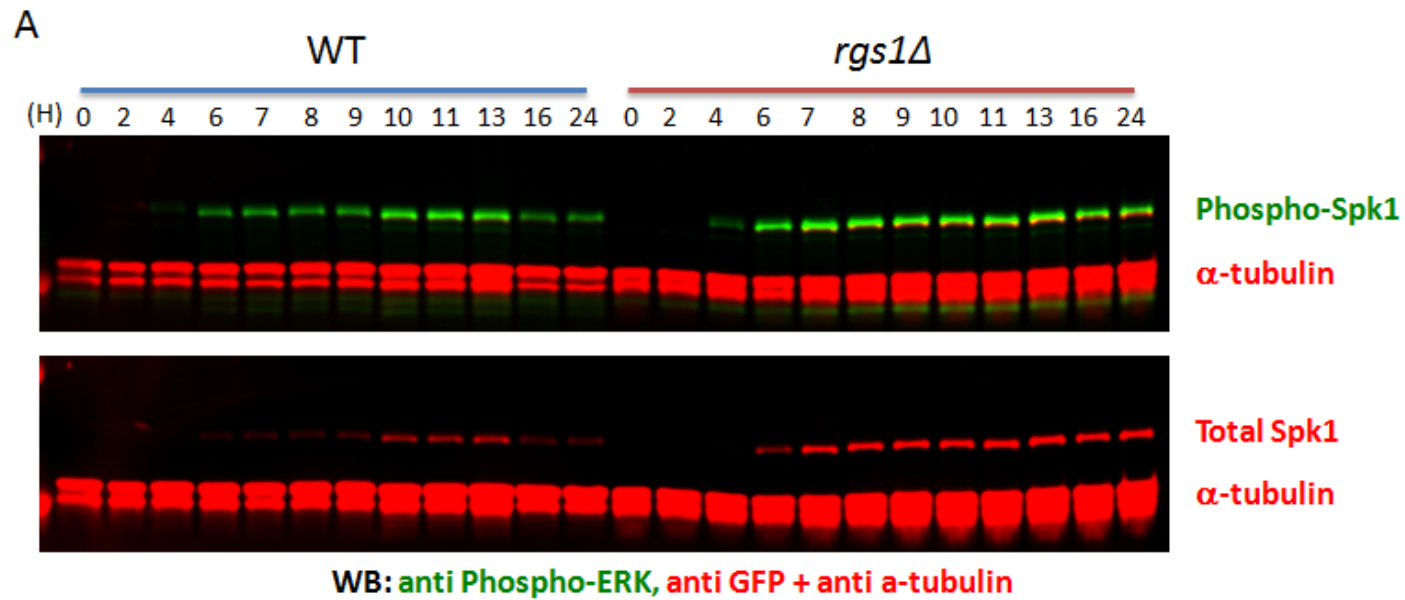


Figure 6.7 A direct comparison of the signalling dynamics in WT and *rgs1Δ* during a mating time-course.

A wildtype strain (KT3082) and *rgs1Δ* strain (KT4161) were subject to a meiotic time-course over 24 hours. (A) Western blot comparing a WT time-course with a *rgs1Δ* time-course. Membrane was blotted for phospho-Spk1 and α -tubulin (upper panel) as a loading control which is used to normalise the amount of phospho-Spk1 signal to the total amount of protein in the extracts. The lower panel shows the total amount of Spk1 protein over the time-course by blotting with anti-GFP. (B) and (C) Quantitation of one biological replicate time course comprising two technical replicate blots. Quantitation was carried out using the Image Studio ver2.1 software supplied with the Licor Odyssey CLx Scanner. (B) represents WT and *rgs1Δ* MAPK phosphorylation (C) Changes in the levels of MAPK over the mating time-course for WT and *rgs1Δ*, quantified using the GFP signal. (H) represents the number of hours post mating induction.

From the imaging in **Figure 6.8** it appears that the elongation phenotype of *rgs1Δ* cells is more subtle compared to *ras1.val17* as the elongation does not start until after 6-hours post mating induction and the nuclear Spk1-GFP signal is not as strong or as evident compared to the *ras1.val17* elongated cells at 24-hours. The more subtle elongation of *rgs1Δ* is also nicely evident in **Figure 6.2**.

In conclusion, regulation of the G-protein, Gpa1, by Rgs1 is essential for mating as *rgs1Δ* cells are sterile and show the elongated phenotype that we predict is associated with an overactive Ras1 protein.

Sxa2, Rgs1 and Gap1 proteins are essential for mating as single deletions of any of their genes results in sterility and morphological defects during starvation. The effects of *rgs1Δ* and *gap1Δ* are more subtle than *sxa2Δ* in terms of the extent of elongation which can be seen in **Figure 6.2**. We propose that this is due to the extent of the hyperactivation of the shmooing response via Ras1-Cdc42.

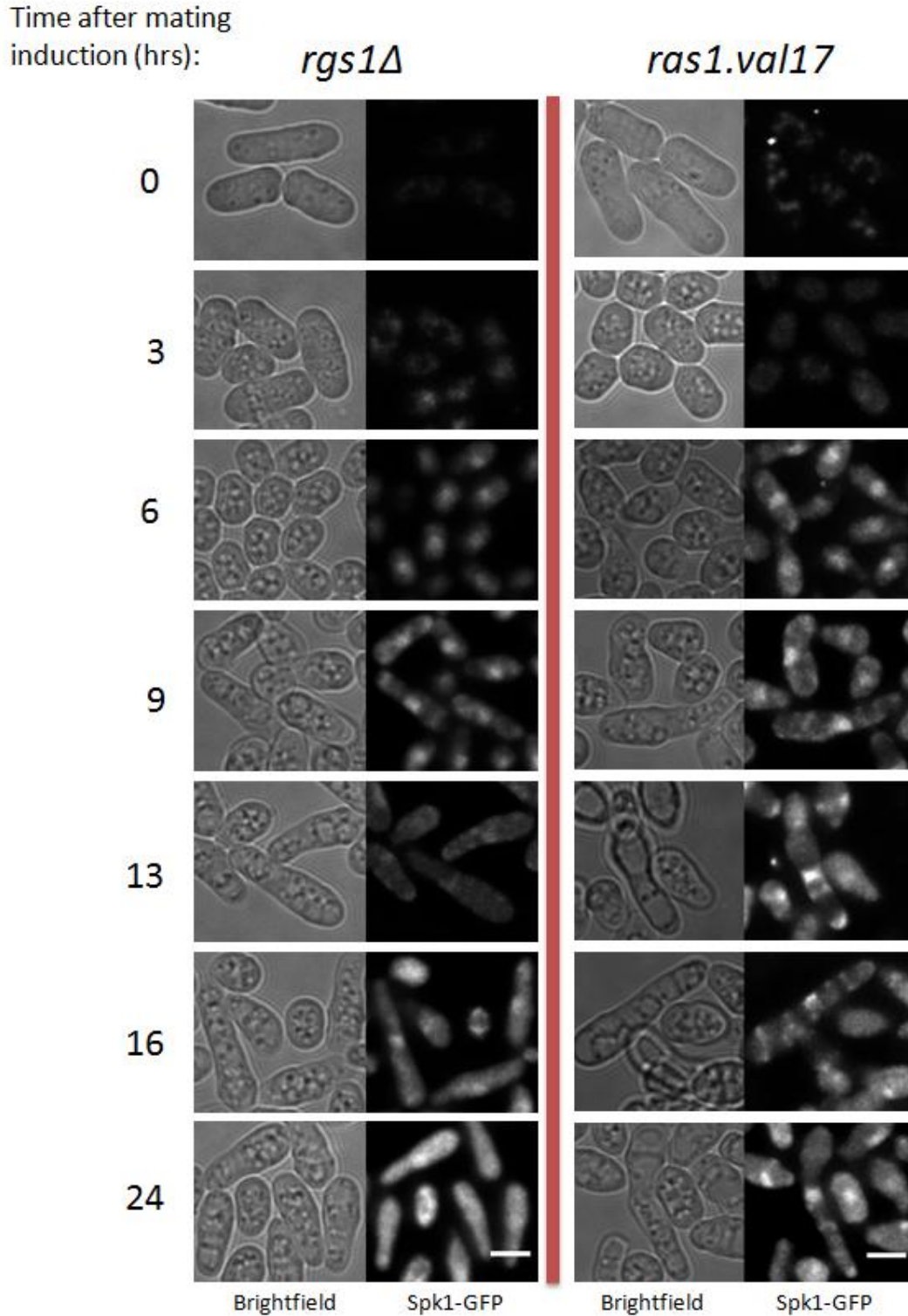


Figure 6.8 Imaging of Spk1-GFP over a 24 hour time-course in *rgs1Δ* cells compared to *ras1.val17* cells.

Live cell imaging of *rgs1Δ* (KT4161) and *ras1.val17* (KT3084) in the brightfield and GFP channels. Each time point comprises 15-25 serial images of 0.4 μm interval along the Z axis taken to span the full thickness of the cell. All of the Spk1-GFP images were deconvolved using the Huygens Essential Deconvolution. Deconvolved images were Z-projected, cropped and combined using ImageJ. Scale bar is 5 μm .

6.5 Discussion - Downregulation of the MFSP

To conclude, investigations into how deletion of each of the negative regulators Gap1, Sxa2 and Rgs1 effect MAPK signalling dynamics has revealed that all three play essential roles in regulating pheromone signal transduction. Sxa2 is the major contributor to down regulate MAPK activation as without Sxa2, control of the MAPK activation is lost with significantly higher levels of phospho-Spk1 compared to WT and the elongation of cells upon pheromone stimulation is much more pronounced when compared to *ras1.val17*, *gap1Δ* and *rgs1Δ* cells.

It is interesting to note that both *sxa2* and *rgs1* mRNA expression require pheromone signalling and not just nutrient starvation as with the majority of the other components of the pathway. This delay in the expression of both negative regulators compared to other components, which are solely dependent on nutrient starvation, is likely to be important for spatial-temporal control of the duration and intensity of MAPK signalling. With all three deletion mutants, the overall MAPK phosphorylation signal shows a decrease over time showing that additional forms of down regulation are still effective in their absence. In the case of *sxa2Δ*, this could either be due to Gap1 and Rgs1 but probably due to receptor internalisation. In addition, the un-identified down-regulators/down-regulatory mechanism at the level of the MEKK (Byr2) or MEK (Byr1) identified in Chapter 3 may also play a vital role.

It appears likely that these negative regulators working upstream of Ras1 in the MFSP also play a role in regulating the Ras1 associated with Cdc42-pathway activity during mating. We have already established that although MAPK activation feeds into the morphology pathway (Chapter 4) it is the activation status of Ras1 which is most indicative of morphological phenotype because the *ras1.val17 byr1.DD* double mutant

shows the elongated phenotype rather than the *byr1.DD* single mutant paired phenotype (Chapter 4 Section 4.3). It is reasonable to predict that in *gap1Δ*, *rgs1Δ* and *sxa2Δ* cells it is the hyperactive status of Ras1 signalling via the Cdc42-pathway which is causing the elongated phenotype.

During this work we have not directly investigated the activation status of Ras1. A current method to determine that amount of Ras-GTP in cell extracts involves pull-down experiments using glutathione S-transferase (GST)- fused to the "Ras Binding Domain" (RBD) of downstream effectors of Ras as this domain binds exclusively to Ras-GTP, this is followed by western blotting for the Ras protein. There are commercially available assay kits for Ras-GTP detection which specifically use the RBD of Raf1 (Cell Signalling Technology #8821) which potentially could be utilised for such experiments in *S.pombe*. The method by which we prepare whole cell protein extracts using TCA does not allow us to carry on pull-down experiments but this can be altered and the conditions optimised to decrease the amount of protein degradation we saw using the Cdc2 STOP-RIPA buffer method (See Materials and Methods). Another option for visualising the intensity and localisation of Ras-GTP is to use the RBD fused to GFP during live cell imaging (de Rooij & Bos, 1997; Bivona *et al.*, 2006; Augsten *et al.*, 2006). The RBD of Byr2 has already been mapped to residues 65-180 in the N-terminal regulatory region of the protein (Tu *et al.*, 1997) but experiments with Byr2RBD-GFP have not been reported in the literature and one possible concern is that expression of Byr2RBD-GFP may dominantly interfere with the downstream MFSP. We predict that this type of approach will show Ras1-GTP localised at the cell cortex at the site of pheromone stimulation where it has an important role in the activation of Byr2. It could also show that Ras1-GTP is concentrated at the site of shmooing. There is surprisingly little evidence that Ras1 is physically acting as part of the Scd1-Scd2-

Cdc42-Pak1 multiprotein complex. A yeast two hybrid experiment was used to show that Ras1 and Scd1 interact in the presence of Scd2 (Chang *et al.*, 1994) but colocalisation studies of endogenously expressed Ras1 and Scd1 have not been reported.

Compartmentalised signalling of Ras1, along with the two non-functionally interchangeable GEFs for Ras1 in *S.pombe* has been proposed as the mechanism by which Ras1 can separately control the mating process and morphology (Papadaki *et al.*, 2002; Onken *et al.*, 2006) although we believe that actually, Ste6 is playing a vital role in activation of the Ras1-Scd1 pathway during mating (Chapter 5 Section 5.4). Live cell imaging of Ras1-GTP, employing Byr2RDB-GFP, along with colocalisation experiments with the Scd1, Scd2 and Cdc42 proteins, may provide evidence that Ras1 is present at the site of shmoo formation. The work by Bendezu and Martin 2013, showed that Scd1, Scd2 and Cdc42-GTP (via CRIB-GFP) colocalise and are present at the site of shmoo formation (Bendezu & Martin, 2013). Therefore to further investigate our hypothesis that the elongated mating phenotype is due to hyperactivated Cdc42, we could investigate whether the intensity of any of these components is increased at the shmoo site in *gap1Δ*, *rgs1Δ*, *sxa2Δ* and *ras1.val17*.

It is interesting that much less is known about negative regulators downstream of Ras1 in the MFSP but we predict from the *byr1.DD* mutant, if MAPK phosphorylation is constitutive then fusion between the mating pairs is unsuccessful (Chapter 3) and that the function of predicted MAPK phosphatases is ineffective in the presence of constitutively activated Byr1 therefore down-regulation of Byr1 is important for concerted MAPK signalling. Down-regulation of MAPK phosphorylation is still effective in the presence of oncogenic Ras1 (Chapter 3) hence the prediction of an unidentified downregulatory mechanism at the level of MEKK and/or MEK, potentially

these could be phosphatases but other mechanism of down-regulation could also be occurring. As seen in Chapter 5, the G-protein is essential for any signal transduced to the MAPK via Ras1 and this signal is not transduced even in the presence of oncogenic Ras1 if the G-protein is missing therefore once the G-protein signal is terminated probably by a combination of the actions of Rgs1, Sxa2 and receptor internalisation, we can assume that Byr2 will no longer be further activated by the proposed Gpa1-Ste4 complex and therefore Byr2 can no longer activate the MAPK pathway even if Ras1 is still in its activated GTP-bound form.

The work by Ozoe *et al.*, 2002 showed that the 14-3-3 proteins, Rad24 and Rad25, play a role as negative regulators of Byr2. Overexpression of either protein lead to a decrease in mating and sporulation efficiency and both proteins were shown to interact with Byr2 in a coimmunoprecipitation experiment. Byr2 was shown to translocate to the plasma membrane quicker when either gene was disrupted linking the function of these 14-3-3 proteins to the negative regulation of Byr2 via sequestering it in the cytoplasm (Ozoe *et al.*, 2002). A potential down-regulation of Byr2 signalling to Byr1 may be achieved by the binding of Rad24 and Rad25 to Byr2 causing inactivation and loss of correct localisation to the cell cortex. A role for 14-3-3 proteins in Raf-mediated signalling has been proposed in mammalian cells (Freed *et al.*, 1994). It was observed that 14-3-3 β and 14-3-3 ζ proteins interact with inactive and activated Raf at a distinct site from Ras and that these 14-3-3 proteins accompany Raf to the membrane in a Ras dependent manner as viewed by immunofluoresence. In contrast to the findings in *S.pombe* where these proteins have a negative effect on MEKK signalling, it was observed that the presence of these 14-3-3 proteins enhanced Raf activity although association with Raf alone was not enough to stimulate activation (Freed *et al.*, 1994).

These findings suggest that the role of 14-3-3 proteins in MEKK regulation are not conserved between mammalian cells and *S.pombe*.

The mechanism for termination of the activity of Byr1 remains to be uncovered but is shown to be of significant importance for successful mating because the constitutively active phospho-mimetic Byr1.DD mutant is defective in cell fusion as shown in Chapter 3 and the phospho-MAPK signal is constitutive in the presence of Byr1.DD therefore the actions of predicted Spk1 phosphatases are not effective if Byr1 is still active.

Little is known about how the activity of Mammalian MEK is terminated. The protein phosphatase 2A (PP2A) is linked with MEK dephosphorylation in PC12 cells (Alessi *et al.*, 1995) and inactivation of PP2A via overexpression of SV40 small t-antigen promotes MEK and ERK activity in CV-1 cells (Sontag *et al.*, 1993) and a number of kinases have been shown to phosphorylate MEK1 including Cdc2, ERK1/2 and Pak1 (Rossomando *et al.*, 1994), (Gotoh *et al.*, 1994; Brunet *et al.*, 1994; Saito *et al.*, 1994; Gardner *et al.*, 1994; Mansour *et al.*, 1994; Frost *et al.*, 1997) however, the effects of these phosphorylations is yet to be determined. The works of Gopalbhani *et al.*, 2003 show that phosphorylation of the conserved serine residue at position 212 results in suppressed activity of both WT and phosphomimetic MEK1. Alanine substitution of the serine resulted in a higher than basal activity whereas substitution with an aspartic acid lead to suppressed activity and they also showed this is conserved with the *S.cerevisiae* MEKs, Pbs2 and Ste7 (Gopalbhai *et al.*, 2003). It would be interesting to mutate this conserved Serine in *S.pombe* Byr1 although they showed that phosphorylation of this residue was effective in suppressing the activity of phosphomimetic MEK1 but we see constitutive activation with phosphomimetic Byr1. However we can predict that if Spk1 is responsible for this inhibition and was phosphorylating Byr1 in a negative feedback manner then perhaps Spk1 cannot bind effectively to Byr1.DD due to the

phosphomimetic mutations. The *S.pombe* genome contains two genes which show homology to the catalytic subunits of mammalian PP2A (*ppa1* and *ppa2*). In a similar manner to mammalian PP2A, *S.pombe* PP2A has been shown to be heterotrimeric consisting of A, B and C subunits (scaffold, regulatory and catalytic subunits) (Goyal & Simanis, 2012) and is strongly linked with cell cycle control. There has been no reported links between the function of *S.pombe* PP2A and meiosis. It is possible that Byr1 regulation does not directly involve a phosphatase and is dependent on inhibitory phosphorylation and changes in cellular localisation for negative regulation and/or proteosomal degradation. Identification of potential MAPK phosphorylation sites plus mutational analysis of the homologous S212 residue may aid in the future investigations into Byr1 regulation. An overall discussion of the *byr1.DD* phenotype is provided in Chapter 7 Section 7.4.

CHAPTER 7 BIOCHEMICAL MANIPULATION OF PHEROMONE SIGNAL TRANSDUCTION

7.1 Introduction

The aims of this Chapter were investigate whether it is possible to rescue Ras1-MAPK mutants using biochemical techniques to not only prevent the mutant mating phenotypes but to promote the WT meiosis. The two mutants of specific interest were *ras1.val17* and *byr1.DD* which we've shown to have significantly different MAPK signalling dynamics and phenotypes upon induction of mating (Chapter 3), these are summarised in **Figure 7.1**

Manipulation of protein function can be achieved in a number of different ways both genetically and biochemically. The observation that *byr1.DD* exhibits constitutive MAPK phosphorylation and is defective at the point of cell fusion led us to hypothesis that down-regulation of the MAPK activity is essential for cells to progress past the point of cell fusion therefore we took the approach of modulating the activity of the MAPK directly. This hypothesis also assumes that the level of the MAPK activity, or the MAPK activation profile, affects the morphological phenotype. The hypothesis was examined by employing the ATP-analogue sensitive kinase approach (Section 7.2).

On the other hand, we've also shown that Ras1 activates two independent pathways upon mating induction, the Ras1-Byr2- MAPK transcriptional branch and the Ras1-Cdc42 morphology branch and that altering the MAPK output in the presence of *ras1.val17* does not change the overall mating morphological phenotype but does effect the timing of a morphological change (Chapter 4). Therefore it was predicted that exclusive manipulation of the MAPK activity was unlikely to bring successful

completion of mating process in the *ras1.val17* mutant and consequently we focused on direct manipulation of Ras1 activity (Section 7.5).

.

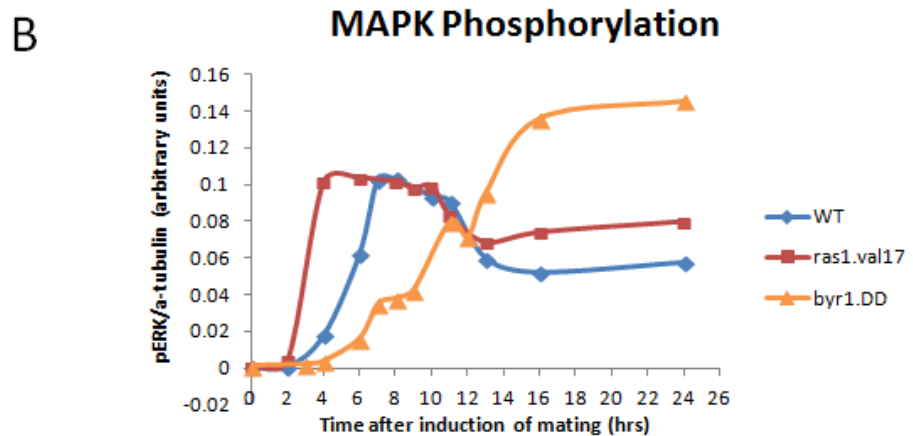
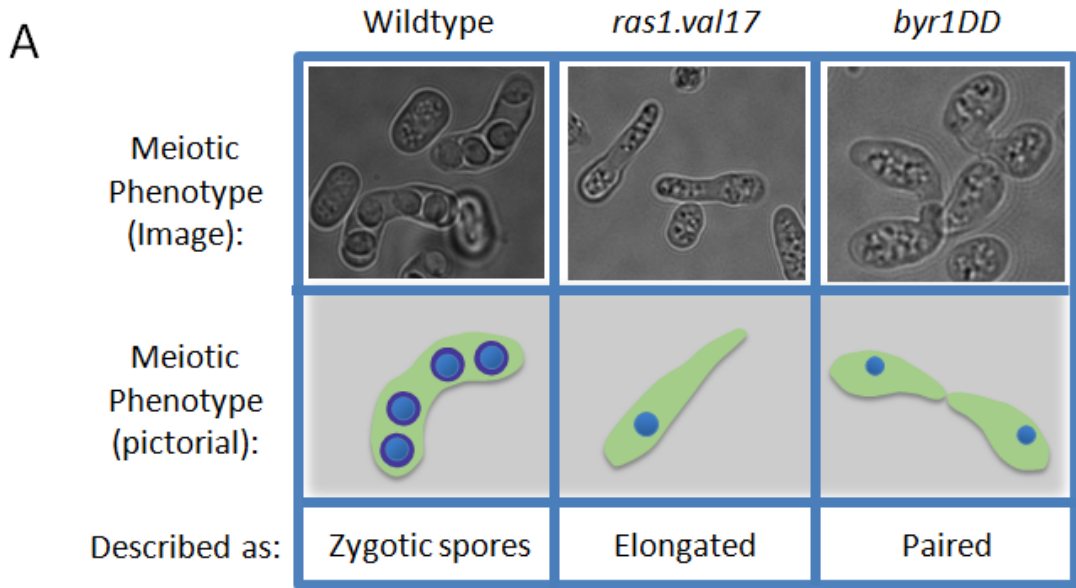


Figure 7.1 Summary of the mating phenotypes and MAPK phosphorylation profiles of WT, *ras1.val17* and *byr1.DD*.

(A) A summary of the phenotypes of WT, *ras1.val17* and *byr1.DD* upon nutrient starvation. WT cells progress through mating and two meiotic divisions to make four haploid spores. The *ras1.val17* mutant cells make elongated conjugation tubes and appear unable to attach themselves to a cell of the opposite mating type. The *byr1.DD* cells form prezygotic pairs but the cells are unable to fuse.

(B) The Phospho-MAPK levels during the 24-hours after cells are induced for mating as observed in Chapter 3. Phospho-MAPK levels are transient over the 24-hours in WT (blue) whereas the signal is much slower to increase in *byr1.DD* (orange) but the signal is constitutive. The phospho-MAPK signal in *ras1.val17* (red) appears much earlier than WT but is then down-regulated to a level similar to WT.

7.2 Creation of an ATP-analogue sensitive MAPK

The approach we wanted to take in an attempt to rescue *byr1.DD* was to manipulate the MAPK activity to prevent the constitutive output of the Spk1 MAPK, preferably by the addition of a specific MAPK inhibitor at a specific time-point. The major problem with a kinase inhibition approach is that there are a vast number of kinases in the genome, all containing a highly conserved active site. Inhibitors designed to target the active site of a specific kinases encounter the problem of selectivity and can therefore affect more than one protein kinase and have an undesired outcome. The kinome of *Schizosaccharomyces pombe* contains 106 serine/threonine kinases (Yan *et al.*, 2006) therefore to specifically inhibit our MAPK of choice, Spk1, we chose to try the ATP-analogue sensitive kinase approach illustrated in **Figure 7.2**.

This is a chemical-genetic strategy which has recently been developed to conditionally inactivate a specific protein kinase of interest (Gregan *et al.*, 2007; Zhang *et al.*, 2005). Mutating a single residue in the ATP-binding pocket, named the gatekeeper residue (GKR), confers sensitivity to specifically designed small-molecule inhibitors (Bishop *et al.*, 2000) where the inhibitor can only bind to the mutant kinase and not to any other wild-type kinase, allowing specific inactivation of the modified kinase. An ATP-analogue sensitive kinase approach provide several advantages over genetic approaches; different degrees of inhibition can be achieved depending on the concentration of inhibitor and upon addition of the inhibitor, the cells have very little time to adapt to the loss of the protein kinase activity (Gregan *et al.*, 2007).

Despite many advantages, this chemical-genetic strategy of protein kinase sensitisation contains a number of limitations. The catalytic activity of the protein kinase may be diminished by mutating the gate-keeper residue and around 30% of kinases tested to

date are intolerant (Zhang *et al.*, 2005). In such cases, a second-site suppressor mutation can be introduced to rescue the kinase activity, the method of which is outlined in Zhang *et al.*, 2005 (**Figure 7.3**). These second sites which can rescue the kinase activity disrupted by mutation of the GKR are termed "suppressors of glycine gatekeeper" or *sogg*. Hot spots for these second site mutations were originally identified using random mutagenesis followed by genetic selection using the intolerant kinase, APH(3')-IIIa, which phosphorylates antibiotics therefore if the kinase function was restored due to a *sogg* then the cells would be resistant to the specific antibiotic. Several mutations were identified that restored APH(3')-IIIa function. Structural based sequence alignments were used to identify the area of focus for *sogg* mutations as the anti-parallel β sheet in the kinase N-terminal subdomain. This was followed by sequence alignments with tolerant kinases leading to identification of *sogg* hot spots (Zhang *et al.*, 2005).

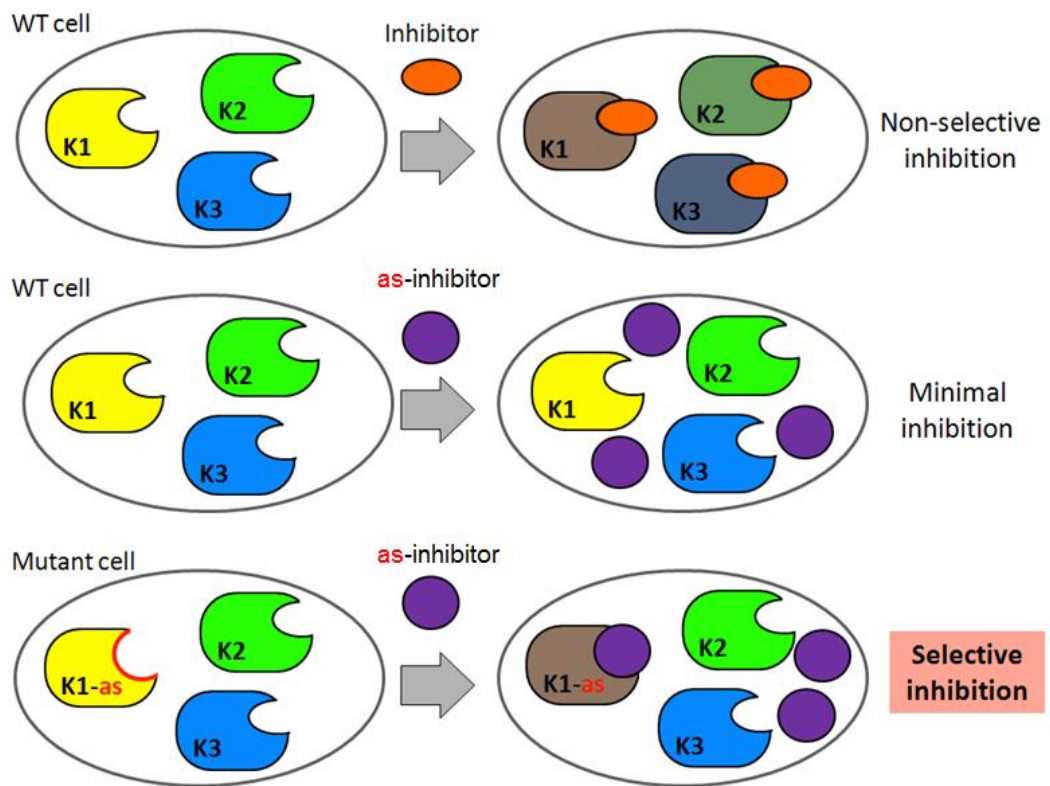


Figure 7.2 The concept of ATP-analogue sensitive kinases.

In the past, kinase inhibitors that target the active site have been fairly non-selective (top line). The addition of an ATP-analogue sensitive inhibitor (*as*-inhibitor) to wildtype cells will provide minimal inhibition as this inhibitor does not efficiently bind into the active sites of any wildtype kinases (middle line). The concept of an ATP-analogue sensitive kinase is a chemical-genetic strategy to conditionally inactivate protein kinases whereby mutating a single residue in the ATP-binding pocket known as the “gatekeeper residue” confers sensitivity to specific small-molecule inhibitors. These inhibitors can only bind to the mutant kinase and not to any other wild-type kinase in the cell, allowing specific inactivation of the modified kinase (bottom line).

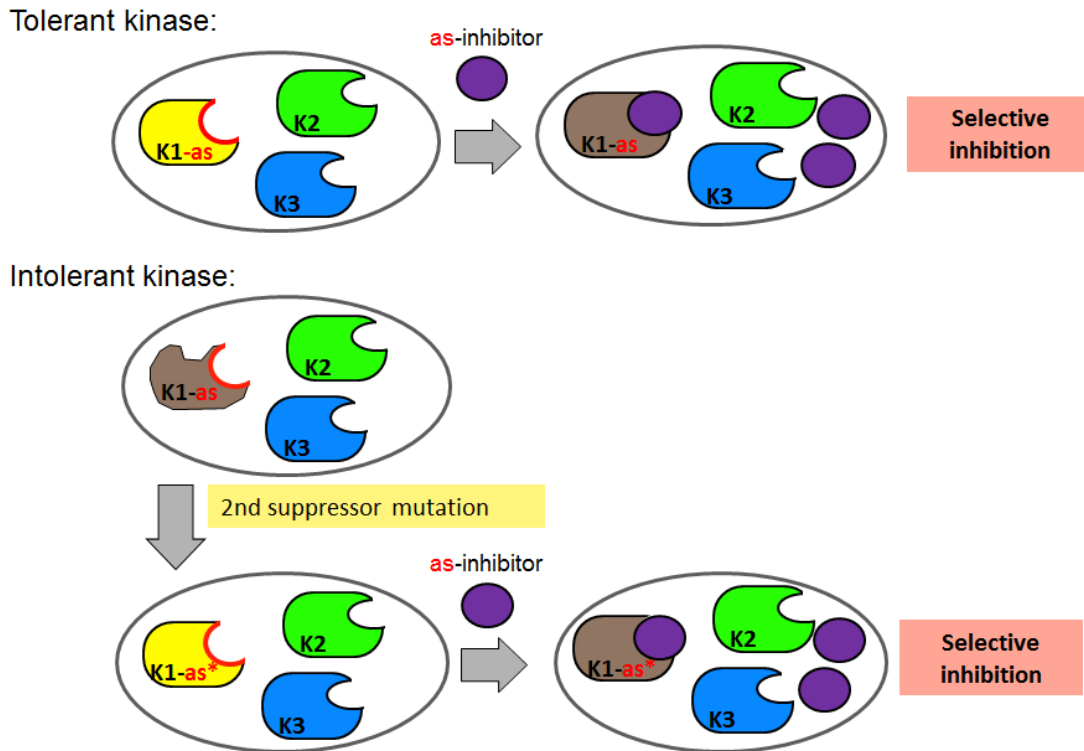


Figure 7.3 Tolerant and intolerant kinases

Many kinases can tolerate gatekeeper mutations without loss of affinity for ATP or catalytic activity and therefore upon the addition of an *as*-kinase inhibitor there will be selective inhibition of the kinase of interest (top line). Experimentally, it has been found that around 30% of kinases are intolerant to mutation of the gatekeeper residue (Zhang *et al.*, 2005) (middle line). An approach has been developed to rescue the kinase activity of intolerant kinases by introducing a second site mutation and still allow selective inhibition by *as*-inhibitors (bottom line). The process by which to identify these potential second sites is outlined in Zhang *et al.* 2005.

The GKR is located within the ATP-binding pocket of a kinase and is the residue which comes into close contact with N6 group of ATP, within the active site (**Figure 7.4A**). Creation of such a kinase follows the method summarised in **Figure 7.4B** and relies on the accurate identification of the GKR. This residue is conserved as a bulky hydrophobic amino acid in the protein kinase super-family. Mutation of the gate-keeper to a small residue (alanine or glycine) creates a novel pocket that can be uniquely targeted by ATP analogues that are chemically modified at the N6 position, these include inhibitors which have been designed with properly enlarged substituents and a number of *as*-inhibitors are commercially available (**Figure 7.4C**). The mutation thus confers inhibitor sensitivity but does not interfere with kinase function in the absence of inhibitor. The gate-keeper residue can be easily identified from primary sequence alignments in many protein kinases from various kinase subfamilies which has already been done for a huge number of kinases, the results of which can be found in the Kinase Sequence Database (Buzko & Shokat, 2002).

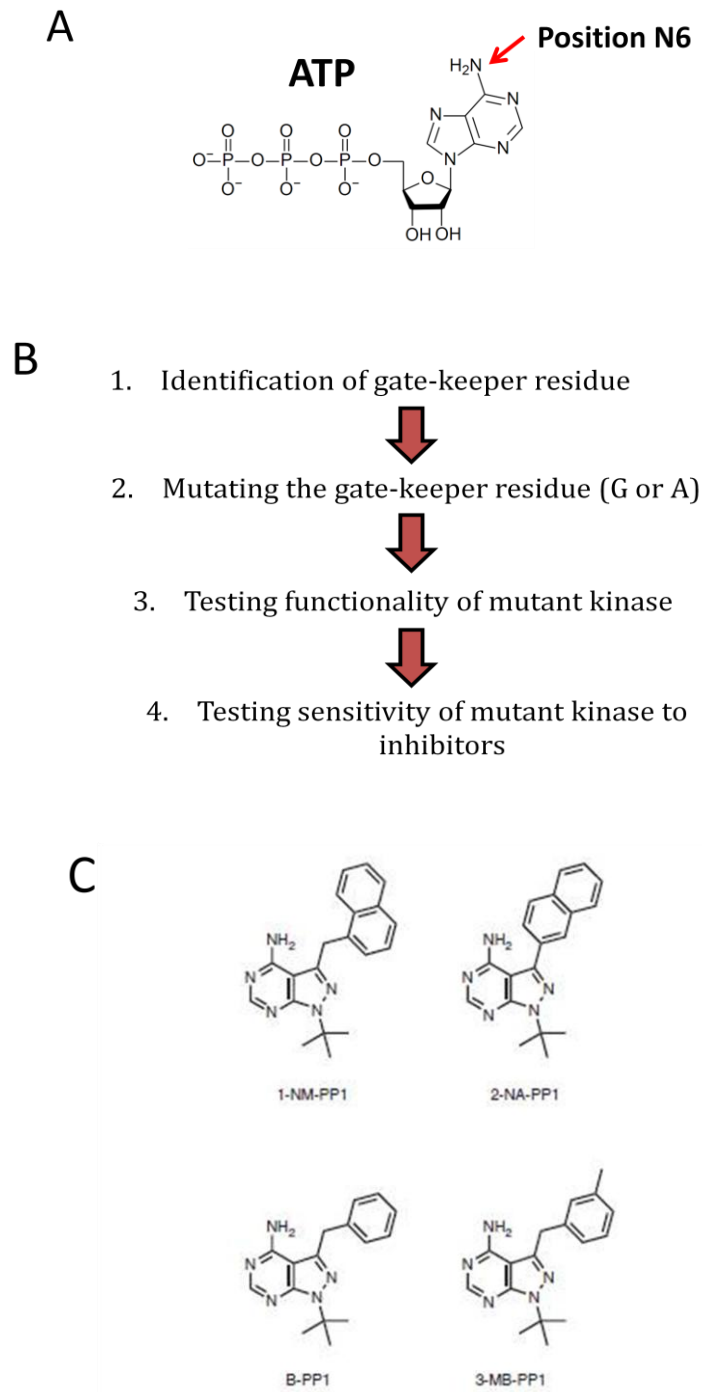


Figure 7.4 Generating an ATP-analogue sensitive kinase

(A) ATP with the red arrow identifying the N6 position (B) Following identification of the gate-keeper residue (GKR) using the Kinase Sequence Database, this residue is mutated to either a glycine or an alanine. Functionality of the kinase should then be tested as around a third of all kinases lose functionality after introducing this mutation. (C) A number of ATP-analogue sensitive kinase inhibitors are available commercially (Reproduced from (Gregan *et al.*, 2007)).

7.2.1 Creation of ATP-analogue sensitive Spk1

7.2.1.1 Mutation of the Gatekeeper residue

The initial mutation of the gatekeeper residue (GKR) of Spk1 was carried out by a previous Masters student in the lab, Shubhchintan Randhawa, in 2009 as described below.

Following the identification of the gatekeeper residue for Spk1, glutamate-119, using the Kinase Sequence Database (<http://sequoia.ucsf.edu/ksd/>) (Buzko & Shokat, 2002), this residue was mutated to an alanine or a glycine (Q119A/Q119G). These mutations were introduced into the *spk1* gene using site-directed mutagenesis of *S.pombe* genomic DNA and the two-step PCR method. An Spk1 deleted strain was transformed, using the TRAF0 method (Gietz, 2006), with the DNA fragment containing the mutated sequence. Positive transformation colonies were selected for kanamycin resistance and the functionality of the mutant kinase was tested. In this case the positively transformed cells needed to be able to mate at the same frequency as the strain with wild type Spk1, however both the Q119A and Q119G mutations caused Spk1 to lose its functionality and cells showed an exceptionally low mating and sporulation rate, therefore Spk1 is an “intolerant kinase” and we would have to undertake the second site suppressor strategy to create a functional Spk1-*as* kinase.

The paper describing the second site suppressor strategy (Zhang *et al.*, 2005) lists Fus3 as a tolerant kinase (**Figure 7.5A**). This is significant because Fus3 is the Spk1 homologue in *S.cerevisiae* which is involved in the mating pathway induced by pheromone and nitrogen/carbon limitation. By aligning the amino acid sequence of Spk1 and Fus3 and by identifying the corresponding residues in the β -sheets β 2, β 3 and β 5, which are illustrated in the paper are prime locations for the suppressor mutations,

two residues were chosen to be mutated individually, V67I in β 3 and V118I in β 5 (**Figure 7.5B**) along with the Q119A gatekeeper residue mutation. We chose to use the Q119A GKR mutation instead of Q119G as Spk1 containing Q119A appeared slightly more functional than Q119G in terms of mating frequency.

7.2.1.2 Mutation of second site suppressor residues

PCR fragments containing the selected two mutations were created using *S.pombe* genomic DNA using two different approaches. As can be seen in **Figure 7.5B** the V67I mutation in the $\beta 3$ region is relatively far away from the gatekeeper residue (Q119) highlighted in blue, therefore V67I mutation primers were designed and the PCR product for transformation was created using genomic DNA isolated from a strain already containing the Q119A mutation and the Spk1 gene marked with the kanamycin resistance gene (KT2875) as illustrated in **Figure 7.6**. PCR products from the three reactions were run on a 1% agarose gel to confirm the presence of successfully generation of the *Spk1-V67I-Q119A-Kan^R* fragment running at the correct molecular weight (data not shown).

The V118I mutation and the gatekeeper residue Q119 are directly adjacent to each other therefore both the mutations were introduced into genomic DNA from a yeast strain containing the Spk1 ORF marked with the kanamycin resistance cassette (KT2863, KT2864 and KT2865) using one set of primers (Spk1-SHO-IA-F and Spk1-SHO-IA-R) as outlined in **Figure 7.7A**. The three PCR products from the PCR reactions to create *Spk1-V118I-Q119A::Kan^R* were ran on a 1% agarose gel to confirm the presence of a fragment confirming that the two products from reactions 1 and 2 have been "sewn" together successfully (**Figure 7.7B**).

For the generation of both mutant strains an Spk1 deleted strain (KT2852) was transformed with either of the generated PCR products using the TRAF0 method (Gietz, 2006). DNA from positive colonies was extracted and checked for Spk1 genome integration at the Spk1 locus using the Spk1-F1 and Spk1-CHK-R primers shown in **Figure 7.6** and **Figure 7.7A**. This PCR product was purified and prepared for sequencing using the Big Dye Terminators V3.1 method (see Materials and Methods

for sequencing protocol) to confirm the presence of the mutations. Sequence alignments were carried out using the ClustalW2 sequence alignment program on the EBI database website and are shown in **Figure 7.8** to confirm the presence of the specifically desired mutations.

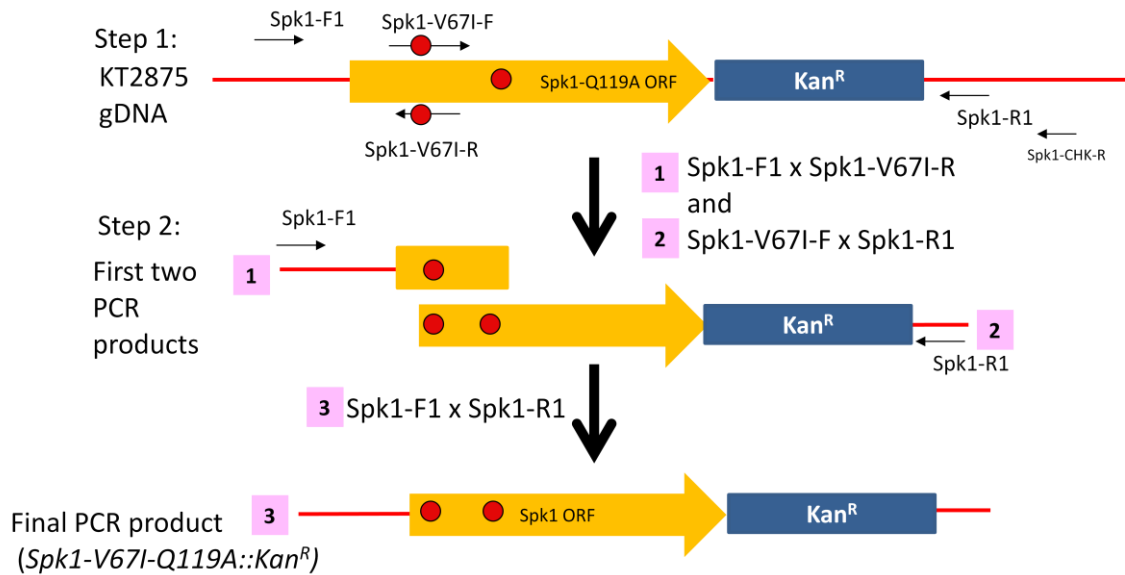


Figure 7.6 Spk1-V67I-Q119A Generation

The V67I and Q119A mutations were introduced into *S.pombe* genomic DNA separately due to the relatively large distance between them. Genomic DNA from a strain already containing *Spk1-Q119A::Kan^R* (KT2875) was isolated the V67I mutation was introduced using the Spk1-V67I-F and Spk1-V67I-R primers using the two-step PCR approach to create a PCR fragment containing both the V67I and Q119A mutations.

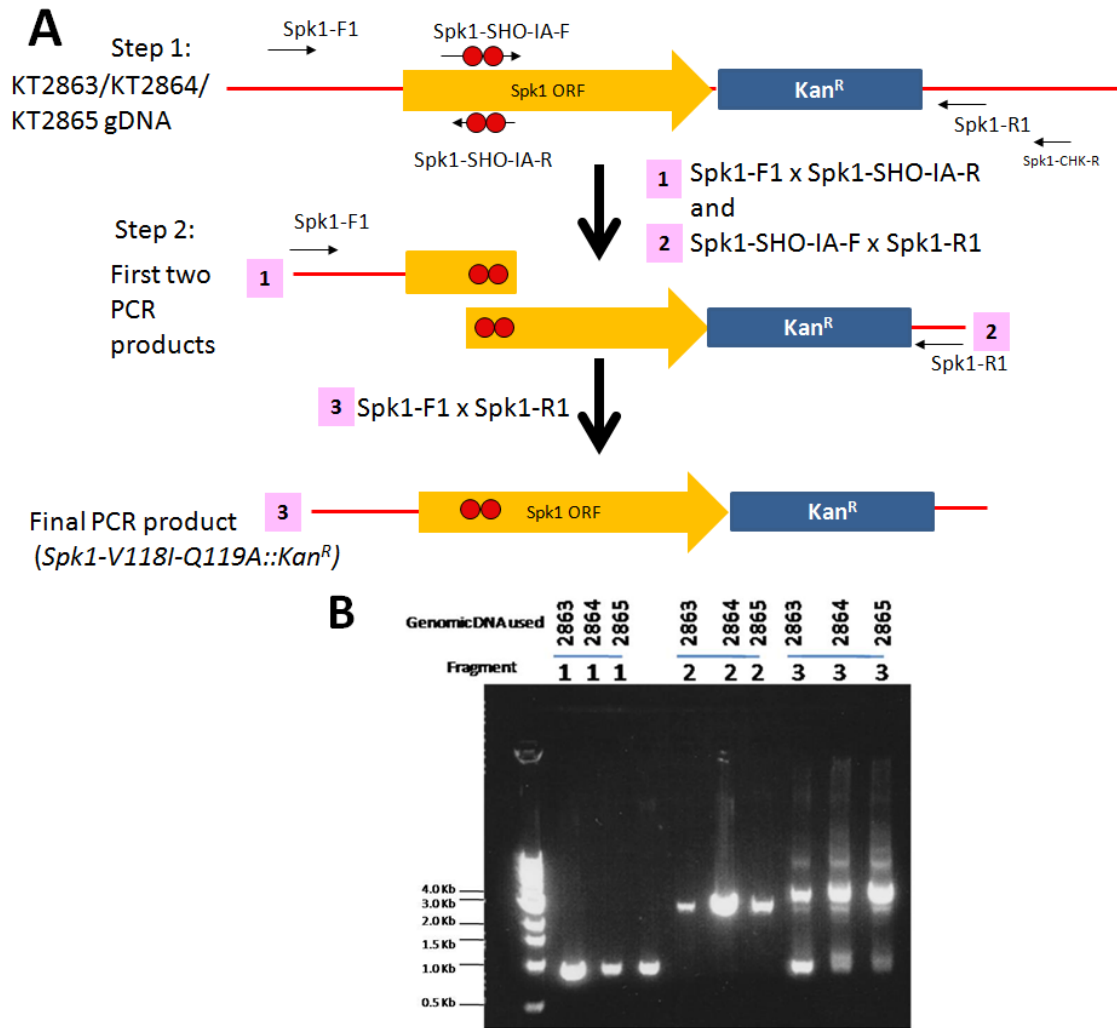


Figure 7.7 Spk1-Sho-IA generation

(A) Site-directed mutagenesis strategy specifically for Spk1-SHO-IA generation. gDNA for the PCR reactions was isolated from a strain already containing the Spk1ORF marked with the Kanamycin resistance cassette (KT2863, KT2864 and KT2865).

(B) An example of the three PCR products generated by the 2-step PCR method outlined in (A). PCR products were ran on a 1% agarose gel. Fragment 1 was created using the Spk1-F1 and Spk1-SHO-IA-R primers from three different genomic DNA's (KT2863, KT2864 and KT2865) is around 1.0Kbps, fragment 2 created using the spk1-SHO-IA-F and Spk1-R1 primers is around 3.0Kbps. The last three lanes are the PCR results made from fragment 1 plus fragment 2 and the PCR primers Spk1-F1 and Spk1-R1. This third fragment should be the sum of the molecular weight of fragment 1 plus fragment 2 which it is confirmed to be running at around 4.0Kbps.

Two independent clones that contain both V67I-Q119A mutations (KT2945 and KT2946 - clones 1 and 2 respectively)

```

spk1-WT          GCTTCACAAACCCAGCGGCCTAAAGGTGGCTGTTAAAAAATACATCCTTTCAATCATCC
Spk1-V67I-Q119A-1 GCTTCACAAACCCAGCGGCCTAAAGGTGGCTATTAAAAAATACATCCTTTCAATCATCC
Spk1-V67I-Q119A-2 GCTTCACAAACCCAGCGGCCTAAAGGTGGCTATTAAAAAATACATCCTTTCAATCATCC

```

V67I

```

spk1-WT          TATTGTACAAAGAGCTTATGGAAACGGATTTGTACCGTGTATACGTTTCGAGCCCTTAAG
Spk1-V67I-Q119A-1 TATTGTAGCAGAGCTTATGGAAACGGATTTGTACCGTGTATACGTTTCGAGCCCTTAAG
Spk1-V67I-Q119A-2 TATTGTAGCAGAGCTTATGGAAACGGATTTGTACCGTGTATACGTTTCGAGCCCTTAAG

```

Q119A

Three independent clones that contain both V118I-Q119A mutations (KT2948, KT2949 and KT2950 - clones 1,2 and 3 respectively)

```

spk1-WT          GAGCTACCAGGAATTGGAAGATGTTTATATTGTACAAAGAGCTTATGGAAACGGATTTGT
Spk1-V118I-Q119A-1 GAGCTACCAGGAATTGGAAGATGTTTATATTATAGCAGAGCTTATGGAAACGGATTTGT
Spk1-V118I-Q119A-2 GAGCTACCAGGAATTGGAAGATGTTTATATTATAGCAGAGCTTATGGAAACGGATTTGT
Spk1-V118I-Q119A-3 GAGCTACCAGGAATTGGAAGATGTTTATATTATAGCAGAGCTTATGGAAACGGATTTGT

```

V118I and Q119A

Figure 7.8 Sequence alignments confirming the GKR mutation and the second site mutations.

Genomic DNA was extracted from positive kanamycin resistant colonies. Correct genomic DNA integration at the Spk1 locus was confirmed using the Spk1-F1 and Spk1-CHK-R primers. This PCR product was purified and prepared for sequencing using the Big Dye Terminators V3.1 method. Sequences were aligned using the ClustalW2 programme on the EBI database website:

<http://www.ebi.ac.uk/Tools/clustalw2/index.html>. The Q119A mutation involves a change of codon 119 from CAA to GCA. The V67I involves a change of GTT to ATT and V118I involves a change of GTA to ATA.

7.2.1.3 Testing the Functionality of the Mutant Kinase

100µl of the yeast strains containing wild-type Spk1 (KT301), the V67I-Q119A mutations (KT2945) or V118I-Q119A mutations (KT2948) were incubated with either DMSO or the *as*-kinase inhibitor 1-NM-PP1 (PP1 Analog II 1NM-PP1 Cat. No. 529581, Calbiochem) at a final concentration of 1 µM in 20 ml tubes at a cell density of 1×10^7 cells/ml for 24 hours. Cells were then visualised under the microscope to determine firstly if either V67I or V118I had rescued the function of Spk1 and secondly if either mutant was sensitive to 1-NM-PP1, results are shown in **Figure 7.9**

The Spk1-V67I-Q119A strain was able to mate at a relatively high efficiency which appears comparable to WT (not quantified) confirming that the activity of Spk1 has been somewhat restored. The Spk1-V118I-Q119A strain could mate at very low efficiency therefore the kinase activity of Spk1 is still compromised in this mutant. In the presence of 1-NM-PP1, mating in the WT strain is unaffected but in both the ATP-analogue sensitive strains mating was completely abolished, showing selective inhibition of the mutated Spk1. For future experiments Spk1-V67I-Q119A was used and is referred to as Spk1.*as*.

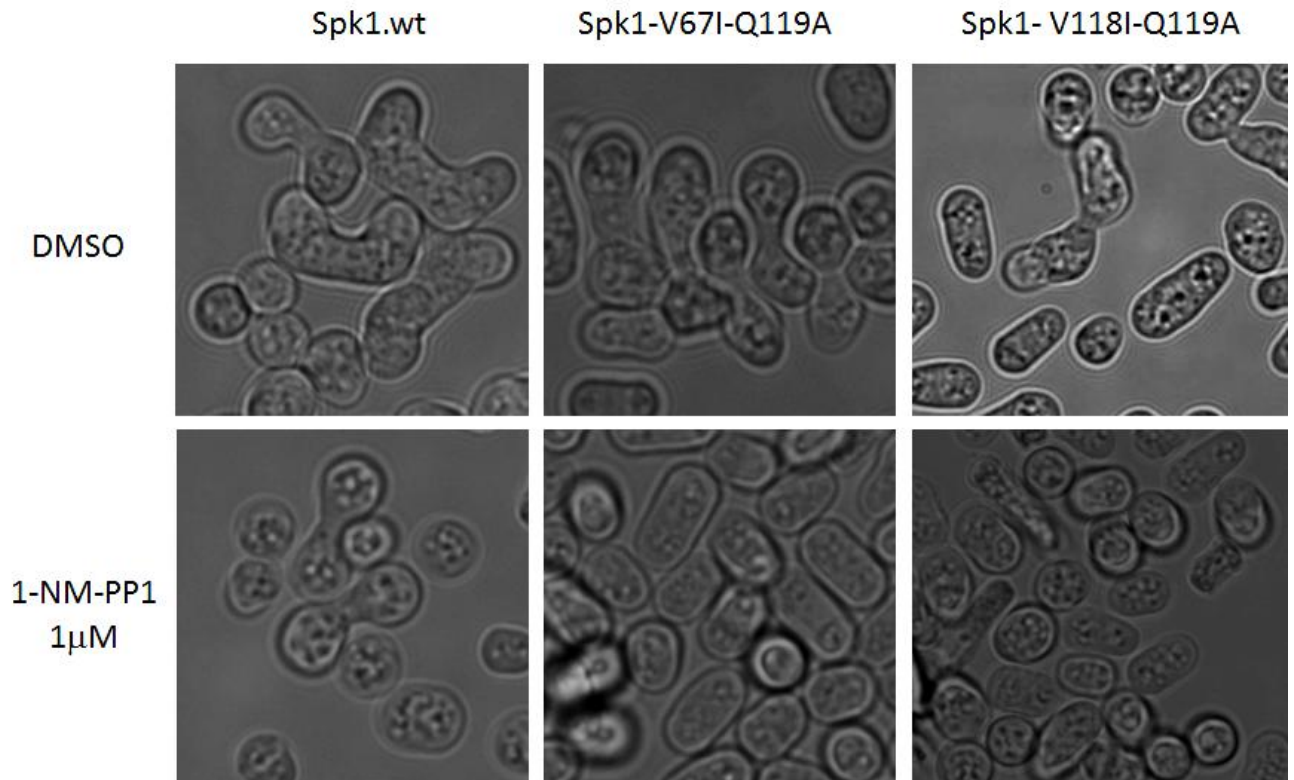


Figure 7.9 Rescuing *Spk1-as* activity and testing 1-NM-PP1 selectivity.

Two mutations were introduced independently (V67I and Q118I) along with the gatekeeper residue mutation (Q119A). Cells were incubated with either DMSO or 1-NM-PP1 at a final concentration of 1 μM in 20 ml tubes at a cell density of 1×10^7 cells/ml for 24 hours and then visualised using a light microscope.

7.2.2 Rescue of *byr1.DD*

Experiments with the *Spk1.as* to rescue *byr1.DD* have so far been unsuccessful in restoring further progress in meiosis. All original experiments with *spk1.as* were carried out in liquid cultures so that the concentration of 1-NM-PP1 could be calculated accurately. One of the major issues we came across when using liquid cultures was that the appearance of the prezygotic phenotype was exceptionally low in *byr1.DD spk1.as* strains compared with *byr1.DD spk1.wt* strains. We conclude that the activity of *Spk1.as* is still compromised. Since the development of the plate assay, we would expect a much higher percentage of *byr1.DD spk1.as* cells to show the prezygotic phenotype using this method and preliminary experiments have indicated that this is the case. An advantage of the plate assay is that membranes can be transferred from inhibitor free medium to media containing various concentrations of inhibitor at various time points. These experiments are yet to be revisited.

Our original prediction was that the activated MAPK merely needs to be terminated at the correct time for cells to fuse and then go on to complete meiosis. It could be a case of the timings and assay conditions are not fully optimised. We already know that the *Spk1-GFP* localisation in *byr1.DD* cells is predominantly nuclear once *Spk1-GFP* is expressed during a 24-hour mating time-course (Chapter 3 **Figure 3.11**) therefore it is important that the signal is terminated effectively in the nucleus and it is presently unknown if analogue sensitive kinase inhibitors are able to penetrate the nucleus in *S.pombe*. An alternative to this analogue sensitive kinase approach could be to screen for a temperature sensitive mutant of *Spk1* using error prone PCR to introduce random mutations into the *Spk1* allele then screen for a mutant that is able to sporulate at one temperature (e.g. 25°C) but not at another (e.g. 34°C). This would enable us to selectively switch off *Spk1* at a wide range of timings relatively easily and does not rely

on the penetration of inhibitors into the nucleus which is the dominant Spk1-GFP location. We could also try other inhibitors such the MEK inhibitor U0126 which may be effective against Byr1.DD.

7.2.3 Potential use of *spk1.as* to identify direct Spk1 substrates

Although experiments with *spk1.as* have so far been unsuccessful in rescuing *byr1.DD*, the ATP-analogue sensitive Spk1 protein can be used to identify direct Spk1 MAPK substrates. This could be achieved by using a protocol described by Zheng *et al.*, 2010 using a radiolabeled ATP analogue - that can only be exclusively used by the *as*-kinase - and an *in vitro* kinase assay. Their method relies on the basis that specific kinase substrates will be coimmunoprecipitated with the *as*-kinase . This is then followed by mass spectrometry to identify radiolabeled proteins (Zheng *et al.*, 2010). This type of experiment would be extremely informative as Ste11 is the only Spk1 substrate identified to date (Kjaerulff *et al.*, 2005). This may be able to identify potential unknown down-regulators/feedback loops within the MFSP and the morphology pathway target may also be revealed if it is directly linked to Spk1 phosphorylation.

We wanted to further investigate what might be preventing the *byr1.DD* mutant from fusing. Another mutant which shows this characteristic "prezygotic" phenotype is *fus1Δ* (Petersen *et al.*, 1995). Fus1 is a formin protein which is required for cell fusion and is required for stabilisation of actin at the fusion tip (Petersen *et al.*, 1998b). Polymerised actin (also known as filamentous or F-actin) is required for cell fusion as treatment of cells with the actin depolymerising drug, Latrunculin A, prevented this process. F-actin is also required for spore formation (Petersen *et al.*, 1998a). In *fus1⁻* cells, actin can localises to the projection tip and cells exhibit successful polarised growth but after cell-cell contact the actin is redistributed throughout the cytoplasm therefore Fus1 is thought to coordinate actin for cell fusion but not polarised growth (Petersen *et al.*,

1998b). The expression of *fus1* requires both nutrient starvation and pheromone signalling (Petersen *et al.*, 1995) and localisation of Fus1 to the projection tip requires contact with a cell of the opposite mating type (Petersen *et al.*, 1998b). The reason that *fus1Δ* cells cannot conjugate is likely due to a disorganisation of actin after cell-cell contact which may be required for the transport of vesicles containing proteins involved in cell wall degradation/remodelling. This led us to investigate the localisation of actin in *byr1.DD* cells to determine if the conjugation defect was of a similar nature to that of *fus1Δ*. In order to visualise actin in live cells we used a peptide called Lifeact (Riedl *et al.*, 2008) tagged with GFP.

7.3 Lifeact – Visualisation of F-actin in live cells

Lifeact (LA) is a 17 amino-acid peptide that stains filamentous actin in living or fixed cells. The peptide was initially derived from the first 17 amino acids of the protein ABP140 in *Saccharomyces cerevisiae*. Most importantly, Lifeact does not interfere with actin dynamics *in vitro* and *in vivo* (Riedl *et al.*, 2008).

Lifeact (MGVADLIKKFESISKEE) was cloned into the pDUAL vector which is capable of single copy chromosome integration in *S.pombe* at the *leu1* locus via homologous recombination. Part of the pDUAL vector was amplified using *leu1*-3' F and *leu1*-5' R primers (**Figure 7.10A**) in order to create an amplified PCR product which was then used for transformation of an *S. pombe* host strain. The host strain contained the leucine auxotroph (*leu1.32*) so that successful integration lead to a fully functional leucine locus and positive clones were selected due to their ability to grow in the absence of leucine.

7.3.1 *Actin Localisation in Wildtype Cells*

The WT strain (KT3001), with LA-GFP successfully integrated into the genome, was set up for live imaging using a Nikon Eclipse Ti-E microscope and images taken every 3 minutes in the green and brightfield channels, selected images are shown in **Figure 7.10B**. The images clearly show actin localising to the cell tips before and during conjugation, for example, it is clear at 66 minutes that actin is accumulating at the tips of both cells where the cell membranes will eventually start to fuse which happens about 60-70 minutes later (132 minutes). Actin stays localised here for a further 30 minutes while the conjugation of the two cells takes place (timings labelled in red) and has fully dissipated 207 minutes after the first image was taken.

This data corresponds with the results of (Petersen *et al.*, 1998a). They used rhodamine conjugated phalloidin in fixed cells to visualise F-actin and in agreement with their work, we also see that even though actin is localised to the projection tips it appears absent from the exact region of cell fusion. **Figure 7.10C** shows a diagrammatic representation of actin dynamics during conjugation from their findings (Petersen *et al.*, 1998a). My results are the first reported data showing live images of actin reorganisation during *S.pombe* conjugation and a movie of the process has been created and is included on the CD provided. This reorganisation of actin is crucial for successful conjugation and therefore successful meiosis, therefore investigations into the actin localisation in Ras1-MAPK mutants was of interest. Unfortunately live imaging of *ras1.vall7* strains containing LA-GFP (KT3017 and KT3005), which have been set up in the same way as for WT, have been unsuccessful in capturing the formation of the mutant elongated phenotype; this may be due to the need for cells to agglutinate extensively and for the cells to be at a high density to form their characteristic mating phenotypes. Capturing the formation of the “prezygotic”

phenotype of *byr1.DD* cells has also been unsuccessful so far which is probably down to a similar reason as *ras1.val17* and the cells aren't at an density which allows them to form the phenotype but a high density of cells is not ideal for live cell imaging (because a single layer of the cells would be ideal for clear images) and therefore requires further optimisation to be successful. As an alternative, *ras1.val17* (KT3017), *sxa2Δ* (KT3992), *byr1.DD* (KT3051) and *fus1Δ* (KT3035) strains containing LA-GFP were subject to the SPA plate mating assay setup to achieve a high density of synchronous cells and then still images of cells were taken at various time-points, the results of which can be seen in **Figure 7.11**.

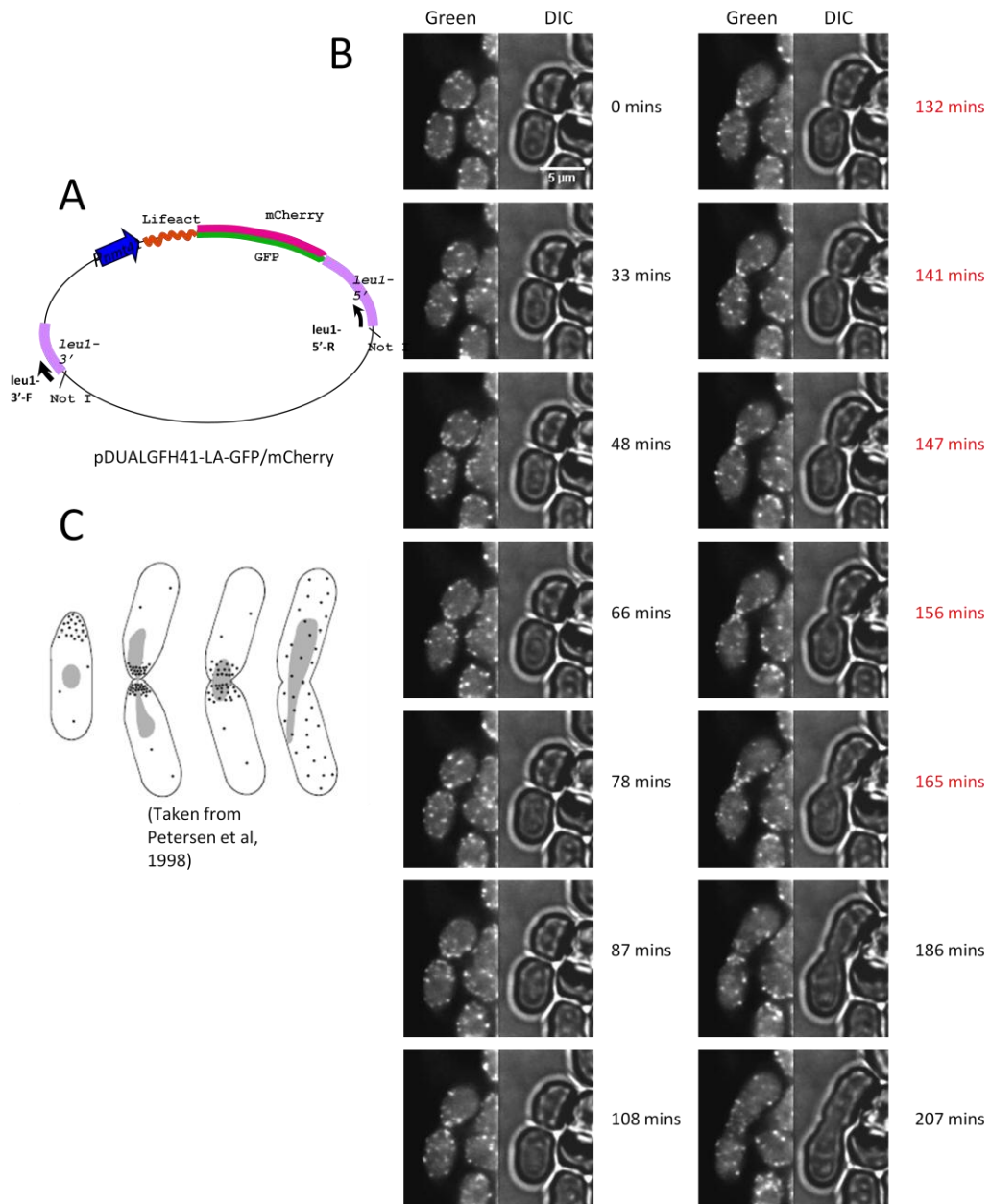


Figure 7.10 Lifact imaging during conjugation in WT cells.

(A) The pDUAL plasmid with LA-GFP cloned in and relative primer positions for amplification. (B) Live imaging of KT3001 (WT plus chromosomally integrated LA-GFP). Timings are labelled relative to the first image. Timings labelled in red highlight the conjugation process specifically. Images were deconvolved using the Huygens Essential software and then processed using Image J. (C) Summary of F-actin localisation during conjugation from Petersen et al, 1998). Scale bar is 5 μ m.

7.3.2 *Actin localisation in Ras-MAPK mutants*

WT cells (KT3001) were set up to act as a reference using the plate assay system to induce mating and visualise actin rather than continual imaging as described for the images in **Figure 7.10**. The assay system had to be slightly modified as the expression of Lifeact-GFP is under the control of the inducible *nmt1* promoter that is repressed by thiamine. Therefore overnight cultures were grown in thiamine-free MM+N rather than thiamine-containing YE+ade as previously described for the plate mating assay (Chapter Section 3.2.2). We observed that WT cells started to conjugate and form diploid zygotes at an accelerated rate when grown in MM+N compared to overnight YE+ade cultures, presumably because the synthetic MM+N media lacks some nutrition compared to the rich YE+ade media that is efficient in preventing cells to commit into sexual differentiation.

Mating pairs and zygotes were clearly seen already at 3.5 hours after mating induction (**Figure 7.11**). The WT 3.5-hour image shows Lifeact-GFP localised at the point of cell fusion in one mating pair (yellow arrow) and in a zygote (red arrow) where Lifeact-GFP is being redistributed after cell fusion. After cells have fused actin remains dispersed throughout and is eventually incorporated into spores (8-, 12- and 24-hour images). No image was taken for 55-hours post induction for WT cells as a high percentage of cells had sporulated and most asci had broken down to release mature spores.

In the *ras1.val17* mutant (KT3017), actin can be seen localising more predominantly at one end of cells at most time-points when images were taken - indicated by yellow arrows in **Figure 7.11**, however this localisation is not permanent as there are elongated cells in the 24- and 55-hour post induction images where actin is not at the tip and after actin has delocalised from the tips cells probably do not continue to elongate which would explain why elongation does not continue over a prolonged period of time. This

indicates that actin is localised to the tip in a transient manner which is also likely to be the case with the *sxa2Δ* mutant (KT3992) although localisation to the elongating tip is also not as obvious as in *ras1.val17*, it can be seen in the 8- and 24-hour images and is absent at the later time-points (38- and 55-hours). *sxa2Δ* cells show extensively longer elongated conjugation tubes compared to *ras1.val17* which may be a consequence of having actin at the tip for an extended period of time but our images do not reflect this currently and for this mutant in particular it may be more suitable to image cells more intensively over the mating time-course, specifically between 4- to 12-hours post induction when cells show the greatest change in shape. It may also be the case that the shmooing response is activated to a greater extent in the absence of *sxa2* which is reflected in the MAPK phosphorylation profile (Chapter 6 **Figure 6.5**) and actin may be present at a higher intensity at the tips during the period of elongation.

To summarise, not all cells showing the elongated phenotype in the *ras1.val17* and *sxa2Δ* images have actin localised to the tips which again indicates that this actin localisation is probably a relatively transient event and cells that have delocalised actin from the tips are unlikely to elongate any further indicating that cells have desensitised themselves from the pheromone signal and have ceased polarised growth. The extremely high levels of pheromone pathway stimulation seen in *sxa2Δ* (Chapter 6 **Figure 6.5**) judged by the levels of phospho-MAPK, correlate well with the extent of hyperactive shmooing but this particular experiment has been inconclusive in relating the extent of shmooing to a increased amount of actin localised at the shmoo tip in *ras1.val17* and *sxa2Δ* strains.

To compare actin localisation in mutants showing the "prezygotic" phenotype we directly compared the *fus1Δ* directly compared the *fus1Δ* and *byr1.DD* mutants. *byr1.DD* (KT3051) cells show Lifact-GFP localised at the Lifact-GFP localised at the projection tips (Figure 7.11

Figure 7.11, yellow arrows) at the location where the mating pair would fuse in order to successfully conjugate. This localisation is sustained throughout the time-course and is still evident after 55- hours post induction. It was interesting to note that cells continue to elongate their conjugation tubes with time which probably reflects the permanent localisation of actin to that region.

*fus1*Δ (KT3035) also has actin localised to the tips during pheromone induced polarisation (**Figure 7.11**, yellow arrows) which was originally shown in (Petersen *et al.*, 1998a). In agreement with their findings, we found F-actin to be sustained at the tips for a prolonged period of time compared to WT but F-actin gets redistributed after cells fail to fuse suggesting that Fus1 is required to stabilise actin at the projection tip (Petersen *et al.*, 1998b). When cells start to pair up actin was clearly localised to the cell tips where cells would normally fuse (8- and 12-hours post induction) whereas this localisation is not obvious at later time-points (24-hours and 38- hours post induction, indicated by the green arrows).

It was evident that, even though we like to describe both *byr1.DD* and *fus1*Δ as showing the prezygotic phenotype, these two mutants are unlikely to be caused by the same molecular defect as the conjugation tubes of *byr1.DD* continue to elongate as long skinny tubes compared to *fus1*Δ which exhibit much wider fatter tubes. The "chubby" conjugation tubes of *fus1*Δ are more indicative of normal mitotic cell tip elongation in terms of a more uniform elongation in contrast to *byr1.DD* where cell tip shmooing is resulting in long "skinny" tubes. This is evident when comparing the brightfield images between the two mutants in **Figure 7.11**. Although conjugation tubes in the *fus1*Δ mutant elongate, it is not to the same extent as the *byr1.DD* mutant which may be explained by the lack of permanently localised actin at the shmoo tip in *fus1*Δ.

It would appear that Fus1 is functioning correctly in *byr1.DD* as actin is sustained at the tips and therefore the reason for fusion failure in this mutant remains unclear.

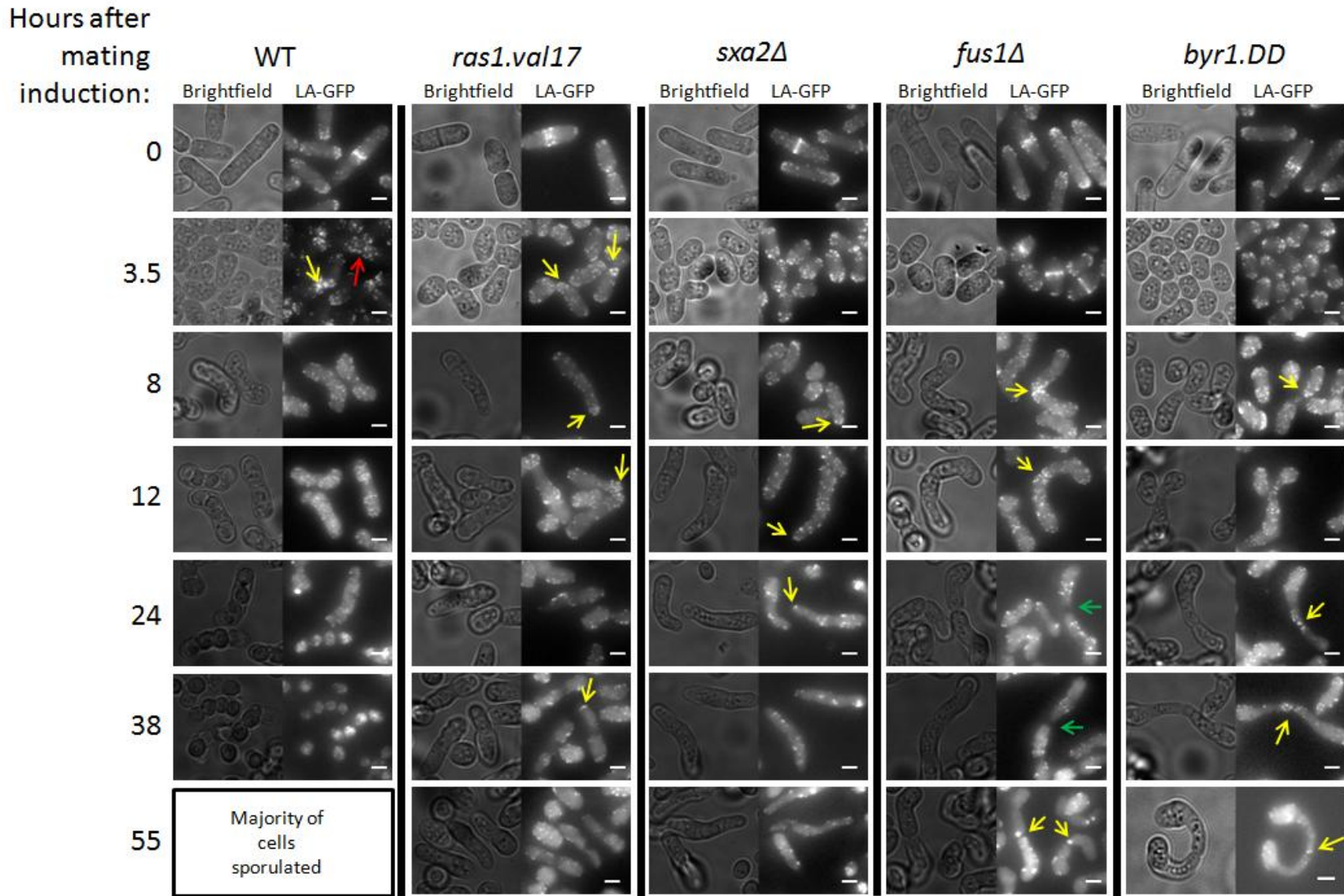


Figure 7.11 Lifeact-GFP localisation in Ras1-MAPK mutants.

WT (KT3001), *ras1.val17* (KT3017), *sxa2Δ* (KT3992), *fus1Δ* (KT3035) and *byr1.DD* (KT3051) all contain Lifeact-GFP expressed under the control of the *nmt1* promoter integrated at the *leu1* locus. All cells were imaged at defined time-points after mating induction using the SPA plate assay. Arrows specify cells of interest mentioned within the text. Scale bar is 5 μm.

7.4 Discussion of the *byr1.DD* phenotype

Generation of the ATP-analogue sensitive Spk1 MAPK has given us a valuable tool with which we can manipulate Spk1 activity in *S.pombe* but experiments so far to "unlock" to characteristic paired phenotype of *byr1.DD* have been unsuccessful.

However, there are a number of conditions to optimise for these experiments which are yet to be revisited. For example, originally assay conditions involved the use of liquid cultures in 20 ml tubes which were incubated in a shaker, at the time this seemed like the most logical choice so that the concentration of *as*-inhibitor could be accurately calculated and we could be sure that all cells within the culture were subjected to the same concentration. However, inducing mating using liquid culture is never as efficient as the plate mating assay described in Chapter 3. Also, it was noted that all positive clones isolated as *byr1.DD spk1-as* double mutants showed a decrease in the amount of cells which formed the paired phenotype when spotted on SPA, indicating that Spk1-*as* probably still has compromised activity compared to WT Spk1 even with the second site mutation. We are now designing an assay system that is based on the plate mating assay in which we are able to define the amount of *as*-inhibitor that cells receive.

An *spk1.as* allele containing all three mutations - the GKR mutation (Q119A) plus the two potential *sogg* mutations identified from alignment with Fus3 (V67I and V118I) - was generated to determine whether *spk1.as* kinase activity could be further increased, this however was not the case and the triple mutant was found to have lower activity than the allele containing only the GKR mutation and the single additional *sogg* V67I (*spk1-V67I-Q119A*).

The Lifeact data demonstrates that although the *byr1.DD* and *fus1Δ* mutants morphologically appear to be stuck at a similar stage in the mating process, the reason

behind the lack of fusion may be for distinctly different reasons. It is evident from our results that in *byr1.DD* cells, actin is able to localise to the projection tips successfully and remain there for a substantial amount of time yet there is a lack of cell wall degradation. The reason for this remains unclear. Fus1 plays an essential role in cell fusion and is exclusively expressed in response to pheromone (Petersen *et al.*, 1995). Tropomyosin (Cdc8) and Myo51 (a type-V myosin) also localise at the fusion site and are essential for successful conjugation (Kurahashi *et al.*, 2002; Doyle *et al.*, 2009). The protein, Dni1, is also required for fusion, localisation of Dni1 to the shmoo tip is dependent on Fus1 (Angel Clemente-Ramos *et al.*, 2009) although little is known about the function of Dni1. Further investigations into the reason why *byr1.DD* cannot fuse could involve localisation studies of Fus1 and Dni1, although from the Lifeact data in **Figure 7.11** we presume that Fus1 would be localised correctly as actin seems to be stabilised at the tips. The localisation of other important proteins involved in cell fusion such as proteins involved in cell wall synthesis and degradation enzymes should also be investigated. These proteins include the glucan synthases, Bgs1, Bgs3 and Bgs4 and the glucanase, Ang1 (Merlini *et al.*, 2013) and Bgs1 and Bgs4 have been previously shown to localise strongly to the project tip (Bendezu & Martin, 2013; Cortes *et al.*, 2005). It is important to note that Fus1, actin and all the formentioned enzymes are correctly localised in the *dni1Δ* mutant (Angel Clemente-Ramos *et al.*, 2009). The type I myosin, Myo1 shows the same localisation pattern as F-actin during the mating process although homothallic *myo1* disrupted strains could mate and sporulate at a frequency similar to WT (Toya *et al.*, 2001). They also showed that Myo1 plays a role in controlling the redistribution of F-actin patches during the cell cycle and hypothesise that Myo1 function may be linked with conjugation tube formation as mating in heterothallic *myo1* disrupted strains -when the h^+ and h^- cell populations were mixed - was significantly

lower than in a equivalent homothallic strain. Our observation that conjugation tube formation is severely delayed in *byr1.DD* may indicate a role for Spk1 influencing Myo1 function.

Overall, cell fusion is a highly complex coordinated process and we are a long way from understanding this process in *S.pombe*. We can speculate that concerted pheromone signalling is required for the induction of specific genes required for cell fusion such as the glucan synthases and glucanase mentioned above and that the functions of these proteins are directly or indirectly affected by Spk1 MAPK phosphorylation. How the MFSP contributes to the regulation of cell fusion is a novel and interesting concept which remains to be explored.

It is interesting to note that the works by (Kjaerulff *et al.*, 2007), relating to Ste11 phosphorylation by Cdk during mitosis, showed that Ste11 with a phosphomimetic mutant mimicking Cdk phosphorylation (*ste11.T82D*) may also show the "prezygotic" phenotype. This mutant results in low Ste11 protein expression associated with preventing the initiation of meiotic differentiation during mitosis. This brings in an entire new angle to the *byr1.DD* story in that the paired phenotype could be associated with the slow phospho-MAPK/MFSP activity seen over the first 12-hours after mating induction rather than the constitutive phosphorylation (Chapter 3 **Figure 3.10**). We hypothesise that Spk1 protein expression is slower in *byr1.DD* because of the ineffectiveness of the phosphomimetic mutations to fully mimic true phosphorylation therefore resulting in a kinase with lower activity or less effective binding to Spk1. This will cause slower activation of the positive feedback loop for Spk1 expression associated with MFSP activation. Lower output from the MFSP will result in lower activity/expression of Ste11. To investigate whether it is low levels of Ste11 at the earlier stages that is responsible for the paired phenotype in *byr1.DD*, we could

introduce WT *byr1* into the *byr1.DD* mutant. In the presence of both WT Byr1 and Byr1.DD mutant, activation of Spk1 (and Ste11 accumulation) is expected to occur as quickly as in wildtype cells whilst Spk1 will remain phosphorylated because of the *byr1.DD* mutation. If the phenotype stays the same as the *byr1.DD* mutant, then the paired phenotype is the result of constitutive MFSP activation but if the phenotype becomes WT then, the paired phenotype is associated with slow expression of Spk1. Levels of Ste11 protein can also be investigated by western blotting comparing a WT and a *byr1.DD* strain containing Ste11 tagged with a HA-tag. We can speculate that the delay in Spk1 phosphorylation in the *byr1.DD* mutant can cause a failure in the coordination of the highly synchronised events that take place during cell fusion. Alternatively if it is indeed the constitutive activation of Spk1 MAPK that is resulting in the failure of cell fusion, we can predict that downregulation of the phospho-MAPK signal acts as a signal that cells are ready to fuse. This is a critical decision for the cell to make as premature lysis of the cell wall will be fatal.

Our final objective was to investigate potential rescue experiments of MFSP mutants with the elongated phenotype, such as *ras1.val17*. This approach was likely to require direct manipulation of Ras1 or components upstream of Ras1 in order to modulate the MFSP at a level before the pheromone signal input splits into the MAPK-transcriptional branch activation and the morphology branch activation which we found to be the case in Chapter 4, therefore we concentrated on direct manipulation of the activity of Ras1.

7.5 Direct manipulation of Ras1

We have proven that the presence of oncogenic Ras1 in *S.pombe* does not cause constitutive activation of Spk1 MAPK in the MFSP (Chapter 3 and **Figure 7.1**). We have also proven that Ras1 is signalling to both the MAPK cascade and the morphology pathway as a direct consequence of pheromone G-protein activation (Chapter 5). Our hypothesis - as outlined at the end of Chapter 6 - is that the terminal mating phenotype of the oncogenic Ras1 mutant is mainly a consequence of hyper-activation of the morphology branch therefore the most effective way to suppress *ras1.val17* would be to target the Ras1 molecule itself rather than manipulating any of the downstream effectors as was the approach for the rescue of *byr1.DD*.

A prime candidate for Ras1 manipulation would be via its GTPase activating protein, Gap1. The nature of the oncogenic Ras Gly12Val mutation in mammalian cells is that it is resistant to the effects of Ras-GAPs, this is thought to be because of the steric hindrance caused by the valine 12 of Ras and Arginine 789 of Ras-GAP (Scheffzek *et al.*, 1996) therefore the intrinsic GTPase activity of Ras cannot be activated and Ras proteins stay permanently in their activated GTP bound state. However a paper from Wang *et al.*, 1991 specified that overexpression of Gap1 in *S.pombe* could rescue the *ras1.val17* phenotype and so we went about confirming this by setting up Gap1 overexpression experiments.

7.5.1 Gap1 overexpression in *ras1.val17*

In order to overexpress Gap1, plasmids with an inducible promoters, pREP1 and pREP41 were chosen, these plasmids contain the *nmt1* and *nmt41* promoters respectively (Maundrell, 1993). These inducible promoters are highly induced in the absence of thiamine with the induced expression level of *nmt1* being about eighty times

greater than the repressed level although there is significant basal expression when repressed. *nmt41* has a seven times lower induced expression level than *nmt1* and a significantly lower basal level of expression. The gene fragment for *gap1* was inserted into both pREP1 and pREP41 using restriction enzymes and DNA ligation as outlined in Material and Methods Section 2.2.3. As a control experiment, the empty pREP41 plasmid and the pREP41 *gap1* containing plasmids were transformed into a *gap1Δ* strain (KT3289). Only the plasmid containing *gap1* could rescue the deletion phenotype and not the empty plasmid (data not shown).

A *ras1.val17* (KT2673) strain was transformed with the empty or *gap1* containing pREP1 and pREP41 plasmids and positive colonies that took up the plasmid were selected for using an SD agar plate. Only cells carrying the plasmid will grow as the budding yeast *LEU2* gene in the plasmid complements the *leu1.32* mutation in these parental strains. Positive cells were cultured for 18 hours in MM+N media to induce the *nmt1* promoter, SPA spotted and observed after a further 24 hours, results are shown in **Figure 7.12**. Both pREP1-*gap1* and pREP41-*gap1* induced mating and the production of zygotic spores in the *ras1.val17* strain in contrast to the elongated conjugation tubes seen in the control cells which were transformed with the empty plasmids. We confirm that the overexpression of *gap1* rescues the *ras1.val17* phenotype and allows cells to complete meiosis. This result highlights that oncogenic Ras1 activity can still be influenced by GAPs and this is probably due to the presence of an excess amount of Gap1 protein being enough to associate with and regulate the Ras1.val17 mutant protein at a molecular level whereas endogenous levels of Gap1 have little or no effect on Ras1.val17.

The homologous mutation in mammalian Ras proteins is reported to have ten times lower intrinsic GTPase activity compared to WT (Gibbs *et al.*, 1984) but from this data

it would appear that regulation of this specific mutated form of Ras is still possible by GAP proteins if they are present in an excessive amount. Overexpression of Gap in mammalian systems has been unsuccessful in reversing Ras mutant phenotypes most likely because of the effector functions of RasGAPs. For example overexpression of Ras-GAP promotes cell survival by acting as an effector of Ras via the inhibition of Rho-GAP thereby promoting Rho activity (Yang *et al.*, 2009). RasGAP has also been shown to bind and enhance the activity of Akt (Yue *et al.*, 2004) therefore the use of GAPs as therapeutic agents has not received too much attention in the past.

All GAP proteins contain a conserved GAP domain which is responsible for providing the GAP activity (Imai *et al.*, 1991). Unlike *S.pombe* Gap1, mammalian Ras-GAP has other characteristic signalling domains N-terminal to the GAP domain, including an SH3 domain, two SH2 domains and a PH domain which have been proven to be responsible for downstream signalling effects independent of Ras signalling (Yang *et al.* 2009).

Early experiments, carried out in 1986 (Nadin-Davis *et al.*, 1986a), introduced a human Ras protein sequence into fission yeast cells containing a null allele of Ras1, which restored meiosis with limited success, thus indicating that the human sequence can complement *S. pombe* Ras1. This also indicates that pombe Gap1 is effective against human RAS in an *S.pombe* environment therefore potentially *S.pombe* Gap1 may have a functionally effect on human oncogenic Ras in a mammalian environment without the side effects caused by the effector functions of mammalian GAPs as *S.pombe* Gap1 lacks the additional SH2, SH3 and PH domains.

We followed up the overexpression of full length Gap1 by overexpressing truncated and mutated versions of Gap1 to try and identify what regions of the protein are required for *ras1.val17* rescue. The specific *gap1* constructs are illustrated in **Figure 7.14**.

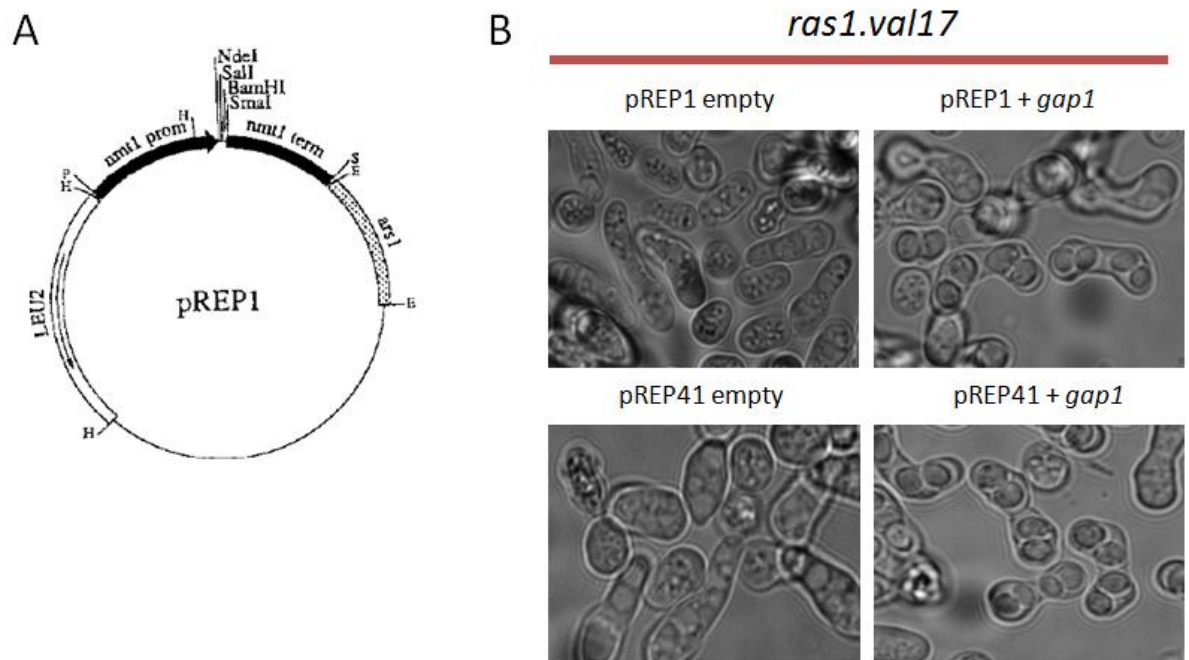


Figure 7.12 Gap1 overexpression in *ras1.val17*.

The *ras1.val17* strain KT2673 was transformed with the pREP1/pREP41 plasmid which was either empty as a control or containing the full *gap1* gene sequence inserted in order to establish Gap1 overexpression. (A) pREP1 vector (B) Live cell images of the cells after 24-hours on SPA.

7.5.2 Overexpression of GAP deficient and N- and C-terminal truncation

Gap1 mutants

The next steps for this project would be to investigate whether this rescue is dependent on the GAP activity of Gap1 or just the binding of the Gap1 to *ras1.val17*. The reason behind trying this approach is to try and establish why oncogenic Ras1 is still able to be regulated by its GAP if the oncogenic mutation is proposed to make Ras resistant to the effect of GAPs due to steric hindrance (Scheffzek *et al.*, 1997). This group solved the crystal structure of p120GAP and proposed that RasGAP is responsible for the stabilisation of glutamine 61 of Ras with a water molecule for hydrolysis of the γ -phosphate of GTP as well as what is known as the "arginine finger" of RasGAP which stabilises the transition state of the hydrolysis reaction. Mutations to glycine 12 of RAS prevent to correct orientation of the arginine finger of GAPs thereby preventing GTP hydrolysis, therefore even in the presence of an excess amount of Gap1 we would not expect the catalytic activity of Gap1 to be influencing the activity of Ras1.val17.

One explanation may be that Gap1 interacts with downstream effectors of Ras1 and overexpression of Gap1 may titrate out the effectors, acting as a competitive inhibitor for Ras1, Gap1 could be potentially be binding and sequestering Ras1 effectors thereby reducing the hyperactivation effect of *ras1.val17*. Another possibility may be that Gap1 interacts with Ras1.val17 and prevents Ras1 interacting with its effectors. In either case, GTPase activity of Gap1 is not expected to be required for the rescue of *ras1.val17*. Therefore, we aimed to generate a *gap1* mutant allele that encodes GTPase-deficient Gap1.

Figure 7.13 -taken from (Wang *et al.*, 1991) identifies blocks containing conserved residues between *S.pombe gap1 (sar1)*, *S.cerevisiae Ira1* and *Ira2*, and mammalian *GAP* and *NF1*. They identified the conserved "FLR_PA_P" motif and concluded it is

characteristic of GAP proteins and no others. (Brownbridge *et al.*, 1993) identified and characterised a number of mammalian RasGAP mutants with different GAP activities and binding affinities for Ras. From this work we chose to mutate the conserved arginine in the "FLR" to a lysine which they have shown to have severely compromised GAP activity and only a minor effect on binding to Ras. The *S.pombe gap1-R340K* mutant was created using site-directed mutagenesis and inserted into the pREP1 and pREP41 plasmids, neither plasmid containing the mutated Gap1 could rescue *gap1Δ* confirming that the R340 is essential for Gap1 function and R340K mutation is likely to have severely depleted GTPase activity. Strikingly, these plasmids failed to revert the *ras1.val17* phenotype concluding that GAP activity is indeed required for the rescue of *ras1.val17*.

The next step was to investigate the minimal regions of Gap1 which were required for *ras1.val17* rescue therefore C-terminal and N-terminal truncations of Gap1 were created to test if the whole protein is required for the rescuing effect or just the RasGAP domain (residues 175-379) as found using <http://pfam.sanger.ac.uk/search/sequence>. Full length Gap1 is 766 amino acids, the C-terminal deletion protein is amino acids 1-379 and the N-terminal deletion protein is amino acids 169-766 therefore both truncated mutants contained the RasGAP domain as illustrated in **Figure 7.14**. Neither the N-terminal nor C-terminal truncated proteins could rescue *ras1.val17* (data not shown) but a key control experiment to show that these truncated proteins are still capable of rescuing *gap1Δ* are missing therefore we cannot conclude if the truncated proteins are catalytically active. Further truncation experiments could help to narrow down the minimal region required for *ras1.val17* rescue. It is important to note that one of the original papers to isolate *gap1* defines the catalytic domain of Gap1 as residues 148-492

(Imai *et al.*, 1991) and therefore it is unclear as to the true minimal region required for *gap1Δ* rescue but this has not been pursued further in this work.

Residues		Block 1 $p=2.2e-2$			
170	HLLLSLQFQVLT	EFEATSDVLSLLRANTPVSRMLTTYTR	RGPGQAYLRSILY	<i>sar1</i>	
917	HLLYQLLWNMFSK	EVELADSMQTLFRGNSLASKIMTFCFK	-VYGATYLQKLLD	<i>NF1</i>	
764	KLESLLLCTLNDR	EISMEDEATTLFRATTLASTLMEQYMK	-ATATQFVHHALK	<i>GAP</i>	
1571	NASHILVTELLKQ	EIKRAARSDDILRRNSCATRALSLYTR	-SRGNKYLIKTLR	<i>IRA1</i>	
1717	NATHIVVAQLIKN	EIEKSSRPDIILRRNSCATRSLMLAR	-SKGNEYLIRTLO	<i>IRA2</i>	
		EIE.....LLR.NS.ASR.L..Y.R		Consensus	
223	QCINDVAIHDPDLQLDIHPLSVYRYLVNTGQLSPSEDDNLLTNEEVSEFPVAVKNAIQ			<i>sar1</i>	
969	PLLRIVITSSDWQHV-----SFEVDPTRLEPSESLE-----			<i>NF1</i>	
816	DSILKIMESKQ-----SCELSPSKLEKNEDVN-----			<i>GAP</i>	
1623	PVLQGIVDNKE-----SFEID--KMKPGSENS-----			<i>IRA1</i>	
1769	PLLKKIIQNRD-----FFEIE--KLKPEDSDA-----			<i>IRA2</i>	
		Block 2 $p=1.9e-5$			
279	ERSAQLLL-LTK	RFLDAVLNSIDEIPYGIKRWVCKLIRNLTNRLFFSISDS	TICS	<i>sar1</i>	
1000	ENQRNLLQ-MTE	KFFHAIISSSSEFPQLRSVCHCLYQVVSQRFPQNSIG	----	<i>NF1</i>	
843	TNLTHLLN-ILS	ELVEKIFMASEILPPTLRYIYGCLQKSVQHKWPTNTTM	R-TR	<i>GAP</i>	
1648	EKMLDLFEKYMT	RLIDAITSSIDDFP IELVDICKTIYNAASVNFPEYAYI	----	<i>IRA1</i>	
1794	ERQIELEFVKYMN	ELLESISNSVSYFPPPLFYICQNIYKVACEKFPDHAI	----	<i>IRA2</i>	
		.LL.AI..S...FPP.LR.IC..IY.....FP.....		Consensus	
		Block 3A $p=0$	Block 3B $p=5.2e-5$		
332	LIGGFFFLRFVNP AIISPQTSMLLD	SCPSDNV	RKTLATIAKIIQSVAN	GTSS	
1049	AVGSAMFLRF INPAIVSPYEAGILD	KKPPPRI	ERGLKLMKILQSIAN	HVLF	
895	VVSGFVFLRLICPA ILNPRMFIIS	DSPSPIA	ARTLILVAKSVQNLAN	LVEF	
1698	AVGSFVFLRF IGPALVSPDSENIIS	VTHAHD-	RKPFITLAKVIQSLAN	GREN	
1844	AAGSFVFLRFFCP ALVSPDSENIID	ISHLSE-	KRTFISLAKVIQNIAN	GSEN	
	AVGSFVFLRFI.PAIVSP...NIID		RRTLII..AK.IQS.AN	Consensus	
384	-TKTHLDVVSFQPMLEDEYEKVINLLRKL	410		<i>sar1</i>	
1101	-TKEEHMRPFNDFVKSNEFDAARRFFLDI	1127		<i>NF1</i>	
947	GAKEPYMEGVNPFIKSNKHRMIMFLDEL	974		<i>GAP</i>	
1749	IFKDIILVSKEEFLKTCSDKIFNFLSEL	1776		<i>IRA1</i>	
1895	FSRNPALCSQKDFLKECSDRIFRFLAEL	1922		<i>IRA2</i>	

Figure 7.13 Identifying a residue to mutant to create a GTPase deficient Gap1

Reproduced from Wang *et al.*, 1991. Identification of blocks of amino acids containing conserved residues between *S.pombe gap1 (sar1)*, *S.cerevisiae Ira1* and *Ira2*, and mammalian *GAP* and *NF1*. They identified the “FLR_PA_P” motif in Block 3A and concluded it is characteristic of GAP proteins and no others. The conserved residues highlighted in bold.

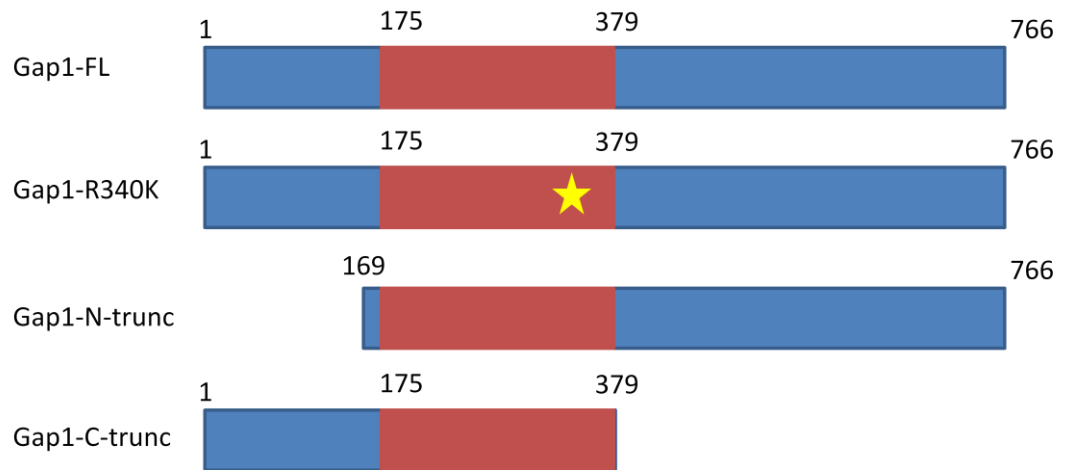


Figure 7.14 Gap1 constructs.

A schematic illustration of the protein structures of Gap1 inserted into the pREP1 and pREP41 plasmids. The GAP domain consists of residues 175-379 (red) as found using <http://pfam.sanger.ac.uk/search/sequence>. and is present in all four constructs tested. Gap1-FL is Gap1-full length. Gap1-R340K is a GTPase activity compromised mutant. Gap1-N-truncated is amino acids 169-766 and Gap1-C-truncated is amino acids 1-379.

7.6 Discussion - GAPs as potential therapeutics

In relation to translating this result into a mammalian context, it is important to note that past experiments have shown that mammalian GAP and the catalytic domain of NF1 cannot rescue *S.pombe ras1.val17* and *S.pombe* Gap1 cannot rescue *S.cerevisiae Ras2.val19* (Wang *et al.*, 1991). Therefore any potential minimal *gap1* domain capable of suppressing *ras1.val17* is unlikely to have a major effect in a mammalian background as there is limited complementation between the functions of these GAPs between species. This is also reflected in the low sequence similarity between them. There is however partial complementation as mammalian GAP and NF1 can rescue *S.pombe gap1Δ* to a limited extent and *gap1* can complement the deletion of either of the RAS GAPs *Ira1* and *Ira2* in *S.cerevisiae*. However, partial complementation may be enough to prevent the oncogenic phenotype as (Eccleston *et al.*, 1993) found that relatively low GTPase activity is sufficient to prevent transformation. This was seen using a Ras proline 12 mutant which, in the same manner as the Ras valine 12 mutant, is not activated by the binding of p120GAP but was found to have a two fold increase in its intrinsic GTPase activity compared to WT Ras. The transforming potential of the Ras proline 12 mutant is classified as low when the proline 12 mutant was overexpressed in Rat-1 fibroblast and was found to be only slightly more effective at transforming these cells than overexpression of the WT glycine 12 Ras protein (Ricketts & Levinson, 1988).

Investigations into the functional complementation of human Ras proteins in *S.pombe* has shown that the human isoforms have distinct cellular localisations (Bond *et al.*, 2013). *ras1Δ* cells overexpressing the human isoforms cannot shmoo but can activate pheromone responsive transcription (Bond *et al.*, 2013). This provides a potential

screening strategy in *S.pombe* for inhibitors of human oncogenic Ras isoforms using a pheromone transcription reporter assay.

It has been known for over two decades that oncogenic Ras can still bind to GAPs but they are unable to promote the intrinsic GTPase activity of Ras (Eccleston *et al.*, 1993; Vogel *et al.*, 1988). The findings that RasGAP is also a potent effector protein of Ras and has a positive effect on proliferation, migration and cell survival through a number of protein-protein interaction motifs in the N-terminal domain has ruled out the use as RasGAP as a potential therapeutic against oncogenic Ras. The C-terminal domain of RasGAP contains the GAP domain and is therefore separate from the N-terminal effector domain containing two SH2 domains, an SH3 domain, a PH domain and a calcium dependent phospholipid binding domain (Pamonsinlapatham *et al.*, 2009). The role of RasGAP as a downstream effector is reviewed in Pamonsinlapatham *et al.*, 2009. Also, because the mechanism of hydrolysis was unveiled a number of years ago (Scheffzek *et al.*, 1996), GAPs have always been thought to be ineffective against oncogenic Ras and have not received a lot of attention in terms of their use in cancer therapy. However, our findings highlight that GAPs may still be effective against oncogenic Ras mutants. A molecule that can mimic the GTPase activating domain of RasGAPs without promoting any of the downstream effector functions would be ideal in this case and *S.pombe* Gap1 should be considered as a prime candidate for this type of molecule as it lacks any of the protein-protein interaction domains of mammalian RasGAP.

In conclusion, we have reconfirmed that overexpression of *gap1* suppresses *ras1.val17* in *S.pombe*. This highlights the importance of oncogenic Ras regulation in promoting a WT phenotype and suggests that attempts to manipulate Ras1 activity directly should be reassessed as a potential therapeutic approach. Indeed, published work by (Bossu *et al.*,

2000) has shown that sequestering of oncogenic Ras by a dominant negative GEF can attenuate the amount of Ras-GTP in mouse fibroblasts and somewhat revert the oncogenic phenotype to that of WT in terms of morphology and anchorage dependent growth. Furthermore, they observed a delay in tumour formation in xenotransplants. This idea of diluting out the amount of oncogenic Ras as a means of reverting back to a WT phenotype is not entirely a new concept as it was shown by Wang *et al.*, 1991 in *S.pombe* that -along with *gap1* overexpression - wildtype *ras1* overexpression was the only other suppressor of *ras1.val17* identified in their screen and this was thought to be due to competition between oncogenic and WT Ras1 for downstream effectors. These observations confirm that direct Ras manipulation is a promising approach for not only preventing the oncogenic phenotype in cells but actually promoting the WT phenotype.

CHAPTER 8 DISCUSSION AND FUTURE DIRECTIONS

8.1 Original aims and objectives

In this study, we have used the process of *S.pombe* mating as a model system to study Ras protein signalling . In the past, the role of the Ras protein homologue in fission yeast, Ras1, in coordinating meiotic differentiation has only been vaguely described. Ras1 plays an essential role in the maintenance of the elongated cell shape as cells containing a defective Ras1 are rounded in morphology. The function of Ras1 during meiosis is strongly linked to the activation of the pheromone stimulated MAPK cascade consisting of Byr2, Byr1 and Spk1 but the predicted role of Ras1 in coordinating a polarised growth response remained undefined. We aimed to provide evidence for the coordination of the Ras1-MAPK pathway and Ras1-morphology pathway to test our hypothesis that Ras1 is activating these two pathways independently upon pheromone stimulation. Although the oncogenic Ras1 (*ras1.val17*) mating phenotype in *S.pombe* was observed over two decades ago, the molecular nature of this mutation remains unexplored. We aimed to assess the molecular reasoning behind the observation that constitutively active Ras1 (*ras1.val17*) and constitutively active MEK (*byr1.DD*) show distinctly different phenotypes upon the induction of mating. We also wanted to identify a hypothesis as to why *ras1.val17* has little/no effect in mitosis but a prominent effect in meiosis. In order to do this we employed genetic, biochemical and cell biology approaches. Specifically we aimed to devise an assay to monitor the activation of the pheromone response pathway that would allow us to quantify the activation of Spk1 MAPK in various mutant strains. We further aimed to define the contribution of various components of the pathway to MAPK activation, particularly those of the

negative regulators, Gap1, Rgs1 and Sxa2 along with the G-protein, Gpa1, Ste4 and Ste6. Our integrated model is proposed in **Figure 8.1**.

Ras proteins are highly conserved GTPases present in yeasts through to humans. Ras proteins play pivotal roles in a number of fundamental signalling pathways and are found to be mutated in around a third of all human cancers (Downward, 2003) as well as a number of RASopathies making the understanding of their molecular biology of high importance. The aim of this work was to further our understanding of the coordination and regulation of Ras-protein signalling and to highlight basic regulatory concepts to potentially provide direction for therapeutic investigations.

Individual discussion sections have been provided at the end of each results chapter. This chapter brings together the main conclusions, which are summarised in **Figure 8.1**, and outlines future directions for further investigations.

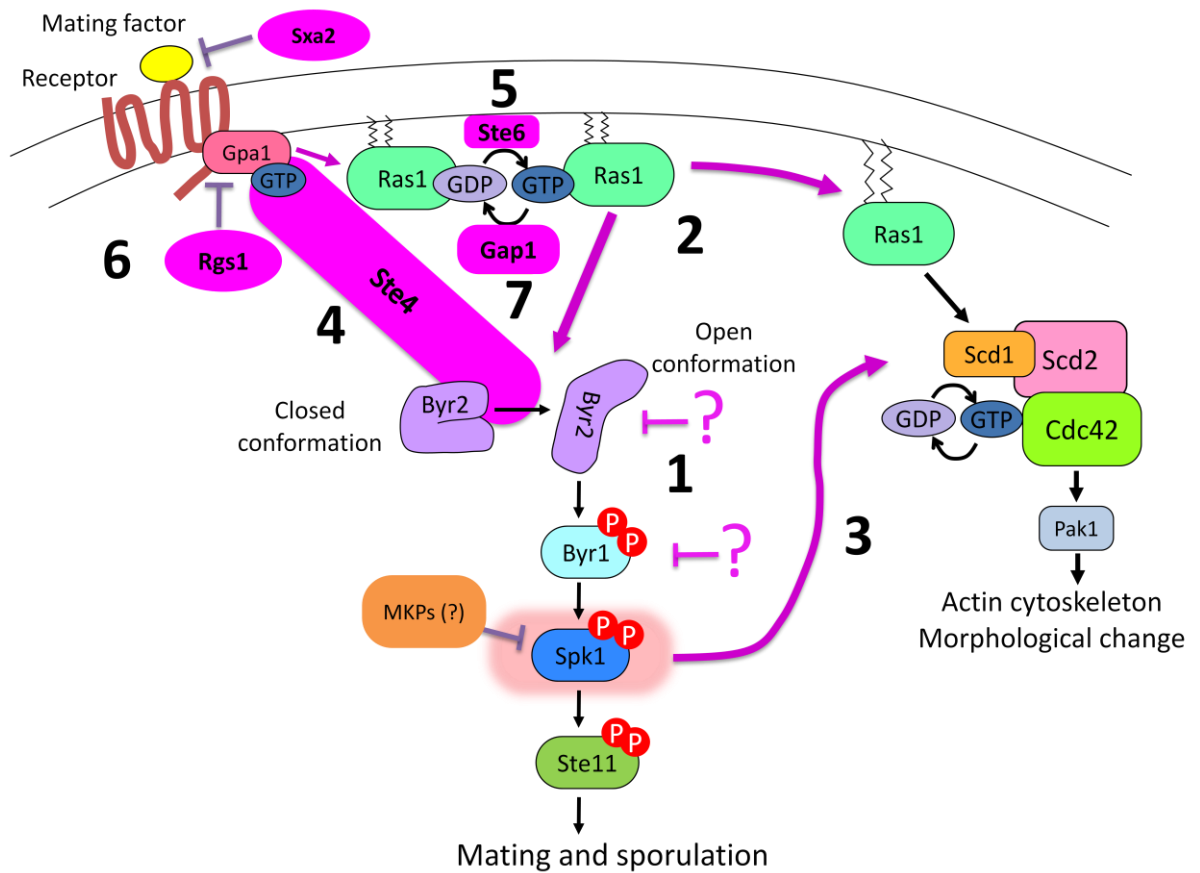


Figure 8.1 Summary of the main findings of this work

1. Chapter 3: The role for a undefined downregulatory step
2. Chapter 4: Ras1 activates two independent pathways
3. Chapter 4: MAPK signalling is required for a morphological response
4. Chapter 5: Gpa1 and Ste4 are essential for activation of the MAPK cascade
5. Chapter 5: Ste6 is the Ras1 GEF controlling the activation of both the MAPK branch and the morphology branch
6. Chapter 6: Sxa2, Gap1 and Rgs1 all play essential roles in MFSP regulation
7. Chapter 7: Gap1 overexpression rescues the oncogenic Ras1 phenotype

8.1.1 An undefined down regulatory mechanism at the level of MEKK or MEK

Once an effective mating assay had been designed and validated along with the use of a commercially available phospho-ERK antibody for quantitation of the activity of the MFSP via the detection of phospho-Spk1 we went on to investigate the spatiotemporal dynamics of Spk1 MAPK in the presence of a constitutively activated MEK (*byr1.DD*) or an oncogenic Ras1 mutant (*ras1.val17*). These experiments revealed a number of key points about the regulation of the MFSP. Firstly, Byr1 must be down-regulated to prevent constitutive MAPK phosphorylation and that proposed MAPK phosphatases (Pmp1 and Pyp1 (Didmon *et al.*, 2002)) are ineffective if Byr1 is not downregulated. The previously reported hypersensitive nature of *ras1.val17* (Nadin-Davis *et al.*, 1986a) is reflected in the hypersensitive MAPK phosphorylation dynamics where the phospho-MAPK signal appears significantly earlier in this mutant. Most importantly there is effective downregulation of the phospho-MAPK signal in the presence of oncogenic Ras1 when expressed from its endogenous locus which has also been reported in mammalian cells (Tuveson *et al.*, 2004). Therefore it is evident that the mutant phenotype is not a consequence of constitutive MAPK output. Our results clearly shows that there is effective down regulation of the phospho-MAPK signal, acting downstream of Ras1 which does not appear to be effective in the *byr1.DD* mutant. There are potential unidentified down-regulator acting at the level of MEKK or MEK itself which are yet to be identified for the *S.pombe* MFSP. Negative regulatory mechanisms which act downstream of Ras1 in the WT situation are no longer effective in the presence of Byr1.DD due to its constitutive nature and therefore it is important to terminate Byr1 activity. The fact that Byr1 is phosphorylated for activation promotes the idea that dephosphorylation by protein phosphatases is a likely form of downregulation. In the

mammalian RTK pathway, involving Ras-Raf-MEK-ERK which is activated in response to growth factors, there is significant regulation of Raf (MAPKKK) by PP1, PP2A and PP5 (Dhillon *et al.*, 2007) but the homologues of these proteins in fission yeast play important roles in other essential pathways. For example, PP1 and PP2A have distinct roles as mitotic regulators involved in the DNA damage checkpoint, regulation of homologous chromosome segregation and regulation of mitotic sister chromatid segregation (Kinoshita *et al.*, 1990). Currently there is no evidence for a role of either PP1 or PP2A phosphatases during meiosis and expression profiles, viewed using the Bahler lab expression viewer, show no distinct changes during pheromone signalling or sporulation.

There is no reported homologue of mammalian PP5 in *S. pombe*, therefore a database search was carried out to try and identify one. The omniBLAST results indicated one potential homologue, SPBC3F6.01c, which has 50% identity and 69% similarity to PP5. Additional hits were those of the PP1 and PP2A homologues mentioned previously. An MSc student in the lab, Huda Ali, carried out deletion experiments to try and identify a role for SPBC3F6.01c during meiosis but a single deletion strain was able to undergo mating and sporulation with no obvious defects. Other phosphatases were selected for investigation based on potential MAPK docking sites with multiple single and double deletion strains created but all showed no defect in meiosis therefore, presently, a specific phosphatase for either Byr2 or Byr1 remains unidentified.

We cannot rule out that the regulation of Byr1 may be down to proteosomal degradation which is dependent on recognition of phosphorylated Byr1. It is also possible that the activity of Byr1 could be inhibited by the addition of an inhibitory phosphorylation in a negative feedback manner potentially by Spk1 itself. The works of Gopalbhani *et al.*, 2003 show that phosphorylation of the conserved serine residue at position 212 of

mammalian MEK1 results in suppressed activity of both WT and phosphomimetic MEK1. Alanine substitution of the serine resulted in a higher than basal activity whereas substitution with an aspartic acid lead to suppressed activity and they also showed this is conserved with the *S.cerevisiae* MEKs, Pbs2 and Ste7 (Gopalbhai *et al.*, 2003). It would be interesting to mutate this conserved Serine in *S.pombe* Byr1 although they showed that phosphorylation of this residue was effective in suppressing the activity of phosphomimetic MEK1 but we see constitutive activation with phosphomimetic Byr1. However we can predict that if Spk1 was phosphorylating Byr1 in a negative feedback manner then perhaps Spk1 cannot bind effectively to Byr1.DD due to the phosphomimetic mutations.

In terms of explaining why *byr1.DD* results in the paired phenotype where cells fail to undergo fusion it is important to distinguish whether the reason is linked to slower MFSP activity or constitutive activity as outlined in Chapter 7 Section 7.4. We observed that Spk1 protein expression is slower in *byr1.DD* and hypothesised that it is because of the ineffectiveness of the phosphomimetic mutations to fully mimic true phosphorylation therefore resulting in a kinase with lower activity or less effective binding to Spk1. This will cause slower activation of the positive feedback loop for Spk1 expression associated with MFSP activation. Lower output from the MFSP will result in lower activity/expression of Ste11 which directly cause the delay/significant decrease in expression of a huge number of pheromone responsive genes including *sxa2*, *rgs1* and *fus1*. To investigate whether it is low levels of Ste11 at the earlier stages that is responsible for the paired phenotype in *byr1.DD* we could introduce WT *byr1* into the *byr1.DD* mutant. If the phenotype stays the same then the paired phenotype is the result of constitutive MFSP activation but if the phenotype becomes WT then, in the case of *byr1.DD*, the paired phenotype is associated with slow expression of Spk1.

Levels of Ste11 protein can also be investigated by western blotting comparing a WT and a *byr1.DD* strain containing Ste11 tagged with a HA-tag which has already been generated in the lab.

8.1.2 Ras1 plays an essential role in coordination *S.pombe* mating events

In Chapter 4, we provide evidence that Ras1 is activating the morphology pathway independently of the MAPK cascade during mating. We also show that MAPK activation is essential for a morphological response. This was firstly considered when it was observed that *byr2Δ*, *byr1Δ* and *spk1Δ* strains are all completely sterile and do not undergo any shmooing response in the presence of mating factor. We further contribute to this observation by showing that artificial activation of the morphology pathway by the addition of *ras1.vall7* cannot restore a morphological response in the absence of Byr2 or Byr1 hence concluding that MAPK activation is essential for shmooing. We propose a number of hypothesis as to how MAPK could be contributing to the activation of shmooing. The morphology complex may require MAPK for activation, for stability or for correct localisation to the site of pheromone stimulation at the cell cortex. We can test this by investigating the localisation of activated Cdc42 in WT cells and in the absence of MAPK signalling using CRIB-GFP which acts as a fluorescent marker which only binds to Cdc42-GTP. We can also check the localisation of other components of the morphology complex (i.e. Scd1 and Scd2) using fluorescently tagged versions of these proteins to confirm whether these components are correctly associated with the complex in the absence of MAPK activation.

We tested the hypothesis that the morphology pathway is feeding into MAPK cascade activation which was first proposed by Tu *et al.*, 1997 when they observed that Pak1 can promote the open conformation of Byr2. However, when we quantified MAPK phosphorylation in the absence of Scd1 (a Cdc42 GEF) we did not see a decrease in

MAPK phosphorylation as expected and instead we found a reproducible advancement in MAPK activation. We hypothesize that this is likely due to an increase in the amount of "free" Ras protein which would usually be involved in signalling to the morphology complex through Scd1 which is now available to activate the MAPK cascade in the absence of Scd1. A proposed experiment to investigate the contribution of Cdc42-Pak1 to MAPK cascade activation is to use mutated versions of these two proteins which have compromised activity, for example, Pak1 K415R (Chang *et al.*, 1999), Pak1 G517E (Das *et al.*, 2012) and Cdc42-L160S (Estravis *et al.*, 2012).

8.1.3 Gpa1 and Ste4 are essential for activation of the MAPK cascade

We have shown through quantitative western blotting that the G-protein, Gpa1, is essential for Spk1 phosphorylation even in the presence of *ras1.val17* concluding that activated Ras1 alone is not enough to cause Byr2 activation. It is possible that the primary role of Ras1 could be Byr2 translocation to the plasma membrane where it is activated by additional means through Gpa1-Ste4. We have not ruled out that Ste4 may also have a role in targeting Byr2 to the membrane as we observed a small amount of phospho-MAPK in the absence of *ras1* but the level was severely reduced compared to WT. An important experiment to test this hypothesis is to investigate the localisation of Byr2 - using Byr2-GFP - in the absence of *ste4*. We also found that restoration of MAPK phosphorylation in the absence of Gpa1 was not sufficient to simultaneously activate a morphological response. However, artificially activating both the MAPK pathway and the morphology pathway by the generation of the triple mutant, *gpa1Δ byr1.DD ras1.val17*, resulting in a shmooing response thereby confirming that activation of both signalling pathways represents activation of the G-protein and Gpa1 plays a crucial role in coordinating this activation at the site of pheromone stimulation. The *gpa1Δ byr1.DD ras1.val17* probably feels no pheromone signal orientation yet still

subtly elongates which supports the default end shmooing reported in Bendezu and Martin., 2013.

Following up the conclusion that Gpa1 is essential for MAPK phosphorylation we also found that the adaptor protein Ste4 is also essential for MAPK phosphorylation. In contrast to Gpa1 we found that Ste4 is not required for Ras1-Scd1-Cdc42 activation as the restoration of MAPK phosphorylation via *byr1.DD* in *ste4Δ* resulted in the paired phenotype associated with the *byr1.DD* mutant. We hypothesise that Ste4 links Gpa1 to Byr2 activation potentially through dimerisation/oligomerisation of Byr2 resulting in autophosphorylation. This fits well with the model proposed by Tu *et al.*, 1997 which is outlined in Chapter 5 **Figure 5.14**. An important future experiment is to investigate the localisation of Byr2 in the absence of Gpa1-Ste4 to discover if localisation to the cell cortex is solely dependent on Ras1 activation. This can be further confirmed using a Byr2 mutant artificially localised to the membrane via the addition of the membrane localisation signal of Ras1. This experiment was originally outlined in Leever *et al.*, 1994 to investigate if Ras1 is no longer required for MAPK phosphorylation. In this paper, they fused the membrane localisation signal of K-Ras4B containing the last 20 amino acids and the essential membrane localisation CAAX motif to the C-terminus of Raf and found Raf to be continuously associated with the membrane and have constitutive activity (Hancock *et al.*, 1989; Leever *et al.*, 1994).

In future, a crucial experiment to support our hypothesis that Ste4 links Gpa1 activation to Byr2 activation is to prove that Gpa1 and Ste4 interact. Previously, using yeast-2-hybrid, Barr *et al.*, 1996 could not show an interaction between Ste4 and Gpa1 or Ras1, this could be due to the difficulty of using G-proteins in Y2H experiments as the interactions are usually dependent on the binding of GTP. Goddard *et al.*, 2006 successfully showed an interaction between Gpa1 and the predicted G β -subunit Gnr1

but this interaction may not be dependent on the GTP/GDP binding state of Gpa1. As I have shown that Gpa1.QL mimics mating factor signalling without pheromone stimulation it will be interesting to investigate if Gpa1.QL interacts with Ste4 but not Gpa1-wt using the yeast two hybrid system which may firstly confirm if the two proteins interact and whether their interaction is dependent on G-protein activation. A number of other proteins should also be tested to check for an interaction with Gpa1.QL, these include Ste6 and Ral2 (a predicted upstream component required for Ras1 activation (Fukui *et al.*, 1989) - See Chapter 5 Discussion) as well as Spk1 MAPK and Cdc42. In *S.cerevisiae*, pheromone activated MAPK, Fus3 is localised to the shmoo via *Gα* (Metodiev *et al.*, 2002) and is important for polarised growth as it phosphorylates an important formin protein required for actin assembly, Bni1 (Matheos *et al.*, 2004) and Fus3 phosphorylates $G\beta$ to stabilise the Far1- $G\beta$ complex and keep it at the cell cortex (Metodiev *et al.*, 2002). Far1 is a scaffold which localises activated Cdc42 to the site of polarised growth via Cdc24. During mitosis, Far1 sequesters Cdc24 in the nucleus and is released upon Far1 phosphorylation and degradation (Shimada *et al.*, 2000; Nern & Arkowitz, 2000) but during meiosis the Far1-Cdc24 complex relocates to the cell cortex and recruits Cdc42 and Bem1 away from the bud site to activate a shmoo site (Valtz *et al.*, 1995; Wiget *et al.*, 2004). Relating this to the *S.pombe* system, perhaps the G-protein (Gpa1 and possibly Gnr1) can interact with a number of components in order to coordinate the MFSP response.

We have shown that Ste4 is essential for Spk1 activation but the mechanism as to how this is achieved is still undefined. Ste4 has been shown to directly bind to Byr2 and is thought to potentially dimerise/oligomerise Byr2 to promote autophosphorylation (Ramachander *et al.*, 2002, Tu *et al.*, 1997). Regions of Ste4 show homology to the *S.cerevisiae* protein Ste50 which has been shown to bind to the regulatory region of

Ste11 (the MAPKKK of the pheromone response pathway). Yeast-2-hybrid studies showed that Ste50 cannot bind Byr2 and Ste4 cannot bind STE11 and that the region of Ste4 required for the interactions between another Ste4 protein and Byr2 are not conserved between Ste4 and Ste50 (Barr *et al.*, 1996) therefore it is difficult to draw similarities about the function of *S.pombe* Ste4 when comparing to *S.cerevisiae* Ste50.

8.1.4 Ste6 is the Ras1 GEF controlling the activation of both the MAPK branch and the morphology branch

We discovered that Ste6 is not essential for MAPK phosphorylation as opposed to Gpa1 and Ste4. We already concluded in Chapter 4 that Ras1 is not essential for MAPK phosphorylation but phosphorylation is greatly diminished in the absence of Ras1. The addition of *ras1.val17* into *ste6Δ* is enough to cause the elongated phenotype exhibited by the single *ras1.val17* mutant showing that the sole role of Ste6 is to activate Ras1. Further quantitation of *ste6Δ*, *ras1Δ* and a *ste6Δ ras1Δ* double mutant will help to uncover whether the MAPK phosphorylation seen in *ste6Δ* is a result of Ras1 activation through alternative means, perhaps through the additional Ras1 GEF Efc25.

Importantly, we have shown that Ste6 is required for activation of Ras1 for both the MAPK pathway and the morphology pathway in response to pheromone. It is likely that Ste6 is part of the multiprotein morphology complex along with Gap1 as these have both been seen to colocalise with Scd2 - personal communication with Sophie Martin's lab - perhaps forming a meiosis specific morphology complex. The function of Ral2 (Fukui *et al.*, 1989) in Ras1 activation should be assessed to further our understanding of how Ras1 is activated upon pheromone stimulation, it would be interesting to investigate whether Ral2 interacts with Gpa1, Ste4 and/or Ste6 as well as Ras1 itself.

8.1.5 The Importance of Negative Regulators

Investigations into the effects of deleting the known negative regulators *gap1*, *rgs1* and *sxa2* on MAPK phosphorylation revealed that all three are essential for the mating process and in their absence cells exhibit the elongated phenotype we associate with hyperactivated Ras1. All three mutants exhibit hypersensitive MAPK phosphorylation. We have shown that both the MAPK branch and the morphology branch are activated via Gpa1 and Ras1 therefore we assume that if the MAPK branch is being activated at an earlier stage after induction of mating compared to WT then so is the morphology branch and that it is activation of the morphology branch that is dictating the elongated phenotype in these mutants. In order to prove this hypothesis we require a quantitative read out for the activity of the Cdc42 pathway. One possibility is quantitation of the amount of Cdc42-GTP either via quantitative fluorescent imaging with the use of CRIB-GFP or by using a similar method as described for quantitation of the amount of Ras1-GTP (Chapter 6 Discussion) but using a PAK-CRIB pull-down assay, the CRIB (also known as the p21 binding domain, PBD) domain of PAK binds specifically to Cdc42-GTP and assay kits of this design are available commercially (Millipore 17-441, Cytoskeleton, inc #BK034). Manipulation of the activity of the Cdc42 pathway may also be efficient in rescuing the *ras1.val17* elongated phenotype, there are commercially available Cdc42 inhibitors (e.g. ML141 from Millipore), more specifically, a ATP-analogue sensitive version of *S.pombe* Pak1 could be generated following the method outlined in Chapter 7 Section 7.2.

8.1.6 GAPs as therapeutic targets

It has been well established that the oncogenic Ras mutant, Ras.G12V, in human cancer cell lines is resistant to the effects of Ras-GAP (Gibbs *et al.*, 1984) and that overexpression of Ras-GAP promotes cell survival by acting as an effector of Ras via

the inhibition of Rho-GAP thereby promoting Rho activity (Yang *et al.*, 2009). In these experiments with fission yeast, it appears that Ras1.val17 is still able to be affected by Gap1 if Gap1 is overexpressed. All GAP proteins contain a conserved GAP domain which is responsible for providing the GAP activity (Imai *et al.*, 1991). Unlike *S.pombe* Gap1, mammalian Ras-GAP has other characteristic signalling domains N-terminal to the GAP domain, including an SH3 domain, two SH2 domains and a PH domain which have been proven to be responsible for downstream signalling effects independent of Ras signalling (Yang *et al* 2009). Early experiments, carried out in 1986 (Nadin-Davis *et al.*, 1986a), introduced a human Ras sequence into *S.pombe* containing a null allele of Ras1, which restored meiosis with limited success, thus indicating that the human Ras sequence can complement *S. pombe* Ras1. This also indicates that *S.pombe* Gap1 is effective against human Ras in a *S.pombe* environment. These observations confirm that direct Ras manipulation is a promising approach for not only preventing the oncogenic phenotype in cells but actually promoting the WT phenotype. This highlights the importance of oncogenic Ras regulation in promoting a WT phenotype and suggests that attempts to manipulate Ras1 activity directly should be reassessed as a potential therapeutic approach.

8.1.7 Targeting the Cdc42 pathway as a therapeutic approach

In Chapter 4 we conclude that it is the activation status of Ras that is indicative of the final cellular phenotype independently of the duration of MAPK phosphorylation and that the *ras1.val17* oncogenic phenotype can only be prevented if MAPK phosphorylation is abolished completely as is the case of *ras1.val17 byr1Δ*. The complete inhibition of ERK MAPKs in Ras-transformed tumour cells is potentially unachievable and unrealistic in terms of a treatment strategy. Recently the contribution of the ERK effector pathway to Ras induced oncogenesis has been called into question

(Luo *et al.*, 2009) especially as MEK inhibition has had variable success in Ras malignancies compared with B-Raf driven malignancies which is probably because of the diverse number of Ras effector pathways. The work by Tuveson *et al.*, 2004 showed that endogenously expressed oncogenic Ras did not cause aberrant ERK activation in MEFs and was therefore unlikely to be causing the partial transformation phenotype seen in these cells. This has led to the quest for a more relevant and effective target for Ras-driven tumours. Published work by (Stengel & Zheng, 2012) has shown that gene targeting of Cdc42 impaired oncogenic H-Ras to drive tumour formation in mice and that this effect was partially dependent on Akt but not MEK and ERK therefore highlighting that Cdc42 is an attractive therapeutic target. This ties in with our work which suggests that targeting of the morphology pathway is likely to be more successful in preventing the oncogenic Ras phenotype compared to targeting the MAPK pathway.

8.1.8 The *ras1.val17* elongated phenotype

As described in 8.1.5 the hypothesis for why *ras1.val17* results in the formation of a single elongated conjugation tube during *S.pombe* mating is through hyperactivation of the Cdc42-morphology pathway and further experiments have been described to investigate this. We can hypothesise that an overactive Ras1-Cdc42 pathway is resulting in cells where partner recognition is defective. It is the role of agglutinins in the membrane to "stick" cells together therefore the agglutinins responsible for partner recognition could be mislocalised due to the uncoordinated timing of Cdc42/MAPK activation. Hyperactive Ras1 could also be hyperactivating the proteasome as part of its role in autophagy therefore important proteins may be prematurely degraded. It is also possible that the majority of the Ras1.val17 protein is localised on the plasma membrane and resulting in an inadequate pool of Ras1 on the endomembranes where is

has been shown to have a role in vesicle transportation thereby preventing the transport of specific proteins to the plasma membrane which are required for partner recognition.

Another important observation we wanted to address was as to why *ras1.val17* has no mitotic phenotype. We hypothesised that, as in WT cells, in *ras1.val17* mitotic growing cells, the Cdc42 GAPs, Rga4 and possibly Rga6, have the major role of limiting the areas of Cdc42 activation to the elongating cell tips and that Ras1 is primarily in an activated state. This could explain why there is no obvious deformation of cell shape in the *ras1.val17* mutant. Through personal communications with Graham Ladds and John Davey's groups at the University of Warwick, *ras1.val17* cells may be slightly chubbier than WT. We also observed this but have not quantified these cells for "chubbiness" therefore this currently remains to be an observation. We speculate that during mitosis, *ras1.val17* could be causing unwanted areas of Cdc42 activation resulting in a slight loss of the strictly controlled Cdc42-GTP gradient usually present at the cell tips (Tatebe *et al.*, 2008; Kelly & Nurse, 2011; Das *et al.*, 2007). The observation that the mitotic *ras1.val17* phenotype is subtle leads us to speculate that the activity of the Cdc42-morphology pathway must be subject to tight regulation downstream of Ras1. The fact that there is no mitotic phenotype in *gap1Δ* cells also highlights that either Ras1 activity is being controlled through a different unidentified RasGAP during mitosis or Ras1 is primarily in an activated state in mitotic cells.

Indeed, it has already been reported in the literature that the localisation of the Cdc42 GAP, Rga4, is extremely important in dictating the localisation of activated Cdc42 at the cell tips in mitotic cells (Tatebe *et al.*, 2008; Kelly & Nurse, 2011; Das *et al.*, 2007). Interestingly, when *rga4Δ* was introduced into the *ras1.val17* background (KT3084) the cells became large and rounded in morphology during vegetative growth compared to the WT phenotype usually observed in *ras1.val17* (data not shown). This provides firm

evidence that during mitosis the activation of Cdc42 is very tightly regulated at the level of Cdc42 itself and not at the level of Ras1.

In Chapter 4, we proposed two hypothesis as to how Spk1 could be contributing to the activation of shmooing; the Scd2 hypothesis and the Rga4/Rga6 hypothesis. Future experiments to investigate the Scd2 hypothesis are described in Chapter 4 discussion and involve an *in vitro* kinase assay using recombinant Scd2 and phospho-Spk1 followed by mass spectrometry. Potentially Spk1 could play a role in controlling the location of active Cdc42 at the shmoo site by indirectly regulating the activity of Rga4 or Rga6 which has recently been shown to be an additional Cdc42 GAP (Perez lab, Pombe 2013 - International Fission Yeast conference 2013). Both *rga4Δ* and *rga6Δ* strains have been generated in the lab but are still fully able to mate and sporulate at high efficiency when induced for meiosis.. We hypothesis that during mating, Spk1 could be phosphorylating and thereby inactivating Rga4 which would allow a concentrated level of Cdc42-GTP to accumulate at the site of pheromone stimulation. To investigate this further, we propose an experiment using the *h⁺gpa1.QL* mutant described in Chapter 5 which we have shown exhibits an elongated phenotype upon nitrogen starvation. If we delete *byr1* in *h⁺gpa1.QL* to abolish signalling via the MAPK cascade we predict that there will be no morphological change. Following this, if Rga4 or Rga6 were the Spk1 target, deletion of *rga4* (or *rga6*) would result in a morphological change as deletion of the Rga protein would mimic inhibition by Spk1. This experimental design is outlined in Appendix Figure 3.

8.2 Conclusions

In conclusion, the work presented in this thesis clearly defines the role of Ras1 in coordinating the mating response in *S.pombe* in terms of the activation of two

independent pathways; pheromone induced MAPK activation and the polarised growth response. There remains a number of important questions yet to be addressed which would make valuable additions to the works presented here. For example, what is the downregulatory mechanism for the MFSP downstream of Ras1? How is MAPK activation feeding into activation of the morphological response? And can the elongated phenotype be rescued by manipulation of the activity of the Cdc42-pathway - thereby making the Cdc42 pathway an important focus for therapeutic intervention? In order to investigate these questions a number of potential experiments have been proposed to further our understanding of the complexities governing the mating process in *S.pombe*.

APPENDICES

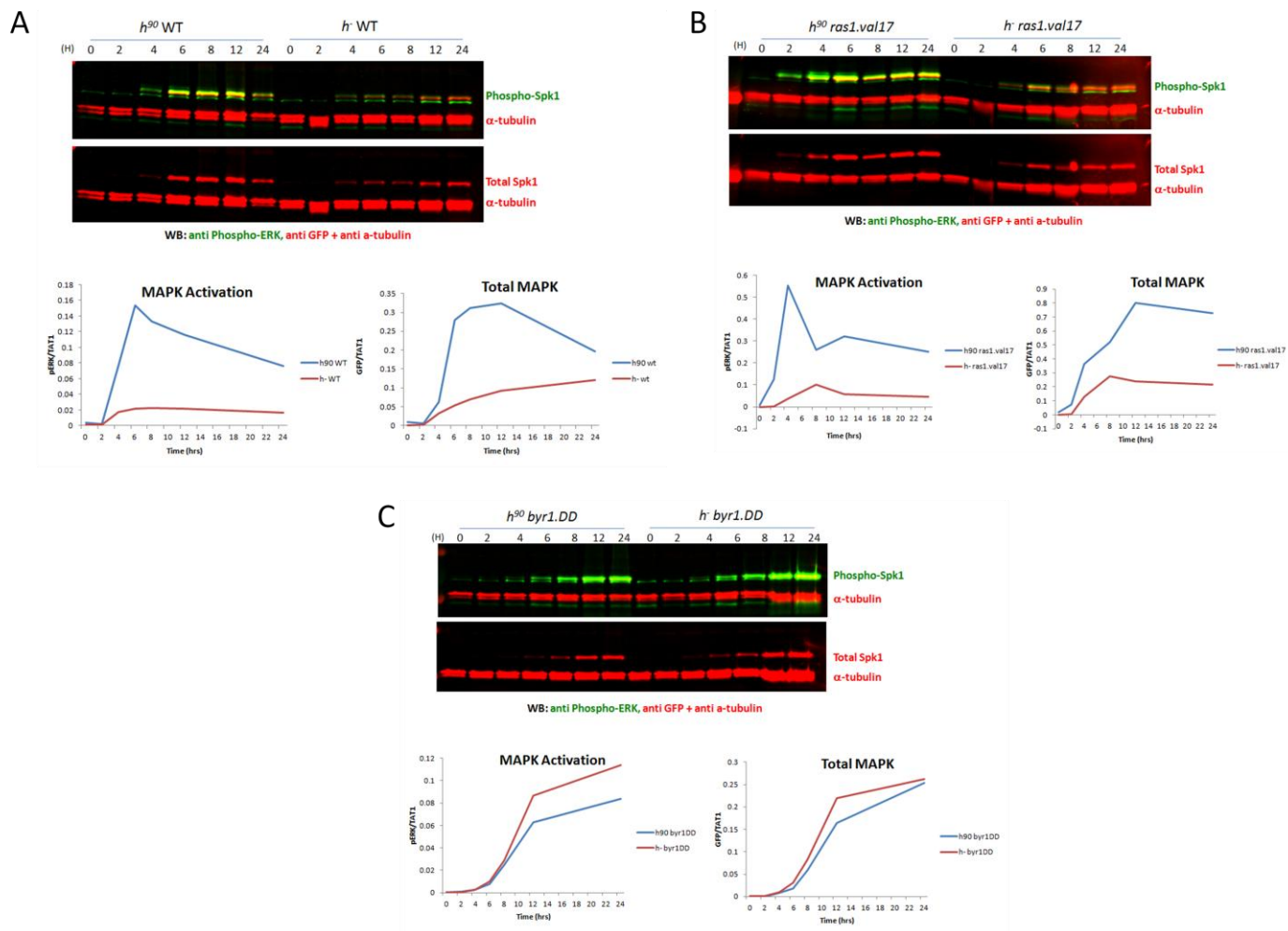


Figure 1. Phospho-Spk1 levels in *h⁻* WT, *h⁻ ras1.val17* and *h⁻ byr1.DD*

Western blot of *h⁻* WT (KT4190), *h⁻ ras1.val17* (KT4233) and *h⁻ byr1.DD* (KT4194) cell extracts directly ran against their *h⁹⁰* equivalent strains, KT3082, KT3084 and KT3453 respectively, membrane was blotted for phospho-ERK, GFP and α -tubulin. Extracts represent one technical replicate of one biological replicate. Below each western is the quantification of Phospho-MAPK/ α -tubulin and total-MAPK/ α -tubulin carried out using the Image Studio Ver2.1.

CD containing the movie file
attached to back page

Figure 2. Lifeact-GFP localisation in WT (KT3001) during conjugation.

The WT strain (KT3001), with LA-GFP successfully integrated into the genome, was set up for live imaging using a Nikon Eclipse Ti-E microscope and images taken every 3 minutes in the green and brightfield channels, selected images are shown in **Figure 7.10B**. Images were taken at each time-point in both the brightfield and GFP channels in order to visualise LA-GFP. Each time point comprises 15-25 serial images of 0.4 μm interval along the Z axis taken to span the full thickness of the cell. All of the LA-GFP images were deconvolved using the Huygens Essential Deconvolution. Deconvolved images were Z-projected, cropped and combined using ImageJ.

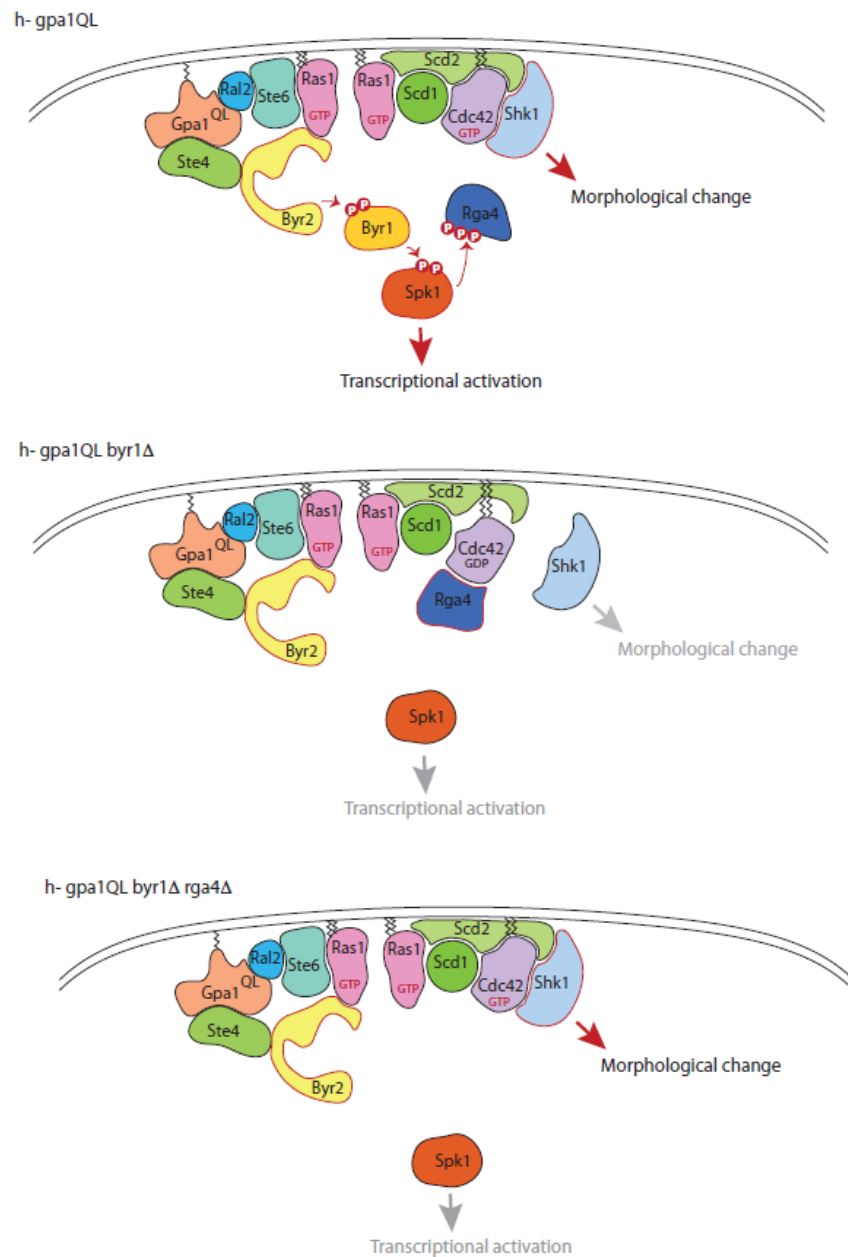


Figure 3. Experimental design to support Rga4/Rga6 hypothesis.

To investigate the hypothesis that Rga4 or Rga6 is the Spk1 target of the morphology pathway, we propose an experiment using the *h⁻gpa1.QL* mutant described in Chapter 5 which we have shown exhibits an elongated phenotype upon nitrogen starvation independently of pheromone (Top line). If we delete *byr1* in *h⁻gpa1.QL* to abolish signalling via the MAPK cascade we predict that there will be no morphological change (Middle line). Following this, if Rga4 or Rga6 were the Spk1 target, deletion of *rga4* (or *rga6*) would result in a morphological change as deletion of the Rga protein would mimic inhibition by Spk1 (Bottom line).

BIBLIOGRAPHY

Websites:

- PomBase <http://www.pombase.org/>
- Wikipedia http://en.wikipedia.org/wiki/Schizosaccharomyces_pombe
- Keogh Lab Protocols <https://sites.google.com/site/mckeogh2/protocols>
- Kinase Sequence Database <http://sequoia.ucsf.edu/ksd/>
- ClustalW <http://www.ebi.ac.uk/Tools/clustalw2/index.html>.
- pfam.sanger <http://pfam.sanger.ac.uk/search/sequence>.

Posters:

"Rga6 is a Cdc42 GAP that collaborates with Rga4 in the maintenance of fission yeast shape" Perez lab, Pombe 2013 - International Fission Yeast conference, London 2013

Thesis:

S Randhawa, MSc Thesis, University of Leicester, 2009

Journal Papers

Adachi, M., Fukuda, M., Nishida, E., 2000. Nuclear export of MAP kinase (ERK) involves a MAP kinase kinase (MEK)-dependent active transport mechanism. *The Journal of Cell Biology*. **148**, 849-856.

Aguilar, P.S., Engel, A., Walter, P., 2007. The plasma membrane proteins Prm1 and Fig1 ascertain fidelity of membrane fusion during yeast mating. *Molecular Biology of the Cell*. **18**, 547-556.

Alessi, D.R., Gomez, N., Moorhead, G., Lewis, T., Keyse, S.M., Cohen, P., 1995. Inactivation of p42 MAP kinase by protein phosphatase 2A and a protein tyrosine phosphatase, but not CL100, in various cell lines. *Current Biology : CB*. **5**, 283-295.

Alfa, C., Fantes, P., Hyams, J., McLeod, M. & Warwick, E., 1993. Experiments with Fission Yeast: A laboratory Manual. *Cold Spring Harbor Laboratory Press*.

Alvarez, B. & Moreno, S., 2006. Fission yeast Tor2 promotes cell growth and represses cell differentiation. *Journal of Cell Science*. **119**, 4475-4485.

Amoah-Buahin, E., Bone, N., Armstrong, J., 2005. Hyphal Growth in the Fission Yeast *Schizosaccharomyces pombe*. *Eukaryotic Cell*. **4**, 1287-1297.

- Angel Clemente-Ramos, J., Martin-Garcia, R., Sharifmoghadam, M.R., Konomi, M., Osumi, M., Valdivieso, M.-., 2009. The tetraspan protein Dni1p is required for correct membrane organization and cell wall remodelling during mating in *Schizosaccharomyces pombe*. *Molecular Microbiology*. **73**, 695-709.
- Asakawa, H., Haraguchi, T., Hiraoka, Y., 2007. Reconstruction of the kinetochore: A prelude to meiosis. *Cell Division*. **2**, .
- Augsten, M., Pusch, R., Biskup, C., Rennert, K., Wittig, U., Beyer, K., Blume, A., Wetzker, R., Friedrich, K., Rubio, I., 2006. Live-cell imaging of endogenous Ras-GTP illustrates predominant Ras activation at the plasma membrane. *EMBO Reports*. **7**, 46-51.
- Bahler, J., Schuchert, P., Grimm, C., Kohli, J., 1991. Synchronized meiosis and recombination in fission yeast: observations with pat1-114 diploid cells. *Current Genetics*. **19**, 445-451.
- Bahler, J., Wu, J.Q., Longtine, M.S., Shah, N.G., McKenzie, A.,3rd, Steever, A.B., Wach, A., Philippsen, P., Pringle, J.R., 1998. Heterologous modules for efficient and versatile PCR-based gene targeting in *Schizosaccharomyces pombe*. *Yeast (Chichester, England)*. **14**, 943-951.
- Barale, S., McCusker, D., Arkowitz, R.A., 2006. Cdc42p GDP/GTP cycling is necessary for efficient cell fusion during yeast mating. *Molecular Biology of the Cell*. **17**, 2824-2838.
- Barr, M.M., Tu, H., VanAelst, L., Wigler, M., 1996. Identification of Ste4 as a potential regulator of Byr2 in the sexual response pathway of *Schizosaccharomyces pombe*. *Molecular and Cellular Biology*. **16**, 5597-5603.
- Bar-Sagi, D., 2001. A Ras by any other name. *Molecular and Cellular Biology*. **21**, 1441-1443.
- Bauman, P., Cheng, Q.C., Albright, C.F., 1998. The Byr2 kinase translocates to the plasma membrane in a Ras1-dependent manner. *Biochemical & Biophysical Research Communications*. **244**, 468-474.
- Beach, D., Rodgers, L., Gould, J., 1985. Ran1+ Controls the Transition from Mitotic Division to Meiosis in Fission Yeast. *Current Genetics*. **10**, 297-311.
- Beeser, A., Jaffer, Z.M., Hofmann, C., Chernoff, J., 2005. Role of group A p21-activated kinases in activation of extracellular-regulated kinase by growth factors. *The Journal of Biological Chemistry*. **280**, 36609-36615.
- Bendezu, F.O. & Martin, S.G., 2013. Cdc42 explores the cell periphery for mate selection in fission yeast. *Current Biology : CB*. **23**, 42-47.
- Bishop, A.C., Ubersax, J.A., Petsch, D.T., Matheos, D.P., Gray, N.S., Blethrow, J., Shimizu, E., Tsien, J.Z., Schultz, P.G., Rose, M.D., Wood, J.L., Morgan, D.O., Shokat, K.M., 2000. A chemical switch for inhibitor-sensitive alleles of any protein kinase. *Nature*. **407**, 395-401.
- Bivona, T.G., Quatela, S., Philips, M.R., 2006. Analysis of Ras activation in living cells with GFP-RBD. *Methods in Enzymology*. **407**, 128-143.
- Bond, M., Croft, W., Tyson, R., Bretschneider, T., Davey, J., Ladds, G., 2013. Quantitative analysis of human ras localization and function in the fission yeast *Schizosaccharomyces pombe*. *Yeast (Chichester, England)*. **30**, 145-156.
- Bos, J.L., 1989. Ras Oncogenes in Human Cancer: a Review. *Cancer Research*. **49**, 4682-4689.
- Bossu, P., Vanoni, M., Wanke, V., Cesaroni, M.P., Tropea, F., Melillo, G., Asti, C., Porzio, S., Ruggiero, P., Di Cioccio, V., Maurizi, G., Ciabini, A., Alberghina, L., 2000. A dominant negative RAS-specific

- guanine nucleotide exchange factor reverses neoplastic phenotype in K-ras transformed mouse fibroblasts. *Oncogene*. **19**, 2147-2154.
- Bourne, H.R., Sanders, D.A., McCormick, F., 1990. The GTPase superfamily: a conserved switch for diverse cell functions. *Nature*. **348**, 125-132.
- Bresch, C., Muller, G., Egel, R., 1968. Genes involved in meiosis and sporulation of a yeast. *Molecular & General Genetics : MGG*. **102**, 301-306.
- Brizzio, V., Gammie, A.E., Nijbroek, G., Michaelis, S., Rose, M.D., 1996. Cell fusion during yeast mating requires high levels of a-factor mating pheromone. *The Journal of Cell Biology*. **135**, 1727-1739.
- Brownbridge, G.G., Lowe, P.N., Moore, K.J., Skinner, R.H., Webb, M.R., 1993. Interaction of GTPase activating proteins (GAPs) with p21ras measured by a novel fluorescence anisotropy method. Essential role of Arg-903 of GAP in activation of GTP hydrolysis on p21ras. *The Journal of Biological Chemistry*. **268**, 10914-10919.
- Brunet, A., Pages, G., Pouyssegur, J., 1994. Growth factor-stimulated MAP kinase induces rapid retrophosphorylation and inhibition of MAP kinase kinase (MEK1). *FEBS Letters*. **346**, 299-303.
- Butty, A.C., Pryciak, P.M., Huang, L.S., Herskowitz, I., Peter, M., 1998. The role of Far1p in linking the heterotrimeric G protein to polarity establishment proteins during yeast mating. *Science (New York, N.Y.)*. **282**, 1511-1516.
- Buzko, O. & Shokat, K.M., 2002. A kinase sequence database: sequence alignments and family assignment. *Bioinformatics (Oxford, England)*. **18**, 1274-1275.
- Capon, D.J., Chen, E.Y., Levinson, A.D., Seeburg, P.H., Goeddel, D.V., 1983. Complete nucleotide sequences of the T24 human bladder carcinoma oncogene and its normal homologue. *Nature*. **302**, 33-37.
- Chalmers, C.J., Gilley, R., March, H.N., Balmanno, K., Cook, S.J., 2007. The duration of ERK1/2 activity determines the activation of c-Fos and Fra-1 and the composition and quantitative transcriptional output of AP-1. *Cellular Signalling*. **19**, 695-704.
- Chan, R.K. & Otte, C.A., 1982. Physiological characterization of *Saccharomyces cerevisiae* mutants supersensitive to G1 arrest by a factor and alpha factor pheromones. *Molecular and Cellular Biology*. **2**, 21-29.
- Chang, E., Bartholomeusz, G., Pimental, R., Chen, J., Lai, H., Wang, L., Yang, P., Marcus, S., 1999. Direct binding and In vivo regulation of the fission yeast p21-activated kinase shk1 by the SH3 domain protein scd2. *Molecular and Cellular Biology*. **19**, 8066-8074.
- Chang, E.C., Barr, M., Wang, Y., Jung, V., Xu, H.P., Wigler, M.H., 1994. Cooperative interaction of *S. pombe* proteins required for mating and morphogenesis. *Cell*. **79**, 131-141.
- Chang, E.C. & Philips, M.R., 2006. Spatial segregation of Ras signaling: new evidence from fission yeast. *Cell Cycle (Georgetown, Tex.)*. **5**, 1936-1939.
- Chang, F. & Peter, M., 2003. Yeasts make their mark. *Nature Cell Biology*. **5**, 294-299.
- Chen, C.R., Li, Y.C., Chen, J., Hou, M.C., Papadaki, P., Chang, E.C., 1999. Moe1, a conserved protein in *Schizosaccharomyces pombe*, interacts with a Ras effector, Scd1, to affect proper spindle formation. *Proceedings of the National Academy of Sciences of the United States of America*. **96**, 517-522.
- Chen, Q. & Konopka, J.B., 1996. Regulation of the G-protein-coupled alpha-factor pheromone receptor by phosphorylation. *Molecular and Cellular Biology*. **16**, 247-257.

- Cheng, C.M., Li, H., Gasman, S., Huang, J., Schiff, R., Chang, E.C., 2011. Compartmentalized Ras proteins transform NIH 3T3 cells with different efficiencies. *Molecular and Cellular Biology*. **31**, 983-997.
- Chikashige, Y., Kurokawa, R., Haraguchi, T., Hiraoka, Y., 2004. Meiosis induced by inactivation of Pat1 kinase proceeds with aberrant nuclear positioning of centromeres in the fission yeast *Schizosaccharomyces pombe*. *Genes to Cells : Devoted to Molecular & Cellular Mechanisms*. **9**, 671-684.
- Coll, P.M., Trillo, Y., Ametzazurra, A., Perez, P., 2003. Gef1p, a new guanine nucleotide exchange factor for Cdc42p, regulates polarity in *Schizosaccharomyces pombe*. *Molecular Biology of the Cell*. **14**, 313-323.
- Cortes, J.C., Carnero, E., Ishiguro, J., Sanchez, Y., Duran, A., Ribas, J.C., 2005. The novel fission yeast (1,3)beta-D-glucan synthase catalytic subunit Bgs4p is essential during both cytokinesis and polarized growth. *Journal of Cell Science*. **118**, 157-174.
- Coudreuse, D., van Bakel, H., Dewez, M., Soutourina, J., Parnell, T., Vandenhoute, J., Cairns, B., Werner, M., Hermand, D., 2010. A gene-specific requirement of RNA polymerase II CTD phosphorylation for sexual differentiation in *S. pombe*. *Current Biology : CB*. **20**, 1053-1064.
- Daniel Gietz, R. & Woods, R.A., Transformation of yeast by lithium acetate/single-stranded carrier DNA/polyethylene glycol method. *Methods in Enzymology*. Academic Press. 87-96.
- Das, M., Drake, T., Wiley, D.J., Buchwald, P., Vavylonis, D., Verde, F., 2012. Oscillatory dynamics of Cdc42 GTPase in the control of polarized growth. *Science (New York, N.Y.)*. **337**, 239-243.
- Das, M., Wiley, D.J., Medina, S., Vincent, H.A., Larrea, M., Oriolo, A., Verde, F., 2007. Regulation of cell diameter, For3p localization, and cell symmetry by fission yeast Rho-GAP Rga4p. *Molecular Biology of the Cell*. **18**, 2090-2101.
- Davey, J., 1992. Mating pheromones of the fission yeast *Schizosaccharomyces pombe*: purification and structural characterization of M-factor and isolation and analysis of two genes encoding the pheromone. *The EMBO Journal*. **11**, 951-960.
- Davey, J. & Nielsen, O., 1994. Mutations in *cyr1* and *pat1* reveal pheromone-induced G1 arrest in the fission yeast *Schizosaccharomyces pombe*. *Current Genetics*. **26**, 105-112.
- de Rooij, J. & Bos, J.L., 1997. Minimal Ras-binding domain of Raf1 can be used as an activation-specific probe for Ras. *Oncogene*. **14**, 623-625.
- De Vries, L., Zheng, B., Fischer, T., Elenko, E., Farquhar, M.G., 2000. The regulator of G protein signaling family. *Annual Review of Pharmacology and Toxicology*. **40**, 235-271.
- Der, C.J., Krontiris, T.G., Cooper, G.M., 1982. Transforming genes of human bladder and lung carcinoma cell lines are homologous to the ras genes of Harvey and Kirsten sarcoma viruses. *Proceedings of the National Academy of Sciences of the United States of America*. **79**, 3637-3640.
- DeVoti, J., Seydoux, G., Beach, D., McLeod, M., 1991. Interaction between *ran1+* protein kinase and cAMP dependent protein kinase as negative regulators of fission yeast meiosis. *The EMBO Journal*. **10**, 3759-3768.
- Dhillon, A.S., von Kriegsheim, A., Grindlay, J., Kolch, W., 2007. Phosphatase and feedback regulation of Raf-1 signaling. *Cell Cycle (Georgetown, Tex.)*. **6**, 3-7.
- Didmon, M., Davis, K., Watson, P., Ladds, G., Broad, P., Davey, J., 2002. Identifying regulators of pheromone signalling in the fission yeast *Schizosaccharomyces pombe*. *Current Genetics*. **41**, 241-253.

- Dikic, I., Schlessinger, J., Lax, I., 1994. PC12 cells overexpressing the insulin receptor undergo insulin-dependent neuronal differentiation. *Current Biology : CB*. **4**, 702-708.
- Ding, D.Q., Yamamoto, A., Haraguchi, T., Hiraoka, Y., 2004. Dynamics of homologous chromosome pairing during meiotic prophase in fission yeast. *Developmental Cell*. **6**, 329-341.
- Dohlman, H.G., Song, J., Ma, D., Courchesne, W.E., Thorner, J., 1996. Sst2, a negative regulator of pheromone signaling in the yeast *Saccharomyces cerevisiae*: expression, localization, and genetic interaction and physical association with Gpa1 (the G-protein alpha subunit). *Molecular and Cellular Biology*. **16**, 5194-5209.
- Dohlman, H.G. & Thorner, J., 1997. RGS proteins and signaling by heterotrimeric G proteins. *The Journal of Biological Chemistry*. **272**, 3871-3874.
- Doi, K., Gartner, A., Ammerer, G., Errede, B., Shinkawa, H., Sugimoto, K., Matsumoto, K., 1994. MSG5, a novel protein phosphatase promotes adaptation to pheromone response in *S. cerevisiae*. *The EMBO Journal*. **13**, 61-70.
- Downward, J., 2006. Signal transduction. Prelude to an anniversary for the RAS oncogene. *Science (New York, N.Y.)*. **314**, 433-434.
- Downward, J., 2003. Targeting RAS signalling pathways in cancer therapy. *Nature Reviews.Cancer*. **3**, 11-22.
- Doyle, A., Martin-Garcia, R., Coulton, A.T., Bagley, S., Mulvihill, D.P., 2009. Fission yeast Myo51 is a meiotic spindle pole body component with discrete roles during cell fusion and spore formation. *Journal of Cell Science*. **122**, 4330-4340.
- Ebisuya, M., Kondoh, K., Nishida, E., 2005. The duration, magnitude and compartmentalization of ERK MAP kinase activity: mechanisms for providing signaling specificity. *Journal of Cell Science*. **118**, 2997-3002.
- Eccleston, J.F., Moore, K.J., Morgan, L., Skinner, R.H., Lowe, P.N., 1993. Kinetics of interaction between normal and proline 12 Ras and the GTPase-activating proteins, p120-GAP and neurofibromin. The significance of the intrinsic GTPase rate in determining the transforming ability of ras. *The Journal of Biological Chemistry*. **268**, 27012-27019.
- Egel, R., 1973. Genes involved in mating type expression of fission yeast. *Molecular & General Genetics* : *MGG*. **122**, 339-343.
- Elion, E.A., 2001. The Ste5p scaffold. *Journal of Cell Science*. **114**, 3967-3978.
- Elion, E.A., 2000. Pheromone response, mating and cell biology. *Current Opinion in Microbiology*. **3**, 573-581.
- Endo, M., Shirouzu, M., Yokoyama, S., 2003. The Cdc42 binding and scaffolding activities of the fission yeast adaptor protein Scd2. *The Journal of Biological Chemistry*. **278**, 843-852.
- Estravis, M., Rincon, S., Perez, P., 2012. Cdc42 regulation of polarized traffic in fission yeast. *Communicative & Integrative Biology*. **5**, 370-373.
- Feierbach, B. & Chang, F., 2001. Roles of the fission yeast formin for3p in cell polarity, actin cable formation and symmetric cell division. *Current Biology : CB*. **11**, 1656-1665.
- Fernandez-Medarde, A. & Santos, E., 2011. Ras in cancer and developmental diseases. *Genes & Cancer*. **2**, 344-358.

- Freed, E., Symons, M., Macdonald, S.G., McCormick, F., Ruggieri, R., 1994. Binding of 14-3-3 proteins to the protein kinase Raf and effects on its activation. *Science (New York, N.Y.)*. **265**, 1713-1716.
- Frost, J.A., Steen, H., Shapiro, P., Lewis, T., Ahn, N., Shaw, P.E., Cobb, M.H., 1997. Cross-cascade activation of ERKs and ternary complex factors by Rho family proteins. *The EMBO Journal*. **16**, 6426-6438.
- Fujimura, H.A., 1994. Yeast homolog of mammalian mitogen-activated protein kinase, FUS3/DAC2 kinase, is required both for cell fusion and for G1 arrest of the cell cycle and morphological changes by the *cdc37* mutation. *Journal of Cell Science*. **107 (Pt 9)**, 2617-2622.
- Fukui, Y. & Kaziro, Y., 1985. Molecular cloning and sequence analysis of a ras gene from *Schizosaccharomyces pombe*. *The EMBO Journal*. **4**, 687-691.
- Fukui, Y., Kozasa, T., Kaziro, Y., Takeda, T., Yamamoto, M., 1986. Role of a ras homolog in the life cycle of *Schizosaccharomyces pombe*. *Cell*. **44**, 329-336.
- Fukui, Y., Miyake, S., Satoh, M., Yamamoto, M., 1989. Characterization of the *Schizosaccharomyces pombe* *ral2* gene implicated in activation of the *ras1* gene product. *Molecular and Cellular Biology*. **9**, 5617-5622.
- Fukui, Y. & Yamamoto, M., 1988. Isolation and characterization of *Schizosaccharomyces pombe* mutants phenotypically similar to *ras1-*. *Molecular & General Genetics : MGG*. **215**, 26-31.
- Funaya, C., Samarasinghe, S., Prugnaller, S., Ohta, M., Connolly, Y., Muller, J., Murakami, H., Grallert, A., Yamamoto, M., Smith, D., Antony, C., Tanaka, K., 2012. Transient structure associated with the spindle pole body directs meiotic microtubule reorganization in *S. pombe*. *Current Biology : CB*. **22**, 562-574.
- Gardner, A.M., Vaillancourt, R.R., Lange-Carter, C.A., Johnson, G.L., 1994. MEK-1 phosphorylation by MEK kinase, Raf, and mitogen-activated protein kinase: analysis of phosphopeptides and regulation of activity. *Molecular Biology of the Cell*. **5**, 193-201.
- Gibbs, J.B., Schaber, M.D., Allard, W.J., Sigal, I.S., Scolnick, E.M., 1988. Purification of ras GTPase activating protein from bovine brain. *Proceedings of the National Academy of Sciences of the United States of America*. **85**, 5026-5030.
- Gibbs, J.B., Sigal, I.S., Poe, M., Scolnick, E.M., 1984. Intrinsic GTPase activity distinguishes normal and oncogenic ras p21 molecules. *Proceedings of the National Academy of Sciences of the United States of America*. **81**, 5704-5708.
- Gietz, R.D., 2006. *The Gietz Lab Yeast Transformation Home Page*. [online]. Available at: <http://home.cc.umanitoba.ca/~gietz/> [accessed 01/04 2010].
- Glynn, J.M., Lustig, R.J., Berlin, A., Chang, F., 2001. Role of *bud6p* and *tea1p* in the interaction between actin and microtubules for the establishment of cell polarity in fission yeast. *Current Biology : CB*. **11**, 836-845.
- Goddard, A., Ladds, G., Forfar, R., Davey, J., 2006. Identification of *Gnr1p*, a negative regulator of G alpha signalling in *Schizosaccharomyces pombe*, and its complementation by human G beta subunits. *Fungal Genetics and Biology : FG & B*. **43**, 840-851.
- Good, M., Tang, G., Singleton, J., Remenyi, A., Lim, W.A., 2009. The Ste5 scaffold directs mating signaling by catalytically unlocking the Fus3 MAP kinase for activation. *Cell*. **136**, 1085-1097.

- Gopalbhai, K., Jansen, G., Beauregard, G., Whiteway, M., Dumas, F., Wu, C., Meloche, S., 2003. Negative regulation of MAPKK by phosphorylation of a conserved serine residue equivalent to Ser212 of MEK1. *The Journal of Biological Chemistry*. **278**, 8118-8125.
- Gotoh, Y., Matsuda, S., Takenaka, K., Hattori, S., Iwamatsu, A., Ishikawa, M., Kosako, H., Nishida, E., 1994. Characterization of recombinant *Xenopus* MAP kinase kinases mutated at potential phosphorylation sites. *Oncogene*. **9**, 1891-1898.
- Gotoh, Y., Nishida, E., Shimanuki, M., Toda, T., Imai, Y., Yamamoto, M., 1993. Schizosaccharomyces pombe Spk1 is a tyrosine-phosphorylated protein functionally related to *Xenopus* mitogen-activated protein kinase. *Molecular & Cellular Biology*. **13**, 6427-6434.
- Goyal, A. & Simanis, V., 2012. Characterization of ypa1 and ypa2, the Schizosaccharomyces pombe orthologs of the peptidyl prolyl isomerases that activate PP2A, reveals a role for Ypa2p in the regulation of cytokinesis. *Genetics*. **190**, 1235-1250.
- Gregan, J., Zhang, C., Rumpf, C., Cipak, L., Li, Z., Uluocak, P., Nasmyth, K., Shokat, K.M., 2007. Construction of conditional analog-sensitive kinase alleles in the fission yeast Schizosaccharomyces pombe. *Nature Protocols*. **2**, 2996-3000.
- Grewal, T., Koese, M., Tebar, F., Enrich, C., 2011. Differential Regulation of RasGAPs in Cancer. *Genes & Cancer*. **2**, 288-297.
- Gutz, H. & Doe, F.J., 1973. Two different h- mating types in Schizosaccharomyces pombe. *Genetics*. **74**, 563-569.
- Hancock, J.F., Magee, A.I., Childs, J.E., Marshall, C.J., 1989. All ras proteins are polyisoprenylated but only some are palmitoylated. *Cell*. **57**, 1167-1177.
- Hancock, J.F., Paterson, H., Marshall, C.J., 1990. A polybasic domain or palmitoylation is required in addition to the CAAX motif to localize p21ras to the plasma membrane. *Cell*. **63**, 133-139.
- Harigaya, Y., Tanaka, H., Yamanaka, S., Tanaka, K., Watanabe, Y., Tsutsumi, C., Chikashige, Y., Hiraoka, Y., Yamashita, A., Yamamoto, M., 2006. Selective elimination of messenger RNA prevents an incidence of untimely meiosis. *Nature*. **442**, 45-50.
- Harigaya, Y. & Yamamoto, M., 2007. Molecular mechanisms underlying the mitosis-meiosis decision. *Chromosome Research*. **15**, 523-537.
- Hayles, J. & Nurse, P., 2001. A journey into space. *Nature Reviews.Molecular Cell Biology*. **2**, 647-656.
- Heiman, M.G., Engel, A., Walter, P., 2007. The Golgi-resident protease Kex2 acts in conjunction with Prm1 to facilitate cell fusion during yeast mating. *The Journal of Cell Biology*. **176**, 209-222.
- Heiman, M.G. & Walter, P., 2000. Prm1p, a pheromone-regulated multispinning membrane protein, facilitates plasma membrane fusion during yeast mating. *The Journal of Cell Biology*. **151**, 719-730.
- Hentges, P., Van Driessche, B., Tafforeau, L., Vandenhoute, J., Carr, A.M., 2005. Three novel antibiotic marker cassettes for gene disruption and marker switching in Schizosaccharomyces pombe. *Yeast (Chichester, England)*. **22**, 1013-1019.
- Hirota, K., Tanaka, K., Ohta, K., Yamamoto, M., 2003. Gef1p and Scd1p, the Two GDP-GTP exchange factors for Cdc42p, form a ring structure that shrinks during cytokinesis in Schizosaccharomyces pombe. *Molecular Biology of the Cell*. **14**, 3617-3627.
- Hirota, K., Tanaka, K., Watanabe, Y., Yamamoto, M., 2001. Functional analysis of the C-terminal cytoplasmic region of the M-factor receptor in fission yeast. *Genes to Cells*. **6**, 201-214.

- Hoffman, C.S., 2005. Glucose sensing via the protein kinase A pathway in *Schizosaccharomyces pombe*. *Biochemical Society Transactions*. **33**, 257-260.
- Hoffman, C.S. & Winston, F., 1991. Glucose repression of transcription of the *Schizosaccharomyces pombe* *fbp1* gene occurs by a cAMP signaling pathway. *Genes & Development*. **5**, 561-571.
- Hughes, D.A., 1995. Control of signal transduction and morphogenesis by Ras. *Seminars in Cell Biology*. **6**, 89-94.
- Hughes, D.A., Fukui, Y., Yamamoto, M., 1990. Homologous activators of ras in fission and budding yeast. *Nature*. **344**, 355-357.
- Hughes, D.A., Yabana, N., Yamamoto, M., 1994. Transcriptional regulation of a Ras nucleotide-exchange factor gene by extracellular signals in fission yeast. *Journal of Cell Science*. **107 (Pt 12)**, 3635-3642.
- Iino, Y. & Yamamoto, M., 1985. Negative control for the initiation of meiosis in *Schizosaccharomyces pombe*. *Proceedings of the National Academy of Sciences of the United States of America*. **82**, 2447-2451.
- Imai, Y., Miyake, S., Hughes, D.A., Yamamoto, M., 1991. Identification of a Gtpase-Activating Protein Homolog in *Schizosaccharomyces-Pombe*. *Molecular and Cellular Biology*. **11**, 3088-3094.
- Imai, Y. & Yamamoto, M., 1994. The fission yeast mating pheromone P-factor: its molecular structure, gene structure, and ability to induce gene expression and G1 arrest in the mating partner. *Genes & Development*. **8**, 328-338.
- Imai, Y. & Yamamoto, M., 1992. *Schizosaccharomyces-Pombe* Sxa1+ and Sxa2+ Encode Putative Proteases Involved in the Mating Response. *Molecular and Cellular Biology*. **12**, 1827-1834.
- Isshiki, T., Mochizuki, N., Maeda, T., Yamamoto, M., 1992. Characterization of a fission yeast gene, *gpa2*, that encodes a G alpha subunit involved in the monitoring of nutrition. *Genes & Development*. **6**, 2455-2462.
- Iwaki, N., Karatsu, K., Miyamoto, M., 2003. Role of guanine nucleotide exchange factors for Rho family GTPases in the regulation of cell morphology and actin cytoskeleton in fission yeast. *Biochemical and Biophysical Research Communications*. **312**, 414-420.
- Jaaro, H., Rubinfeld, H., Hanoch, T., Seger, R., 1997. Nuclear translocation of mitogen-activated protein kinase kinase (MEK1) in response to mitogenic stimulation. *Proceedings of the National Academy of Sciences of the United States of America*. **94**, 3742-3747.
- Johnson, D.I., 1999. Cdc42: An essential Rho-type GTPase controlling eukaryotic cell polarity. *Microbiology and Molecular Biology Reviews* : *MMBR*. **63**, 54-105.
- Kanoh, J., Watanabe, Y., Ohsugi, M., Iino, Y., Yamamoto, M., 1996. *Schizosaccharomyces pombe* *gad7+* encodes a phosphoprotein with a bZIP domain, which is required for proper G1 arrest and gene expression under nitrogen starvation. *Genes to Cells : Devoted to Molecular & Cellular Mechanisms*. **1**, 391-408.
- Kataoka, T., Powers, S., McGill, C., Fasano, O., Strathern, J., Broach, J., Wigler, M., 1984. Genetic analysis of yeast RAS1 and RAS2 genes. *Cell*. **37**, 437-445.
- Kawamukai, M., Ferguson, K., Wigler, M., Young, D., 1991. Genetic and biochemical analysis of the adenylyl cyclase of *Schizosaccharomyces pombe*. *Cell Regulation*. **2**, 155-164.

- Kelly, F.D. & Nurse, P., 2011. Spatial control of Cdc42 activation determines cell width in fission yeast. *Molecular Biology of the Cell*.
- Kelly, M., Burke, J., Smith, M., Klar, A., Beach, D., 1988. Four mating-type genes control sexual differentiation in the fission yeast. *EMBO Journal*. **7**, 1537-1547.
- Kim, H., Yang, P., Catanuto, P., Verde, F., Lai, H., Du, H., Chang, F., Marcus, S., 2003. The kelch repeat protein, Teal1, is a potential substrate target of the p21-activated kinase, Shk1, in the fission yeast, *Schizosaccharomyces pombe*. *The Journal of Biological Chemistry*. **278**, 30074-30082.
- King, A.J., Sun, H., Diaz, B., Barnard, D., Miao, W., Bagrodia, S., Marshall, M.S., 1998. The protein kinase Pak3 positively regulates Raf-1 activity through phosphorylation of serine 338. *Nature*. **396**, 180-183.
- Kinoshita, N., Ohkura, H., Yanagida, M., 1990. Distinct, essential roles of type 1 and 2A protein phosphatases in the control of the fission yeast cell division cycle. *Cell*. **63**, 405-415.
- Kitamura, K., Katayama, S., Dhut, S., Sato, M., Watanabe, Y., Yamamoto, M., Toda, T., 2001. Phosphorylation of Mei2 and Ste11 by Pat1 kinase inhibits sexual differentiation via ubiquitin proteolysis and 14-3-3 protein in fission yeast. *Developmental Cell*. **1**, 389-399.
- Kitamura, K. & Shimoda, C., 1991. The *Schizosaccharomyces pombe* mam2 gene encodes a putative pheromone receptor which has a significant homology with the *Saccharomyces cerevisiae* Ste2 protein. *The EMBO Journal*. **10**, 3743-3751.
- Kjaerulff, S., Andersen, N.R., Borup, M.T., Nielsen, O., 2007. Cdk phosphorylation of the Ste11 transcription factor constrains differentiation-specific transcription to G1. *Genes & Development*. **21**, 347-359.
- Kjaerulff, S., Lautrup-Larsen, I., Truelsen, S., Pedersen, M., Nielsen, O., 2005. Constitutive activation of the fission yeast pheromone-responsive pathway induces ectopic meiosis and reveals ste11 as a mitogen-activated protein kinase target. *Molecular & Cellular Biology*. **25**, 2045-2059.
- Kubicek, M., Pacher, M., Abraham, D., Podar, K., Eulitz, M., Baccarini, M., 2002. Dephosphorylation of Ser-259 regulates Raf-1 membrane association. *The Journal of Biological Chemistry*. **277**, 7913-7919.
- Kunitomo, H., Higuchi, T., Iino, Y., Yamamoto, M., 2000. A zinc-finger protein, Rst2p, regulates transcription of the fission yeast ste11(+) gene, which encodes a pivotal transcription factor for sexual development. *Molecular Biology of the Cell*. **11**, 3205-3217.
- Kurahashi, H., Imai, Y., Yamamoto, M., 2002. Tropomyosin is required for the cell fusion process during conjugation in fission yeast. *Genes to Cells : Devoted to Molecular & Cellular Mechanisms*. **7**, 375-384.
- Ladds, G. & Davey, J., 2000. Sxa2 is a serine carboxypeptidase that degrades extracellular P-factor in the fission yeast *Schizosaccharomyces pombe*. *Molecular Microbiology*. **36**, 377-390.
- Ladds, G., Rasmussen, E.M., Young, T., Nielsen, O., Davey, J., 1996. The sxa2-dependent inactivation of the P-factor mating pheromone in the fission yeast *Schizosaccharomyces pombe*. *Molecular Microbiology*. **20**, 35-42.
- Laemmli, U.K., 1970. Cleavage of structural proteins during the assembly of the head of bacteriophage T4. *Nature*. **227**, 680-685.
- Leeuw, T., Fourest-Lieuvain, A., Wu, C., Chenevert, J., Clark, K., Whiteway, M., Thomas, D.Y., Leberer, E., 1995. Pheromone response in yeast: association of Bem1p with proteins of the MAP kinase cascade and actin. *Science (New York, N.Y.)*. **270**, 1210-1213.

- Leeuw, T., Wu, C., Schrag, J.D., Whiteway, M., Thomas, D.Y., Leberer, E., 1998. Interaction of a G-protein beta-subunit with a conserved sequence in Ste20/PAK family protein kinases. *Nature*. **391**, 191-195.
- Leevers, S.J., Paterson, H.F., Marshall, C.J., 1994. Requirement for Ras in Raf activation is overcome by targeting Raf to the plasma membrane. *Nature*. **369**, 411-414.
- Li, P. & McLeod, M., 1996. Molecular mimicry in development: identification of stel1+ as a substrate and mei3+ as a pseudosubstrate inhibitor of ran1+ kinase. *Cell*. **87**, 869-880.
- Li, W., Chong, H., Guan, K.L., 2001. Function of the Rho family GTPases in Ras-stimulated Raf activation. *The Journal of Biological Chemistry*. **276**, 34728-34737.
- Li, Y. & Chang, E.C., 2003. Schizosaccharomyces pombe Ras1 effector, Scd1, interacts with Klp5 and Klp6 kinesins to mediate cytokinesis. *Genetics*. **165**, 477-488.
- Li, Y.C., Chen, C.R., Chang, E.C., 2000. Fission yeast Ras1 effector Scd1 interacts with the spindle and affects its proper formation. *Genetics*. **156**, 995-1004.
- Lobell, R.B., Omer, C.A., Abrams, M.T., Bhimnathwala, H.G., Brucker, M.J., Buser, C.A., Davide, J.P., deSolms, S.J., Dinsmore, C.J., Ellis-Hutchings, M.S., Kral, A.M., Liu, D., Lumma, W.C., Machotka, S.V., Rands, E., Williams, T.M., Graham, S.L., Hartman, G.D., Oliff, A.I., Heimbrook, D.C., Kohl, N.E., 2001. Evaluation of farnesyl:protein transferase and geranylgeranyl:protein transferase inhibitor combinations in preclinical models. *Cancer Research*. **61**, 8758-8768.
- Luo, J., Emanuele, M.J., Li, D., Creighton, C.J., Schlabach, M.R., Westbrook, T.F., Wong, K.K., Elledge, S.J., 2009. A genome-wide RNAi screen identifies multiple synthetic lethal interactions with the Ras oncogene. *Cell*. **137**, 835-848.
- Maeda, T., Mochizuki, N., Yamamoto, M., 1990. Adenylyl cyclase is dispensable for vegetative cell growth in the fission yeast Schizosaccharomyces pombe. *Proceedings of the National Academy of Sciences of the United States of America*. **87**, 7814-7818.
- Maeda, T., Watanabe, Y., Kunitomo, H., Yamamoto, M., 1994. Cloning of the pka1 gene encoding the catalytic subunit of the cAMP-dependent protein kinase in Schizosaccharomyces pombe. *The Journal of Biological Chemistry*. **269**, 9632-9637.
- Mansour, S.J., Resing, K.A., Candi, J.M., Hermann, A.S., Gloor, J.W., Herskind, K.R., Wartmann, M., Davis, R.J., Ahn, N.G., 1994. Mitogen-activated protein (MAP) kinase phosphorylation of MAP kinase kinase: determination of phosphorylation sites by mass spectrometry and site-directed mutagenesis. *Journal of Biochemistry*. **116**, 304-314.
- Marais, R., Light, Y., Paterson, H.F., Marshall, C.J., 1995. Ras recruits Raf-1 to the plasma membrane for activation by tyrosine phosphorylation. *The EMBO Journal*. **14**, 3136-3145.
- Marcus, S., Polverino, A., Chang, E., Robbins, D., Cobb, M.H., Wigler, M.H., 1995. Shk1, a homolog of the Saccharomyces cerevisiae Ste20 and mammalian p65PAK protein kinases, is a component of a Ras/Cdc42 signaling module in the fission yeast Schizosaccharomyces pombe. *Proceedings of the National Academy of Sciences of the United States of America*. **92**, 6180-6184.
- Martin, S.G., 2009. Microtubule-dependent cell morphogenesis in the fission yeast. *Trends in Cell Biology*. **19**, 447-454.
- Martin, S.G. & Chang, F., 2005. New end take off: regulating cell polarity during the fission yeast cell cycle. *Cell Cycle (Georgetown, Tex.)*. **4**, 1046-1049.

- Martin, S.G., McDonald, W.H., Yates, J.R., 3rd, Chang, F., 2005. Tea4p links microtubule plus ends with the formin for3p in the establishment of cell polarity. *Developmental Cell*. **8**, 479-491.
- Martin, S.G., Rincon, S.A., Basu, R., Perez, P., Chang, F., 2007. Regulation of the formin for3p by cdc42p and bud6p. *Molecular Biology of the Cell*. **18**, 4155-4167.
- Masuda, T., Kariya, K., Shinkai, M., Okada, T., Kataoka, T., 1995. Protein kinase Byr2 is a target of Ras1 in the fission yeast *Schizosaccharomyces pombe*. *The Journal of Biological Chemistry*. **270**, 1979-1982.
- Mata, J. & Bahler, J., 2006. Global roles of Ste11p, cell type, and pheromone in the control of gene expression during early sexual differentiation in fission yeast. *Proceedings of the National Academy of Sciences of the United States of America*. **103**, 15517-15522.
- Mata, J., Lyne, R., Burns, G., Bahler, J., 2002. The transcriptional program of meiosis and sporulation in fission yeast. *Nature Genetics*. **32**, 143-147.
- Mata, J. & Nurse, P., 1997. Tea1 and the Microtubular Cytoskeleton are Important for Generating Global Spatial Order within the Fission Yeast Cell. *Cell*. **89**, 939-949.
- Mata, J., Wilbrey, A., Bahler, J., 2007. Transcriptional regulatory network for sexual differentiation in fission yeast. *Genome Biology*. **8**, R217.
- Matheos, D., Metodiev, M., Muller, E., Stone, D., Rose, M.D., 2004. Pheromone-induced polarization is dependent on the Fus3p MAPK acting through the formin Bni1p. *The Journal of Cell Biology*. **165**, 99-109.
- Maundrell, K., 1993. Thiamine-repressible expression vectors pREP and pRIP for fission yeast. *Gene*. **123**, 127-130.
- McGrath, J.P., Capon, D.J., Goeddel, D.V., Levinson, A.D., 1984. Comparative biochemical properties of normal and activated human ras p21 protein. *Nature*. **310**, 644-649.
- McKay, M.M. & Morrison, D.K., 2007. Integrating signals from RTKs to ERK/MAPK. *Oncogene*. **26**, 3113-3121.
- McLeod, M. & Beach, D., 1988. A specific inhibitor of the ran1+ protein kinase regulates entry into meiosis in *Schizosaccharomyces pombe*. *Nature*. **332**, 509-514.
- McLeod, M., Stein, M., Beach, D., 1987. The product of the mei3+ gene, expressed under control of the mating-type locus, induces meiosis and sporulation in fission yeast. *The EMBO Journal*. **6**, 729-736.
- Meade, J.H. & Gutz, H., 1976. Mating-Type Mutations in SCHIZOSACCHAROMYCES POMBE: Isolation of Mutants and Analysis of Strains with an h or h Phenotype. *Genetics*. **83**, 259-273.
- Mercer, K.E. & Pritchard, C.A., 2003. Raf proteins and cancer: B-Raf is identified as a mutational target. *Biochimica Et Biophysica Acta*. **1653**, 25-40.
- Merlini, L., Dudin, O., Martin, S.G., 2013. Mate and fuse: how yeast cells do it. *Open Biology*. **3**, 130008.
- Metodiev, M.V., Matheos, D., Rose, M.D., Stone, D.E., 2002. Regulation of MAPK function by direct interaction with the mating-specific Galpha in yeast. *Science (New York, N.Y.)*. **296**, 1483-1486.
- Millar, J.B., Buck, V., Wilkinson, M.G., 1995. Pyp1 and Pyp2 PTPases dephosphorylate an osmosensing MAP kinase controlling cell size at division in fission yeast. *Genes & Development*. **9**, 2117-2130.

- Miller, P.J. & Johnson, D.I., 1994. Cdc42p GTPase is involved in controlling polarized cell growth in *Schizosaccharomyces pombe*. *Molecular and Cellular Biology*. **14**, 1075-1083.
- Moreno, S., Klar, A., Nurse, P., 1991. Molecular genetic analysis of fission yeast *Schizosaccharomyces pombe*. *Methods in Enzymology*. **194**, 795-823.
- Moskow, J.J., Gladfelder, A.S., Lamson, R.E., Pryciak, P.M., Lew, D.J., 2000. Role of Cdc42p in pheromone-stimulated signal transduction in *Saccharomyces cerevisiae*. *Molecular and Cellular Biology*. **20**, 7559-7571.
- Munz, P., Woldf, K., Kohli, J. and Leupold, U., 1989. Genetic Overview. In Anwar Nasim, Paul Young, Byron F. Johnson, ed, *Molecular Biology of the Fission Yeast*. Academic press.
- Murphy, L.O., MacKeigan, J.P., Blenis, J., 2004. A network of immediate early gene products propagates subtle differences in mitogen-activated protein kinase signal amplitude and duration. *Molecular and Cellular Biology*. **24**, 144-153.
- Murphy, L.O., Smith, S., Chen, R.H., Fingar, D.C., Blenis, J., 2002. Molecular interpretation of ERK signal duration by immediate early gene products. *Nature Cell Biology*. **4**, 556-564.
- Murphy, T., Hori, S., Sewell, J., Gnanapragasam, V.J., 2010. Expression and functional role of negative signalling regulators in tumour development and progression. *International Journal of Cancer. Journal International Du Cancer*. **127**, 2491-2499.
- Murray, J.M. & Johnson, D.I., 2001. The Cdc42p GTPase and its regulators Nrf1p and Scd1p are involved in endocytic trafficking in the fission yeast *Schizosaccharomyces pombe*. *The Journal of Biological Chemistry*. **276**, 3004-3009.
- Nadin-Davis, S.A. & Nasim, A., 1990. *Schizosaccharomyces pombe* ras1 and byr1 are functionally related genes of the ste family that affect starvation-induced transcription of mating-type genes. *Molecular & Cellular Biology*. **10**, 549-560.
- Nadin-Davis, S.A. & Nasim, A., 1988. A gene which encodes a predicted protein kinase can restore some functions of the ras gene in fission yeast. *EMBO Journal*. **7**, 985-993.
- Nadin-Davis, S.A., Nasim, A., Beach, D., 1986a. Involvement of ras in sexual differentiation but not in growth control in fission yeast. *The EMBO Journal*. **5**, 2963-2971.
- Nadin-Davis, S.A., Yang, R.C., Narang, S.A., Nasim, A., 1986b. The cloning and characterization of a RAS gene from *Schizosaccharomyces pombe*. *Journal of Molecular Evolution*. **23**, 41-51.
- Nakano, K., Mutoh, T., Mabuchi, I., 2001. Characterization of GTPase-activating proteins for the function of the Rho-family small GTPases in the fission yeast *Schizosaccharomyces pombe*. *Genes to Cells : Devoted to Molecular & Cellular Mechanisms*. **6**, 1031-1042.
- Neiman, A.M., Stevenson, B.J., Xu, H.P., Sprague, G.F., Jr, Herskowitz, I., Wigler, M., Marcus, S., 1993. Functional homology of protein kinases required for sexual differentiation in *Schizosaccharomyces pombe* and *Saccharomyces cerevisiae* suggests a conserved signal transduction module in eukaryotic organisms. *Molecular Biology of the Cell*. **4**, 107-120.
- Nern, A. & Arkowitz, R.A., 2000. Nucleocytoplasmic shuttling of the Cdc42p exchange factor Cdc24p. *The Journal of Cell Biology*. **148**, 1115-1122.
- Nern, A. & Arkowitz, R.A., 1999. A Cdc24p-Far1p-Gbetagamma protein complex required for yeast orientation during mating. *The Journal of Cell Biology*. **144**, 1187-1202.

- Nern, A. & Arkowitz, R.A., 1998. A GTP-exchange factor required for cell orientation. *Nature*. **391**, 195-198.
- Nguyen, A., Burack, W.R., Stock, J.L., Kortum, R., Chaika, O.V., Afkarian, M., Muller, W.J., Murphy, K.M., Morrison, D.K., Lewis, R.E., McNeish, J., Shaw, A.S., 2002. Kinase suppressor of Ras (KSR) is a scaffold which facilitates mitogen-activated protein kinase activation in vivo. *Molecular and Cellular Biology*. **22**, 3035-3045.
- Niccoli, T. & Nurse, P., 2002. Different mechanisms of cell polarisation in vegetative and shmooing growth in fission yeast. *Journal of Cell Science*. **115**, 1651-1662.
- Nielsen, O. & Davey, J., 1995. Pheromone communication in the fission yeast *Schizosaccharomyces pombe*. *Seminars in Cell Biology*. **6**, 95-104.
- Nielsen, O., Davey, J., Egel, R., 1992. The Ras1 Function of *Schizosaccharomyces-Pombe* Mediates Pheromone-Induced Transcription. *Embo Journal*. **11**, 1391-1395.
- Nurse, P., 1985. Mutants of the fission yeast *Schizosaccharomyces pombe* which alter the shift between cell proliferation and sporulation. *Mol.Gen.Genet.* **198**, 497-502.
- Obara, T., Nakafuku, M., Yamamoto, M., Kaziro, Y., 1991. Isolation and Characterization of a Gene Encoding a G-Protein Alpha Subunit from *Schizosaccharomyces-Pombe* - Involvement in Mating and Sporulation Pathways. *Proceedings of the National Academy of Sciences of the United States of America*. **88**, 5877-5881.
- Okazaki, N., Okazaki, K., Tanaka, K., Okayama, H., 1991. The *ste4+* gene, essential for sexual differentiation of *Schizosaccharomyces pombe*, encodes a protein with a leucine zipper motif. *Nucleic Acids Research*. **19**, 7043-7047.
- Olmo, V.N. & Grote, E., 2010. Prm1 targeting to contact sites enhances fusion during mating in *Saccharomyces cerevisiae*. *Eukaryotic Cell*. **9**, 1538-1548.
- Onken, B., Wiener, H., Philips, M.R., Chang, E.C., 2006. Compartmentalized signaling of Ras in fission yeast. *Proceedings of the National Academy of Sciences of the United States of America*. **103**, 9045-9050.
- Otsubo, Y. & Yamamoto, M., 2008. TOR signaling in fission yeast. *Critical Reviews in Biochemistry and Molecular Biology*. **43**, 277-283.
- Otsubo, Y. & Yamamoto, M., 2012. Signaling pathways for fission yeast sexual differentiation at a glance. *Journal of Cell Science*. **125**, 2789-2793.
- Ottillie, S., Miller, P.J., Johnson, D.I., Creasy, C.L., Sells, M.A., Bagrodia, S., Forsburg, S.L., Chernoff, J., 1995. Fission yeast *pak1+* encodes a protein kinase that interacts with Cdc42p and is involved in the control of cell polarity and mating. *The EMBO Journal*. **14**, 5908-5919.
- Ozoe, F., Kurokawa, R., Kobayashi, Y., Jeong, H.T., Tanaka, K., Sen, K., Nakagawa, T., Matsuda, H., Kawamukai, M., 2002. The 14-3-3 proteins Rad24 and Rad25 negatively regulate Byr2 by affecting its localization in *Schizosaccharomyces pombe*. *Molecular & Cellular Biology*. **22**, 7105-7119.
- Pamonsinlapatham, P., Hadj-Slimane, R., Lepelletier, Y., Allain, B., Toccafondi, M., Garbay, C., Raynaud, F., 2009. P120-Ras GTPase activating protein (RasGAP): a multi-interacting protein in downstream signaling. *Biochimie*. **91**, 320-328.
- Papadaki, P., Pizon, V., Onken, B., Chang, E.C., 2002. Two ras pathways in fission yeast are differentially regulated by two ras guanine nucleotide exchange factors. *Molecular & Cellular Biology*. **22**, 4598-4606.

- Parada, L.F., Tabin, C.J., Shih, C., Weinberg, R.A., 1982. Human EJ bladder carcinoma oncogene is homologue of Harvey sarcoma virus ras gene. *Nature*. **297**, 474-478.
- Park, H.O. & Bi, E., 2007. Central roles of small GTPases in the development of cell polarity in yeast and beyond. *Microbiology and Molecular Biology Reviews : MMBR*. **71**, 48-96.
- Paterson, J.M., Ydenberg, C.A., Rose, M.D., 2008. Dynamic localization of yeast Fus2p to an expanding ring at the cell fusion junction during mating. *The Journal of Cell Biology*. **181**, 697-709.
- Pereira, P.S. & Jones, N.C., 2001. The RGS domain-containing fission yeast protein, Rgs1p, regulates pheromone signalling and is required for mating. *Genes to Cells*. **6**, 789-802.
- Perez, P. & Rincon, S.A., 2010. Rho GTPases: regulation of cell polarity and growth in yeasts. *The Biochemical Journal*. **426**, 243-253.
- Petersen, J., Nielsen, O., Egel, R., Hagan, I.M., 1998a. F-actin distribution and function during sexual differentiation in *Schizosaccharomyces pombe*. *Journal of Cell Science*. **111 (Pt 7)**, 867-876.
- Petersen, J., Nielsen, O., Egel, R., Hagan, I.M., 1998b. FH3, a domain found in formins, targets the fission yeast formin Fus1 to the projection tip during conjugation. *The Journal of Cell Biology*. **141**, 1217-1228.
- Petersen, J., Weilguny, D., Egel, R., Nielsen, O., 1995. Characterization of fus1 of *Schizosaccharomyces pombe*: a developmentally controlled function needed for conjugation. *Molecular and Cellular Biology*. **15**, 3697-3707.
- Plotnikov, A., Zehorai, E., Procaccia, S., Seger, R., 2011. The MAPK cascades: signaling components, nuclear roles and mechanisms of nuclear translocation. *Biochimica Et Biophysica Acta*. **1813**, 1619-1633.
- Polverino, A., Frost, J., Yang, P., Hutchison, M., Neiman, A.M., Cobb, M.H., Marcus, S., 1995. Activation of mitogen-activated protein kinase cascades by p21-activated protein kinases in cell-free extracts of *Xenopus* oocytes. *The Journal of Biological Chemistry*. **270**, 26067-26070.
- Poulikakos, P.I., Zhang, C., Bollag, G., Shokat, K.M., Rosen, N., 2010. RAF inhibitors transactivate RAF dimers and ERK signalling in cells with wild-type BRAF. *Nature*. **464**, 427-430.
- Qin, J., Kang, W., Leung, B., McLeod, M., 2003. Ste11p, a high-mobility-group box DNA-binding protein, undergoes pheromone- and nutrient-regulated nuclear-cytoplasmic shuttling. *Molecular & Cellular Biology*. **23**, 3253-3264.
- Qyang, Y., Yang, P., Du, H., Lai, H., Kim, H., Marcus, S., 2002. The p21-activated kinase, Shk1, is required for proper regulation of microtubule dynamics in the fission yeast, *Schizosaccharomyces pombe*. *Molecular Microbiology*. **44**, 325-334.
- Rajakulendran, T., Sahmi, M., Lefrancois, M., Sicheri, F., Therrien, M., 2009. A dimerization-dependent mechanism drives RAF catalytic activation. *Nature*. **461**, 542-545.
- Ramachander, R., Kim, C.A., Phillips, M.L., Mackereth, C.D., Thanos, C.D., McIntosh, L.P., Bowie, J.U., 2002. Oligomerization-dependent association of the SAM domains from *Schizosaccharomyces pombe* Byr2 and Ste4. *The Journal of Biological Chemistry*. **277**, 39585-39593.
- Ramezani-Rad, M., 2003. The role of adaptor protein Ste50-dependent regulation of the MAPKKK Ste11 in multiple signalling pathways of yeast. *Current Genetics*. **43**, 161-170.
- Ramos, J.W., 2008. The regulation of extracellular signal-regulated kinase (ERK) in mammalian cells. *The International Journal of Biochemistry & Cell Biology*. **40**, 2707-2719.

- Rauen, K.A., 2013. The RASopathies. *Annual Review of Genomics and Human Genetics*.
- Reddy, E.P., Reynolds, R.K., Santos, E., Barbacid, M., 1982. A point mutation is responsible for the acquisition of transforming properties by the T24 human bladder carcinoma oncogene. *Nature*. **300**, 149-152.
- Ricketts, M.H. & Levinson, A.D., 1988. High-level expression of c-H-ras1 fails to fully transform rat-1 cells. *Molecular and Cellular Biology*. **8**, 1460-1468.
- Riedl, J., Crevenna, A.H., Kessenbrock, K., Yu, J.H., Neukirchen, D., Bista, M., Bradke, F., Jenne, D., Holak, T.A., Werb, Z., Sixt, M., Wedlich-Soldner, R., 2008. Lifeact: a versatile marker to visualize F-actin. *Nature Methods*. **5**, 605-607.
- Rincon, S.A., Ye, Y., Villar-Tajadura, M.A., Santos, B., Martin, S.G., Perez, P., 2009. Pob1 participates in the Cdc42 regulation of fission yeast actin cytoskeleton. *Molecular Biology of the Cell*. **20**, 4390-4399.
- Robbins, D.J., Zhen, E., Owaki, H., Vanderbilt, C.A., Ebert, D., Geppert, T.D., Cobb, M.H., 1993. Regulation and properties of extracellular signal-regulated protein kinases 1 and 2 in vitro. *The Journal of Biological Chemistry*. **268**, 5097-5106.
- Rohrer, J., Benedetti, H., Zanolari, B., Riezman, H., 1993. Identification of a novel sequence mediating regulated endocytosis of the G protein-coupled alpha-pheromone receptor in yeast. *Molecular Biology of the Cell*. **4**, 511-521.
- Roskoski, R., Jr, 2012. ERK1/2 MAP kinases: structure, function, and regulation. *Pharmacological Research : The Official Journal of the Italian Pharmacological Society*. **66**, 105-143.
- Roskoski, R., Jr, 2010. RAF protein-serine/threonine kinases: structure and regulation. *Biochemical and Biophysical Research Communications*. **399**, 313-317.
- Rossomando, A.J., Dent, P., Sturgill, T.W., Marshak, D.R., 1994. Mitogen-activated protein kinase kinase 1 (MKK1) is negatively regulated by threonine phosphorylation. *Molecular and Cellular Biology*. **14**, 1594-1602.
- Roy, S., Lane, A., Yan, J., McPherson, R., Hancock, J.F., 1997. Activity of plasma membrane-recruited Raf-1 is regulated by Ras via the Raf zinc finger. *The Journal of Biological Chemistry*. **272**, 20139-20145.
- Saito, Y., Gomez, N., Campbell, D.G., Ashworth, A., Marshall, C.J., Cohen, P., 1994. The threonine residues in MAP kinase kinase 1 phosphorylated by MAP kinase in vitro are also phosphorylated in nerve growth factor-stimulated rat pheochromocytoma (PC12) cells. *FEBS Letters*. **341**, 119-124.
- Sanchez-Paredes, E., Kawasaki, L., Ongay-Larios, L., Coria, R., 2011. The Galpha subunit signals through the Ste50 protein during the mating pheromone response in the yeast *Kluyveromyces lactis*. *Eukaryotic Cell*. **10**, 540-546.
- Santos, E., Tronick, S.R., Aaronson, S.A., Pulciani, S., Barbacid, M., 1982. T24 human bladder carcinoma oncogene is an activated form of the normal human homologue of BALB- and Harvey-MSV transforming genes. *Nature*. **298**, 343-347.
- Sato, M., Dhut, S., Toda, T., 2005. New drug-resistant cassettes for gene disruption and epitope tagging in *Schizosaccharomyces pombe*. *Yeast (Chichester, England)*. **22**, 583-591.
- Sato, M., Watanabe, Y., Akiyoshi, Y., Yamamoto, M., 2002. 14-3-3 protein interferes with the binding of RNA to the phosphorylated form of fission yeast meiotic regulator Mei2p. *Current Biology*. **12**, 141-145.

- Schaeffer, H.J., Catling, A.D., Eblen, S.T., Collier, L.S., Krauss, A., Weber, M.J., 1998. MP1: a MEK binding partner that enhances enzymatic activation of the MAP kinase cascade. *Science (New York, N.Y.)*. **281**, 1668-1671.
- Scheffzek, K., Ahmadian, M.R., Kabsch, W., Wiesmuller, L., Lautwein, A., Schmitz, F., Wittinghofer, A., 1997. The Ras-RasGAP complex: structural basis for GTPase activation and its loss in oncogenic Ras mutants. *Science (New York, N.Y.)*. **277**, 333-338.
- Scheffzek, K., Lautwein, A., Kabsch, W., Ahmadian, M.R., Wittinghofer, A., 1996. Crystal structure of the GTPase-activating domain of human p120GAP and implications for the interaction with Ras. *Nature*. **384**, 591-596.
- Schubbert, S., Shannon, K., Bollag, G., 2007. Hyperactive Ras in developmental disorders and cancer. *Nature Reviews.Cancer*. **7**, 295-308.
- Scolnick, E.M., Papageorge, A.G., Shih, T.Y., 1979. Guanine nucleotide-binding activity as an assay for src protein of rat-derived murine sarcoma viruses. *Proceedings of the National Academy of Sciences of the United States of America*. **76**, 5355-5359.
- Seger, R. & Krebs, E.G., 1995. The MAPK signaling cascade. *FASEB Journal : Official Publication of the Federation of American Societies for Experimental Biology*. **9**, 726-735.
- Sells, M.A., Barratt, J.T., Caviston, J., Otilie, S., Leberer, E., Chernoff, J., 1998. Characterization of Pak2p, a pleckstrin homology domain-containing, p21-activated protein kinase from fission yeast. *The Journal of Biological Chemistry*. **273**, 18490-18498.
- Shields, J.M., Pruitt, K., McFall, A., Shaub, A., Der, C.J., 2000. Understanding Ras: 'it ain't over 'til it's over'. *Trends in Cell Biology*. **10**, 147-154.
- Shimada, T., Yamashita, A., Yamamoto, M., 2003. The fission yeast meiotic regulator Mei2p forms a dot structure in the horse-tail nucleus in association with the sme2 locus on chromosome II. *Molecular Biology of the Cell*. **14**, 2461-2469.
- Shimada, Y., Gulli, M.P., Peter, M., 2000. Nuclear sequestration of the exchange factor Cdc24 by Far1 regulates cell polarity during yeast mating. *Nature Cell Biology*. **2**, 117-124.
- Shiozaki, K. & Russell, P., 1996. Conjugation, meiosis, and the osmotic stress response are regulated by Spc1 kinase through Atf1 transcription factor in fission yeast. *Genes & Development*. **10**, 2276-2288.
- Shiozaki, K. & Russell, P., 1995. Cell-cycle control linked to extracellular environment by MAP kinase pathway in fission yeast. *Nature*. **378**, 739-743.
- Simon, M.N., De Virgilio, C., Souza, B., Pringle, J.R., Abo, A., Reed, S.I., 1995. Role for the Rho-family GTPase Cdc42 in yeast mating-pheromone signal pathway. *Nature*. **376**, 702-705.
- Snaith, H.A., Samejima, I., Sawin, K.E., 2005. Multistep and multimode cortical anchoring of tea1p at cell tips in fission yeast. *The EMBO Journal*. **24**, 3690-3699.
- Snaith, H.A. & Sawin, K.E., 2003. Fission yeast mod5p regulates polarized growth through anchoring of tea1p at cell tips. *Nature*. **423**, 647-651.
- Soderling, T.R., 1990. Protein kinases. Regulation by autoinhibitory domains. *The Journal of Biological Chemistry*. **265**, 1823-1826.
- Sontag, E., Fedorov, S., Kamibayashi, C., Robbins, D., Cobb, M., Mumby, M., 1993. The interaction of SV40 small tumor antigen with protein phosphatase 2A stimulates the map kinase pathway and induces cell proliferation. *Cell*. **75**, 887-897.

- Stengel, K. & Zheng, Y., 2011. Cdc42 in oncogenic transformation, invasion, and tumorigenesis. *Cellular Signalling*. **23**, 1415-1423.
- Stengel, K.R. & Zheng, Y., 2012. Essential role of Cdc42 in Ras-induced transformation revealed by gene targeting. *PLoS One*. **7**, e37317.
- Sugimoto, A., Iino, Y., Maeda, T., Watanabe, Y., Yamamoto, M., 1991. Schizosaccharomyces pombe *stl1+* encodes a transcription factor with an HMG motif that is a critical regulator of sexual development. *Genes & Development*. **5**, 1990-1999.
- Sugiura, R., Toda, T., Shuntoh, H., Yanagida, M., Kuno, T., 1998. *pmp1+*, a suppressor of calcineurin deficiency, encodes a novel MAP kinase phosphatase in fission yeast. *The EMBO Journal*. **17**, 140-148.
- Sukegawa, Y., Yamashita, A., Yamamoto, M., 2011. The fission yeast stress-responsive MAPK pathway promotes meiosis via the phosphorylation of Pol II CTD in response to environmental and feedback cues. *PLoS Genetics*. **7**, e1002387.
- Sweet, R.W., Yokoyama, S., Kamata, T., Feramisco, J.R., Rosenberg, M., Gross, M., 1984. The product of *ras* is a GTPase and the T24 oncogenic mutant is deficient in this activity. *Nature*. **311**, 273-275.
- Tabin, C.J., Bradley, S.M., Bargmann, C.I., Weinberg, R.A., Papageorge, A.G., Scolnick, E.M., Dhar, R., Lowy, D.R., Chang, E.H., 1982. Mechanism of activation of a human oncogene. *Nature*. **300**, 143-149.
- Tanaka, K., Davey, J., Imai, Y., Yamamoto, M., 1993. Schizosaccharomyces pombe *map3+* encodes the putative M-factor receptor. *Molecular and Cellular Biology*. **13**, 80-88.
- Tanaka, K., Kohda, T., Yamashita, A., Nonaka, N., Yamamoto, M., 2005. Hrs1p/Mcp6p on the meiotic SPB organizes astral microtubule arrays for oscillatory nuclear movement. *Current Biology : CB*. **15**, 1479-1486.
- Taparowsky, E., Suard, Y., Fasano, O., Shimizu, K., Goldfarb, M., Wigler, M., 1982. Activation of the T24 bladder carcinoma transforming gene is linked to a single amino acid change. *Nature*. **300**, 762-765.
- Tatebe, H., Nakano, K., Maximo, R., Shiozaki, K., 2008. Pom1 DYRK regulates localization of the Rga4 GAP to ensure bipolar activation of Cdc42 in fission yeast. *Current Biology : CB*. **18**, 322-330.
- Terrell, J., Shih, S., Dunn, R., Hicke, L., 1998. A function for monoubiquitination in the internalization of a G protein-coupled receptor. *Molecular Cell*. **1**, 193-202.
- Tesmer, J.J., Berman, D.M., Gilman, A.G., Sprang, S.R., 1997. Structure of RGS4 bound to AIF4--activated G(i alpha1): stabilization of the transition state for GTP hydrolysis. *Cell*. **89**, 251-261.
- Toda, T., Dhut, S., Superti-Furga, G., Gotoh, Y., Nishida, E., Sugiura, R., Kuno, T., 1996. The fission yeast *pmk1+* gene encodes a novel mitogen-activated protein kinase homolog which regulates cell integrity and functions coordinately with the protein kinase C pathway. *Molecular and Cellular Biology*. **16**, 6752-6764.
- Toda, T., Uno, I., Ishikawa, T., Powers, S., Kataoka, T., Broek, D., Cameron, S., Broach, J., Matsumoto, K., Wigler, M., 1985. In yeast, RAS proteins are controlling elements of adenylate cyclase. *Cell*. **40**, 27-36.
- Tolwinski, N.S., Shapiro, P.S., Goueli, S., Ahn, N.G., 1999. Nuclear localization of mitogen-activated protein kinase kinase 1 (MKK1) is promoted by serum stimulation and G2-M progression. Requirement for phosphorylation at the activation lip and signaling downstream of MKK. *The Journal of Biological Chemistry*. **274**, 6168-6174.

- Toya, M., Motegi, F., Nakano, K., Mabuchi, I., Yamamoto, M., 2001. Identification and functional analysis of the gene for type I myosin in fission yeast. *Genes to Cells : Devoted to Molecular & Cellular Mechanisms*. **6**, 187-199.
- Trahey, M. & McCormick, F., 1987. A cytoplasmic protein stimulates normal N-ras p21 GTPase, but does not affect oncogenic mutants. *Science (New York, N.Y.)*. **238**, 542-545.
- Tratner, I., Fourtqc-Esqueoute, A., Tillit, J., Baldacci, G., 1997. Cloning and characterization of the *S. pombe* gene *efc25+*, a new putative guanine nucleotide exchange factor. *Gene*. **193**, 203-210.
- Traverse, S., Seedorf, K., Paterson, H., Marshall, C.J., Cohen, P., Ullrich, A., 1994. EGF triggers neuronal differentiation of PC12 cells that overexpress the EGF receptor. *Current Biology : CB*. **4**, 694-701.
- Truckses, D.M., Bloomekatz, J.E., Thorner, J., 2006. The RA domain of Ste50 adaptor protein is required for delivery of Ste11 to the plasma membrane in the filamentous growth signaling pathway of the yeast *Saccharomyces cerevisiae*. *Molecular and Cellular Biology*. **26**, 912-928.
- Tu, H., Barr, M., Dong, D.L., Wigler, M., 1997. Multiple regulatory domains on the Byr2 protein kinase. *Molecular and Cellular Biology*. **17**, 5876-5887.
- Tu, H. & Wigler, M., 1999. Genetic evidence for Pak1 autoinhibition and its release by Cdc42. *Molecular and Cellular Biology*. **19**, 602-611.
- Tuveson, D.A., Shaw, A.T., Willis, N.A., Silver, D.P., Jackson, E.L., Chang, S., Mercer, K.L., Grochow, R., Hock, H., Crowley, D., Hingorani, S.R., Zaks, T., King, C., Jacobetz, M.A., Wang, L., Bronson, R.T., Orkin, S.H., DePinho, R.A., Jacks, T., 2004. Endogenous oncogenic K-ras(G12D) stimulates proliferation and widespread neoplastic and developmental defects. *Cancer Cell*. **5**, 375-387.
- Valbuena, N. & Moreno, S., 2010. TOR and PKA pathways synergize at the level of the Ste11 transcription factor to prevent mating and meiosis in fission yeast. *PLoS One*. **5**, e11514.
- Valtz, N., Peter, M., Herskowitz, I., 1995. FAR1 is required for oriented polarization of yeast cells in response to mating pheromones. *The Journal of Cell Biology*. **131**, 863-873.
- Van Heeckeren, W.J., Dorris, D.R., Struhl, K., 1998. The mating-type proteins of fission yeast induce meiosis by directly activating *mei3* transcription. *Molecular & Cellular Biology*. **18**, 7317-7326.
- Verde, F., 1998. On growth and form: control of cell morphogenesis in fission yeast. *Current Opinion in Microbiology*. **1**, 712-718.
- Vogel, U.S., Dixon, R.A., Schaber, M.D., Diehl, R.E., Marshall, M.S., Scolnick, E.M., Sigal, I.S., Gibbs, J.B., 1988. Cloning of bovine GAP and its interaction with oncogenic ras p21. *Nature*. **335**, 90-93.
- Wach, A., 1996. PCR-synthesis of marker cassettes with long flanking homology regions for gene disruptions in *S. cerevisiae*. *Yeast (Chichester, England)*. **12**, 259-265.
- Wan, P.T., Garnett, M.J., Roe, S.M., Lee, S., Niculescu-Duvaz, D., Good, V.M., Jones, C.M., Marshall, C.J., Springer, C.J., Barford, D., Marais, R., Cancer Genome Project, 2004. Mechanism of activation of the RAF-ERK signaling pathway by oncogenic mutations of B-RAF. *Cell*. **116**, 855-867.
- Wang, Y., Boguski, M., Riggs, M., Rodgers, L., Wigler, M., 1991. Sar1, a Gene from *Schizosaccharomyces Pombe* Encoding a Protein that Regulates Ras1. *Cell Regulation*. **2**, 453-465.
- Wang, Y., Chen, W., Simpson, D.M., Elion, E.A., 2005. Cdc24 regulates nuclear shuttling and recruitment of the Ste5 scaffold to a heterotrimeric G protein in *Saccharomyces cerevisiae*. *The Journal of Biological Chemistry*. **280**, 13084-13096.

- Wang, Y., Xu, H.P., Riggs, M., Rodgers, L., Wigler, M., 1991. *byr2*, a *Schizosaccharomyces pombe* gene encoding a protein kinase capable of partial suppression of the *ras1* mutant phenotype. *Molecular & Cellular Biology*. **11**, 3554-3563.
- Watanabe, Y., Lino, Y., Furuhata, K., Shimoda, C., Yamamoto, M., 1988. The *S.pombe mei2* gene encoding a crucial molecule for commitment to meiosis is under the regulation of cAMP. *The EMBO Journal*. **7**, 761-767.
- Watanabe, Y., Shinozaki-Yabana, S., Chikashige, Y., Hiraoka, Y., Yamamoto, M., 1997. Phosphorylation of RNA-binding protein controls cell cycle switch from mitotic to meiotic in fission yeast. *Nature*. **386**, 187-190.
- Watanabe, Y. & Yamamoto, M., 1994. *S. pombe mei2+* encodes an RNA-binding protein essential for premeiotic DNA synthesis and meiosis I, which cooperates with a novel RNA species *meiRNA*. *Cell*. **78**, 487-498.
- Watson, P., Davis, K., Didmon, M., Broad, P., Davey, J., 1999. An RGS protein regulates the pheromone response in the fission yeast *Schizosaccharomyces pombe*. *Molecular Microbiology*. **33**, 623-634.
- Weber, C.K., Slupsky, J.R., Kalmes, H.A., Rapp, U.R., 2001. Active Ras induces heterodimerization of cRaf and B Raf. *Cancer Research*. **61**, 3595-3598.
- Welton, R.M. & Hoffman, C.S., 2000. Glucose monitoring in fission yeast via the Gpa2 galpha, the git5 Gbeta and the git3 putative glucose receptor. *Genetics*. **156**, 513-521.
- Wheatley, E. & Rittinger, K., 2005. Interactions between Cdc42 and the scaffold protein Scd2: requirement of SH3 domains for GTPase binding. *The Biochemical Journal*. **388**, 177-184.
- Whiteway, M.S., Wu, C., Leeuw, T., Clark, K., Fourest-Lieuvain, A., Thomas, D.Y., Leberer, E., 1995. Association of the yeast pheromone response G protein beta gamma subunits with the MAP kinase scaffold Ste5p. *Science (New York, N.Y.)*. **269**, 1572-1575.
- Widmann, C., Gibson, S., Jarpe, M.B., Johnson, G.L., 1999. Mitogen-activated protein kinase: conservation of a three-kinase module from yeast to human. *Physiological Reviews*. **79**, 143-180.
- Wiget, P., Shimada, Y., Butty, A.C., Bi, E., Peter, M., 2004. Site-specific regulation of the GEF Cdc24p by the scaffold protein Far1p during yeast mating. *The EMBO Journal*. **23**, 1063-1074.
- Willer, M., Hoffmann, L., Styrkarsdottir, U., Egel, R., Davey, J., Nielsen, O., 1995. Two-step activation of meiosis by the *mat1* locus in *Schizosaccharomyces pombe*. *Molecular & Cellular Biology*. **15**, 4964-4970.
- Wood, V., Gwilliam, R., Rajandream, M.A., Lyne, M., Lyne, R., Stewart, A., Sgouros, J., Peat, N., Hayles, J., Baker, S., Basham, D., Bowman, S., Brooks, K., Brown, D., Brown, S., Chillingworth, T., Churcher, C., Collins, M., Connor, R., Cronin, A., Davis, P., Feltwell, T., Fraser, A., Gentles, S., Goble, A., Hamlin, N., Harris, D., Hidalgo, J., Hodgson, G., Holroyd, S., Hornsby, T., Howarth, S., Huckle, E.J., Hunt, S., Jagels, K., James, K., Jones, L., Jones, M., Leather, S., McDonald, S., McLean, J., Mooney, P., Moule, S., Mungall, K., Murphy, L., Niblett, D., Odell, C., Oliver, K., O'Neil, S., Pearson, D., Quail, M.A., Rabinowitsch, E., Rutherford, K., Rutter, S., Saunders, D., Seeger, K., Sharp, S., Skelton, J., Simmonds, M., Squares, R., Stevens, K., Taylor, K., Taylor, R.G., Tivey, A., Walsh, S., Warren, T., Whitehead, S., Woodward, J., Volckaert, G., Aert, R., Robben, J., Grymonprez, B., Weltjens, I., Vanstreels, E., Rieger, M., Schafer, M., Muller-Auer, S., Gabel, C., Fuchs, M., Dusterhoft, A., Fritzc, C., Holzer, E., Moestl, D., Hilbert, H., Borzym, K., Langer, I., Beck, A., Lehrach, H., Reinhardt, R., Pohl, T.M., Eger, P., Zimmermann, W., Wedler, H., Wambutt, R., Purnelle, B., Goffeau, A., Cadieu, E., Dreano, S., Gloux, S., Lelaure, V., Mottier, S., Galibert, F., Aves, S.J., Xiang, Z., Hunt, C., Moore, K., Hurst, S.M., Lucas, M., Rochet, M., Gaillardin, C., Tallada, V.A., Garzon, A., Thode, G., Daga, R.R., Cruzado, L., Jimenez, J., Sanchez, M., del Rey, F., Benito, J., Dominguez, A., Revuelta, J.L., Moreno, S., Armstrong, J., Forsburg, S.L., Cerutti, L., Lowe, T., McCombie, W.R., Paulsen, I., Potashkin, J.,

- Shpakovski, G.V., Ussery, D., Barrell, B.G., Nurse, P., 2002. The genome sequence of *Schizosaccharomyces pombe*. *Nature*. **415**, 871-880.
- Wu, C., Jansen, G., Zhang, J., Thomas, D.Y., Whiteway, M., 2006. Adaptor protein Ste50p links the Ste11p MEKK to the HOG pathway through plasma membrane association. *Genes & Development*. **20**, 734-746.
- Xu, H.P., Rajavashisth, T., Grewal, N., Jung, V., Riggs, M., Rodgers, L., Wigler, M., 1992. A gene encoding a protein with seven zinc finger domains acts on the sexual differentiation pathways of *Schizosaccharomyces pombe*. *Molecular Biology of the Cell*. **3**, 721-734.
- Xu, H.P., White, M., Marcus, S., Wigler, M., 1994. Concerted action of RAS and G proteins in the sexual response pathways of *Schizosaccharomyces pombe*. *Molecular & Cellular Biology*. **14**, 50-58.
- Xue-Franzen, Y., Kjaerulff, S., Holmberg, C., Wright, A., Nielsen, O., 2006. Genomewide identification of pheromone-targeted transcription in fission yeast. *BMC Genomics*. **7**, 303.
- Yamamoto, A. & Hiraoka, Y., 2003. Monopolar spindle attachment of sister chromatids is ensured by two distinct mechanisms at the first meiotic division in fission yeast. *The EMBO Journal*. **22**, 2284-2296.
- Yamamoto, M., 2010. The selective elimination of messenger RNA underlies the mitosis-meiosis switch in fission yeast. *Proceedings of the Japan Academy. Series B, Physical and Biological Sciences*. **86**, 788-797.
- Yamamoto, M., 1996. The molecular control mechanisms of meiosis in fission yeast. *Trends in Biochemical Sciences*. **21**, 18-22.
- Yamamoto, T.G., Chikashige, Y., Ozoe, F., Kawamukai, M., Hiraoka, Y., 2004. Activation of the pheromone-responsive MAP kinase drives haploid cells to undergo ectopic meiosis with normal telomere clustering and sister chromatid segregation in fission yeast. *Journal of Cell Science*. **117**, 3875-3886.
- Yamashita, A. & Yamamoto, M., 1998. [Molecular mechanisms for the regulation of meiosis in fission yeast]. *Tanpakushitsu Kakusan Koso - Protein, Nucleic Acid, Enzyme*. **43**, 314-321.
- Yan, S.F., King, F.J., Zhou, Y., Warmuth, M., Xia, G., 2006. Profiling the kinome for drug discovery. *Drug Discovery Today: Technologies*. **3**, 269-276.
- Yang, P., Kansra, S., Pimental, R.A., Gilbreth, M., Marcus, S., 1998. Cloning and characterization of *shk2*, a gene encoding a novel p21-activated protein kinase from fission yeast. *The Journal of Biological Chemistry*. **273**, 18481-18489.
- Yang, X.Y., Guan, M., Vigil, D., Der, C.J., Lowy, D.R., Popescu, N.C., 2009. p120Ras-GAP binds the DLC1 Rho-GAP tumor suppressor protein and inhibits its RhoA GTPase and growth-suppressing activities. *Oncogene*. **28**, 1401-1409.
- Yen, H.C., Gordon, C., Chang, E.C., 2003. *Schizosaccharomyces pombe* Int6 and Ras homologs regulate cell division and mitotic fidelity via the proteasome. *Cell*. **112**, 207-217.
- Yeung, K., Seitz, T., Li, S., Janosch, P., McFerran, B., Kaiser, C., Fee, F., Katsanakis, K.D., Rose, D.W., Mischak, H., Sedivy, J.M., Kolch, W., 1999. Suppression of Raf-1 kinase activity and MAP kinase signalling by RKIP. *Nature*. **401**, 173-177.
- Yue, Y., Lypowy, J., Hedhli, N., Abdellatif, M., 2004. Ras GTPase-activating protein binds to Akt and is required for its activation. *The Journal of Biological Chemistry*. **279**, 12883-12889.

Zhang, C., Kenski, D.M., Paulson, J.L., Bonshtien, A., Sessa, G., Cross, J.V., Templeton, D.J., Shokat, K.M., 2005. A second-site suppressor strategy for chemical genetic analysis of diverse protein kinases. *Nature Methods*. **2**, 435-441.

Zhao, Z.S., Leung, T., Manser, E., Lim, L., 1995. Pheromone signalling in *Saccharomyces cerevisiae* requires the small GTP-binding protein Cdc42p and its activator CDC24. *Molecular and Cellular Biology*. **15**, 5246-5257.

Zheng, C.F. & Guan, K.L., 1994. Activation of MEK family kinases requires phosphorylation of two conserved Ser/Thr residues. *The EMBO Journal*. **13**, 1123-1131.

Zheng, H., Al-Ayoubi, A., Eblen, S.T., 2010. Identification of novel substrates of MAP Kinase cascades using bioengineered kinases that uniquely utilize analogs of ATP to phosphorylate substrates. *Methods in Molecular Biology (Clifton, N.J.)*. **661**, 167-183.